AN ANALYTICAL TREATMENT OF PHOTON TRANSPORT IN TWO-LAYERED MEDIA.

James Andrew Maniscalco

AN ANALYTICAL TREATMENT OF PHOTON TRANSPORT IN TWO-LAYERED MEDIA

A Thesis

Submitted to the Faculty

of

Purdue University

by

James Andrew Maniscalco

In Partial Fulfillment of the

Requirements for the Degree

of

Doctor of Philosophy

May 1973

ACKNOWLEDGMENTS

The author would like to express his sincerest thanks to Professor H. E. Hungerford for providing technical assistance, guidance and encouragement during the study. For Professor Hungerford's patient understanding and readily available expertise the author will be eternally grateful.

Thanks are also due to the other members of the author's committee: Professors F. M. Clikeman, K. J. Yost, and R. S. Christian.

Financial support from the United States Navy, through the Junior Line Officer Advanced Scientific Education Program is gratefully acknowledged. In addition, the author wishes to express his gratitude to Captain Knudsen, Commanding Officer of the Naval Reserve Officer Training Center at Purdue University, for his continuing support and professional guidance.

Finally the author would like to thank his wife, Barbara, for her patience, understanding and cheeful endurance; moreover, should the reader detect any grammatical or spelling errors in this work, the author would like to place the blame fairly and squarely where it belongs--on the shoulders of his wife.

TABLE OF CONTENTS

LIST OF TABLES

Appendix Page

Tables

Appendix Page

Table

Appendix Page

Table

Appendix Page

Table

Appendix Page

Table

Appendix Table — Page

Appendix Page

Table

Appendix Page

Table

LIST OF FIGURES

Appendix Page

Figure

Appendix Page

Figure

Appendix Figure — Page

Appendix

Figure

NOMENCLATURE

Symbol	Description	Dimension
b	Thickness in mean free paths ($b = \mu x$)	None
b_1	Thickness of the first layer in mean free paths	None
b_2	Thickness of the second layer in mean free paths	None
$B_A(b_1+b_2)$	The two-medium energy-absorption buildup factor	None
$B_D(b_1+b_2)$	The two-medium dose buildup factor	None
$B_E(b)$	The single-medium energy buildup factor	None
$B_E(b_1,b_2)$	The energy buildup factor at the interface between the two layers	None
$B_E^S(b_1,b_2)$	The scattered energy buildup factor	None
E	Photon energy	MeV
E_0	The initial photon energy	MeV
E_i	The average photon energy in the ith group	MeV
$E_n(x)$	The exponential integral of order n	None
F	The fractional deviation	None
$I(b_1,E,\vec{\Omega})$	The angular energy flux density at the interface between the slabs, defined as $E\cdot\phi(b_1,E,\vec{\Omega})$	$\frac{\text{MeV}}{\text{cm}^2\text{-sec-MeV-STER}}$
$I^S(b_1,E,\vec{\Omega})$	The scattered angular energy flux at the interface between the slabs	$\frac{\text{MeV}}{\text{cm}^2\text{-sec-MeV-STER}}$

Symbol	Description	Dimension
$I^s(b_1,b_2)$	The scattered energy flux at the interface between the slabs	$\frac{MeV}{cm^2\text{-sec}}$
$I^s(b_1+b_2)$	The scattered energy flux at the outer edge of the second layer	$\frac{MeV}{cm^2\text{-sec}}$
$I^s(b_1+b_2,E)$	The scattered energy flux spectrum at the outer edge of the second layer	$\frac{MeV}{cm^2\text{-sec-MeV}}$
$I^s_\ell(b_1,b_2,E)$	The Legendre expansion coefficients of $I^s(b_1,E,\vec{\Omega})$	$\frac{MeV}{cm^2\text{-sec-MeV}}$
$I^u(b_1+b_2)$	The unscattered energy flux at the outer edge of the second layer	$\frac{MeV}{cm^2\text{-sec}}$
$I^{ss}(b_1+b_2)$	The energy flux which scatters in both layers	$\frac{MeV}{cm^2\text{-sec}}$
$I^{su}(b_1+b_2)$	The energy flux which scatters in the first layer but not in the second layer	MeV
$I^{us}(b_1+b_2)$	The energy flux which does not scatter in the first layer but scatters in the second layer	$\frac{MeV}{cm^2\text{-sec}}$
$I^s_f(b_1)$	The scattered energy flux which results at the interface when the second layer is replaced by a vacuum	$\frac{MeV}{cm^2\text{-sec}}$
$I^s_r(b_1,b_2)$	The scattered energy flux at the interface which is reflected from the second layer	$\frac{MeV}{cm^2\text{-sec}}$
$I^{su}_n(b_1+b_2)$	The energy flux which scatters in the first layer but not the second layer, normalized to an interface flux of $1 MeV/cm^2\text{-sec}$. $[I^{su}_n(b_1+b_2) = I^{su}(b_1+b_2)/I^s(b_1,b_2)]$	None
$M_\ell(b)$	Defined by equation (3.12)	None
m_0	The rest mass of an electron	gm

Symbol	Description	Dimension
N	The atom density	atoms/cm^3
$P_\ell(w)$	Legendre polynomial of order ℓ	None
$R(b_1,b_2)$	The ratio of scattered to unscattered energy flux albedo ($R = \alpha_\phi^s/\alpha_\phi^u$)	None
$\vec{r}$	An independent variable for position	cm
r_e	The classical radius of an electron	cm
S	The standard deviation	None
S_N	The order of angular quadrature	None
w	Cosine of the angle of emergence (see Figure 3.1)	Radians
x	Distance in slab geometry	cm
x_1	Thickness of the first layer	cm
x_2	Thickness of the second layer	cm
z	Atomic number	None
z_1	Atomic number of the material in the first layer	None
z_2	Atomic number of the material in the second layer	None
$\alpha_\phi^u(b)$	The unscattered energy flux albedo	None
$\alpha_\phi^s(b_1,b_2)$	The scattered energy flux albedo	None
δ	The Dirac delta function	None
ΔE_i	Width of the ith energy group	MeV
λ	Photon wavelength in Compton units	.02426°A
μ	The linear attenuation coefficient ($\mu = N\sigma$)	cm^{-1}
μ_1	The linear attenuation coefficient for the material in the first layer	cm^{-1}
μ_2	The linear attenuation coefficient for the material in the second layer	cm^{-1}

Symbol	Description	Dimension
μ_a	The linear absorption coefficient	cm^{-1}
μ_{en}	The linear energy-absorption coefficient	cm^{-1}
μ_{en}/ρ	The mass energy-absorption coefficient	cm^2/gm
σ_a	The microscopic photoelectric and pair production absorption cross section	cm^2
σ_t	The microscopic total cross section (total = absorption + scattering)	cm^2
$\sigma_{s\ell}^{h\to g}$	The P_ℓ down scattering cross sections	cm^2
$\Sigma_s(\vec{r},E'\to E,\vec{\Omega}'\to\vec{\Omega})$	The differential cross section for scattering from the direction $\vec{\Omega}'$ to Ω and from the energy E' to E per unit solid angle and energy range	$\frac{cm^{-1}}{MeV\text{-}STER.}$
$\Sigma_s(\vec{r},E'\to E)$	The Legendre expansion coefficient of $\Sigma_s(\vec{r},E'\to E,\vec{\Omega}'\to\vec{\Omega})$	$\frac{cm^{-1}}{MeV}$
$\phi(b_1,E,\vec{\Omega})$	The angular photon flux, defined so that $\phi(b_1,E,\vec{\Omega})dE\ d\vec{\Omega}$ gives the number of photons at b_1, with energy E in the range dE, going in the direction $\vec{\Omega}$ within the element of solid angle $d\vec{\Omega}$, which cross in unit time a unit differential element of area whose normal is in the direction $\vec{\Omega}$.	$\frac{Photons}{cm^2\text{-}sec\text{-}MeV\text{-}STER.}$

ABSTRACT

Maniscalco, James Andrew. Ph.D., Purdue University, May 1973. AN ANALYTICAL TREATMENT OF PHOTON TRANSPORT IN TWO-LAYERED MEDIA. Major Prcfessor: H. E. Hungerford.

In this thesis the transport of photons in two-layered slabs is examined, and then evaluated by analytically expressing the two-medium buildup factor in terms of single medium buildup factors and parameters which in turn can be characterized as functions of atomic number. The word analytical is used to indicate that the parameters in this formulation are not empirical but rather they are directly related to the basic physics of transport phenomena in two-layered slabs.

In applying the two-medium buildup factor formulation, we assume that the single medium buildup factors and albedos are available and then seek to determine the two-medium parameters. These quantities have been evaluated by using a one-dimensional discrete ordinates transport code (ANISN) to calculate the attenuation of photons in two-layered slabs of water, iron, and lead. Independent verification of some of the ANISN results was made using the stochastic transport code PUGTII. The materials water, iron, and lead were chosen because they are commonly used together in pair combinations

and because they represent the light, intermediate, and heavy elements respectively.

In the process of tabulating and plotting the results, it was observed that the two-medium parameters are slowly varying functions of the first medium and smoothly varying functions of the second medium; moreover, a detailed examination of the plotted results (Appendix D) reveals that the curves for each of the two-medium parameters have the same shape (i.e., functional dependence) for different first-layer thicknesses and/or materials. Because of this functional behavior, these two-medium parameters have been accurately extrapolated to a large number of two-material combinations by simple linear interpolation on atomic number.

Energy and dose buildup factors for more than 15 different two-material combinations have been calculated with the two-medium buildup factor formulation and compared to corresponding ANISN results. These comparisons clearly indicate that the errors resulting from obtaining buildup factors with this formulation are less than 5%.

1. INTRODUCTION

1.1. Statement of the Problem

The advent of the nuclear age has resulted in the development of sophisticated nuclear devices and systems in two vital areas of our material well-being: (1) national security; and (2) energy. The weapons and nuclear power reactors conceived and developed in the many military and civilian programs over the past quarter of a century have been possible only because of our advancement in the understanding of nuclear radiation transport processes within material media. As part of this theoretical undertaking, a considerable amount of effort has been devoted to developing methods of calculating the deep penetrations of photons in material media. These radiation transport calculations usually involve the solution of the Boltzmann transport equation in one of its various forms.

The Boltzmann transport equation is a statistical-mechanical statement of the balance and flow of radiation in terms of position, energy, direction, and time. As such, it is an integro-differential equation which can not be solved exactly for any but a few highly restricted cases; however, numerous methods have been developed and used to provide approximate solutions. They include techniques utilizing:

1. Successive integrations over trial solutions,
2. Polynomial expansions such as spherical harmonics,
3. Fourier transforms,
4. Diffusion theory,
5. Variational techniques and perturbation theory,
6. Expansions in terms of moments,
7. Invariant imbedding,
8. Discrete ordinates S_N theory, and
9. Stochastic Solutions (Lattice Transport and Monte Carlo).

Some of these methods most applicable to photon transport (the topic of interest in this investigation) will be described in the next chapter.

It has become customary to present the results of photon transport theory calculations in the form of a buildup factor. The buildup factor is defined as the ratio of the desired quantity which is a characteristic of the total gamma-ray flux density to a similar quantity which is a characteristic of the unscattered flux density. For example, the energy buildup factor is defined as the ratio of the total energy flux (direct plus scattered) to the unscattered energy flux (direct). The principal advantage of expressing the results of photon attenuation calculations in the form of buildup factors is that these quantities are rather slowly varying functions of attenuation distance, photon source energy, and average atomic composition.

The penetration of gamma-rays in an infinite, homogeneous medium has been explored in detail using the moments method,[1,2,3,4] a technique particularly suited to photon transport in infinite media. Goldstein and Wilkins[1] have used this method to compile an extensive collection of buildup factor data which for 20 years has been and is still considered to be the primary source of buildup factor data for point isotropic and plane monodirectional sources in infinite media. Of more practical interest to shielders is the transmission of photons through finite slabs of material. Much work has been done on single (one-layer) slabs,[5,6,7,8] including calculations of reflection coefficients and transmission buildup factors for several different source distributions (isotropic, perpendicular, and oblique incidence).

A small amount of work has been done on two-layer slabs.[9,10,11,12] However the object of such studies has been to derive corrections to single medium buildup factors and/or empirical formulas[13,14,15,16] which work only in a given set of circumstances. No investigation that the author is aware of has focused on expressing the two-medium buildup factor in terms of general parameters which are directly related to the basic physics of transport phenomena in such layers.

The objective of this thesis is to investigate the transport of gamma-rays in two-layer slabs and to develop an analytical expression for two-medium buildup factors in terms of single-medium buildup factors and parameters which, in

turn, can be characterized as a function of atomic number. The reason for expressing the two-layer results in terms of one-layer results is that one-layer results are readily available in the open literature, and two-layer buildup factors so expressed will be of great practical benefit. The present theoretical investigation of photon transport in two-layered slabs was conducted by first thoroughly reviewing the literature for all existent one- and two-layer buildup and transmission information. As a result of this extensive search, it became evident that the problem of two-layer buildup factors could best be handled by utilizing both discrete ordinates and stochastic transport techniques to calculate, as accurately as possible, the attenuation of gamma-rays in two-layered material combinations of water, iron, and lead. These elements were chosen for the study because they are commonly used together in pair combinations, and they represent the light, intermediate, and heavy elements respectively. The results of these calculations were then used to determine a set of parameters required in the formulation of the two-material buildup factors.

As has already been pointed out, a number of computational techniques are available for determining the transport of gamma-rays in two-layered media. However, these techniques usually involve the extensive use of a large computing facility, and when a large number of calculations on complex shielding configurations are to be undertaken, this method is unduly slow, awkward, and costly. We looked, therefore,

for ways to simplify the approach for others, performing in advance (as it were) the long computer calculations for them. The unique feature of the analytical formulation derived in this work is that two-material buildup factors can be easily hand-calculated, using fairly simple formulas for most of the two-material combinations of interest to shield designers. In fact, the major limitation on the number of two-material combinations which can be investigated is the lack of one-medium data.

2. THE TRANSPORT OF GAMMA RAYS: REVIEW OF THE LITERATURE AND METHODS

The attenuation of gamma-rays in material media is relatively simple to predict when each interaction process (collision) results in the disappearance of a photon, i.e., the medium is purely absorptive. For example, consider the case of a monodirectional beam of gamma-rays of energy E in such an absorptive medium; then, the change in the flux intensity of the beam dI(x), as it traverses the medium, is given by

$$\frac{dI(x)}{dx} = -\mu\, I(x) \quad \frac{\text{MeV}}{\text{cm}^3\text{-sec}} \quad , \tag{2.1}$$

where the constant of proportionality μ is known as the linear attenuation coefficient. The solution of equation (2.1) is the well-known Lambert's law of absorption,

$$I(x) = I_o\, e^{-\mu x} \quad \frac{\text{MeV}}{\text{cm}^2\text{-sec}} \quad . \tag{2.2}$$

Unfortunately, Lambert's Law is not an accurate description of photon attenuation in material media. First, the law assumes that the medium is purely absorptive and does not account for scattering. Second, the law does not account for

the energy change which results from photons of lower energy contributing to the flux at x.

Lambert's law can be corrected to account for scattered radiation by using a multiplicative factor called the buildup factor. The term "buildup factor" was first introduced during the Manhattan Project. Its usefulness stems from the fact that radiation quantities resulting from unscattered photons, i.e., photons which emerge without suffering any collisions, are relatively simple to calculate. There are many different quantities of interest in shield design (particle flux, energy flux, dose rate, etc.) and we can define a buildup factor for each of them. To show how this can be done, let the superscripts u and s refer to unscattered and scattered photons respectively and let the quantity of interest be represented by the functional F(I); then, the buildup factor for the quantity F(I) is defined by[1]

$$F(I) = B_f \, F(I^u) \, . \qquad (2.3)$$

In words, equation (2.3) defines the buildup factor as the ratio of a desired quantity which is a characteristic of the total flux density (unscattered plus scattered) to a similar quantity which is a characteristic of the unscattered flux density. From this definition, it is obvious that the buildup factor concept is meaningless when the unscattered quantity does not exist.

Buildup factors of interest in shield design include:

1. The energy buildup factor B_E (with F(I) representing the integrated energy flux) defined as

$$B_E(x) = \frac{\int_E I(x,E)\, dE}{\int_E I^u(x,E)\, dE} \quad . \tag{2.4}$$

The total energy flux I(x,E) is the sum of the scattered and unscattered contributions. That is,

$$I(x,E) = I^u(x,E) + I^s(x,E) \tag{2.5}$$

Hence,

$$B_E(x) = 1 + \frac{\int_E I^s(x,E)\, dE}{\int_E I^u(x,E)\, dE} \quad . \tag{2.6}$$

2. The dose buildup factor B_D (with F(I) representing the dose-rate in air) defined as

$$B_D(x) = 1 + \frac{\int_E \mu_{en}^{air}(E)\, I^s(x,E)\, dE}{\int_E \mu_{en}^{air}(E)\, I^u(x,E)\, dE} \quad , \tag{2.7}$$

where $\mu_{en}^{air}(E)$ is the energy absorption coefficient of air.

3. The energy absorption buildup factor B_A (with F(I) representing the energy density absorbed by the medium from the photons in unit time) defined as

$$B_A(x) = 1 + \frac{\int_E \mu_{en}(E)\, I^s(x,E)\, dE}{\int_E \mu_{en}(E)\, I^u(x,E)\, dE} \quad , \tag{2.8}$$

where μ_{en} (E) is the energy absorption coefficient for the medium. It should be mentioned that in all of the definitions cited, the functional F depends only on the energy flux; therefore, for a monoenergetic source, $F(I^u)$ is given by a constant, F_u, times the integrated, unscattered energy flux $I^u(x)$. In these cases, the buildup factor is simply defined by

$$F(I) = B_F \, F_u \, I^u(x) \, . \tag{2.9}$$

2.1. Transport Theory

The fundamental equation governing the transport of gamma rays in material media is an integro-differential equation known as the Boltzmann transport equation. It is basically a bookkeeping statement which accounts for photon increases and decreases in a given increment of space, angle, energy, and time. For shield analyses, a steady state is normally assumed and the time variable is not required. Briefly, the equation of continuity is applied to a six-dimensional phase space consisting of three spatial coordinates $\vec{r}$, two directional coordinates $\vec{\Omega}$ and one energy coordinate E; and the resulting integro-differential form of the Boltzmann transport equation is given as

$$\vec{\nabla} \cdot \vec{\Omega} \, \phi \, (\vec{r},E,\vec{\Omega}) + \mu\phi(\vec{r},E,\vec{\Omega}) = S(\vec{r},E,\vec{\Omega}) + \int_{E'} \int_{\vec{\Omega}} \Sigma_s \, (\vec{r},E' \to E, \, \vec{\Omega}' \to \vec{\Omega}) \, \phi(\vec{r},E', \, \vec{\Omega}') \, dE' \, d\vec{\Omega}' \, . \tag{2.10}$$

In the above equation, the quantity μ is the linear attenuation coefficient and the angular flux $\phi(\vec{r},E,\vec{\Omega})$ is defined so that

$$\phi(\vec{r},E,\vec{\Omega})\ dE\ d\vec{\Omega} \tag{2.11}$$

gives the number of photons at $\vec{r}$, with energy E in the range dE, going in the direction $\vec{\Omega}$ within the element of solid angle $d\vec{\Omega}$, which cross in unit time a unit differential element of area whose normal is in the direction $\vec{\Omega}$. The various terms in equation (2.10) are defined as follows:

$\vec{\nabla} \cdot \vec{\Omega}\ \phi$ is the loss rate due to leakage from the phase space cell $(d\vec{r},\ dE,\ d\vec{\Omega})$,

$\mu\ \phi$ is the loss rate due to collisions in the phase space cell which either absorb the photons or change their energy and direction,

S is the independent generating source of photons, and

$$\int_{E'}\int_{\vec{\Omega}} \Sigma_s(\vec{r},\ E'\to E,\ \vec{\Omega}'\to\vec{\Omega})\ \ \phi(\vec{r},\ E'\vec{\Omega})\ dE'\ d\Omega' \tag{2.12}$$

represents the rate at which photons are scattered into the phase space cell. The transport kernel, $\Sigma_s(\vec{r},E'\to E,\vec{\Omega}'\to\vec{\Omega})$, represents the differential macroscopic cross section for scattering from the direction $\vec{\Omega}'$ to $\vec{\Omega}$ and from the energy E' to E per unit solid angle and energy range. For Compton scattered photons, the transport kernel is given by the well-known Klein-Nishina formula. This formula takes a

particularly simple form if the energy dependence is expressed in terms of photon wavelength in Compton units,*

$$\lambda(\text{Compton units}) = \frac{m_o C^2}{E(\text{MeV})} = \frac{.511}{E(\text{MeV})} . \qquad (2.13)$$

In these units, the transport kernel is

$$\Sigma_s(\vec{r},\lambda'\to\lambda,\vec{\Omega}'\to\vec{\Omega}) = \frac{n}{2} r_e^2 \left(\frac{\lambda'}{\lambda}\right)^2 \left[\frac{\lambda}{\lambda'} + \frac{\lambda'}{\lambda} + 2(\lambda' - \lambda) + (\lambda' - \lambda)^2\right] \delta(1 + \lambda' - \lambda - \vec{\Omega} \cdot \vec{\Omega}') , \qquad (2.14)$$

where n is the electron density and r_e is the classical radius of an electron (2.817×10^{-13} cm). The Dirac delta function δ accounts for the fact that wavelength (energy) and angle changes are related by the Compton shift equation

$$\lambda' - \lambda = 1 - \vec{\Omega}' \cdot \vec{\Omega} . \qquad (2.15)$$

In shielding problems where absorbed energy density and biological dose are the quantities of interest, it is convenient to work with the angular energy flux which is defined as

$$I(\vec{r},E,\vec{\Omega}) = E \cdot \phi(\vec{r},E,\vec{\Omega}). \qquad (2.16)$$

---

* One unit of Compton wavelength = $h/m_o C$ = .02425°A, where h is Planck's constant, m_o is the rest mass of an electron, and C is the velocity of light.

This preference arises from the fact that absorbed energy density and biological dose are more nearly proportional to energy flux than particle flux. The transport equation is written in terms of $I(\vec{r},\lambda,\vec{\Omega})$ by multiplying equation (2.10) by E and noting that

$$dE = \frac{.511}{\lambda^2}\, d\lambda \quad , \tag{2.17}$$

$$E \cdot S(\vec{r},E,\vec{\Omega}) = S(\vec{r},\lambda,\vec{\Omega}) \quad , \tag{2.18}$$

$$I(\vec{r},E,\vec{\Omega}) = I(\vec{r},\lambda,\vec{\Omega}) \quad , \tag{2.19}$$

and

$$\Sigma_s(\vec{r},E'\to E,\vec{\Omega}'\to\vec{\Omega}) = \frac{\lambda^2}{.511}\,\Sigma_s'(\vec{r},\lambda'\to\lambda,\vec{\Omega}'\to\vec{\Omega}) \; ; \tag{2.20}$$

then,

$$\vec{\nabla}\cdot\vec{\Omega}\, I(\vec{r},\lambda,\vec{\Omega}) + \mu\, I(\vec{r},\lambda,\vec{\Omega}) = S(\vec{r},\lambda,\vec{\Omega}) + \int_{\lambda}\int_{\vec{\Omega}} \frac{\lambda}{\lambda'}\,\Sigma_s(\vec{r},\lambda'\to\lambda,\vec{\Omega}'\to\vec{\Omega})\, I(\vec{r},\lambda',\vec{\Omega}')\, d\lambda'\, d\vec{\Omega}' . \tag{2.21}$$

A direct, analytical solution of the Boltzmann transport equation is feasible only for a very small number of simple and highly idealistic problems. There are, however, many methods available which provide approximate solutions to the transport equation, several of which are described below. In general, methods utilizing numerical techniques with high speed computers provide more accurate solutions than methods which employ simplifying assumptions to alter the transport equation such that an analytical solution is

obtainable. An example of the latter type is the elementary one-speed diffusion equation of reactor physics which can be derived from the transport equation by invoking the following assumptions:

1. Scattering is isotropic in the laboratory co-ordinate system.
2. There are no strong absorbers in the medium i.e., $\Sigma_a \ll \Sigma_s$.
3. The region of interest is two or more mean free paths from any intense sources or boundaries.

The existence of these limiting assumptions (especially the first assumption) is a clear indication that diffusion theory is inadequate for problems involving photon transport because the scattering of photons is not isotropic at any energy.

2.1.1. The Method of Successive Scattering

A relatively simple and straightforward approach for calculating the contribution of scattered photons to the penetration of gamma-rays is found in the method of successive scatterings.[17] This method is a semianalytical technique which considers the total photon flux to be the sum of the unscattered flux, the once scattered flux, the twice scattered flux, etc. In notational form

$$\phi(x) = \sum_{i=0}^{\infty} \phi_i(x) \quad , \tag{2.22}$$

where $\phi_i(x)$ is the flux at x which results from the ith scattering. As previously mentioned calculations for the unscattered flux are relatively simple to perform; however, this is not so for the scattered flux. In the successive scattering method, the unscattered flux provides the collision density for first scattering which is used as a source in calculating the once scattered flux. The process is then repeated with an integral recursion formula which gives a relationship between $\phi_{i+1}(x)$ and $\phi_i(x)$. In other words, the higher-order scattered fluxes are expressed as integral operators of the next lower-order scattered flux. After the first scattering, the mathematics becomes quite involved and there is a tendency to limit this type of calculation to only one or two orders of scattering.[17] However, this simplistic approach yields unreliable results for deep penetration problems where many scatterings contribute to the flux and the once and twice scattered contributions are only a small part of the total flux.

The method of successive scattering was first used by Peebles and Plesset[18,19] to calculate the transmission of monodirectional gamma-rays through finite slabs of iron and lead. The error in these calculations is estimated to be as high as 20% for slab thicknesses up to 20 mean free paths. A variation of the method of successive scattering has been developed by Peebles[20] and elaborated upon by Yarmush.[21] It consists of considering the photon

transmission through a thick slab to be composed of a succession of transmissions through thin slabs which are taken thin enough to make the contributions of photons scattered three or more times negligible. Gamma-ray transmission in the thick slab is then obtained by successive matrix multiplication of the thin slab results.

2.1.2. The Spherical Harmonics Method*

The method of spherical harmonics, as applied to the transport equation, consists of expressing the various angular dependent terms in a complete set of elementary functions such as a series of polynomials. In three-dimensional geometry, spherical harmonics are the logical choice; however, these reduce to Legendre polynomials for one-dimensional geometry with azimuthal symmetry. When the polynomial expansions are substituted into the transport equation, it separates into an infinite set of coupled differential equations which no longer involve the directional variables. Practical methods of solution require that the infinite set be limited to a finite number of coupled equations, and this is achieved by truncating the polynomial expansions to some finite number of terms. For

*Although not widely used today, this method embodies concepts which are used in other techniques described in this Chapter. It has therefore been included for pedagogical reasons rather than its potential for problem solving.

example, a P_n (or nth order) approximation represents a solution in which the polynomial expansions are limited to n+1 terms.

In general, the degree of anistropic scattering dictates the order of expansion required to yield accurate results. The P_1 approximation is equivalent to diffusion theory which, as previously indicated, provides adequate results only when the scattered flux is nearly isotropic. It has been shown that a P_3 approximation provides a vast improvement over diffusion theory[22] and that the most severe anisotropy resulting from Compton scattered photons with energies less than 10 MeV can be adequately resolved with a P_5 approximation.[23] Lanning[24] has used the spherical harmonics method to investigate gamma-ray heating in multi-slab geometry. He successfully calculated the spatial distribution of the energy flux spectra out to ten mean free paths with a P_3 approximation.

2.1.3. The Moments Method

The moments-method of Spencer and Fano[25] is a semi-analytical technique which solves the Boltzmann transport equation in infinite geometry. With this method, as in the spherical harmonics method, the angular flux is expanded in terms of Legendre polynomials. In addition, spatial moments of the Legendre coefficients, $I_\ell(x,E)$, which serve to separate energy and spatial dependence, are introduced by the definitions

$$b_{m\ell}(E) = \frac{\mu_o^{m+1}}{m!} \int_{-\infty}^{+\infty} I_\ell(x,E)\, x^m\, dx \ , \qquad (2.23)$$

where μ_o is the linear attenuation coefficient at the source energy E_o. In terms of these moments, the transport equation reduces to a set of interlinked integral equations of the Volterra type[26] with energy as the only independent variable. The spatial moments are straightforwardly evaluated by numerically integrating these integral equations. It should be emphasized that the calculations to this point are rigorous because no assumptions have been made. The major source of error in this method results from reconstructing the spatial dependence of the flux with only a finite number of known moments. Usually six to eight properly chosen moments are sufficient to reconstruct the spatial flux with reasonable accuracy.*

The method of moments is generally considered to be the technique of choice for problems involving photon transport in infinite media. Goldstein and Wilkins[1] have used the moments method to investigate in detail the penetration of monoenergetic gamma-rays in infinite homogeneous media, and they have used their results to develop an extensive compilation of energy flux spectra and buildup factors for

---

*The interested reader is referred to Reference [1] for a detailed description of two methods used to reconstruct the spatial flux The polynimial expansion method and the method of undetermined parameters.

infinite plane and point isotropic sources. Advantages of the moments method, as stated by Golstein,[27] include:

1. A detailed energy spectrum of the flux can be obtained.
2. The required computing time for penetrations up to 20 mean free paths is relatively short.
3. Most photon source configurations of interest are amenable to the method. (Spencer and Lamkin[28,29] have successfully employed the method to calculate the slant penetrations of photons in water and concrete.)
4. Angular distributions of the flux may be obtained. (Certaine[30] used the moments method to calculate angular distributions from plane monoenergetic sources.)

The most serious limitation of the moments method is that it is applicable only to infinite homogeneous media. Another disadvantage, less restrictive but still noteworthy, involves the difficulty in reconstructing and determining the flux behavior near the source* (less than one mean free path). Because of this, the method of moments is not a good technique for evaluating reflection coefficients (albedos).

---

*Berger[31] has developed a method to alleviate the difficulty for point isotropic sources.

2.1.4. The Method of Invariant Imbedding

The invariant imbedding technique was originally developed and used to calculate the reflection of diffuse light from a stellar atmosphere by the astrophysist Ambrazumian.[32,33] Bellman, Kalaba, and Wing[34] have extended the method into a general approach, and shown that it can be applied to a much broader class of problems which includes neutron and gamma-ray transport. As applied to radiation, the invariant embedding formulation is not another method for solving the transport equation but rather a new fundamental approach to the transport of radiation in material media.

Unlike the Boltzmann equation, the dependent variables of the invariant embedding formulation are reflection and transmission functions. Each of these parameters is defined by and thus satisfies a non-linear integro-differential equation which cannot be solved analytically. Hence, all of the solutions are numerical in nature. The reflection and transmission equations represent problems of the "initial-value" type. In contrast, the Boltzmann equation, as applied to photon transport in slab geometries, forms "boundary-value" type problems. In general, initial-value problems are more amenable to numerical solution with a computer. As a consequence, the invariant embedding formulation has a computational advantage over the Boltzmann approach.

Mizuta and Shimizu[35,36] have applied the method of invariant imbedding to the problem of photon transport in slabs and demonstrated that it is competitive in accuracy to other established methods such as Monte Carlo and the method of moments. Compared to stochastic methods, invariant imbedding has the advantage that it requires less computing time. Compared to the moments method, it has the advantage of being applicable to slab geometries. The disadvantages of the method are that it is difficult to apply to other than slab geometry and that it is inefficient for thin shields. (Thin shields require almost as much computing time as thick shields.)

2.1.5. The Discrete Ordinates S_N Method

G. C. Wick[37] in 1943 was the first to suggest the use of discrete ordinates (or discrete directions) in transport theory. In the years that followed, S. Chandrasekhar[38] further developed the method and applied it to the study of radiation transport in stellar atmospheres. Early applications of the discrete ordinates method were primarily limited to the transport of isotropically scattered radiation in slab geometries. Carlson,[39] with some success, applied discrete ordinates to curvilinear geometries by using an "S_N approximation." In the S_N version, the angular dependence of the flux is approximated by a series of connected straight line segments; hence, the letter S signifies segments and the subscript N indicates the number of segments

used to construct the angular dependence. It was subsequently recognized by Carlson and Lathrop[40] that the S_N approximation was only a special case of a more general formulation and this led to the development of the discrete ordinates S_N method.

The discrete ordinates S_N method, as presently employed, is a means of numerically solving the Boltzmann transport equation with finite difference equations. The finite difference equations are formulated as flow balances for differential phase space cells ($dV\ dE\ d\vec{\Omega}$). The more recent versions of the method accurately treat anisotropic scattering by using a Legendre series expansion to describe the scattering cross section, $\Sigma_s(\vec{r},E'\rightarrow E,\vec{\Omega}'\rightarrow\vec{\Omega})$. The fundamental assumption in the discrete ordinates method is that the inscattering integral can be approximated by a quadrature scheme which evaluates the integral as the sum of a discrete distribution. In one-dimensional geometries a Gauss-Legendre quadrature formula[41] may be used to provide the discrete distribution, with discrete direction cosines corresponding to the Gaussian zeroes.

The discrete ordinates S_N method has been shown to be a versatile and powerful method for accurately solving the transport equation in both one-dimensional geometries (DTF IV,[42] ANISN[43]) and two-dimensional geometries (DOT[44]). It has been successfully applied to neutron and gamma-ray deep penetration calculations[45,46,47] as well

as to general core criticality problems.[48] The results of these calculations and many others clearly indicate that the discrete ordinates method, as applied to shielding problems, has the following advantages:*

1. Depending somewhat on the sophistication desired, the S_N calculations are easy to prepare.
2. The method is not stochastic and flux errors at deep penetration are systematic rather than statistical.
3. Secondary gammas may be calculated by the same method, either as a second calculation or simultaneously with the neutrons. The gamma yield distribution may be dependent on the neutron energy at capture.
4. The neutron energy range from highest fission energies to thermal, including upscatter, may be calculated by the same method.
5. The one-dimensional calculations are much faster (in computer time) than similar Monte Carlo calculations. In two dimensions the type of problem and the desired answers determine whether S_N or Monte Carlo is better.

---

*These advantages were compiled from a listing given by F. R. Mynatt[49].

The major disadvantage of the method is that it is not applicable to three-dimensional geometries.

The discrete ordinates method is one of the methods used in this work to calculate the penetration of photons in two-layered slabs; therefore, a derivation is given in Appendix A which establishes the equivalence of the one-dimensional discrete ordinates equations with the transport equation and which also shows how the Gaussian quadrature is employed to evaluate the inscattering integral.

2.1.6. Stochastic Methods

Many physical processes including the emission and transport of radiation are probabilistic in nature. As a result, many types of problems in mathematics and physics can be solved by random sampling or stochastic techniques. The Monte Carlo method, as applied to radiation transport, represents a system of probabilistic solutions in which probabilities relating to microscopic emission and interaction processes are used to predict macroscopic phenomena such as flux and dose-rate. Simply stated, the Monte Carlo approach consists of constructing a series of analogue experiments (histories) which mathematically simulates the emission and transport of particles, and then analyzing the outcomes of a large number of histories to obtain relevant quantities. Each history (or experiment) includes the generation of a particle, its random walk through the medium, and its death which results when the particle is absorbed, exceeds some

physical energy or time boundary, or when its importance becomes insignificant.

The method of random sampling was first applied to the solution of radiation transport problems by Ulam and Von Neumann[50,51] in the mid-1940's. In the early stages of development, the Monte Carlo method was based on direct simulation of the transport problem and was therefore found to be prohibitively costly and time consuming in calculating deep penetrations with reasonable accuracy. In the years that followed, several techniques were developed to reduce the variance associated with the statistical behavior of a particle history. Some of these variance reducing (or biasing) techniques, as described by Kahn,[52,53] include:

1. Importance Sampling: The selection of events (source parameters, path lengths, etc.) or omission of events (absorption) is based on an altered probability distribution which allows the more important events to be sampled more frequently. The exponential transform is one of the more widely used means of importance sampling because it is easier to alter selection of path length. Particle weighting is another widely used importance sampling technique in which absorption is not allowed but accounted for by reducing the weight of a scattered particle.

2. Use of Expected Value: A portion of the random walk process is replaced by its average value.
3. Russian Roulette and Splitting: Unimportant histories (i.e., those which are unlikely to contribute to the answer) are terminated with some probability while important histories are multiplied to give several semi-independent estimates.

In general, Monte Carlo is not the technique of choice for one-dimensional steady-state transport problems because other methods such as discrete ordinates are usually much faster (in computer time) and just as accurate. In two-dimensions the type of problem (deep penetration, irregular geometry, ducts) determines whether Monte Carlo or discrete ordinates is better; but, there is no competitor to Monte Carlo for obtaining rigorous solutions to three-dimensional or time-dependent transport problems.

The Lattice Model Concept of Stochastic Transport was developed and successfully applied to neutron transport by H. E. Hungerford.[54] It differs from conventional Monte Carlo methods in that the random walks of particles are constructed by sampling their motion at predetermined points using a direct simulation of the transport process. In the "Lattice Model Concept" space can be envisioned as being made up of a large number of small cubes whose sides are equal to a distance called the unit lattice distance. The method of sampling particle motion within this framework is

best described by H. E. Hungerford[54] in the following excerpt:

> If we now restrict the locations of the sampling points to be only at the corners of the cubes, and nowhere else, we have already chosen our allowed directions of emission, namely, these directions represented by lines which can be drawn from any corner of the unit cube to any other, neglecting the repeats. There are altogether 26 allowed directions of motion, outward from any given source point (considered at the origin)--6 along the 6 axial directions, 12 in-plane diagonal directions (the planes being defined by any 2 of 3 axes), and 8 skew diagonal directions (to opposite corners of the cube). Actually, to show all these directions emanating from one point, one has to make a larger cube from 8 unit cubes and place the source at the central point common to all cubes. These 8 cubes correspond to the 8 octants of a sphere. The larger cube [may be] referred to as the representative cube.

A. Razani[55] applied the lattice concept to gamma-ray transport by developing a stochastic gamma-ray transport code called PUGT I. Another version of the code, PUGT II, which uses particle weighting will be used in this work to calculate the penetration of photons in two-layered slabs, and thereby provide independent verification of the discrete ordinates results; therefore, a derivation which relates the transport of photons in the lattice model to the integral form of the transport equation is given in Appendix B.

3. THEORY OF PHOTON TRANSMISSION AND BUILDUP IN A TWO-LAYER SLAB

3.1. Analytical Formulation of the Two-Medium Buildup Factor

Given two slabs of different materials and a plane, monoenergetic gamma-radiation source incident on one of them, the problem under consideration is to develop a relatively simple expression which will predict the buildup and therefore the transmission of radiation through the slabs, without having to resort to expensive and time-consuming computer calculations. The choice of the radiation quantity selected as the prime variable* is the angular energy flux density, $I(b_1,E,\vec{\Omega})$ in MeV per cm^2 per second per steradian and per unit energy, where

$$I(b_1,E,\vec{\Omega}) = E \cdot \phi(b_1,E,\vec{\Omega})$$

and $\phi(b_1,E,\vec{\Omega})$ is the angular photon flux density. (The number of photons of energy E at b_1 passing through a unit of area in the direction $\vec{\Omega}$, per unit time, per steradian, and per unit energy.) The analytical formulation to be

---

*Quantities used in this development are defined in the Nomenclature preceding the text.

developed is based on the buildup factor concepts, as given in Chapter 2, and the geometrical configuration shown in Figure 3.1. More rigorously stated and referring to Figure 3.1, the objective of the formulation to be developed is to determine the buildup factor which when used with Lambert's Law correctly predicts the energy flux density at the detector (point C) resulting from a plane, monoenergetic, monodirectional photon source at point A. The two-medium buildup factor, as derived, will be a function of quantities which characterize the angular energy flux at the interface between the two slabs. As nearly as possible the formulation for two-layer buildups will follow that for one layer. The single-medium buildup factors previously defined contained two terms, one describing the scattered energy flux and, the other describing the unscattered energy flux. The same scheme will be followed here. In addition, a distinction will be made between photons which scatter in the first layer and those that scatter in the second layer. In order that the reader fully understand the terminology and import of this development, a series of terms used herein is defined. The superscript s is used to refer to the scattered radiation and the superscript u refers to the unscattered radiation. These superscripts may be used alone or in combination. Thus:

1. I^s is the scattered energy flux,

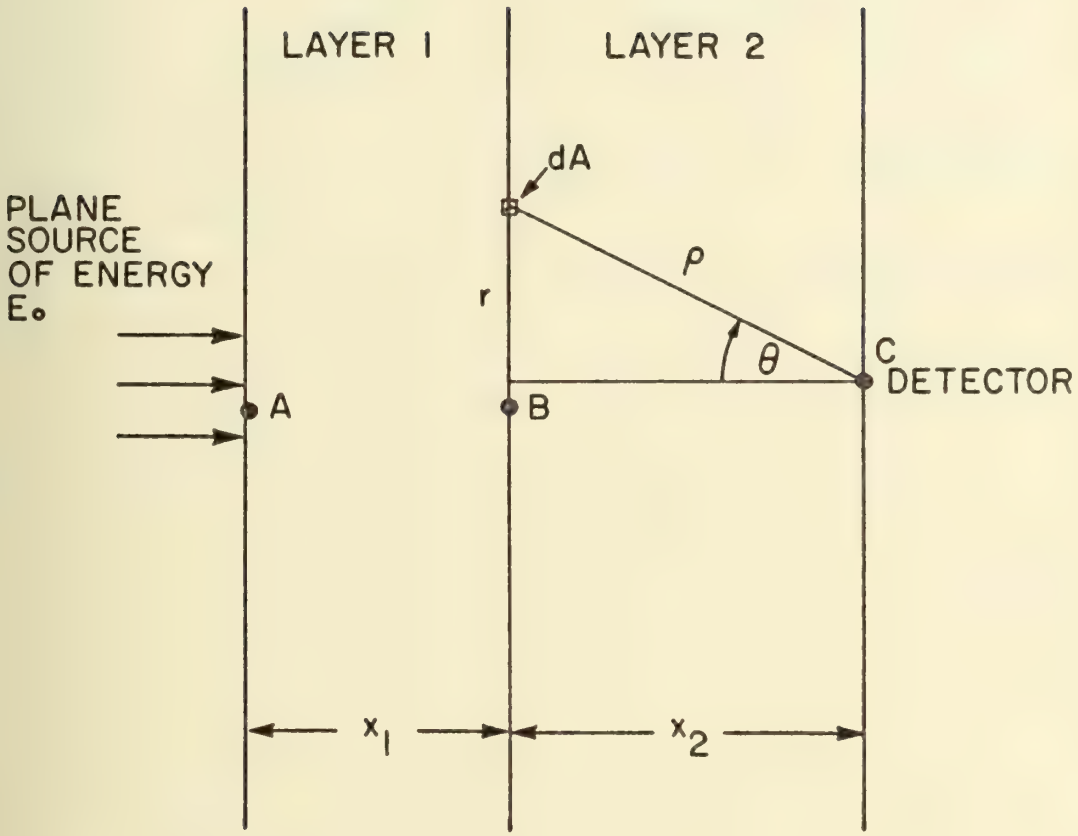

Figure 3.1. Geometrical Configuration for a Two-Layer Slab.

2. I^u is the unscattered energy flux,
3. I^{su} refers to the energy flux which has scattered in the first layer but not in the second layer,
4. I^{us} refers to the energy flux which doesn't scatter in the first layer, but scatters in the second layer, and
5. I^{ss} refers to the energy flux which scatters in both layers.

These and other terms will be more fully described as the detailed development unfolds.

The scattered energy flux at the detector (point C) may now be written as the sum of three components

$$I^s(b_1+b_2) = I^{su}(b_1+b_2) + I^{us}(b_1+b_2) + I^{ss}(b_1+b_2) \ \frac{\text{MeV}}{\text{cm}^2 \ \text{sec}}, \tag{3.1}$$

where $I^{su}(b_1+b_2)$ is the scattered energy flux at the detector arising from the scattered energy flux at the interface which doesn't scatter again in traversing the second layer, $I^{us}(b_1+b_2)$ is the scattered energy flux at the detector arising from the unscattered flux at the interface which scatters at least once in traversing the second layer, and $I^{ss}(b_1+b_2)$ is the scattered energy flux at the detector arising from the scattered energy flux at the interface which scatters at least one more time in traversing the second layer. Here, as in the rest of this work, the

quantity b_1 denotes the number of mean free paths in the first slab at the source energy E_o and b_2 is analogously defined for the second slab. That is, $b_1 = \mu_1(E_o)x_1$, and $b_2 = \mu_2(E_o)x_2$ where μ_1 and μ_2 are the linear attenuation coefficients of the first and second media.

The relationship between the energy flux $I^{su}(b_1+b_2)$ and the scattered angular energy flux at the interface, $I^s(b_1,E,\vec{\Omega})$, is given by

$$I^{su}(b_1+b_2) = \int_0^{E_o} dE \int_{4\pi} I^s(b_1,E,\vec{\Omega})\, e^{-\mu_2(E)\rho}\, d\vec{\Omega} \quad \frac{MeV}{cm^2\text{-sec}} . \tag{3.2}$$

In slab geometry the angular energy flux can be expressed as

$$I^s(b_1,E,\vec{\Omega}) = \frac{I^s(b_1,E,w)}{2\pi} \quad \frac{MeV}{cm^2\text{-sec-MeV-STER.}} ; \tag{3.3}$$

and the differential solid angle is given by

$$d\vec{\Omega} = w\,\frac{2\pi\, r\, dr}{\rho^2} \quad \text{steradians}, \tag{3.4}$$

where $w = \cos\theta$, and ρ and r are shown in Figure 3.1. Substituting these relationships into equation (3.2) yields

$$I^{su}(b_1+b_2) = \int_0^{E_o} dE \int_0^{\infty} I^s(b_1,E,w)\, e^{-\mu_2(E)\rho}\, \frac{w\, r\, dr}{\rho^2} \quad \frac{MeV}{cm^2\text{-sec}} . \tag{3.5}$$

The integration variable may be changed to w by using the relations $\rho = x_2/w$, $r = x_2 \tan\theta$, and $rdr = - x_2^2\, dw/w^3$. Referring again to Figure 3.1, one sees that $w \to 0$ as $r \to \infty$, and $w \to 1$ as $r \to 0$. Substitution of these variables and limits into equation (3.5) yields

$$I^{su}(b_1+b_2) = \int_0^{E_o} dE \int_0^1 I^s(b_1,E,w)\, e^{-b_2(E)/w}\, dw \quad \frac{MeV}{cm^2\text{-}sec}, \tag{3.6}$$

where $b_2(E) = \mu_2(E)x_2$.

In proceeding further it will be necessary to expand the scattered, angular energy flux, $I^s(b_1,E,w)$, in a series of Legendre polynomials. For a plane source, the Legendre series expansion takes the form

$$I^s(b_1,E,w) = \sum_{\ell=0}^{\infty} \frac{2\ell+1}{2}\, I_\ell^s(b_1,b_2,E)\, P_\ell(w) \cdot \tag{3.7}$$

It can be shown that beyond a certain number of terms $\ell = m$, there is a negligible contribution to the scattered angular energy flux; therefore, the series is truncated at m where m indicates the order of the expansion.* The terms $P_\ell(w)$ are the Legendre polynomials of order ℓ, and the expansion coefficients are given by

$$I_\ell^s(b_1,b_2,E) = \int_{-1}^{1} I^s(b_1,E,w)\, P_\ell(w)\, dw \quad \frac{MeV}{cm^2\text{-}sec\text{-}MeV} \cdot \tag{3.8}$$

*It is anticipated that a fifth order expansion will be sufficient to describe $I^s(b_1,E,w)$ to very good accuracy.

The physical significance of the expansion coefficients can be ascertained by noting that for $\ell = 0$ and $\ell = 1$, these quantities represent the scattered energy flux spectrum and the scattered energy current spectrum at the interface between the two layers. The higher ℓ terms define moments of these. In addition, the scattered energy flux at the interface is related to the zeroeth order Legendre expansion coefficient by

$$I^s(b_1,b_2) = \int_0^{E_o} I_o^s(b_1,b_2,E)\, dE \quad \frac{MeV}{cm^2\text{-sec}} \quad . \qquad (3.9)$$

Substituting the Legendre expansion for $I^s(b_1,E,w)$ into equation (3.6) gives

$$I^{su}(b_1+b_2) = \sum_{\ell=o}^{m} \frac{2\ell+1}{2} \int_0^{E_o} dE \int_0^1 I_\ell^s(b_1,b_2,E)\, P_\ell(w)\, e^{-b_2(E)/w}\, dw \quad \frac{MeV}{cm^2\text{-sec}} \quad . \qquad (3.10)$$

For convenience in later analyzing and tabulating, it is desirable to consider a two-medium parameter which is a slowly varying function of the thickness of the first slab. This quantity results when both sides of equation (3.10) are divided by the scattered energy flux at the interface as defined in equation (3.9). Thus,

$$I_n^{su}(b_1+b_2) = \sum_{\ell=o}^{m} \frac{2\ \ell+1}{2} \int_0^{E_o} dE \int_0^1 \frac{I_\ell^s(b_1,b_2,E)}{I^s(b_1,b_2)}\, P_\ell(w)\, e^{-b_2(E)/w}\, dw \,, \qquad (3.11)$$

where $I_n^{su}(b_1+b_2)$ is nothing more than $I^{su}(b_1+b_2)$ normalized to a scattered energy flux at the interface of 1MeV/cm^2-sec. For convenience in carrying out the integration with respect to w, let $b = b_2(E)$. Note that $b \neq b_2(E_o)$. Also, let us define a set of quantities

$$M_\ell(b) = \int_o^1 P_\ell(w)\, e^{-b/w}\, dw \qquad \text{for } \ell = 1,2,\ldots,m. \quad (3.12)$$

Substitution of $M_\ell(b)$ into equation (3.11) yields

$$I_n^{su}(b_1+b_2) = \sum_{\ell=o}^{m} \frac{2\ell+1}{2} \int_o^{E_o} \frac{I_\ell^s(b_1,b_2,E)}{I^s(b_1,b_2)}\, M_\ell(b)\, dE. \quad (3.13)$$

The evaluation of $M_\ell(b)$ is accomplished by comparing it to the exponential integrals which are defined as

$$E_n(b) = b^{n-1} \int_o^\infty \frac{e^{-v}\, dv}{v^n} \quad . \quad (3.14)$$

The relationship between $M_\ell(b)$ and the exponential integrals is made clearer by substituting $v = b/w$ into equation (3.12) so that

$$M_\ell(b) = \int_b^\infty P_\ell\left(\frac{b}{v}\right) \frac{e^{-v}\, b\, dv}{v^2} \quad . \quad (3.15)$$

Specifically for $\ell = o$, $P_o(b/v) = 1$, and

$$M_o(b) = E_2(b) \quad , \quad (3.16)$$

for $\ell = 1$, $P_1(b/v) = b/v$, and

$$M_1(b) = E_3(b), \tag{3.17}$$

for $\ell = 2$, $P_2(b/v) = \frac{1}{2}[3(b/v)^2 - 1]$, and

$$M_2(b) = \frac{1}{2}[3\ E_4(b) - E_2(b)], \tag{3.18}$$

etc.

Since $P_\ell(w)$ is a polynomial in w, $M_\ell(b)$ can be expressed in shorthand form as

$$M_\ell(b) = P_\ell[E_{j+2}(b)] \quad . \tag{3.19}$$

Here the somewhat strange notation signifies that whenever w^j occurs in $P_\ell(w)$, it is to be replaced by $E_{j+2}(b)$. For example, when $\ell = 3$,

$$P_3(w) = \frac{1}{2}[5\ w^3 - 3\ w] \ , \tag{3.20}$$

and

$$M_3(b) = \frac{1}{2}[5\ E_5(b) - 3\ E_3(b)] \ . \tag{3.21}$$

With $M_\ell(b)$ now expressed as an exponential integral function of energy, the final step in evaluating $I_n^{su}(b_1+b_2)$, as indicated in equation (3.13), involves integration with respect to energy. In performing this integration it is necessary to specify the expansion coefficients, $I_\ell^s(b_1,b_2,E)$; therefore, the energy flux $I_n^{su}(b_1+b_2)$ will be calculated in the next chapter after the expansion coefficients are determined.

The scattered energy flux at the detector which was previously expressed as

$$I^{s}(b_1+b_2) = I^{su}(b_1+b_2) + I^{us}(b_1+b_2) + I^{ss}(b_1+b_2) \quad \frac{\text{MeV}}{\text{cm}^2\text{-sec}} \tag{3.22}$$

can be displayed in a more convenient form by defining a scattered energy buildup factor, $B_E^s(b_1,b_2)$, as the variable which gives the buildup of the scattered energy flux at the interface as it traverses the second medium. That is,

$$B_E^s(b_1,b_2) = \frac{I^{su}(b_1+b_2) + I^{ss}(b_1+b_2)}{I^{su}(b_1+b_2)} ,$$

$$= 1 + \frac{I^{ss}(b_1+b_2)}{I^{su}(b_1+b_2)} . \tag{3.23}$$

With the scattered energy buildup factor defined in this manner, it follows that

$$I^{s}(b_1+b_2) = B_E^s(b_1,b_2)\, I^{s}(b_1,b_2)\, I_n^{su}(b_1+b_2) + I^{us}(b_1+b_2) \quad \frac{\text{MeV}}{\text{cm}^2\text{-sec}} . \tag{3.24}$$

Further simplification is achieved by expressing I^{us} in terms of the previously defined single-medium energy buildup factor, that is

$$I^{us}(b_1+b_2) = E_o\, e^{-(b_1+b_2)} [B_E(b_2) - 1] \quad \frac{\text{MeV}}{\text{cm}^2\text{-sec}} , \tag{3.25}$$

where

$$B_E(b_2) = 1 + \frac{I^{us}(b_1+b_2)}{I^{u}(b_1+b_2)} , \qquad (3.26)$$

and

$$I^{u}(b_1+b_2) = E_o\, e^{-(b_1+b_2)} \quad \frac{MeV}{cm^2\text{-sec}} \quad . \qquad (3.27)$$

Substituting this expression for I^{us} into equation (3.24) yields

$$I^{s}(b_1+b_2) = B_E^{s}(b_1,b_2)\; I^{s}(b_1,b_2)\; I_n^{su}(b_1+b_2)$$

$$+ E_o\, e^{-(b_1+b_2)} \left[B_E(b_1) - 1\right] \quad \frac{MeV}{cm^2\text{-sec}} \quad . \qquad (3.28)$$

In keeping with the definitions for single-medium buildup factors, the two-medium energy buildup factor, $B_E(b_1+b_2)$, is defined as the ratio of total energy flux to unscattered energy flux. Specifically, in formula notation

$$B_E(b_1+b_2) = \frac{I^{u}(b_1+b_2) + I^{s}(b_1+b_2)}{I^{u}(b_1+b_2)}$$

$$= 1 + \frac{I^{s}(b_1+b_2)}{E_o\, e^{-(b_1+b_2)}} \quad . \qquad (3.29)$$

Substituting the expression for $I^{s}(b_1+b_2)$, as given in equation (3.28), into equation (3.29) yields

$$B_E(b_1+b_2) = B_E(b_2) + \frac{B_E^s(b_1,b_2)\ I^s(b_1,b_2)\ I_n^{su}(b_1+b_2)}{E_o\ e^{-(b_1+b_2)}} \quad . (3.30)$$

Equation (3.30) can be further simplified by noting that the energy buildup factor at the interface between the two layers is given by

$$B_E(b_1,b_2) = 1 + \frac{I^s(b_1,b_2)}{E_o\ e^{-b_1}} \quad , \qquad (3.31)$$

where $I^s(b_1,b_2)$ is the scattered energy flux at the interface. Thus,

$$B_E(b_1+b_2) = B_E(b_2) + \frac{B_E^s(b_1,b_2)[B_E(b_1,b_2)-1]\ I_n^{su}(b_1+b_2)}{\exp(-b_2)} . (3.32)$$

This is the formulation which will be used to evaluate energy buildup factors for two-material combinations, other than those of water, iron, and lead which are calculated in the next chapter. It will be shown in the discussion of results that the two-medium parameters $B_E^s(b_1,b_2)$ and $I_n^{su}(b_1,b_2)$ are slowly varying functions of b_1 and smoothly varying functions of b_2 which can be accurately evaluated for many two-material combinations by simple linear interpolation over atomic number.

The energy buildup factor at the interface between the two layers, $B_E(b_1,b_2)$, needs further clarification so that it can be evaluated from available single-medium parameters such as buildup factors and albedos. The scattered energy

flux at the interface is composed of the following fluxes:

$I_f^s(b_1)$ - The scattered energy flux which results at the interface when the second medium is replaced by a vacuum.

$I_r^s(b_1,b_2)$ - The scattered energy flux at the interface which is reflected from the second layer.

In notational form,

$$I^s(b_1,b_2) = I_f^s(b_1) + I_r^s(b_1,b_2) \quad \frac{\text{MeV}}{\text{cm}^2\text{-sec}} \quad . \qquad (3.33)$$

Now, the scattered energy flux which is reflected can be expressed in terms of flux albedos as

$$I_r^s(b_1,b_2) = I^u(b_1)\ \alpha_\phi^u(b_2) + I_f^s(b_1)\ \alpha_\phi^s(b_1,b_2) \ \frac{\text{MeV}}{\text{cm}^2\text{-sec}} \ , \qquad (3.34)$$

where the unscattered energy flux albedo α_ϕ^u is defined as the ratio of reflected energy flux to incident, unscattered energy flux; and the scattered energy flux albedo α_ϕ^s is defined as the ratio of reflected energy flux to incident, scattered energy flux. Since the unscattered energy flux is both monoenergetic and monodirectional, α_ϕ^u is equivalent to the energy flux albedos for normally incident sources found in the open literature.[5] However, the scattered energy flux albedo is not dealt with in the open literature; therefore, it will be calculated and tabulated in this work.

Substituting equation (3.34) into equation (3.33) and dividing by the unscattered energy flux $I^u(b_1)$ yields

$$B_E(b_1,b_2) = B_E(b_1) + \alpha_\phi^u(b_2) + [B_E(b_1)-1]\,\alpha_\phi^s(b_1,b_2), \quad (3.35)$$

where $B_E(b_1)$ is the single-medium energy buildup factor for a normally incident source in slab geometry which has been evaluated in Reference [5]. It will be shown in the discussion of results that the interface energy buildup factor can be accurately evaluated for a large number of two-material combinations by using equation (3.35).

4. CALCULATIONS

4.1. General

The transport of monoenergetic gamma-rays normally incident on two-layered slabs of water, iron, and lead has been investigated by using both discrete ordinates and stochastic methods to solve the Boltzmann transport equation in slab geometry. Source energies of 1, 3, and 6 MeV were chosen so that the two-medium buildup factor formulation, as derived in the previous chapter, could later be verified for the primary photon interaction processes: The photoelectric effect, Compton scattering, and pair production. The production of annihilation radiation has also been included in these calculations, but other secondary interaction processes such as fluorescence radiation and bremsstrahlung have not. The consequences of not dealing with these photon interactions in the calculations will be considered and accounted for in the discussion of results.

The discrete ordinates calculations were carried out with the Westinghouse version of a transport code called ANISN,[56] and the stochastic calculations were carried out with PUGT II,[55] a gamma-ray transport code developed at Purdue University. On the average, the PUGT II stochastic calculations required much more computer running time than

the ANISN discrete ordinates calculations, especially for slab configurations of more than three mean free paths.* Therefore, the stochastic calculations were limited to two-layered slab configurations of up to five mean free paths and primarily used to verify the accuracy of the discrete ordinates results. One of the major goals of this work will be to establish definitive accuracy limits for the two-layered buildup factor results.

4.2. Stochastic Calculations

Over 150 independent stochastic calculations have been carried out with the transport code PUGT II to evaluate the transmission and buildup of monoenergetic photons normally incident on two-layered slabs of water, iron, and lead. PUGT II (Purdue University Gamma-Ray Transport) is a stochastic computer code which is based on the "Lattice Model Concept" as discussed in Chapter 2 and Appendix B. In brief, the code generates source gamma-rays and runs analogue experiments in which the photons are followed through a material medium until they exceed some physical, energy, or time boundary. The record of each photon from birth to death is called its history, and quantities of interest such as fluxes, currents, and albedos are obtained by summing the results of many thousands of histories. Reference (55) should be consulted for a more detailed description of PUGT II.

*A typical ANISN run for slab configurations up to 13 mean free paths required approximately 250 seconds of time on the CDC 6500 computer at Purdue University while a PUGT II run for a slab configuration of 4 mean free paths required 1500 seconds of computer time.

The results of these stochastic calculations for two-layered slabs of water, iron, and lead will be primarily used to determine the accuracy of the discrete ordinates calculations; therefore, it is imperative to estimate and limit the inherent statistical inaccuracies. For statistical purposes, the transmission of photons through a slab can be considered to be a series of independent Bernoulli trials where M, the fractional number of photons transmitted through the slab in N histories (trials), represents the probability that a photon will be transmitted through the slab on any given history. The standard deviation for this statistical quantity is then estimated by

$$S = \left[\frac{M(1-M)}{N}\right]^{1/2} \tag{4.1}$$

and the fractional deviation which indicates the percentage of deviation from the mean value of the fractional number of photons transmitted is given as

$$F = 100 \frac{S}{M} \% \tag{4.2}$$

It is believed that a fractional deviation limit of 2% will provide a sound basis for determining the accuracy of the discrete ordinates calculations; therefore, the number of histories for each of the stochastic problems in this work was chosen large enough to limit the fractional deviation to within 2%.* On the average 10,000, 20,000, and 30,000

*The fractional deviation was less than 1.5% for problems in which the second material was not lead.

histories were required for slab configurations totaling 2, 3, and 4 mean free paths respectively.

It should be noted that the statistical model, as presented above, does not account for the effects of biasing. Particle weighting is the only biasing technique used in the PUGT II code. This weighting procedure reduces the statistical variance by analytically accounting for photoelectric absorption. However, the resulting decrease in the fractional deviation cannot be quantitatively determined.

4.3. Discrete Ordinates Calculations

Over 900 independent discrete ordinates calculations were carried out to calculate, as accurately as possible, the buildup and transmission of monoenergetic gamma-rays normally incident on two-layered slabs. The bulk of these calculations dealt with two-layered slabs of water, iron and lead, source energies of 1, 3, and 6 MeV, and shield thicknesses of up to 5 mean free paths of the first layer followed by up to 8 mean free paths of the second layer. The materials water, iron, and lead were chosen because they are commonly used together in pair combinations, and they represent the light, intermediate, and heavy elements respectively. The source energies of 1, 3, and 6 MeV were chosen in order to account for buildup and transmission characteristics resulting from all of the primary gamma-ray interaction processes: The photoelectric effect, pair production, and Compton scattering.

The discrete ordinates calculations in this work were carried out with the one-dimensional, discrete-ordinates code ANISN.[56] This computer program is written in FORTRAN IV and solves the one-dimensional Boltzmann transport equation in slab, cylindrical or spherical geometries.

Theoretical considerations, as discussed in Appendix A, indicate that solution accuracy is highly dependent on the following parameters:

1. Order of scattering (P_ℓ).
2. Order of angular quadrature (S_N).
3. Mesh interval spacing (r).
4. Cross section set used.

The order of scattering (P_ℓ) represents the number of terms in the truncated Legendre series used to approximate the inscattering function. In general, the degree of anisotropic scattering dictates the order of scattering required to give accurate results. A (P_5) expansion was selected for the ANISN calculations in this work.

The quadrature data sets used in the ANISN code consist of direction cosines and associated weights which specify the discrete directions over which the inscattering function is evaluated. Symmetric sets corresponding to the Gaussian zeroes are given for various orders of angular quadrature in the ANISN User's Manual.[57] In general, for anisotropic scattering, the order of angular quadrature (S_N) should be at least twice as large as the order of

scattering (P_ℓ).* An (S_{16}) quadrature set in slab geometry was used for all of the discrete ordinates calculations in this work.

The discrete ordinates derivation given in Appendix A emphasizes that solution accuracy requires adequate mesh spacing. Stringent requirements to insure adequate mesh spacing are presented in the ANISN User's Manual.[58] The calculations in this thesis comply with these criteria in all cases. Specifically, the mesh interval spacings for these calculations were kept smaller than $(4\ \Sigma_g^t)^{-1}$, where Σ_g^t is the largest total group cross section.

ANISN fixed source calculations require the following group-averaged cross sections

σ_A - the photo electric and pair production absorption cross sections

σ_T - the total attenuation cross section (total = absorption + scattering)

$\sigma_{g\to g}$ - the ingroup scattering cross section

$\sigma_{s\ell}^{h\to g}$ h = 1,2,...,g-1 - The P_ℓ down scattering cross sections.

These group-averaged cross sections were generated with the Westinghouse version of a computer program called GAMLEG-W.[59] With the absorption cross-section data** and the group energy

---

*The quadrature requirements are treated in Appendix A.

**The photoelectric and pair-production cross section data were obtained from the tabulations of Storm and Israel.[60]

bounds as input, this code performs the numerical integrations necessary to produce group-averaged absorption, scattering and total cross sections. The down scattering cross sections are determined by averaging the Klein-Nishina differential scattering cross section over the appropriate initial and final photon energy intervals. This version of GAMLEG does not account for the production of the annihilation radiation that results when positions created during pair-production events are destroyed. The code was therefore modified to include the production of annhiliation radiation by treating this generation process as a pseudo-scattering event. In this modification, the two (0.511MeV) annhiliation photons are assumed to be emitted isotropically at the same time and place that the pair-production event occurs, since the lifetime and range of a position are relatively very short in comparison to photon transport. With this assumption, the zeroth order down scattering cross sections are modified according to

$$\sigma_{so}^{i\to g}(\text{modified}) = \sigma_{so}^{i\to g} + \sigma_{pp}^{i} \cdot 2 \cdot \delta(g - p) \qquad (4.3)$$

where σ_{pp}^{i} is the average pair production cross section for group i, p is the index number of the energy group corresponding to 0.511MeV, and δ represents the Dirac delta function.

Flux weighted 20-group cross section sets were used for all of the P_5 - S_{16} discrete ordinates calculations.

The 20-group energy structures used for the 1, 3, and 6MeV sources are tabulated in Tables C.59 - C.61. The weighting fluxes were obtained from the infinite-medium energy flux spectrum tabulations of Goldstein and Wilkins.[1] When the energy flux spectra, as calculated in this work, differed significantly from the corresponding infinite medium tabulations, the cross sections were reweighted using the energy flux spectra obtained in the preliminary solutions.

The following quantities were obtained directly from the output of the ANISN code:

$I^S(b_1+b_2,E)$ - The scattered energy flux spectrum at the outer edge of the second slab.

$B_E(b_1+b_2)$ - The two-medium energy buildup factor.

$I^S_\ell(b_1,b_2,E)$ for $\ell=1,2,\ldots5$ - The Legendre expansion coefficients of the scattered angular energy flux at the interface, $I^S(b_1,E,\vec{\Omega})$.

$I^S(b_1,b_2)$ The scattered energy flux at the interface. Note that,

$$I^S(b_1,b_2) = \int_0^{E_o} I^S_o(b_1,b_2,E)\, dE$$

The two-medium energy buildup factors, $B_e(b_1+b_2)$, and the normalized scattered energy flux spectra, $I^S(b_1+b_2,E)/I^S(b_1+b_2)$, are tabulated in Appendix C for three source energies, six two-material configurations, and forty thickness combinations. The Legendre expansion

coefficients, $I_{\ell}^{s}(b_1,b_2,E)$, are used in the next section to calculate the energy flux which scatters in the first layer but not in the second layer, while the scattered energy flux at the interface is used to determine the interface energy buildup factor, $B_E(b_1,b_2)$, which in turn is used to evaluate the scattered energy flux albedo, $\alpha_{\phi}^{s}(b_1,b_2)$.

4.4. Calculation of the Parameters in the Two-Medium Buildup Factor Formulation

The two-medium buildup factor formulation which was derived in Chapter 3 is rewritten here as

$$B_E(b_1+b_2) = B_E(b_2) + \frac{B_E^s(b_1,b_2)[B_E(b_1,b_2)-1]I_n^{su}(b_1+b_2)}{\exp(-b_2)}, \quad (4.4)$$

where

$$B_E(b_1,b_2) = B_E(b_1) + \alpha_{\phi}^{u}(b_2) + [B_E(b_1)-1]\,\alpha_{\phi}^{s}(b_1,b_2) . \quad (4.5)$$

For organizing purposes, the quantities in this formulation are separated into two categories:

1. Single-medium parameters
   - $B_E(b)$ - The single-medium energy buildup factor
   - $\alpha_{\phi}^{u}(b)$ - The unscattered energy flux albedo
2. Two-medium parameters
   - $B_E^s(b_1,b_2)$ - The scattered energy buildup factor
   - $B_E(b_1,b_2)$ - The interface energy buildup factor
   - $\alpha_{\phi}^{s}(b_1,b_2)$ - The scattered energy flux albedo

$I_n^{su}(b_1+b_2)$ - The energy flux which scatters in the first layer but not the second layer. Normalized to an interface flux of 1MeV/cm^2-sec.

The single-medium parameters are assumed to be available in the open literature; however, for convenience, these quantities are calculated and tabulated in this work for three source energies (1, 3, and 6 MeV) and five materials (water, aluminum, iron, tin, and lead). The remainder of this chapter will be concerned with evaluating the two-medium parameters for two-layered slabs of water, iron, and lead. It will then be shown in the next chapter that these quantities can be accurately extrapolated to many other two-material combinations by interpolating over atomic number.

4.4.1. Calculation of the Interface Energy Buildup Factor and the Scattered Energy Flux Albedo

The energy buildup factor at the interface between the two layers is obtained by applying the energy buildup factor definition to the discrete ordinates results for the scattered energy flux at the interface. Thus,

$$B_E(b_1,b_2) = 1 + \frac{I^s(b_1,b_2)}{I^u(b_1)} = 1 + \frac{I^s(b_1,b_2)}{E_o\, e^{-b_1}} . \quad (4.6)$$

This two-medium parameter, as calculated, can't be directly extrapolated to other material combination with reasonable accuracy; however, accurate extrapolations can be achieved

by using the expression for $B_E(b_1,b_2)$ as given by equation (4.5). That is,

$$B_E(b_1,b_2) = B_E(b_1) + \alpha_\phi^u(b_2) + [B_E(b_1)-1]\ \alpha_\phi^s(b_1,b_2) . \quad (4.7)$$

As will be shown in the next chapter, the scattered energy flux albedo, $\alpha_\phi^s(b_1,b_2)$, can be extrapolated to many other material combinations. This two-medium parameter is evaluated for all the two-material combinations of water, iron, and lead by rearranging equation (4.7) to yield

$$\alpha_\phi^s(b_1,b_2) = \frac{B_E(b_1,b_2) - B_E(b_1) - \alpha_\phi^u(b_2)}{B_E(b_1) - 1} . \quad (4.8)$$

It should be noted that the scattered energy flux albedos, as calculated from the above expression, have values ranging in order of magnitude from 10^{-2} to 10^{-1} while the buildup factors in this equation range in order of magnitude from 10^0 to 10^1. This indicates that third place accuracy in the interface and single-medium energy buildup factors can, on the average, be expected to provide, at best, first place accuracy in the scattered energy flux albedos. At first glance, the resulting inaccuracy appears to be a shortcoming, however, it must be remembered that the scattered energy flux albedos are calculated and tabulated solely for the purpose of providing a means to accurately extrapolate interface energy buildup factors. When equation (4.6) is

employed for this purpose, it can be seen that, in reverse, first order accuracy in the scattered energy flux-albedo provides third place accuracy in the extrapolated interface energy buildup factor.

4.4.2. Calculation of the Energy Flux which Scatters in the First Layer but not in the Second Layer

In Chapter 3, the energy flux which scatters in the first medium but not the second medium, $I^{su}(b_1+b_2)$, was normalized and expressed in terms of a truncated Legendre expansion of the angular energy flux at the interface between the two layers. That is,

$$I_n^{su}(b_1+b_2) = \sum_{\ell=0}^{5} \frac{2\ell+1}{2} \int_0^{E_o} \frac{I_\ell^s(b_1,b_2,E)}{I^s(b_1,b_2)} M_\ell(b)\, dE \qquad (4.9)$$

where $I_\ell^s(b_1,b_2,E)$ are the Legendre expansion coefficients, $I^s(b_1,b_2)$ is the scattered energy flux at the interface, $M_\ell(b) = P_\ell[E_{j+2}(b)]$, $E_{j+2}(b)$ is an exponential integral of order j+2, and $b = \mu_2(E)x_2$. Note that $b \neq b_2(E_o)$. The Legendre expansion coefficients, $I_\ell^s(b_1,b_2,E)$ for $\ell=1,2,\ldots,5$, are obtained in 20-group structure from the discrete ordinates calculations while the attenuation coefficient data are obtained from the tabulations of Storm and Israel.[60] These discrete quantities along with the exponential integrals in $M_\ell(b)$ must be expressed as functions of energy in order to perform the indicated integration in equation (4.9).

A computer program called NINT was developed by the author to express the integration variables as functions of energy and then numerically integrate equation (4.9). This program utilizes a least-squares polynomial-curve-fitting routine to approximate and express the attenuation and Legendre expansion coefficient data as polynomial functions of energy. In formula notation, we have

$$I^{s}_{\ell}(b_1,b_2,E) = \sum_{n=1}^{j} g_{\ell,n} E^{n-1} \frac{MeV}{cm^2\text{-sec-MeV}} \text{ for } \ell=1,2,\ldots,5 \tag{4.10}$$

and

$$b_2(E) = x_2 \mu_2(E) = x_2 \sum_{n=1}^{k} h_n E^{n-1} , \tag{4.11}$$

where g and h are the polynomial expansion coefficients, and the indices j and k indicate the orders of the polynomial expansions. (The curve fitting routine was limited to 12th order expansions.)

The exponential integrals occurring in $M_{\ell}(b)$ are expressed as functions of energy by first approximating $E_1(b)$ and then using a recursion relationship to determine the higher order exponential integrals in terms of $E_1(b)$. The following Rand approximation for $E_1(b)$[61] is accurate to at least one part in a million in the range $1 \leq b \leq 110$:

$$E_1(b) = \frac{e^{-b}}{b} \left[\frac{a_0 + a_1 b + a_2 b^2 + b^3}{c_0 + c_1 b + a_2 b^2 + b^3}\right] \tag{4.12}$$

where

$a_0 = 0.2372905$ $\quad$ $c_0 = 2.4776331$

$a_1 = 4.5307924$ $\quad$ $c_1 = 8.6660126$

$a_2 = 5.1266902$ $\quad$ $c_2 = 6.1265272$

The higher order exponential integrals are obtained by repeated use of the recursion formula

$$E_n(b) = \frac{1}{n-1}\left[e^{-b} - b\, E_{n-1}(b)\right] \quad \text{for } n \cdot 1 \ . \qquad (4.13)$$

With the integration variables expressed as functions of energy, equation (4.9) is integrated in NINT with a numerical integrating subroutine called CADRE* (Cautious Adaptive Romberg Extrapolation). The two-medium parameter $I_n^{su}(b_1+b_2)$ is evaluated in this manner and tabulated in Appendix C for all of the two-material combinations of water, iron, and lead; three source energies (1, 3, and 6 MeV); and 40 different mean free path combinations.

4.4.3. Calculation of the Scattered Energy Buildup Factor

The scattered energy buildup factor $B_E^s(b_1,b_2)$ was defined in Chapter 3 as a two-medium parameter which gives the buildup of the scattered energy flux at the interface as

---

*CADRE is a CDC 6500 system library program of the Computer Sciences Center at Purdue University.

it traverses the second medium. In formula notation,

$$B_E^s(b_1,b_2) = \frac{I^{su}(b_1+b_2) + I^{ss}(b_1+b_2)}{I^{su}(b_1+b_2)} \quad , \qquad (4.14)$$

where $I^{ss}(b_1+b_2)$ is the energy flux which scatters in both layers and $I^{su}(b_1+b_2)$ has already been evaluated. There is no need to evaluate $I^{ss}(b_1+b_2)$ because the scattered energy buildup factor is simply calculated by rearranging the two-medium buildup factor formula to yield

$$B_E^s(b_1,b_2) = \frac{[B_E(b_1+b_2) - B_E(b_2)]\, e^{-b_2}}{[B_E(b_1,b_2)-1]\, I_n^{su}(b_1+b_2)} \quad . \qquad (4.15)$$

$B_E^s(b_1,b_2)$, like all of the other two-medium parameters in equation (4.15) is evaluated and tabulated for all of the two-material combinations of water, iron, and lead; three source energies (1, 3, and 6MeV); and forty different slab thicknesses.

4.5. Determination of the Two-Medium Dose Buildup Factor

Of all the different buildup factor forms, the dose buildup factor is perhaps one of the more useful to shield designers, since many shield systems are designed to limit dose rate. In this section, the two-medium dose buildup factor will be evaluated by expressing it in terms of the previously determined two-medium energy buildup factor. This approach has been chosen because it allows the two-medium dose buildup factor to be calculated without evaluating

a new set of two-medium parameters.

Consistent with the single-medium definition of dose buildup, the two-medium dose buildup factor is defined as the ratio of total dose rate to the dose rate resulting from the unscattered flux. In formula notation,

$$B_D(b_1+b_2) = 1 + \int_o^{E_o} \frac{\mu_{en}^{air}(E)\ I^s(b_1+b_2,E)\ dE}{\mu_{en}^{air}(E_o)\ I^u(b_1+b_2)} \qquad (4.16)$$

where μ_{en}^{air} is the energy-absorption coefficient for air, and $I^s(b_1+b_2,E)$ is the scattered energy flux spectrum at the outer edge of the second slab. Multiplying and dividing the numerator in equation (4.16) by the scattered energy flux and noting that the unscattered energy flux can be expressed as

$$I^u(b_1+b_2) = E_o \exp[-(b_1+b_2)] \frac{MeV}{cm^2\text{-sec}} , \qquad (4.17)$$

yields

$$B_D(b_1+b_2) = 1 + \frac{I^s(b_1+b_2) \int_o^{E_o} \mu_{en}^{air}(E) \frac{I^s(b_1+b_2,E)}{I^s(b_1+b_2)}\ dE}{\mu_{en}^{air}(E_o)\ E_o \exp[-b_1+b_2)]} ,$$

$$= 1 + [B_E(b_1+b_2)-1] \int_o^{E_o} \frac{\mu_{en}^{air}(E)}{\mu_{en}^{air}(E_o)} \frac{I^s(b_1+b_2,E)}{I^s(b_1+b_2)}\ dE \qquad (4.18)$$

where $B_E(b_1+b_2)$ is the two-medium energy buildup factor,

and $I^s(b_1+b_2,E)/I^s(b_1+b_2)$ is the normalized scattered energy flux spectrum which is tabulated in Appendix C. The integral in equation (4.18) which represents the average value of the quantity $\mu_{en}^{air}(E)/\mu_{en}^{air}(E_o)$ is evaluated in terms of the 20-group energy structures used in the discrete ordinates calculations as follows:

$$\frac{\bar{\mu}_{en}^{air}}{\mu_{en}^{air}(E_o)} = \sum_{i=1}^{20} \frac{\mu_{en}^{air}(E_i)}{\mu_{en}^{air}(E_o)} \frac{I^s(b_1+b_2,E_i)}{I^s(b_1+b_2)} \Delta E_i \quad , \quad (4.19)$$

where the average energies E_i, group widths ΔE_i and group averaged energy absorption coefficients of air $\mu_{en}^{air}(E_i)^*$ are tabulated for the 20-group structures of 1, 3, and 6MeV in Tables C.59 - C.61. Substituting equation (4.19) into equation (4.18) yields

$$B_D(b_1+b_2) = 1 + [B_E(b_1+b_2)-1]\ \bar{\mu}_{en}^{air}/\mu_{en}^{air}(E_o) \quad (4.20)$$

Using equations (4.19) and (4.20), the two-medium dose buildup factor, $B_D(b_1+b_2)$, and the normalized, average energy-absorption coefficient of air, $\bar{\mu}_{en}^{air}/\mu_{en}^{air}(E_o)$, are calculated and then tabulated along with the two-medium energy buildup factor in Appendix C.

---

*The group averaged energy absorption coefficients of air were constructed from the tabulations of Hubbell.[62]

5. PRESENTATION AND DISCUSSION OF RESULTS

5.1. Description of Tables and Figures

Almost all of the results obtained in the preceding chapter are presented in tabular form in Appendix C. A selected portion of the tabulated information is also reproduced in graphical form in Appendix D. It is intended that the graphical representations be used primarily to facilitate visualization and analyzation of the extensive collection of tables. The purpose of this section is to present the calculated results and to aid the reader in wading through the lengthy collection of tables and figures.

Buildup factors and the parameters in the two-medium buildup factor formulation form the bulk of both the tables and figures. For convenience, a summary of the tables which defines the tabulated quantities and indicates their location and order of arrangement is provided at the beginning of Appendix C. The same procedure is employed for the graphical representations in Appendix D. In general, the two-medium buildup factors and parameters have been evaluated and tabulated for all of the two-material combinations of water, iron, and lead; three source energies (1, 3, and 6 MeV); and slab thicknesses of up to five mean free paths of the first material followed by up to eight mean free paths of the second

material. The calculated results for any one of the two-medium quantities are grouped first by source energy and then by material configuration. Within this scheme, the paired material combinations are arranged by the increasing order of their atomic numbers with the material in the second medium taking priority over the material in the first medium. For example, application of this arrangement scheme to all the paired combinations of water, iron, and lead yields*

1. Iron-water (26 - 6)
2. Lead-Water (82 - 6)
3. Water-Iron (6 - 26)
4. Lead-Iron (82 - 26)
5. Water-Lead (6 - 82)
6. Iron-Lead (26 - 82)

This somewhat unusual arrangement was chosen to emphasize and later utilize the important fact that most of the two-medium quantities are similar in both magnitude and shape for configurations with the same material in the second layer.

Appendix D presents a small number of tables of Appendix C in graphical form. These plots are not intended to replace the tables but rather to show how the results change with source energy, material configuration, and slab thickness. Being more specific, the reproduction limitations for graph size and grid-line detail are not compatible with the

---

*The atomic number of water is taken as six for both arrangement and interpolation purposes.

conditions for accurate reading of the graphs. It is therefore anticipated that the reader making serious use of these results will want to plot his own curves for purposes of interpolation.

5.2. Aids in Applying the Results

When energy or dose buildup factors for two-layer slabs of water, iron, and lead are required, they can be obtained from the corresponding tables in Appendix C (Tables C.1 - C.32). It will probably be frequently desired to apply these results to practical problems which differ in several aspects from the calculated results. Source energies may be different or the two-layer media may differ in thickness or material from those tabulated. In addition, other buildup factor forms such as energy absorption may be required. For use in such problems, the given results must be interpolated or extrapolated. Some of these manipulations are quite obvious and need no further discussion. For example, the simplest extensions involve obtaining buildup factors for different source energies and slab thicknesses. In these cases the tabulated results are plotted and directly interpolated. In contrast, the extension of these results to other material combinations is quite involved because two-medium buildup factors can't be directly extrapolated with reasonable accuracy. However, as will be shown in Section 5.3, accurate extrapolations to other materials can be achieved by employing the two-medium buildup factor

formulation which was derived in Chapter 3.

When other buildup factor forms are desired they can be obtained in terms of the energy buildup factors by using the calculated results for the normalized, scattered energy flux at the outer edge of the second slab, $I^s(b_1+b_2,E)/I^s(b_1+b_2)$ (Tables C.62 - C.93). For example, consider the energy-absorption buildup factor which is defined as the ratio of total energy-absorption rate to the energy-absorption rate which results from the unscattered flux. With this definition, the two-medium energy-absorption buildup factor is given as

$$B_A(b_1+b_2) = 1 + \frac{\int_0^{E_o} \mu_{en}(E)\, I^s(b_1+b_2,E)\, dE}{\mu_{en}(E_o)\, E_o\, e^{-(b_1+b_2)}} , \qquad (5.1)$$

where μ_{en} is the energy-absorption coefficient for the absorbing medium. It should be noted that when the absorbing medium is air, the energy-absorption and dose buildup factors are identical. It is therefore not surprising that the procedure for evaluating the energy-absorption buildup factor by expressing it in terms of the energy buildup factor is identical to the procedure for obtaining the dose buildup factor which was given in Section 4.5. Thus,

$$B_A(b_1+b_2) = 1 + [B_E(b_1+b_2) - 1]\, \bar{\mu}_{en}/\mu_{en}(E_o) , \qquad (5.2)$$

where the normalized average energy-absorption coefficient is given by

$$\frac{\bar{\mu}_{en}}{\mu_{en}(E_o)} = \sum_{i=1}^{20} \frac{\mu_{en}(E_i)}{\mu_{en}(E_o)} \frac{I^S(b_1+b_2,E_i)}{I^S(b_1+b_2)} \Delta E_i \quad , \qquad (5.3)$$

and where the average energies E_i and the group widths ΔE_i are tabulated for the 20-group structures of 1, 3, and 6 MeV in Tables C.59 - C.61.

5.3. Extrapolating the Calculated Results to Other Two-Material Combinations

The two-medium buildup factor formulation was derived and set forth in Chapter 3. This formulation will now be used to obtain buildup factors for two-material combinations other than those of water, iron and lead. For convenience, it is rewritten here as

$$B_E(b_1+b_2) = B_E(b_2) + \frac{B_E^S(b_1,b_2)[B_E(b_1,b_2)-1]\ I_n^{su}(b_1+b_2)}{\exp(-b_2)} \quad , \qquad (5.4)$$

where

$$B_E(b_1,b_2) = B_E(b_1) + \mathcal{L}_E^u(b_2) + [B_E(b_1)-1]\ \mathcal{L}_E^S(b_1,b_2) \quad . \qquad (5.5)$$

The reason for expecting these formulas to provide accurate extrapolations where direct interpolation of the desired two-medium buildup factor fails is made clearer by examining the two-medium parameters in equation (5.4). In this formula there are three, two-medium parameters which must be evaluated for other material combinations before the two-medium buildup factor can be determined. These are

(1) $B_E^s(b_1,b_2)$ - The scattered energy buildup factor,

(2) $I_n^{su}(b_1+b_2)$ - The energy flux which scatters in the first layer but not in the second layer, normalized to an interface flux of 1 MeV/cm^2-sec,

(3) $B_E(b_1,b_2)$ - The energy buildup factor at the interface between the two slabs.

The first two parameters, B_E^s and I_n^{su}, are tabulated in Appendix C and plotted in Appendix D for all of the two-material combinations of water, iron, and lead. The plots show that these two-medium parameters are slowly varying functions of the first layer and smoothly varying functions of the second layer. Closer scrutiny of these figures reveals that the curves for each of the quantities have the same shape for different first layer thicknesses and/or materials. In other words, the curves for all the two-layer configurations having the same material in the second layer differ only by a constant. With this type of functional behavior, it is reasonable to expect that both B_E^s and I_n^{su} can be accurately extrapolated to other material combinations by interpolating over atomic number. Moreover, it is obvious that these quantities can be very accurately interpolated to two-layered slab configurations with materials in the first layer other than those calculated.

In contrast, the third two-medium parameter, $B_E(b_1,b_2)$ is strongly dependent on the material and thickness of the

first layer. Furthermore, this quantity cannot be directly extrapolated to other material combinations with reasonable accuracy; however, accurate extrapolations can be achieved by using equation (5.5). In this formula, the influence of the second medium on the interface energy buildup factor is represented by the albedos for both unscattered and scattered energy fluxes. The unscattered energy flux albedo is nothing more than the albedo for a monoenergetic, normally incident photon source which has been evaluated in the open literature.[5] However, for convenience, this quantity has been recalculated and tabulated in Table C.55 for three source energies (1, 3, and 6MeV) and five materials (water, aluminum, iron, tin, and lead). During the process of calculating the scattered energy flux albedo, it became evident that this two-medium parameter could best be characterized in terms of the unscattered energy flux albedo for a finite reflecting medium. Therefore, the ratio, $R(b_1,b_2)$, of scattered to unscattered albedo is tabulated along with the scattered energy flux albedo in Tables C.56 - C.58. One of the outstanding features of these results is the rapidity with which the albedos assume their maximum value with respect to the thickness of the reflecting medium. A reflecting medium of two mean free paths is, for all practical purposes, equivalent to an infinite medium. Hence, these albedo results have been tabulated only for reflecting medium thicknesses of one and two mean free paths.

In formula notation, the ratio of the scattered to the unscattered energy flux albedo is given as

$$R(b_1,b_2) = \frac{\alpha_{\phi}^{s}(b_1,b_2)}{\alpha_{\phi}^{u}(b_2)} \quad . \tag{5.6}$$

Substituting this relationship into equation (5.5) yields

$$B_E(b_1,b_2) = B_E(b_1) + \alpha_{\phi}^{u}(b_2) + [B_E(b_1) - 1]\, R(b_1,b_2)\, \alpha_{\phi}^{u}(b_2) \quad . \tag{5.7}$$

The advantage of extrapolating R instead of α_{ϕ}^{s} to other material configurations becomes apparent when one observes that this ratio varies only from a value of one to four over the entire spectrum of calculated results. This advantage, coupled with the fact that the albedo contributions to $B_E(b_1,b_2)$ are relatively small,* can be expected to yield highly accurate extrapolations for the interface energy buildup factor.

5.3.1. The Extrapolation Technique

Before describing the procedure for extrapolating buildup factors with the two-medium buildup factor formulation, it is desirable to first define the sets of two-material combinations for which the extrapolation technique is applicable. They can most effectively be delineated in terms of

---

* In Section 4.4.1, it was pointed out that the albedos are approximately two orders of magnitude smaller than the corresponding buildup factors.

Z_1 and Z_2, the atomic numbers of the materials in the first and second layer respectively. Using this terminology, the range of two-material combinations between water (Z = 6) and lead (Z = 82) is given as

$$6 \leq Z_1 \leq 82 , \quad 6 \leq Z_2 \leq 82 .$$

Within the limits of this complete set, eight distinct subsets are defined and herein considered. These eight ranges of material interpolation, as set forth in Table 5.1, have been chosen so that the extrapolation technique may be applied to and evaluated for most of the two-material combinations of interest in shield design. The extrapolation technique will be described in the remainder of this section and evaluated in Section 5.4 by establishing accuracy limits for each of the ranges of interpolation.

The manipulations and methods employed to extrapolate the tabulated results can be most easily illustrated by changing the arguments in the two-medium buildup factor formulation. The mean free path variables in these formulas actually represent slab thickness and material dependence, where the material dependence is accounted for with an attenuation coefficient. In this section, slab thicknesses will be held constant and material dependence will be expressed in terms of atomic number. Specifically, the independent variables b_1 and b_2 are replaced by Z_1 and Z_2, and the two-medium buildup factor formulas, equations (5.4) and (5.5), are rewritten as

Table 5.1. Ranges of Material Interpolation.

Range Number	Interpolation Range* (in atomic number)
	Single Interpolation Ranges
1	$26 < z_1 < 82, \quad z_2 = 6$
2	$z_1 = 26, \quad 6 < z_2 < 26$
3	$z_1 = 82, \quad 6 < z_2 < 26$
4	$6 < z_1 < 26, \quad z_2 = 26$
5	$z_1 = 6, \quad 26 < z_2 < 82$
6	$6 < z_1 < 26, \quad z_2 = 82$
	Double Interpolation Ranges
7	$26 < z_1 < 82, \quad 6 < z_2 < 26$
8	$6 < z_2 < 26, \quad 26 < z_2 < 82$

*z_1 and z_2 are the atomic numbers of the materials in the first and second layer, respectively.

$$B_E(Z_1+Z_2) = B_E(Z_2) + \frac{B_E^s(Z_1,Z_2)[B_E(Z_1,Z_2)-1]I_n^{su}(Z_1+Z_2)}{\exp(-b_2)} , \quad (5.9)$$

and

$$B_E(Z_1,Z_2) = B_E(Z_1) + \alpha_\Phi^u(Z_2) + [B_E(Z_1)-1]\, R(Z_1,Z_2)\alpha_\Phi^u(Z_2) . \quad (5.10)$$

The two-medium buildup factor is extrapolated with equations (5.9) and (5.10) by interpolating the calculated results for the quantities B_E^s, I_n^{su}, and R. More precisely, these two-medium parameters are linearly interpolated over atomic number with a general set of formulas. For convenience, the linear interpolation formulas are presented along with the ranges of material interpolation in Table 5.2.

A working knowledge of the above described extrapolation technique can be achieved by applying the formulas in Table 5.2 to a few specific problems. For example, consider the case of a 3-MeV photon source with four mean free paths of tin followed by two mean free paths of water. This two-material combination lies within the first interpolation range of Table 5.2. Therefore, the linear interpolation formula,

$$X(Sn4,H_2O2) = X(Fe4,H_2O2) + \frac{Z(Sn)-26}{82-26}\,[X(Pb4,H_2O2) - X(Fe4,H_2O2)] \quad (5.11)$$

(text continued on page 71)

Table 5.2. Summary of the Extrapolation Technique.

I. The Two-Medium Buildup Factor Formula

Let: z_1 = the atomic number of the material in the first layer,
z_2 = the atomic number of the material in the second layer,

then

$$B_E(z_1+z_2) = B_E(z_2) + \frac{B_E^s(z_1,z_2)\ [B_E(z_1,z_2)-1]\ I_N^{su}(z_1+z_2)}{\exp(-b_2)},$$

where

$$B_E(z_1,z_2) = B_E(z_1) + \alpha_\phi^u(z_2) + [B_E(z_1)-1]R(z_1,z_2)\ \alpha_\phi^u(z_2).$$

II. Linear Interpolation Formula for Each Set of Two-Material Combinations

Let $X(z_1,z_2)$ represent any of the following two-medium parameters:

1. $B_E^s(z_1,z_2)$

2. $I_N^{su}(z_1+z_2)$

3. $R(z_1,z_2) = \alpha_\phi^s(z_1,z_2)/\alpha_\phi^u(z_2)$

A. Single Interpolation Ranges

1. $26 < z_1 < 82, \qquad z_2 = z(h_20) = 6$

$$X(z_1,6) = X(26,6) + \frac{z_1-26}{82-26}\,[X(82,6) - X(26,6)]$$

2. $z_1 = z(Fe) = 26, \qquad 6 < z_2 < 26$

$$X(26,z_2) = X(26,6) + \frac{z_2-6}{82-6}\,[X(26,82) - X(26,6)]$$

Table 5.2. Continued.

3. $z_1 = z(Pb) = 82, \quad 6 < z_2 < 26$

$$X(82,z_2) = X(82,6) + \frac{z_2-6}{26-6}\,[X(82,26) - X(82,6)]$$

4. $6 < z_1 < 26, \quad z_2 = z(Fe) = 26$

$$X(z_1,26) = x(6,26) + \frac{z_1-6}{82-6}\,[X(82,26) - X(6,26)$$

5. $z_1 = z(H_2O) = 6, \quad 26 < z_2 < 82$

$$X(6,z_2) = X(6,26) + \frac{z_2-26}{82-26}\,[X(6,82) - X(6,26)]$$

6. $6 < z_1 < 26, \quad z_2 = z(Pb) = 82$

$$X(z_1,82) = X(6,82) + \frac{z_1-6}{26-6}\,[X(26,82) - X(6,82)]$$

B. Double Interpolation Ranges

7. $26 < z_1 < 82, \quad 6 < z_2 < 26$

$$X(z_1,z_2) = X(z_1,6) + \frac{z_2-6}{26-6}\,[X(82,26) - X(82,6)]$$

where $X(z_1,6)$ is obtained from formula (1)

8. $6 < z_1 < 26, \quad 26 < z_2 < 82$

$$X(z_1,z_2) = X(6,z_2) + \frac{z_1-6}{26-6}\,[X(26,82) - X(6,82)]$$

where $X(6,z_2)$ is obtained from formula (5)

is used to interpolate the two medium parameters B_E^S, I_n^{su}, and R. Specifically, in formula notation

$$B_E^S(Sn4,H_2O2) = B_E^S(Fe4,H_2O2) + \frac{50-26}{82-26}\,[B_E^S(Pb4,H_2O2) - B_E^S(Fe4,H_2O2)] \quad . \tag{5.12}$$

Values for the bracketed quantities are obtained from Table C.36 as

$$B_E^S(Pb4,H_2O2) = 2.256$$

$$B_E^S(Fe4,H_2O2) = 2.313$$

Substituting these values into equation (5.12) yields

$$B_E^S(Sn4,H_2O2) = 2.313 + \frac{24}{56}\,[2.256 - 2.313]$$

$$= 2.289 \quad . \tag{5.13}$$

Moreover, the same interpolation formula with

$I_n^{su}(Pb4,H_2O2) = 6.452 \times 10^{-2}$,

and

$I_n^{su}(Fe4,H_2O2) = 5.406 \times 10^{-2}$

obtained from Table C.45 gives

$$I_n^{su}(Sn4,H_2O2) = 5.406 \times 10^{-2} + \frac{24}{56}\left[6.45 \times 10^{-2} - 5.406 \times 10^{-2}\right]$$

$$= 5.854 \times 10^{-2} \qquad (5.14)$$

Likewise, with the values

$$R(Pb4,H_2O2) = 1.82 \text{ and } R(Fe4,H_2O2) = 3.35$$

obtained from Table C.57,

$$R(Sn4,H_2O2) = 3.35 + \frac{24}{56}\left[1.82 - 3.35\right]$$

$$= 2.694 \qquad (5.15)$$

The interface energy buildup factor for this problem is given by equation (5.10) as

$$B_E(Sn4,H_2O2) = B_E(Sn4) + \alpha_{\phi}^{u}(H_2O2) + \left[B_E(Sn4) - 1\right] R(Sn4,H_2O2)\, \alpha_{\phi}^{u}(H_2O2) \quad , \qquad (5.16)$$

where the single-medium buildup factor and the unscattered flux albedo obtained from Tables C.54 and C.55 are

$$B_E(Sn4) = 2.642 \text{ and } \alpha_{\phi}^{u}(H_2O2) = .0249.$$

Hence,

$$B_E(Sn4,H_2O2) = 2.642 + .0249 + (1.642)(2.694)(.0249)$$

$$= 2.777 \quad . \qquad (5.17)$$

Now, with all of the two-medium parameters evaluated, the two-medium energy buildup factor is calculated with the aid of equation (5.9). That is,

$$B_E(Sn4+H_2O2) = B_E(H_2O2) + \frac{B_E^s(Sn4,H_2O2)[B_E(Sn4,H_2O2)-1]I_n^{su}(Sn4,H_2O2)}{\exp(-2)}$$

$$= 1.996 + \frac{(2.289)(1.777)(5.854\times10^{-2})}{1.353\times10^{-1}} \qquad (5.18)$$

$$= 3.756$$

which is the desired result.

A material extrapolation problem requiring double interpolation can be illustrated by considering the case of a 3-MeV photon source with four mean free paths of tin followed by two mean free paths of aluminum. This two-material combination lies within the seventh interpolation range of Table 5.2. Thus, the linear interpolation formula for the two-medium parameters B_E^s, I_n^{su}, and R is given as

$$X(Sn4,Al2) = X(Sn4,H_2O2) + \frac{Z(Al)-6}{26-6}[X(Pb4,Fe2)-X(Pb4,H_2O2)] \qquad (5.19)$$

where the parameters denoted by $X(Sn4,H_2O2)$ have been interpolated in the preceding example. Once more, in formula notation,

$$B_E^s(Sn4,Al2) = B_E^s(Sn4,H_2O2) + \frac{13-6}{26-6}[B_E^s(Pb4,Fe2)-B_E^s(Pb4,H_2O2)] , \qquad (5.20)$$

where $B_E^s(Sn4,H_2O2)$ has been interpolated in the preceding example and the values of the bracketed quantities are given in Tables C.36 and C.37 as

$$B_E^s(Pb4,Fe2) = 2.126 \quad \text{and} \quad B_E^s(Pb4,H_2O2) = 2.256.$$

Substituting these values into formula (5.20) yields

$$B_E^s(Sn4,Al2) = 2.289 + \frac{7}{20}\,[2.126 - 2.256]$$

$$= 2.244 \ . \qquad (5.21)$$

Again, the same interpolation formula with $I_n^{su}(Sn4,H_2O2) = 5.854\times10^{-2}$ obtained from the preceding example and with $I_n^{su}(Pb4,Fe2) = 7.22\times10^{-2}$ and $I_n^{su}(Pb4,H_2O2) = 6.452\times10^{-2}$ obtained from Tables C.46 and C.45 gives

$$I_n^{su}(Sn4,Al2) = 5.854\times10^{-2} + \frac{7}{20}\,[7.221\times10^{-2} - 6.452\times10^{-2}]$$

$$= 5.881\times10^{-2} \ . \qquad (5.22)$$

Likewise, with $R(Sn4,H_2O2) = 2.694$ obtained from the preceding example and with $R(Pb4,Fe2) = 1.73$ and $R(Pb4,H_2O2) = 1.82$ obtained from Table C.57,

$$R(Sn4,Al2) = 2.694 + \frac{7}{20}\,[1.73 - 1.82]$$

$$= 2.662 \ . \qquad (5.23)$$

The interface energy buildup factor for this problem is given by equation (5.10) as

$$B_E^s(Sn4,Al2) = B_E(Sn4) + \alpha_\phi^u(Al2)$$

$$+ [B_E(Sn4) - 1]\, R(Sn4,Al2)\, \alpha_\phi^u(Al2) \qquad (5.24)$$

where the single medium buildup factor and the unscattered flux albedo obtained from Tables C.54 and C.55 are

$$B_E(Sn4) = 2.642, \quad \text{and} \quad \alpha_\phi^u(Al2) = 0.023 .$$

Thus,

$$B_E(Sn4),Al2) = 2.642 + 0.023 + (1.642)(2.66)(0.023)$$

$$= 2.765 . \qquad (5.25)$$

The two-medium energy buildup factor is now evaluated by substituting these interpolated values into equation (5.9). That is

$$B_E(Sn4+Al2) = B_E(Al2) + \frac{B_E^s(Sn4,Al2)[B_E(Sn4,Al2)-1]I_n^{su}(Sn4,Al2)}{\exp(-b_2)}$$

$$= 1.976 + \frac{(2.244)(1.765)(5.88\times10^{-2})}{1.353\times10^{-1}}$$

$$= 3.698 \qquad (5.26)$$

which is the desired result.

5.4. Discussion of Accuracy and Comparison of Results

In order to use the results of this work it is necessary to have some idea of the expected range of error in both the calculated and extrapolated results . There are obviously many sources of error in a work of this nature.

Some of them are inherent in the computational methods while others are due to data inaccuracies. It is convenient to classify these sources of error in two categories:

1. Errors resulting from incorrectly solving the Boltzmann transport equation.
2. Errors occurring in extrapolating the calculated results (especially to other two-material combinations).

In the first category we seek to determine how well the chosen computational methods solve the transport equation by considering the sources of error and comparing the results. A major goal of this work is to establish definitive accuracy limits for the calculated results. In particular, it is most important to verify the discrete ordinates results. The importance of this is made clear when one recalls that most of the parameters in the two-medium build-up factor formulation were obtained from the discrete ordinates calculations. Furthermore, the extrapolation technique, as set forth in Section 5.3.1, will be evaluated later by comparing the extrapolated results to corresponding discrete ordinates calculations for a number of two-material combinations.

Perhaps the best method of determining the accuracy of the discrete ordinates results would be to compare them to corresponding experimental results. However, for many reasons, some obvious, this was not possible. In searching

the literature, the author only found an inadequately small number of experimental results for two-layered slabs.[14,63,64] On the other hand, if a large number of experimental results existed or if they could be easily obtained, there would be no need for this work. It goes without question, that an undertaking to experimentally verify the calculated results is beyond the scope of this work.

In the absence of experimental results, it seems reasonable to verify the discrete ordinates results by comparing them to results of other computational methods found in the literature. Here, one finds that the bulk of photon attenuation calculations have dealt with single-layered media. However, a number of calculations for multiple layered media have been carried out. Some of these of particular importance to this work are listed in Table 5.3 along with the method of solution. A relevant feature shared by the results of all of these works is that their accuracy is estimated to be at best 10%. A considerable amount of computing time and effort has been expended in this work to calculate, as accurately as possible, the attenuation of photons in two-layered media. In particular, the discrete ordinates calculations were carried out with the expectation of obtaining results which are accurate to within five percent. It is obvious that the discrete ordinates results cannot be verified to this accuracy by comparing them to results which are, at best, accurate to within 10 percent.

Table 5.3. Summary of Gamma-ray Attenuation Calculations for Multi-layer Slabs.

Reference Number	Authors	Multi-layered Configuration	Method of Solution
13	Kalos	Pb-H_2O, H_2O-Pb	Empirical fit to Monte Carlo Calculations
9	Auslender	Pb-H_2O, H_2O-Pb	Monte Carlo
10	Bowman and Trubey	Pb-H_2O, H_2O-Pb	Monte Carlo
14	Broder et al.	Multi-layer slabs of Al, Fe, Pb, and polyethylene	Empirical fit to experimental data
15	Tsuruo	Pb-H_2O, H_2O-Pb, three-layer slabs of Al, Fe, and Pb	Spectrum matrix method
16	Kitazume, et al.	H_2O-Fe, Fe-H_2O, Pb-H_2O	Empirical fit to numerical integration calculations
11	Shimizu	H_2O-Fe, Fe-H_2O H_2O-Pb, Pb-H_2O	Invariant imbedding
12	Sharp and Carnesale	H_2O-Fe, Fe-H_2O H_2O-Pb, Pb-H_2O	Empirical fit to Monte Carlo calculations

With this in mind, the results of the works listed above will not be used to establish definitive accuracy limits on the discrete ordinates results. Instead, some of them will be included in the comparisons of Section 5.4.2 with the intention of enhancing the credibility of all results in this work.

Without experimental results or calculated results which are accurate enough, verification of the discrete ordinates calculations to within 5 percent accuracy is primarily dependent on comparing these results to the results obtained from the stochastic calculations of this work. In comparing the results from these two independent methods of solution, it is necessary to consider the sources of error inherent in each of the methods, paying particular attention to those sources of error which are common to both methods. More precisely, errors which are common to both methods of solution must be quantitatively estimated before any meaningful conclusions can be obtained from the comparison of results.

5.4.1. Sources of Error in the Calculated Results

Many possible sources of error are found within both methods (discrete ordinates and stochastic calculations). Thus, it may be helpful, before discussing them, to list these sources of error and to indicate the methods of solution in which they are found:

1. statistical errors (stochastic method)
2. biasing errors (stochastic method)
3. mesh interval spacing (discrete ordinates)
4. angular quadrature scheme (discrete ordinates)
5. group averaging of cross section data (discrete ordinates)
6. truncation of Legendre expansions (discrete ordinates)
7. cross section data inaccuracies (both methods)
8. omission of coherent scattering (both methods)
9. omission of flouresence radiation (both methods)
10. omission of bremsstrahlung (both methods).

In this section we will first briefly consider the sources of error which are not common to both methods of solution. Here, it is only necessary to show that the resulting inaccuracies are small because the total effect of these errors on the attenuation calculations will be accounted for by comparing the results of both methods. On the other hand, it is necessary to consider, in detail, those sources of error which are common to both methods. Therefore, the bulk of this section will be devoted to quantitatively estimating the inaccuracies resulting from common sources of error.

Stochastic methods, by definition, provide probabilistic solutions. It is therefore meaningless to present stochastic results for a quantity of interest without specifying the statistical variance. (Statistical variance is a

measure of dispersion about the mean value.) In the stochastic calculations of this work, the variance has been estimated in terms of fractional deviation. Specifically, a statistical model was developed and used in Section 4.2 to express the fractional deviation as a function of the number of histories. With the resulting formulation, equations (4.1) and (4.2), the number of histories for each of the stochastic calculations was chosen large enough to limit the fractional deviation to within 2 percent. It should be noted that the statistical model, as set forth, does not account for the effects of biasing. The stochastic code PUGT II uses a particle weighting technique to analytically account for photoelectric absorption.* The statistical variance is obviously reduced with this type of biasing. However, the resulting decrease in the fractional deviation cannot be easily determined. It is the authors belief that the fractional deviation is less than 1 percent for all of the build-up factor results obtained from PUGT II. In any event, it is known to be less than 2 percent.

The next four sources of error, numbered three through six, are pertinent only to the discrete ordinates calculations. All of these have been dealt with in Section 4.3 and Appendix A. As shown in the discrete ordinates derivation

---

*This is the only type of biasing used in the PUGT II code.

of Appendix A, the definition of a finite-difference phase space mesh and the subsequent approximations involved in integrating the differential equations over the mesh constitute the major sources of error. A great deal of work has been done to establish criteria for determining adequate angle, energy, and space meshes.[58,65,66] The discrete ordinates calculations of this work comply with these criteria in all cases.

The error resulting from the group-averaging of cross section data is, of course, closely related to the energy mesh. It follows that in-group energy dependence can be more accurately estimated for finer group structures. The multigroup constants, as defined in Appendix A, can be exactly determined only when the weighting functions (i.e., in-group energy dependence) are exactly known. In practice these weighting functions are not precisely known and they must be estimated from similar results of other works or from calculations with finer group structures. In this work, infinite-medium flux spectra from Reference [1] were used as weighting functions to provide the required multigroup constants. However, when the flux spectra, as calculated with this group-averaged data, differed significantly from the infinite medium tabulations, the cross sections were reweighted with the calculated flux spectra.

The remaining approximation which is only relevant to the discrete ordinates method is the truncated polynomial

expansion of the differential scattering cross section. In general, the degree of anisotropic scattering dictates the order of the Legendre expansion required to achieve accurate results. Experience has shown that the most severe anisotropy, which results from Compton scattered photons with energies less than 10MeV, can be adequately resolved with a P_5 or P_6 expansion.[23] With this in mind, a P_5 Legendre expansion was used for all of the discrete ordinates calculations in this work.

The listed sources of error which are common to both methods of solution can be categorized as follows:

1. Omission of photon interaction processes which are assumed to have a small effect on the calculated results.
2. Inaccuracies in the cross section data.

The subject of photon interactions has been treated at length in the literature.[67,68,69] Many of the more detailed treatments indicate that even in the restricted range from 20Kev to 10MeV, the number of processes by which photons interact with matter is quite large. It is beyond the scope of this work to present an extended description of these various interaction processes. Moreover, it is unnecessary since, as indicated, this area has been excellently covered in the literature. However, for the readers convenience, a listing of the various interaction processes which indicates their relative importance in attenuation calculations

is presented in Table 5.4. This listing was reproduced from Table 5.1 of Reference [27].

Both the discrete ordinates and stochastic calculations herein account for all of the primary interaction processes (photoelectric effect, pair production and Compton scattering). However, these calculations only account for one of the secondary reactions (annihilation radiation). Here, we shall be concerned with quantitatively estimating the effect of neglecting the remaining interaction processes which are assumed to be of small importance (coherent scattering, fluorescence radiation, and Bremsstrahlung).

Coherent Scattering. In the primary interaction process of Compton scattering, the electrons are considered to be unbound. In reality, they are bound to the atom. The binding makes little difference in the predictions for Compton scattering; however, it does make coherent scattering possible. That is the scattering of photons by the electron cloud of the atom. In this interaction process, the recoil momentum is taken up by the heavy atom. Therefore, the photon experiences almost no change in energy and very little change in direction. In fact, it has been demonstrated that for 1MeV and higher energy photons, deflection angles are less than 2° in aluminum and less than 4° in lead.[69] In proportion to the total absorption coefficient, coherent scattering is most important for middle Z elements (Z = 25-75) and energies below 500Kev. At higher

Table 5.4. Gamma-ray Interaction Processes 20Kev to 10MeV.

A. Of Primary Importance

1. Photoelectric effect
2. Pair production
3. Compton scattering

B. Of small importance

4. Coherent (Rayleigh) electron scattering
5. Annihilation radiation
6. Fluorescence radiation
7. Bremsstrahlung

C. Negligible

8. Thomson scattering from the nucleus
9. Delbrück or potential scattering
10. Coherent molecular or crystal scattering
11. Nuclear interactions
    a. Nuclear photoeffect
    b. Nuclear scattering
12. Radiative corrections to lower order processes

energies the cross section falls of rapidly because the binding effects are negligible. Further proof of the small importance of coherent scattering in shielding calculations is found in Reference [1]. Here, calculations both including and omitting coherent scattering were performed and the results differed by only a few percent.

From the above discussion it seems reasonable to neglect coherent scattering. However, it should be neglected in the correct manner. The angular distribution of scattered photons, as obtained from the Klein-Nishina formula, does not include coherent scattering. If this interaction process is then included in the attenuation coefficient data, the resulting effect is equivalent to treating coherent scattering as an absorption process which it is definitely not. This is the reason that attenuation coefficients without coherent scattering have been used throughout this work.

Fluorescence Radiation. This interaction process refers to the emission of characteristic x-rays and less energetic photons by an atom subsequent to the ejection of atomic electrons in the photoelectric effect. More precisely, x-rays of relatively low energy are given off when free electrons fill the electron vacancies created by the photoelectric effect. The effects of fluorescence radiation are most pronounced for low source energies and high Z materials. However, even in these cases, the intensity of this radiation is usually less than 1% of the intensity of the

radiation producing the original photoelectric effect. In fact, according to Reference [70], the fluorescence radiation contribution to dose rate from a 500 Kev source in lead is less than 2%. Hence, it is obvious that the omission of fluorescence radiation has a negligible effect on the calculated results in this work.

Bremsstralung. Bremsstrahlung are gamma-rays produced when charged particles are decelerated in the atomic electric field. The effects of this interaction process are most pronounced for high-energy photons (greater than 5MeV) in heavy materials such as lead. It has been customary to assume that bremsstrahlung are of little importance for source energies below 10MeV. However, recent works[71,72] have incorporated theoretical models for bremsstrahlung into stochastic calculations and shown that the effects of this interaction process are quite significant for source energies of 6 MeV or higher.* Dutton[71] has considered in detail the effects of Bremsstrahlung for photons of 6MeV and 10MeV in slab shields of iron and lead. His results clearly indicate that inaccuracies resulting from the neglect of bremsstrahlung in the 6MeV calculations of this work could be as large as 6% when iron is the material in the second layer and 20% when lead is the material in the second layer.

---

*Recent experimental results[73] have also confirmed that the effects of bremsstrahlung are quite significant for source energies of 6 MeV or higher.

Fortunately, Dutton has presented his results in such a manner that they can be utilized to correct the 6-MeV results of this work. Specifically, a portion of his results are presented in terms of bremsstrahlung contributions to the total flux spectra (Figures 20, 21, 22, and 25 of Reference [71]). With these results as a basis, the following method has been devised to approximate the effect of bremsstrahlung in the 6-MeV results of this work.

In what follows, let a prime sign (') denote quantities which have been corrected to account for bremsstrahlung and let C_i denote the correction factor for the energy flux in the ith energy group. Then the normalized scattered energy flux spectrum at the outer edge of the second layer which has been tabulated in Appendix C is corrected to account for bremsstrahlung with the formulas

$$\frac{I^S(b_1+b_2,E_i)'}{I^S(b_1+b_2)} = C_i \frac{I^S(b_1+b_2,E_i)}{I^S(b_1+b_2)} \quad \text{for } i=1,2,\ldots,20 \qquad (5.27)$$

where E_i is the average energy of the ith group and the correction factors C_i are obtained from Reference [71]. Specifically,

A. When iron is the material in the second layer

1. $C_i = 1.25$ for $0.0 < E_i \leq 1.0$
2. $C_i = 1.12$ for $1.0 < C_i \leq 1.8$
3. $C_i = 1.0$ for $1.8 < E_i$

B. When lead is the material in the second layer

1. $C_i = 2.0$ for $0.0 < E_i \leq 1.4$
2. $C_i = 1.5$ for $1.4 < E_i \leq 2.6$
3. $C_i = 1.0$ for $2.6 < E_i$

By definition, the bremsstrahlung-corrected two-medium energy buildup factor is given as

$$B_E(b_1+b_2)' = 1 + \frac{\int_0^{E_o} I^s(b_1+b_2,E)' \, dE}{I^u(b_1+b_2)} \qquad (5.28)$$

This quantity is actually evaluated in terms of the 20-group structure of the 6MeV calculations. That is

$$B_E(b_1+b_2)' = 1 + \sum_{i=1}^{20} \frac{I^s(b_1+b_2,E_i)' \, \Delta E_i}{I^u(b_1+b_2)} \qquad (5.29)$$

where the average energies E_i, and the group widths ΔE_i are given in Tables C.59 - C.61. Multiplying and dividing equation (5.29) by the scattered energy flux $I^s(b_1+b_2)$ and noting that

$$B_E(b_1+b_2) = 1 + \frac{I^s(b_1+b_2)}{I^u(b_1+b_2)} \quad , \qquad (5.30)$$

yields

$$B_E(b_1+b_2)' = 1 + [B_E(b_1+b_2)-1] \sum_{i=1}^{20} \frac{I^s(b_1+b_2,E_i)' \, \Delta E_i}{I^s(b_1+b_2)} \qquad (5.31)$$

where the normalized scattered energy flux spectrum has already been corrected to account for bremsstrahlung in

equation (5.27).

In Section 4.5, the two-medium dose buildup factor was evaluated in terms of the two-medium energy buildup factor as

$$B_D(b_1+b_2) = 1 + [B_E(b_1+b_2)-1] \frac{\bar{\mu}_{en}^{air}}{\mu_{en}^{air}(E_o)} , \qquad (5.32)$$

where

$$\frac{\bar{\mu}_{en}^{air}}{\mu_{en}^{air}(E_o)} = \sum_{i=1}^{20} \frac{\mu_{en}(E_i)\ I^S(b_1+b_2,E_i)}{\mu_{en}(E_o)\ I^S(b_1+b_2)} \Delta E_i \qquad (5.33)$$

This quantity is also corrected to account for bremsstrahlung by again using the bremsstrahlung corrected scattered energy flux spectra. Hence,

$$B_D(b_1+b_2)' = 1 + [B_E(b_1+b_2)-1] \frac{\bar{\mu}_{en}^{air'}}{\mu_{en}^{air}(E_o)} \qquad (5.34)$$

where

$$\frac{\bar{\mu}_{en}^{air'}}{\mu_{en}^{air}(E_o)} = \sum_{i=1}^{20} \frac{\mu_{en}^{air}(E_i)\ I^S(b_1+b_2,E_i)'}{\mu_{en}^{air}(E_o)\ I^S(b_1+b_2)} \Delta E_i . \qquad (5.35)$$

Before estimating the increase in accuracy which results from these corrections, it should be mentioned that Dutton's results are for isotropic sources in single-layered slabs whereas the calculations in this work are for monodirectional sources in two-layered slabs. These inconsistencies can be placed in perspective by referring to the

energy flux spectrum tabulations of Appendix C. In particular, it can be seen that the lower energy portions of the flux spectra are quite insensitive to the material and thickness in the first layer. Furthermore, the tabulations of Reference [1], indicate that there is not much difference in the spectra for isotropic and monodirectional sources. It is therefore reasonable to expect the above-described method of accounting for bremsstrahlung to provide some improvement in the accuracy of the 6-MeV results. A conservative estimate would be that the existing inaccuracies are reduced by 50%, thereby limiting the uncertainties resulting from the omission of bremsstrahlung in the 6-MeV calculations to 3% when iron is the material in the second layer and 10% when lead is the material in the second layer.

The final source of error which is common to both methods of solution involves inaccuracies in the microscopic cross section data. The status of cross section data is still changing, and it is possible that the cross section tabulations used in this work[60,62] may be in error by as much as 5%. This uncertainty obviously results in large errors for such quantities as dose rates and energy fluxes. For example, at 10 mean free paths, a 5% change in the total attenuation coefficient results in a 65% change ($e^{1/2}$) in the unscattered flux. On the other hand, normalized flux spectra and buildup factors which represent flux ratios are known to be relatively insensitive to small changes in

the microscopic data. An estimate of this insensitivity can be obtained by again referring to Reference [1] where calculations both omitting and including coherent scattering were performed. For the case of a 4-MeV source in iron, the cross section data with and without coherent scattering differ by up to 7% for energies above 200 kev. However, the corresponding moments method results differed by less than 4%.

5.4.2. Comparison and Verification of the Calculated Results

Both discrete ordinates and stochastic methods have been employed in this work to calculate, as accurately as possible, the attenuation of photons in two-layered slabs. It is the purpose of this section to verify the tabulated results by comparing dose buildup factors from these two independent methods of solution to each other and to corresponding results from the following references:

1. Invariant imbedding calculations of Shimizu, Reference [11].
2. Monte Carlo calculations of Bowman and Trubey, Reference [10].
3. Empirically fitted Monte Carlo calculations of Sharp and Carnesale, Reference [12].

Before presenting the results of this comparison it should be noted that quantities of interest from the above listed references are claimed to be accurate to, at best, 10% and

that these results represent the more accurate of those found in the literature. One of the major goals of this work is to establish definitive accuracy limits for all of the results. Moreover, the discrete ordinates calculations were carried out with the intention of obtaining results which are accurate to within 5%. It is obvious that results which are accurate to, at best, 10% can not be used to verify accuracies to within 5%. Therefore, the results from the above listed references have been included in the comparisons only for purposes of enhancing the credibility of this work. Without results from other works which are accurate enough, definitive accuracy limits will be established by comparing the results from both the discrete ordinates and stochastic calculations of this work. This procedure can be expected to yield reliable accuracy limits because errors common to both methods of solution have already been quantitatively estimated.

More than 600 buildup factor comparisons have been carried out to evaluate differences between the ANISN and PUGT II results of this work and the corresponding results from the above listed references. In general, dose buildup factors were compared for two-layered slabs of water, iron, and lead; gamma-ray source energies of 1, 3, and 6 MeV; and shield thicknesses of up to five mean free paths of the first layer followed by up to eight mean free paths of the second layer. The results of these comparisons have been

expressed in terms of deviations with respect to the discrete ordinates dose buildup factors, and summarized in Table 5.5 by presenting maximum and average percent differences along with the number of comparisons made for each of the given configurations. In general, buildup factors from this work agreed best with those of Shimizu, Reference [11]. As shown in the summary, the maximum differences are all less than 10%, the accuracy that Shimizu has placed on his results.

In order to further characterize general trends in these comparisons, some of the more representative results are plotted in Figures 5.1 through 5.5. In line with the summary, the plots illustrate the consistently good agreement between the results of Shimizu and this work. Moreover, these plots provide some insight to the relatively poor agreement between the results of this work and the Monte Carlo results of References [10] and [12]. In this case, they indicate that the maximum differences occur at the larger mean free path values where statistical approaches are known to be less accurate.

In establishing definitive accuracy limits it is most important to measure the differences between the results of the discrete ordinates and stochastic calculations of this work (ANISN and PUGT II). The comparative summary in Table 5.5 reveals that dose buildup factors from these independent methods of solution differed by less than 1.5% for all of

Table 5.5. Comparison of the Discrete Ordinates Dose Buildup Factors with Corresponding Results from Other Methods and Works.*

Shield Configuration	PUGT II (This Work)		Bowman + Trubey Ref. (10)		Shimizu Ref. (11)		Sharp + Carnesale Ref. (12)	
	Number of Comparisons	Max./Avg. Diff.(%)	Number of Comparisons	Max./Avg. Diff.(%)	Number of Comparisons	Max./Avg. Diff.(%)	Number of Comparisons	Max./Avg. Diff.(%)
Iron-Water(1MeV)	9	0.7/0.4			12	7.2/5.0	20	10.2/7.1
Lead-Water(1MeV)	9	1.2/0.7	12	11.0/5.0	12	8.0/4.5	20	13.0/6.0
Water-Iron(1MeV)	8	0.8/0.5			12	3.0/2.4	20	15.5/9.5
Water-Lead(1MeV)	7	1.0/0.7	12	10.3/7.4	12	3.5/2.7	20	16.8/9.2
Iron-Water(3MeV)	8	1.1/0.6			8	4.2/2.0	20	13.0/7.2
Lead-Water(3MeV)	9	0.9/0.4	12	6.0/3.5	8	5.1/2.6	20	8.5/5.0
Water-Iron(3MeV)	8	0.7/0.4			8	4.8/3.0	20	11.0/7.0
Water-Lead(3MeV)	7	0.9/0.6	12	23.0/15.4	8	3.9/2.6	20	9.8/5.0
Iron-Water(6MeV)	9	0.8/0.4					20	8.1/4.0
Lead-Water(6MeV)	9	1.3/0.7	12	12.0/5.5	12	4.3/2.4	20	7.1/3.7
Water-Iron(6MeV)	8	0.7/0.5					20	11.9/8.5
Water-Lead(6MeV)	7	0.9/0.6	12	24.0/11.0	10	4.9/3.3	20	10.6/7.5
Lead-Iron(1-3-6MeV)	25	1.2/0.5			20	3.9/2.5		
Iron-Lead(1-3-6MeV)	22	1.4/0.6			20	4.4/2.7		
Total	145		72		142		240	

*The discrete ordinates (ANISN) results are the reference data for which maximum and average differences are given.

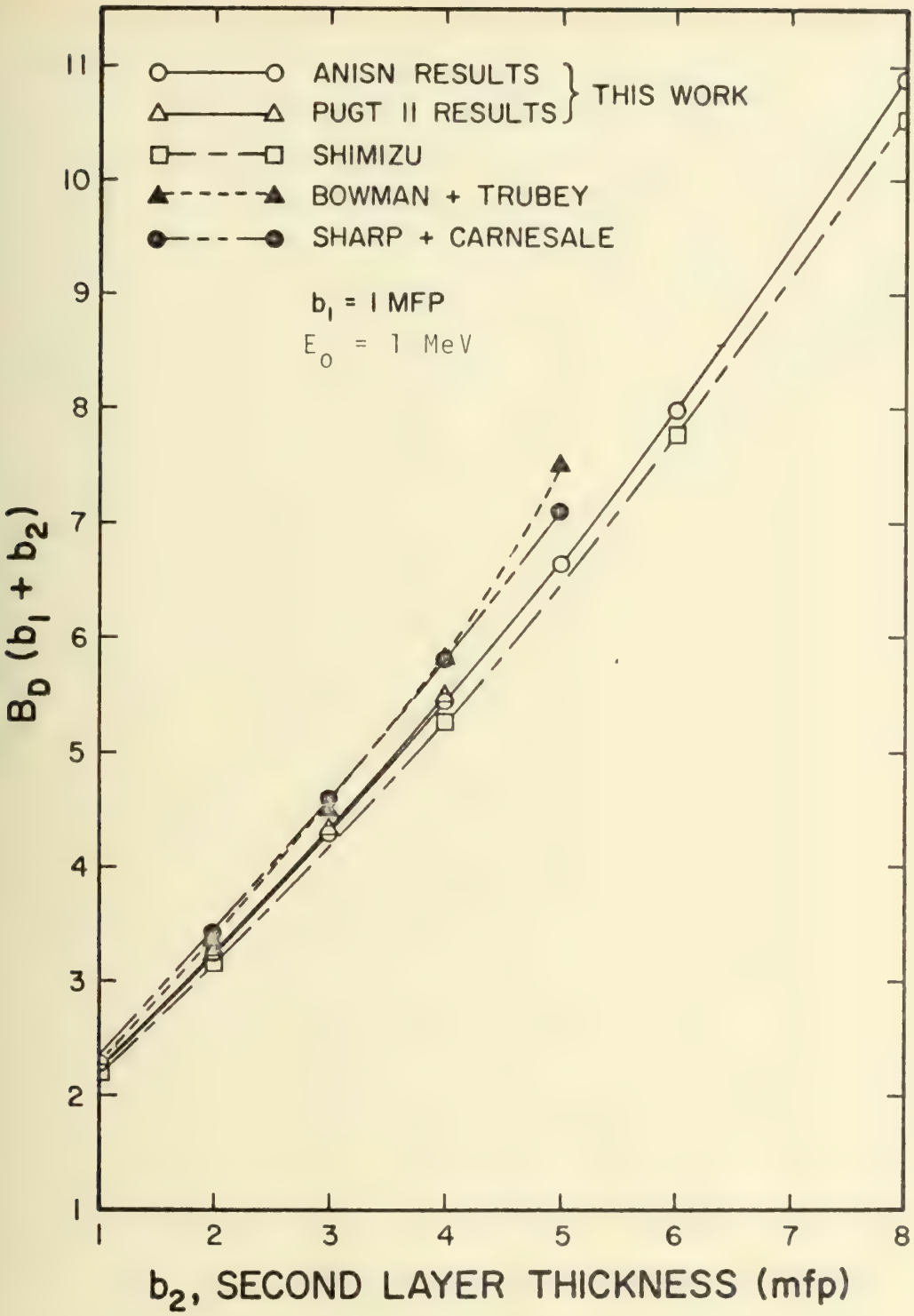

Figure 5.1. Comparison of Dose Buildup Factors for 1-MeV Photons in Two-Layered Slabs of Lead Followed by Water.

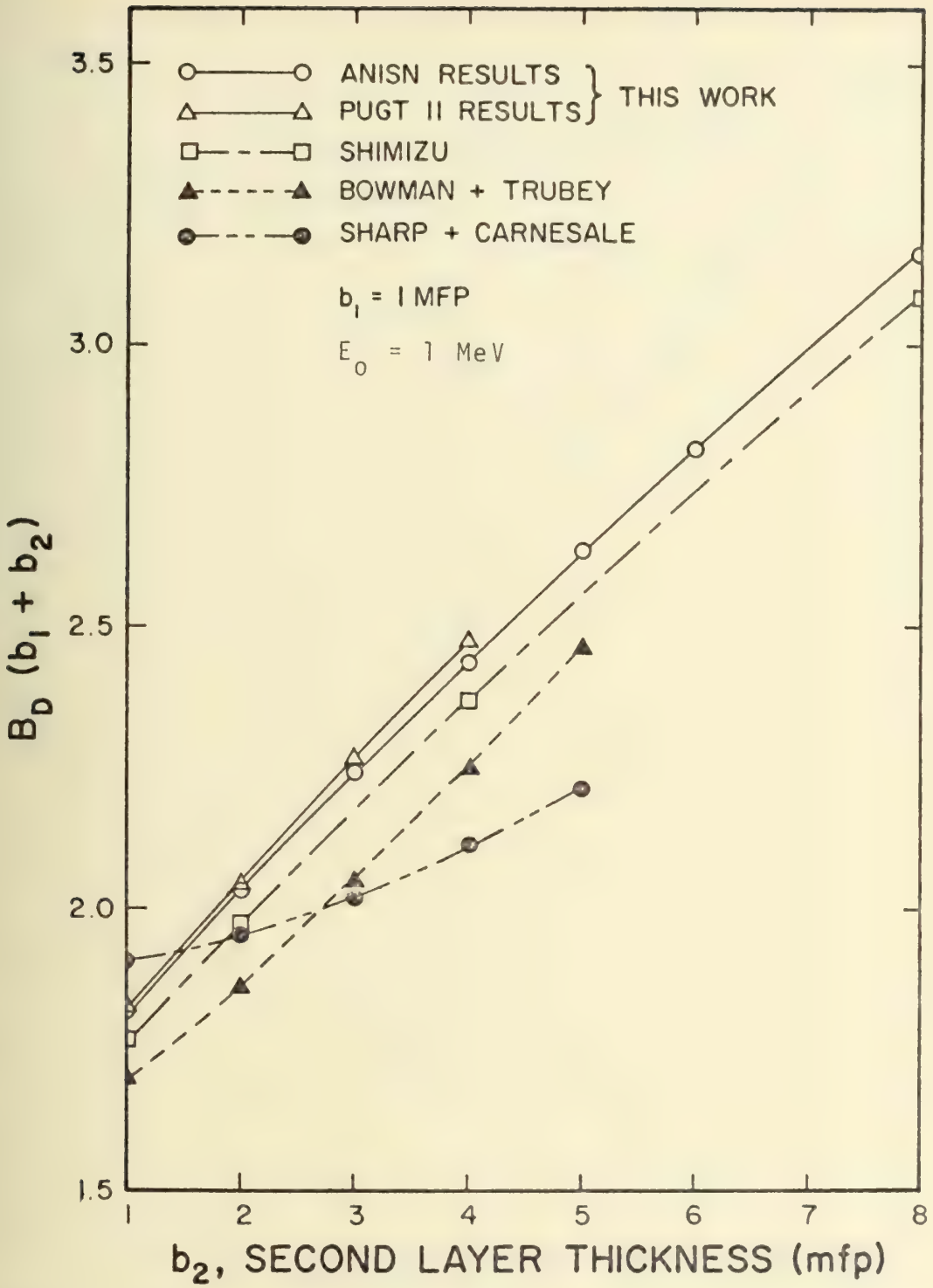

Figure 5.2. Comparison of Dose Buildup Factors for 1-MeV Photons in Two-Layered Slabs of Water Followed by Lead.

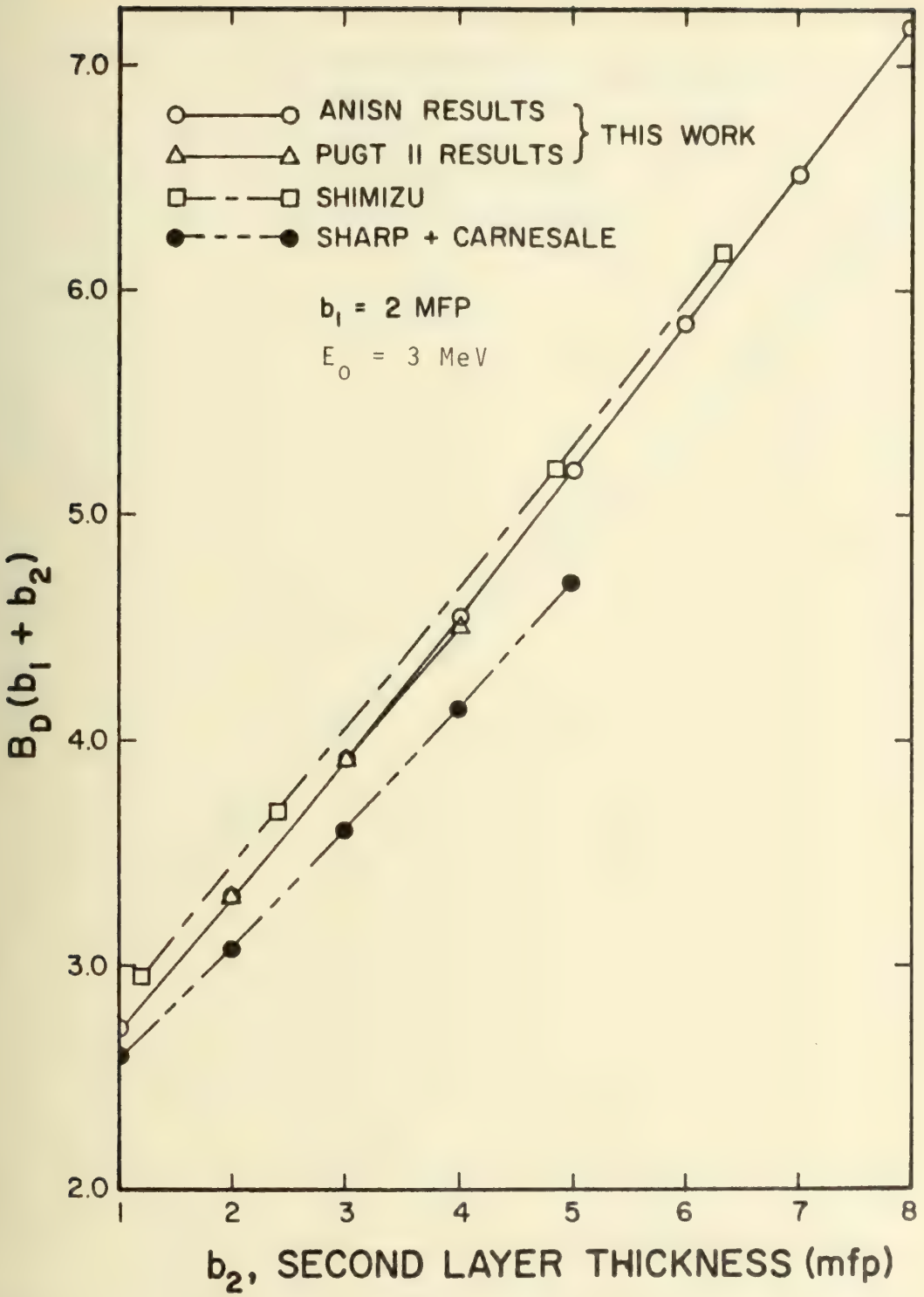

Figure 5.3. Comparison of Dose Buildup Factors for 3-MeV Photons in Two-Layered Slabs of Water Followed by Iron.

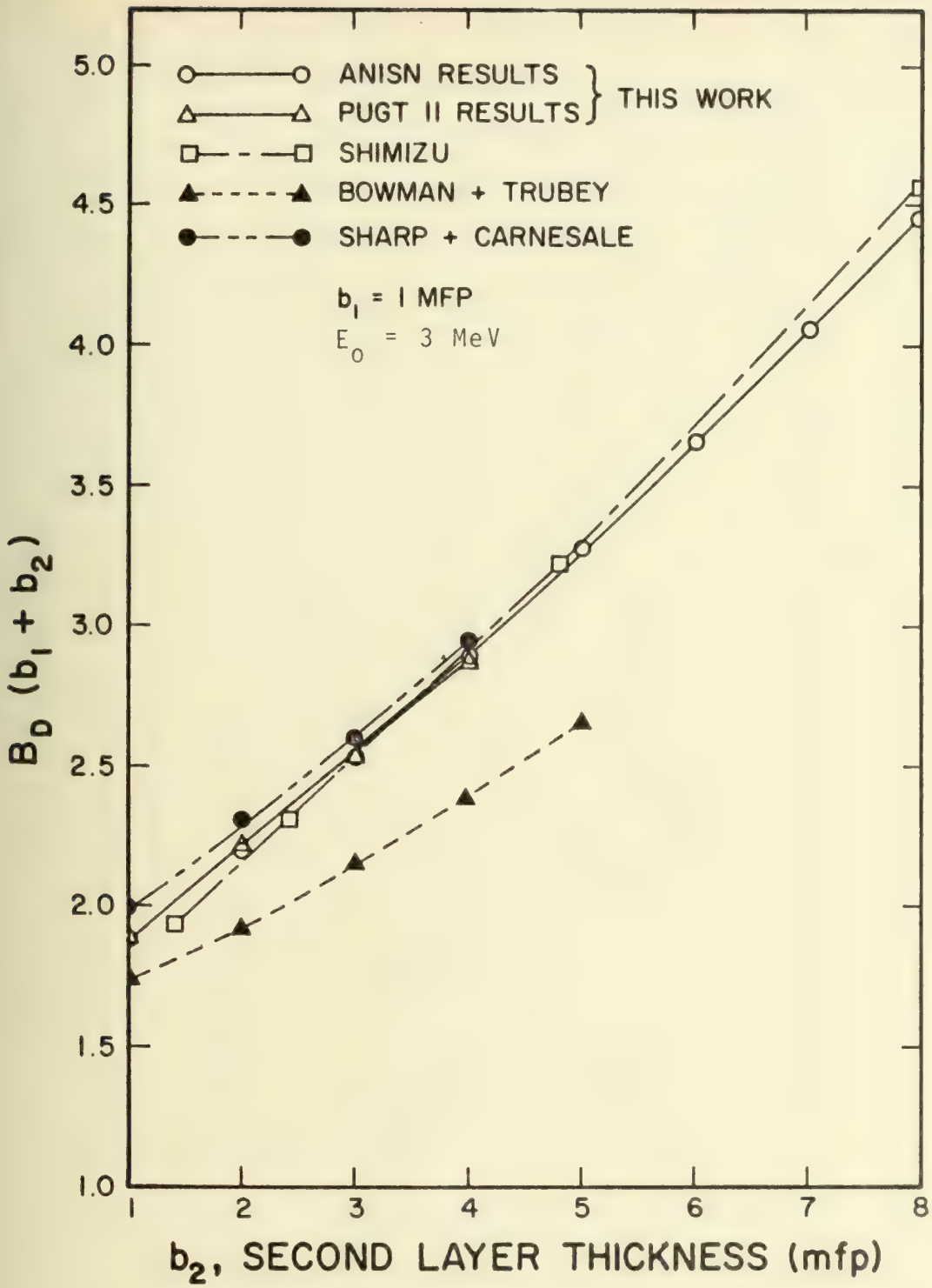

Figure 5.4. Comparison of Dose Buildup Factors for 3-MeV Photons in Two-Layered Slabs of Water Followed by Lead.

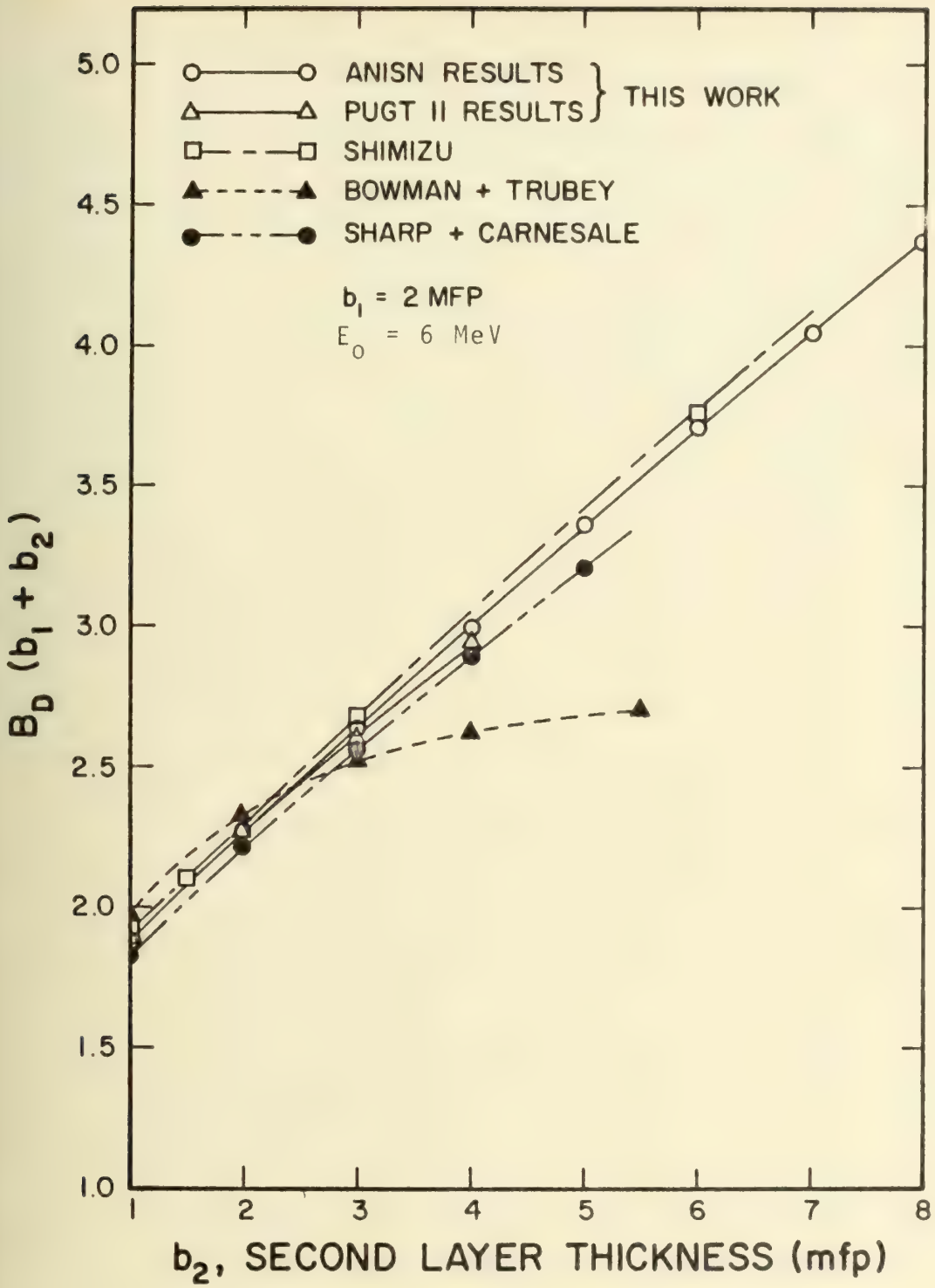

Figure 5.5. Comparison of Dose Buildup Factors for 6-MeV Photons in Two-Layered Slabs of Lead Followed by Water.

comparisons. Moreover, it should be noted that over 90% of the results differed by less than 1%. These remarkably small differences unequivocally substantiate the conclusion that sources of error which are not common to both methods of solution are negligible; furthermore, by taking these differences into account along with the discussion on common sources of error, the results of this work can be verified to the following accuracies. With the exception of the 6-MeV results, energy flux spectra and buildup factors, as tabulated, are conservatively estimated to be accurate to within 5%. The 6-MeV results are known to be less accurate because both methods of solution do not account for bremsstrahlung. In fact, it was shown that the inaccuracies resulting from the omission of bremsstrahlung could be as large as 6% when iron is the material in the second layer and 20% when lead is the material in the second layer. Because of these inaccuracies, a method of approximating the effects of bremsstrahlung was set forth in section 5.4.1, and shown to reduce the existing errors by 50%. When corrected, the 6-MeV energy flux spectra and buildup factors are believed to be accurate to within

1. 5% when water is the material in the second layer,
2. 7% when iron is the material in the second layer, and
3. 12% when lead is the material in the second layer.

5.4.3. Verification of the Extrapolated Results

The procedure for extrapolating buildup factors with the two-medium buildup factor formulation has been presented in Section 5.3 along with the eight ranges of material interpolation. In this section, energy buildup factors for a number of representative material combinations are calculated with the two-medium buildup factor formulation and compared to corresponding results from discrete ordinates calculations. In order to use these comparisons to establish reliable accuracy limits, it is necessary to choose two-material combinations for which the extrapolation technique is known to be least accurate.

In general, quantities which characterize photon transport in material media are mainly determined by the variation of the attenuation coefficient with energy; moreover, materials of similar atomic number have attenuation coefficients which display similar energy dependence. With this view in mind, it is reasonable to expect that the extraplated results will be least accurate for materials with atomic numbers which differ significantly from those of water, iron, and lead. For example, consider the fifth range of material interpolation,

$$z_1 = 6, \quad 26 < z_2 < 82 \quad .$$

Within this range of interpolation, the extrapolation technique should be least accurate for the element tin with

atomic number 50 because most other materials of interest in this range will have atomic numbers closer to either iron or lead.

In line with the preceding discussion, the two material combinations which were chosen for the comparative calculations have atomic numbers that lie in the middle of the interpolation ranges. These representative two-material combinations are categorized by applicable interpolation range and listed in the comparative summaries, Tables 5.6, 5.7, and 5.8. The percent differences, as given in the summaries, represent the maximum deviation between the energy buildup factors which were calculated with ANISN and those which were obtained with the two-medium buildup factor formulation. In order to characterize general trends, the comparative results for two-material combinations in which the largest differences occur have been plotted in Figures 5.6 through 5.9. Both the summaries and the figures demonstrate that the largest differences occur in the fifth and seventh interpolation ranges where the materials in the second layer range in atomic number from 26 to 82. (Even in these ranges the differences are at most 5%.) The fact that these two ranges of interpolation consistently produce the largest differences can be explained by referring to Section 5.3 where the functional behavior of the two-medium parameters has been analyzed. In particular it was shown that the two-medium parameters, B_E^s and I_n^{su}, are slowly varying functions of the first layer and smoothly varying

Table 5.6. A Comparison between Energy Buildup Factors Obtained with the Two-Medium Buildup Factor Formulation and ANISN for a 1-MeV Photon Source.

	Range of Interpolation* (in atomic number)	Comparison Calculations	Maximum Diff. (%)
	Single Interpolation Ranges		
1.	$26 < z_1 < 82$, $z_2 = 6$	Sn-H_2O, 16 pts.	1.5
2.	$z_1 = 26$, $6 < z_2 < 26$	Fe-Al, 12 pts.	1.5
3.	$z_1 = 82$, $6 < z_2 < 26$	Pb-Al, 16 pts.	1.1
4.	$6 < z_1 < 26$, $z_2 = 26$	Al-Fe, 12 pts.	1.0
5.	$z_1 = 6$, $26 < z_2 < 82$	H_2O-Sn, 16 pts.	3.5
6.	$6 < z_1 < 26$, $z_2 = 82$	Al-Pb, 16 pts.	1.0
	Double Interpolation Ranges		
7.	$26 < z_1 < 82$, $6 < z_2 < 26$	Sn-Al, 16 pts.	1.3
8.	$6 < z_1 < 26$, $26 < z_2 < 82$	Al-Sn, 16 pts.	2.0 for $b_1 \leq 2$ 3.5 for $b_1 > 2$

*z_1 and z_2 are the atomic numbers of the materials in the first and second layer, respectively.

Table 5.7. A Comparison between Energy Buildup Factors Obtained with the Two-Medium Buildup Factor Formulation and ANISN for a 3-MeV Photon Source.

	Range of Interpolation* (in atomic number)	Comparison Calculations		Maximum Diff. (%)
		Single Interpolation Ranges		
1.	$26 < z_1 < 82$, $z_2 = 6$	$Sn-H_2O$,	16 pts.	0.80
2.	$z_1 = 26$, $6 < z_2 < 26$	Fe-Al,	12 pts.	1.50
3.	$z_1 = 82$, $6 < z_2 < 26$	Pb-Al,	16 pts.	0.60
4.	$6 < z_1 < 26$, $z_2 = 26$	Al-Fe,	12 pts.	1.00
5.	$z_1 = 6$, $26 < z_2 < 82$	H_2O-Sn,	16 pts.	3.0 for $b_1 \leq 2$ 4.5 for $b_1 > 2$
6.	$6 < z_1 < 26$, $z_2 = 82$	Al-Pb,	16 pts.	0.50
		Double Interpolation Ranges		
7.	$26 < z_1 < 82$, $6 < z_2 < 26$	Sn-Al,	16 pts.	1.0
8.	$6 < z_1 < 26$, $26 < z_2 < 82$	Al-Sn,	16 pts.	3.0 for $b_1 \leq 2$ 4.0 for $b_1 > 2$

*z_1 and z_2 are the atomic numbers of the materials in the first and second layer, respectively.

Table 5.8. A Comparison between Energy Buildup Factors Obtained with the Two-Medium Buildup Factor Formulation and ANISN for a 6-MeV Photon Source.

	Range of Interpolation* (in atomic number)	Comparison Calculations	Maximum Diff. (%)
	Single Interpolation Ranges		
1.	$26 < z_1 < 82$, $z_2 = 6$	Sn-H_2O, 16 pts.	1.7
2.	$z_1 = 26$, $6 < z_2 < 26$	Fe-Al, 12 pts.	1.8
3.	$z_1 = 82$, $6 < z_2 < 26$	Pb-Al, 16 pts.	1.0
4.	$6 < z_1 < 26$, $z_2 = 26$	Al-Fe, 12 pts.	1.1
5.	$z_1 = 6$, $26 < z_2 < 82$	H_2O-Sn, 16 pts.	4.0 for $b_1 \leq 2$ 5.0 for $b_1 > 2$
6.	$6 < z_1 < 26$, $z_2 = 82$	Al-Pb, 16 pts.	0.60
	Double Interpolation Ranges		
7.	$26 < z_1 < 82$, $6 < z_2 < 26$	Sn-Al, 16 pts.	2.50
8.	$6 < z_1 < 26$, $26 < z_2 < 82$	Al-Sn, 16 pts.	3.5 for $b_1 \leq 2$ 5.0 for $b_1 > 2$

*z_1 and z_2 are the atomic numbers of the materials in the first and second layer, respectively.

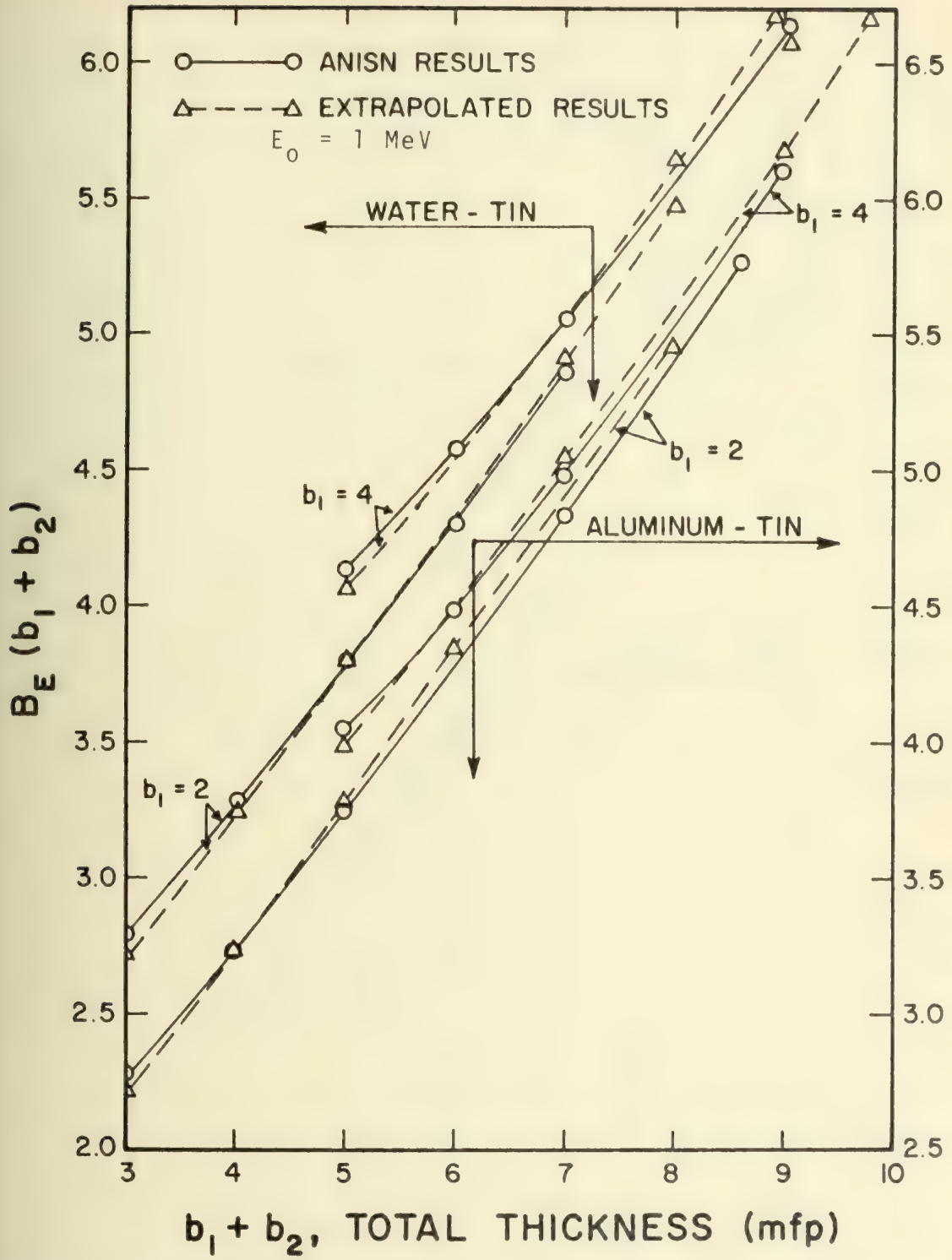

Figure 5.6. Comparison of Energy Buildup Factors for 1-MeV Photons in Two-Layered Slabs of Water-Tin and Aluminum-Tin.

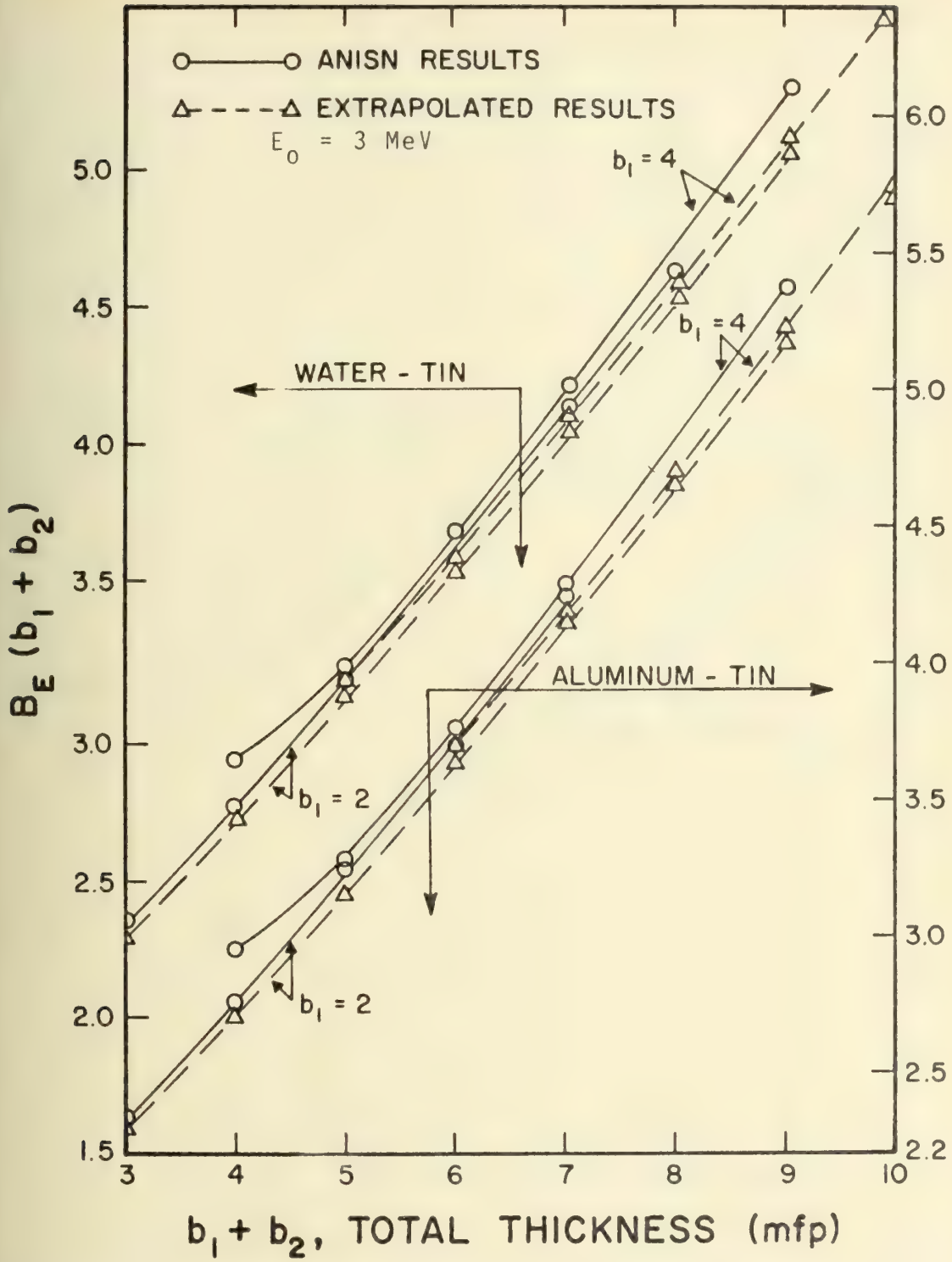

Figure 5.7. Comparison of Energy Buildup Factors for 3-MeV Photons in Two-Layered Slabs of Water-Tin and Aluminum-Tin.

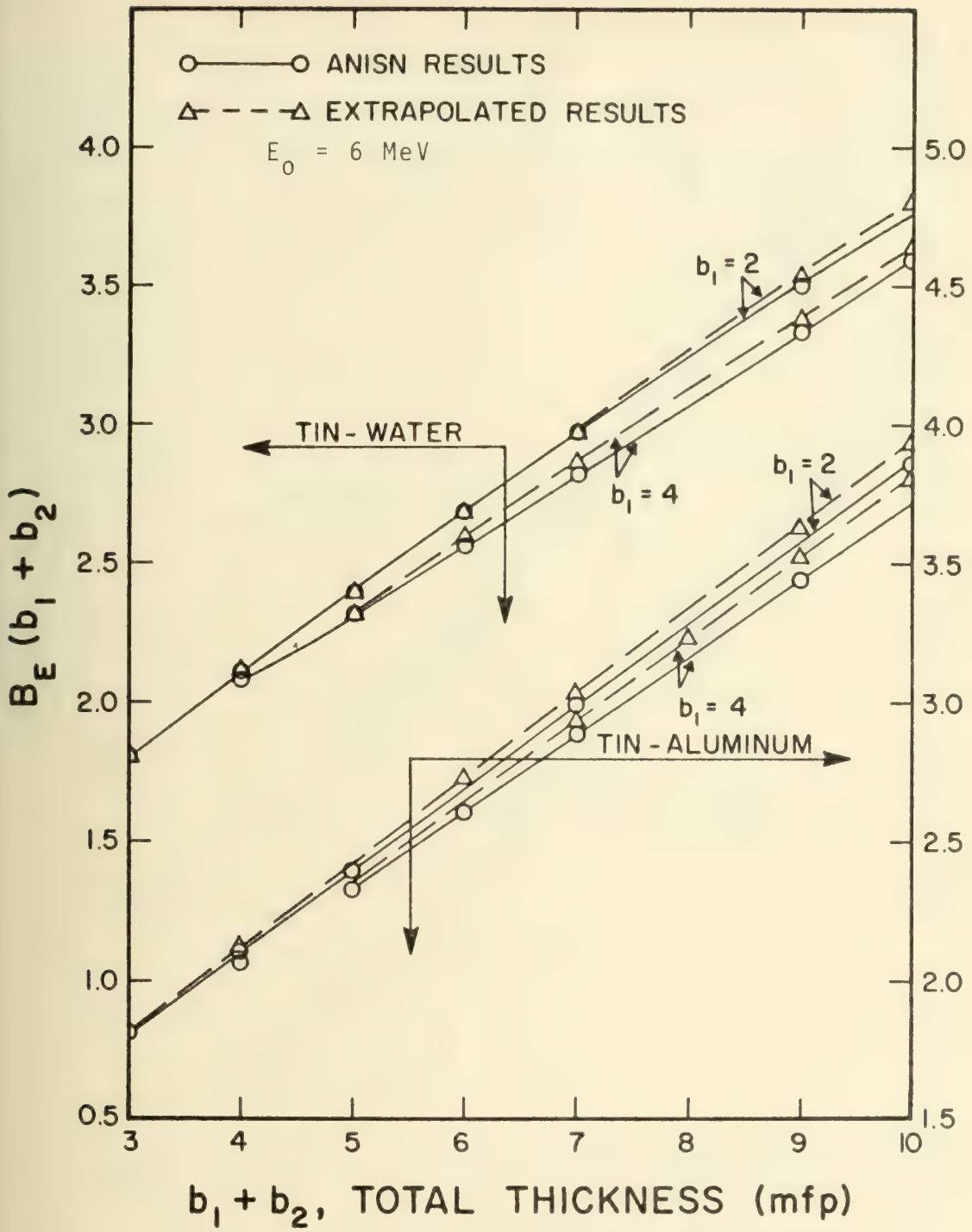

Figure 5.8. Comparison of Energy Buildup Factors for 6-MeV Photons in Two-Layered Slabs of Tin-Water and Tin-Aluminum.

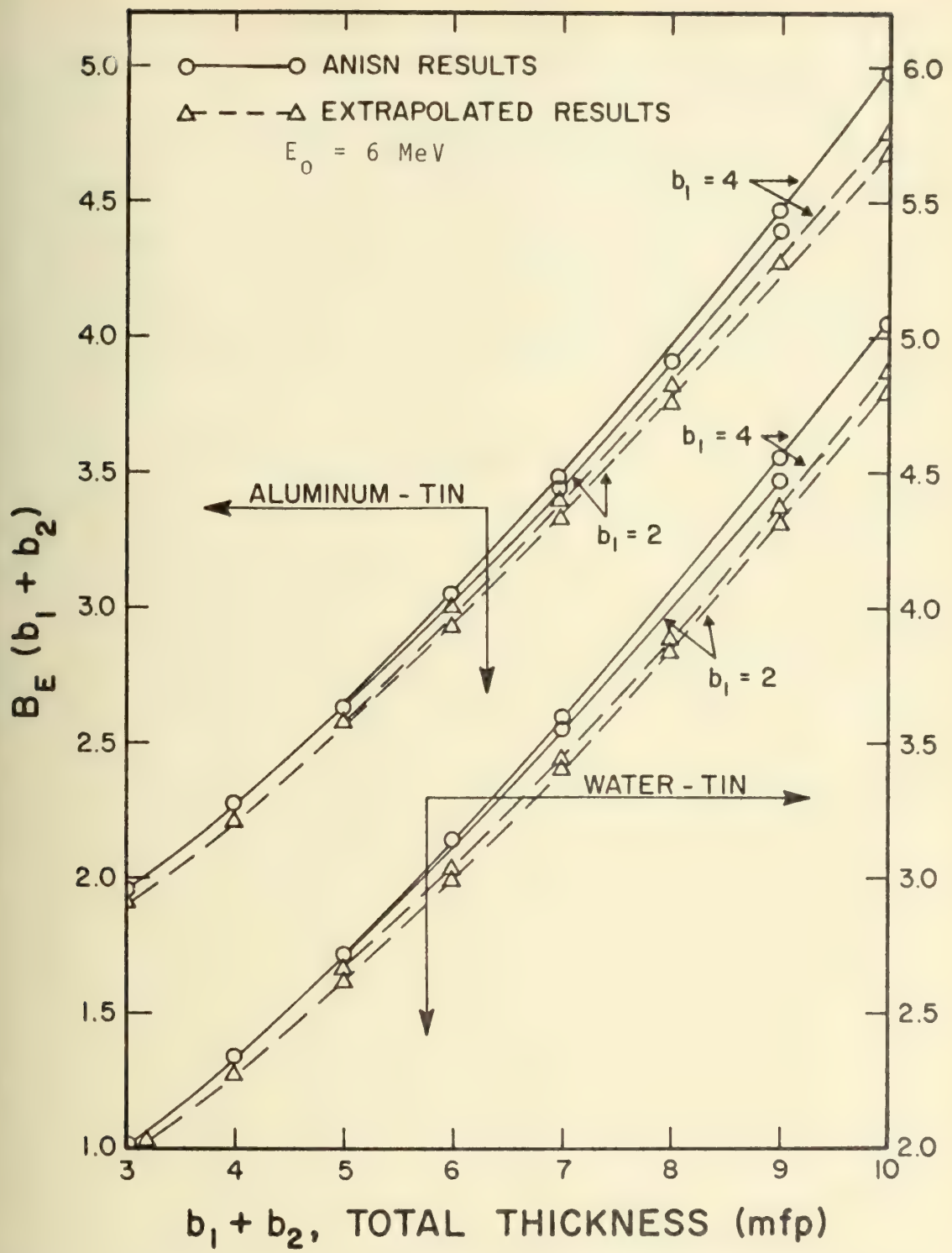

Figure 5.9. Comparison of Energy Buildup Factors for 6-MeV Photons in Two-Layered Slabs of Water-Tin and Aluminum-Tin.

functions of the second layer; moreover, a detailed examination of the plotted results reveals that the curves for each of these two-medium parameters have the same shape for different first layer thicknesses and/or materials. Hence, it is reasonable to expect the extrapolated results to be least accurate for interpolation ranges which encompass the largest variation in the atomic number of the material of the second layer.

The differences, as set forth in the summaries, clearly indicate that errors resulting from obtaining buildup factors with the two-medium buildup factor formulation are

1. At most 5% for two-material combinations which lie in the fifth and seventh interpolation ranges, and
2. At most 2.5% for two-material combinations which lie in all the other interpolation ranges.

6. CONCLUSIONS AND RECOMMENDATIONS

6.1. Conclusions

The theory of photon transmission and buildup in two-layered slabs has been investigated and set forth in this work. As a result, the two-medium buildup factor has been analytically expressed in terms of single medium buildup factors and parameters which in turn can be characterized as functions of atomic number. It should be noted that the two-medium parameters in this formulation are not empirical, but rather they are directly related to the basic physics of transport phenomena in two-layered slabs.

In applying the two-medium buildup factor formulation, we assume that the single medium buildup factors and albedos are available and then seek to determine the two-medium parameters. These quantities have been evaluated by using ANISN, a discrete ordinates code, to calculate the attenuation of photons in two-layered slabs of water, iron, and lead. In the process of tabulating and plotting the results it was observed that the two-medium parameters are slowly varying functions of the first medium and smoothly varying functions of the second medium; moreover, a detailed examination of the plotted results (Appendix D) reveals that the curves for each of the two-medium parameters have the same

shape for different first layer thicknesses and/or materials. Because of this functional behavior, these two-medium parameters have been accurately extrapolated to a large number of two-material combinations by simple linear interpolation in atomic number.

Energy and dose buildup factors for more than 15 different two-material combinations have been calculated with the two-medium buildup factor formulation and compared to corresponding ANISN results. These comparisons clearly indicate that the errors resulting from obtaining buildup factors with this formulation are at most 5%. The unique feature of the method and results herein described is that buildup factors can be accurately hand-calculated using fairly simple formulas for most of the two-material combinations of interest in shield design. In fact, the major limitation on the number of materials which can be investigated is the lack of single medium data.

6.2. Recommendations

The methods and results of this work should prove to be useful tools of the shield designer, especially in the area of determining the optimum two-material combination for a given application. Future development and improvement should therefore be aimed at extending the application of the two-medium buildup factor formulation and thereby increasing its usefulness.

At present the two-medium buildup factor formulation has been applied only to normally incident photon sources with energies up to 6 MeV. In order to consider higher energies, it is necessary to accurately account for the effects of bremsstrahlung on the parameters in the two-medium buildup factor formulation. This can be accomplished by modifying the discrete ordinates code ANISN to include the contribution of bremsstrahlung. One possible method of including theproduction of bremsstrahlung in a discrete ordinates code is to treat this generation process as a pseudo-scattering event. In so doing, the angle and energy dependent differential cross section for bremsstrahlung can be handled in the same manner as the Klein-Nishina formula for Compton scattering.

Extension of the two-medium buildup factor formulation to other source configurations such as plane isotropic and oblique incident sources is both natural and straightforward. In particular, source configuration differences show up as differences in the expressions for the unscattered flux terms; therefore, definitions for the two-medium parameters, as well as the methods for calculating them, remain the same because these quantities are functions only of the scattered flux.

In verifying the extrapolated results, it was shown that errors resulting from obtaining buildup factors with the two-medium buildup factor formulation are larger for

material interpolation ranges which encompass the largest variation in the atomic number of the material in the second layer. Specifically, the largest errors (5%) were consistently found to occur in the fifth and seventh interpolation ranges (see Tables 5.6-5.8) where the materials in the second layer, range in atomic number from 26 to 82. The error in these interpolation ranges could be reduced by 50% by calculating and tabulating two-medium parameters for the following material combinations:

1. Water-Tin
2. Iron-Tin
3. Lead-Tin

In so doing, errors resulting from obtaining buildup factors with the two-medium buildup factor formulation could be limited to 2.5%.

LIST OF REFERENCES

LIST OF REFERENCES

1. H. Goldstein and J.E. Wilkins, Jr. "Calculations of the Pentration of Gamma-Rays," U.S. Atomic Energy Commission Report NYO-3075 (June 1954).

2. S. Preiser, et al. "Plane Isotropic Gamma-ray Buildup Factors in Lead and Water with Applications to Shielding Problems," Nuclear Data Associates Report NDA 10-144 (Demcember 1954).

3. M.J. Berger and J.A. Doggett. "Gamma Radiations in Air Due to Cloud or Ground Contamination," National Bureau of Standards Report NBS-2224 (June 1953).

4. L.V. Spencer and F. Stinson. "X-ray Diffusion in an Infinite Medium," National Bureau of Standards Report NBS-1151 (1952).

5. M.J. Berger and J.A. Doggett. "Reflection and Transmission of Gamma Radiation by Barriers: Semianalytic Monte Carlo Calcuation," J. Research Nat. Bur. Standards, 56:89 (1956).

6. D.J. Raso. "Transmission of Scattered γ-Rays through Concrete and Iron Slabs," Health Physics, 5:126-141 (1961).

7. A. Shimizu. "Tabulation of Dose Transmission Factors for Homogeneous Slabs," National Bureau of Standards Report NBS-9617 (September 1967).

8. Y. Harima and Y. Nishiwaki. "Analysis of Transmitted Gamma-rays by Multiple Scattering Method (I)--Gamma-rays Transmitted through Slabs of One Material," J. Nucl. Sci. and Technology (Tokyo), 7(8):407-417 (August 1970).

9. S. Auslender. "A Monte Carlo Study of the Gamma-ray Energy Flux, Dose Rate, and Buildup Factors in a Lead-Water Slab Shield of Finite Thickness," Oak Ridge National Laboratory Report ORNL-2194 (February 1957).

10. L.A. Bowman and D.K. Trubey. "Stratified Slab Gamma-ray Dose-Rate Buildup Factors for Lead and Water Shields," ORNL-CF-58-1-41 (January 1958).

11. A. Shimizu. "Tabulation of Dose Transmission Factors for Two-Layer Slabs," National Bureau of Standards Report NBS-9618 (September 1967).

12. D.A. Sharp and A. Carnesale. "Semiempirical Formulas for Gamma-ray Dose Rates through Two-Layer Slab Shields," Nuclear Technology, 12:375-380 (December 1971).

13. M.H. Kalos. "A Monte Carlo Calculation of the Transport of Gamma-rays," Nuclear Data Associates Report NDA56-7 (July 1956).

14. D.L. Broder, et al. "Transmission of Gamma Radiation through Heterogeneous Media," Soviet J. At. Energy (English Translation), 12(1):26-31 (January 1962).

15. A. Tsuruo. "The Spectrum Matrix Method in Gamma-ray Transmission Problems for Multiple Layers," Oak Ridge National Laboratory Report ORNL-TR-241 (February 1964).

16. R.G. Jaeger, et al. (eds.) Engineering Compendium on Radiation Shielding, Vol. I, Section 4.3.2.3:230-233, Berlin, Springer-Verlag (1968).

17. L. Cave, J. Corner, and R. Liston. "The Scattering of Gamma-rays in Extended Media--I: Perpendicular Incidence on a Plane Slab," Proc. Roy. Society A, 204:223 (December 7, 1950).

18. G.H. Peebles and M.S. Plesset. "Transmission of Gamma Rays through Large Thickness of Heavy Materials," Physics Review, 81:430 (1951).

19. G.H. Peebles. "Gamma-ray Transmission through Finite Slabs," Rand Corpaoration Report R-240 (December 1952).

20. G.H. Peebles. "Attenuation of Gamma Rays. I. Transmission Values for Finite Slabs of Lead, Iron, and the Compton Scatterer," J. Applied Physics, 24:1272-1287 (March 1953).

21. D. Yarmush, J. Zell, and R. Aronson. "The Transmission Matrix Method for Penetration Problems," AEC Report WADC-TR-59-772 (1960).

22. A.M. Weinberg and E.P. Wigner. The Physical Theory of Neutron Chain Reactors, Ch. 9:219, Chicago, The University of Chicago Press (1958).

23. D.K. Trubey and B.F. Maskewitz, et al. (eds.). "A Review of the Discrete Ordinates S_N Method for Radiation Transport Calculations," Ch. 2:41, Oak Ridge National Laboratory Report ORNL-RSIC-19 (March 1968).

24. W.D. Lanning. "A FORTRAN Program to Solve the P-3 Gamma-ray Equation in Slab Geometry," AEC Report WAPD-BT-8 (1958).

25. L.V. Spencer and U. Fano. "Calculations of Spatial Distribution by Polynomial Expansion," J. Res. Nat. Bur. Standards, 46:446 (1951).

26. F. Smithies. Integral Equations, London, Cambridge University Press (1958).

27. H. Goldstein, Fundamental Aspects of Reactor Shielding, Ch. 5:172-183, Reading, Massachusetts, Addison-Wesley Publishing Co. (1959).

28. L.V. Spencer and J.C. Lamkin. "Slant Penetration of Gamma-rays in Water," National Bureau of Standards Report NBS-5944 (1958).

29. L.V. Spencer and J.C. Lamkin. "Slant Penetration of Gamma-rays in Concrete," National Bureau of Standards Report NBS-6591 (1959).

30. J. Certaine. "Angular Distribution of Photons from Plane Monoenergetic Sources," AEC Report NYO-3074 (June 1953).

31. M.J. Berger. "Angular Distribution of Multiply Scattered Gamma Radiation from a Plane Isotropic Source," J. Applied Physics, 26:1504 (1955).

32. V.A. Ambrazumian. Theoretical Astrophysics. New York, Pergamon Press (1958).

33. V.A. Ambrazumian. "Diffuse Reflection of Light by a Foggy Medium," Comptes Rendus (Doklady), 38:229 (1943).

34. R. Bellman, R. Kalaba, and G.M. Wing. "Invariant Imbedding and Mathematical Physics-I: Particle Processes," J. Math. Phys., 1:280 (1960).

35. A. Shimizu and H. Mizuta. "Application of Invariant Imbedding to the Reflection and Transmission Problems of Gamma-rays (I)," J. Nucl. Sci. and Technology, 3:57 (1966).

36. A. Shimizu and H. Mizuta. "Application of Invariant Imbedding to the Reflection and Transmission Problems of Gamma-rays (II)," J. Nucl. Sci. and Technology, 3:441 (1966).

37. G.C. Wick. "Uber Ebene Diffusion Problem," Z. Phys., 121:702 (1943).

38. S. Chandrasekhar. Radiative Transfer, Oxford (1950).

39. B.G. Carlson. "Soltuions of the Transport Equation by S_N Approximations," Los Alamos Scientific Laboratory Report LA-1599 (1953).

40. K.D. Lathrop and B.G. Carlson. "Discrete Ordinates Quadrature of the Neutron Transport Equation," Los Alamos Scientific Laboratory Report LA-3186 (1965).

41. A.H. Stroud and D. Secrest. Gaussian Quadrature Formulas, Englewood Cliffs, N.J.: Prentice-Hall Inc. (1966).

42. K.D. Lathrop. "DTF IV, A FORTRAN IV Program for Solving the Multigroup Transport Equation with Anisotropic Scattering," Los Alamos Scientific Laboratory Report LA-3373 (1965).

43. W.W. Engle. "A User's Manual for ANISN, A One Dimensional Discrete Ordinates Transport Code with Anisotropic Scattering," AEC Report K-1693 (1967).

44. F.R. Mynatt. "A User's Manual for DOT, A Two Dimensional Discrete Ordinates Transport Code with Anisotropic Scattering," AEC Report K-1694 (1968).

45. F.B. Kam and F.H. Clark. "Fission Spectrum Neutron Dose Rate Attenuation and Gamma-ray Exposure Dose Buildup Factors for Lithium Hydride," AEC Report ORNL-TM-1477 (1967).

46. H.C. Claiborne. "Survey of Methods for Calculating Gamma-ray Heating," AEC Report ORNL-RSIC-8 (June 1965).

47. D.K. Trubey, S.K. Penny, and K.D. Lathrop. "A Comparison of Three Methods Used to Calculate Gamma-ray Transport in Iron," AEC Report ORNL-RSIC-9 (1965).

48. K.D. Lathrop and A. Leonard. "Comparisons of Exact and S_N Solutions of the Monoenergetic Critical Equation with Anisotropic Scattering," Nucl. Sci. and Engineering, 22:115 (1965).

49. R.G. Jaeger, Ref. 16, p. 164.

50. A.H. Jaub (ed.). John Von Neuman Collected Works. Vol. V:751, Pergamon Press (1963).

51. S. Ulam and N. Metropolis. "The Monte Carlo Method," J. of Am. Stat. Assoc., 44:335 (1949).

52. H. Kahn. "Application of Monte Carlo," AEC Report AECU-3259 (April 1959).

53. H. Meyer, Symposium on Monte Carlo Method, New York: John Wiley and Sons (1956).

54. H.E. Hungerford. "The Lattice Model Concept of Stochastic Neutron Transport," Ph.D. Thesis, Purdue University, Lafayette, Indiana (1965).

55. A. Razani. "Stochastic Gamma-ray Transport and Its Application to Shielding Calculations," Ph.D. Thesis, Purdue University, Lafayette, Indiana (1969).

56. R.G. Soltesz. "Revised WANL ANISN Program User's Manual," Westinghouse Astronuclear Laboratory Report WANL-TML-1967 (April 1969).

57. R.G. Soltesz. Ref. 56, pp. 33-37.

58. R.G. Soltesz. Ref. 56, pp. 40-41.

59. R.K. Disney. "GAMLEG-W User's Manual," Westinghouse Astronuclear Laboratory Report NRD-69-172 (May 1969).

60. E. Storm and H.I. Israel. "Photon Cross Sections from 0.001 to 100MeV for Elements 1 through 100," Los Alamos Scientific Laboratory Report LA-3753 (June 1967).

61. R.G. Jaeger. Ref. 16, p. 411.

62. R.G. Jaeger. Ref. 16, p. 183.

63. L.R. Kimel. "The Buildup Factors for Heterogeneous Shielding," Atomic Energy (USSR), 10:173 (1961).

64. H.G. Vogt. "Determination of the Dose Buildup Factors for Gamma-rays in the Energy Range 0.5-15MeV in Laminated Shields of Iron and Water," Hanover Institute of Technology Report ABS-THH-1029 (1966).

65. D.K. Trubey. Ref. 23, pp. 53-63.

66. G.I. Bell and S. Glasstone. Nuclear Reactory Theory, Ch. 5, New York, Van Nostrand Reinhold Co. (1970).

67. W.H. Heitler. Quantum Theory of Radiation, 3rd ed., New York, Oxford University Press (1954).

68. R.D. Evans. The Atomic Nucleus, New York, McGraw-Hill (1955).

69. H. Goldstein. Ref. 27, pp. 141-159.

70. H. Goldstein. "Estimates of the Effect of Fluorescence and Annihilation on Gamma-ray Penetration," Nuclear Data Associates Report NDA15C-31 (February 1954).

71. L.M.C. Dutton. "The Importance of Bremsstrahlung in the Shielding of Gamma-rays having Energies Less than 10MeV," Atomic Energy Establishment (England) Report AEEW-R675 (October 1969).

72. J.P. Kupsa. "Calculation of Buildup Factors and Energy and Spatial Distributions of Gamma-rays Including the Contribution of Bremsstrahlung," M.S. Thesis, University of Missouri, Rolla, Missouri (1972).

73. W.R. Johnson, et al. "Gamma-ray Attenuation at Energies of Approximately 6 and 8MeV," Nucl. Sci. and Engineering, 43:32-41 (1971).

74. H. Greenspan, et al. (eds.). Computing Methods in Reactor Physics, Ch. 3, New York, Gordon and Breach Science Publishers (1968).

75. E. Guth and E. Inonu. "Random Walk Interpretation and Generalization of Linear Boltzmann Equation, Particularly for Neutron Transport," Physical Review, 118:889 (May 1960).

76. G. Goertzel and M.H. Kalos. Progress in Nuclear Energy, Vol. 2:315-320, Pergamon Press (1958).

APPENDICES

APPENDIX A

A.1. Derivation of the Discrete Ordinates Transport Equation[74]

The general Boltzmann transport equation describing the collective particle* motion in a unit cell in phase space is

$$\vec{\nabla} \cdot \vec{\Omega}\, \phi\, (\vec{r}, E, \vec{\Omega}) + \Sigma_T\, (\vec{r}, E, \vec{\Omega}) = S\, (\vec{r}, E, \vec{\Omega}) \qquad (A.1)$$

where Σ_T is the total macroscopic cross section, $\phi(\vec{r}, E, \vec{\Omega})$ is the angular flux in terms of particles per square cm per second per unit energy and per unit solid angle, $\vec{\nabla} \cdot \vec{\Omega}\, \phi\, (\vec{r}, E, \vec{\Omega})$ represents the loss rate due to leakage from the phase space cell ($dV\, dE\, d\Omega$), $\Sigma_T\, \phi(\vec{r}, E, \vec{\Omega})$ represents the loss rate due to collisions in the phase space cell, and $S\, (\vec{r}, E, \vec{\Omega})$ represents the sum of the sources; that is

$S\, (\vec{r}, E, \vec{\Omega})$ = inscattering source + fission source + independent generating source.

Equation (A.1) is usually obtained by considering the causes for particle increases and decreases in the differential

---

*The development given in this appendix will apply to both neutron and gamma-ray transport; therefore, the word particle will refer to either neutrons or gamma-rays, and the symbol Σ will be used to signify neutron or gamma-ray cross sections.

phase space cell dV dE $d\Omega$. In words, the terms of equation (A.1) represent the following:

LEAKAGE + INTERACTIONS = SOURCES.

In a completely analogous manner, the discrete ordinates formulation of the transport equation can be arrived at by considering the events causing an increase or decrease in the number of neutrons contained in a finite difference cell. A derivation for one dimensional geometries is given following the definitions of the coordinate system used and the group neutron flux averages.

A.1.1. Coordinate Systems

The coordinate systems used in the description of the discrete ordinates equation are in rectangular, spherical, and cylindrical geometries and are shown in Figure A.1. Distances from the origin are given by the variable r_i, with i representing the spatial mesh interval index for the distance r. The cell orthogonal surfaces at distances r_i and r_{i+1} are denoted by the terms A_i and A_{i+1}; and the volume enclosed between r_i and r_{i+1} is denoted by $V_{i+\frac{1}{2}}$, the subscript $\frac{1}{2}$ denoting the center of the cell.

Angular distributions are represented with discrete directions. The solid angle Ω_m associated with each direction is specified by a direction cosine μ_m and a weighting function w_m which is proportional to the surface area subtended by the solid angle.

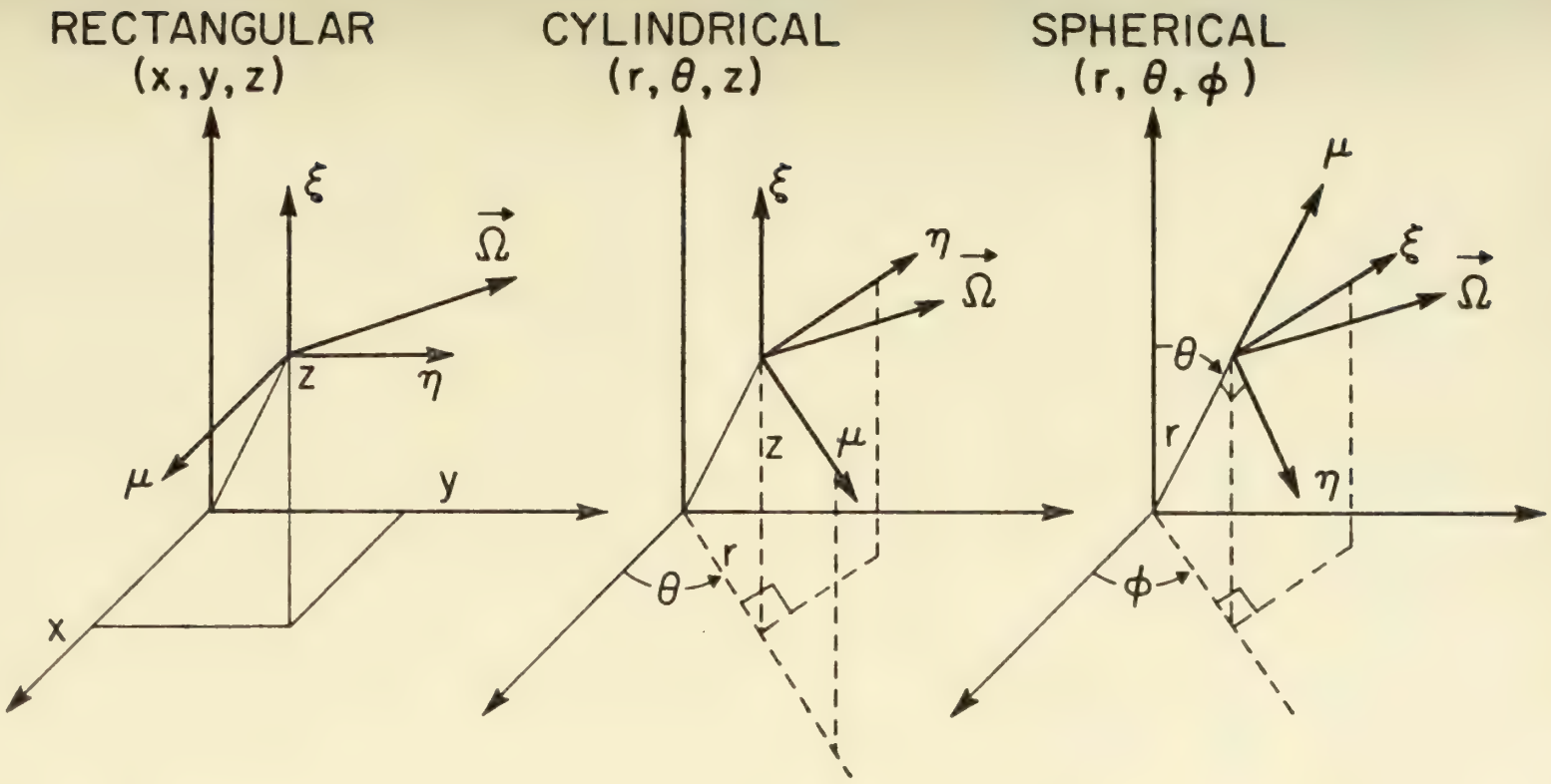

Figure A.1. Geometric and Angular Coordinate Systems.

Table A.1. Geometrical Functions for One Dimensional Geometries.

Geometry	Variable	Area	Volume
Plane	X_i	1	$X_{i+1} - X_i$
Cylinder	r_i	$2\pi r_i$	$\pi(r_{i+1}^2 - r_i^2)$
Sphere	r_i	$4\pi r_i^2$	$\frac{4\pi}{3}(r_{i+1}^3 - r_i^3)$

Energy groups are specified by the group index g with the group having the smallest subscript corresponding to the largest energy.

A.1.2. Distribution Function Averages

The group average angular flux $\phi_g(\vec{r},\vec{\Omega})$ is given as

$$\phi_g(\vec{r},\vec{\Omega}) = \int_{g}^{g-1} \phi(\vec{r},E,\vec{\Omega})\, dE. \qquad (A.2)$$

Several averages of ϕ_g are needed to derive the discrete ordinates transport equation. The mathematical justification for these averages is embodied within the mean value theorem of calculus. First, the average of ϕ_g over the volume $V_{i+\frac{1}{2}}$ and the solid angle Ω_m of the space cell is defined as

$$\phi_{g,i+\frac{1}{2},m} = \frac{1}{V_{i+\frac{1}{2}}, w_m} \int_{V_i}^{V_{i+1}} \int_{\Omega_m} \phi_g(\vec{r},\vec{\Omega})\, dV\, d\Omega. \quad (A.3)$$

Then, the average of ϕ_g over the surface area A_i and the solid angle Ω_m is defined as

$$\phi_{g,i,m} = \frac{1}{A_i\ w_m} \int_{A_i} \int_{\Omega_m} \phi_g(\vec{r},\vec{\Omega})\, dA\, d\Omega \quad (A.4)$$

Finally, the average of ϕ_g over the cell volume and over the directional interfaces of the cell is

$$\phi_{g,i+\frac{1}{2},m-\frac{1}{2}} = \frac{1}{\alpha_{i+\frac{1}{2},m-\frac{1}{2}}} \int_{i+\frac{1}{2}} \int_{m-\frac{1}{2}} \phi_g(\vec{r},\vec{\Omega})\, d\alpha \quad (A.5)$$

A formal definition of the redistribution coefficient α, which accounts for the loss of neutrons due to angular redistribution in curvilinear coordinate systems, will be given later. The averages for the group flux ϕ_g given above are conceptually displayed in Figure A.2.

A.1.3. The Discrete Ordinates Formulation of the Transport Equation

A flow balance for a finite difference cell will be derived in terms of the flux averages given above. The loss rate due to leakage from the face of the phase space cell at r_{i+1} is

$$w_m\, \mu_m\, A_{i+1}\, \phi_{g,i+1,m} \quad . \quad (A.6)$$

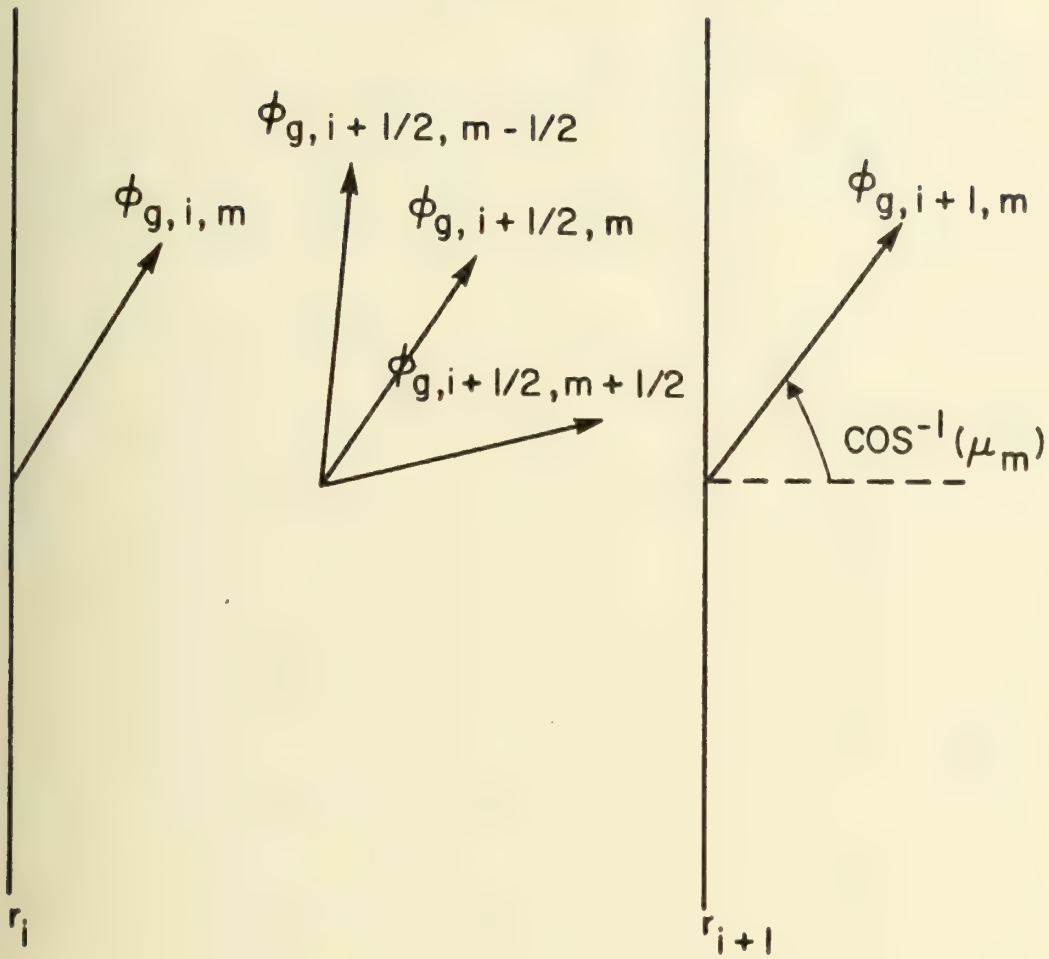

Figure A.2. Average Fluxes for Group g.

Equation (A.6) represents the total exit current in the direction Ω_m from the face A_{i+1} of the cell. The net loss by leakage from the phase space cell is thus

$$w_m \mu_m (A_{i+1} \Phi_{g,i+1,m} - A_i \Phi_{g,i,m}). \qquad (A.7)$$

In a similar manner, the net loss rate by leakage from the interfaces of the direction cell is

$$\alpha_{i+\frac{1}{2},m+\frac{1}{2}} \Phi_{g,i+\frac{1}{2},m+\frac{1}{2}} - \alpha_{i+\frac{1}{2},m-\frac{1}{2}} \Phi_{g,i+\frac{1}{2},m-\frac{1}{2}} \qquad (A.8)$$

In the process of a particle traversing a curved (cylinder or sphere) mesh interval the cosine of the angle associated with the direction of neutron travel is constantly changing. The α terms in equation (A.8) account for the loss rate which results from this angular redistribution.

The particle loss rate from collisions in the phase space cell is given by the product

$$w_m \Sigma_{g,i+\frac{1}{2}} V_{i+\frac{1}{2}} \Phi_{g,i+\frac{1}{2},m} \qquad (A.9)$$

where $\Sigma_{g,i+\frac{1}{2}}$ is the group and space cell averaged macroscopic total cross section. Finally, the average source is defined in the same manner as the average flux given in equation (A.3),

$$S_{g,i+\frac{1}{2},m} = \frac{1}{V_{i+\frac{1}{2}} w_m} \int_{V_i}^{V_{i+1}} \int_{\omega_m} S_g(\vec{r},\vec{\Omega}) \, dV \, d\Omega \qquad (A.10)$$

The discrete ordinates form of the transport equation is obtained by combining equations (A.7, A.8, A.9, and A.10)

to yield

$$w_m \mu_m (A_{i+1} \phi_{g,i+1,m} - A_i \phi_{g,i,m}) + \alpha_{m+\frac{1}{2},i+\frac{1}{2}} \phi_{g,i+\frac{1}{2},m+\frac{1}{2}}$$

$$- \alpha_{m-\frac{1}{2},i+\frac{1}{2}} \phi_{g,i+\frac{1}{2},m-\frac{1}{2}} + w_m \Sigma_{g,i+\frac{1}{2}} V_{i+\frac{1}{2}} \phi_{g,i+\frac{1}{2},m}$$

$$= w_m V_{i+\frac{1}{2}} S_{g,i+\frac{1}{2},m}. \qquad (A.11)$$

For convenience, the centered subscripts are omitted. Then equation (A.11) for each group g becomes

$$w \mu (A_{i+1} \phi_{i+1} - A_i \phi_i) + \alpha_{m+\frac{1}{2}} \phi_{m+\frac{1}{2}} - \alpha_{m-\frac{1}{2}} \phi_{m-\frac{1}{2}}$$

$$+ w \Sigma V \phi - w V S. \qquad (A.12)$$

The angular redistribution coefficient is associated with ray-to-ray transfer in curvilinear coordinates and can be further described by noting that the net angular redistribution must be zero. In other words, angular redistribution does not create or destroy particles. This condition put on α requires that the sum of the terms in equation (A.12) over all the discrete directions must equal zero. That is,

$$\sum_{m=1}^{MM} (\alpha_{m+\frac{1}{2}} \phi_{m+\frac{1}{2}} - \alpha_{m-\frac{1}{2}} \phi_{m-\frac{1}{2}})$$

$$= \alpha_{MM+\frac{1}{2}} \phi_{MM+\frac{1}{2}} - \alpha_{\frac{1}{2}} \phi_{\frac{1}{2}} = 0 \quad . \qquad (A.13)$$

In order to meet this condition on the two limit (or end-point) values, $\alpha_{MM+\frac{1}{2}}$ and $\alpha_{\frac{1}{2}}$, are set equal to zero. Secondly, in the case of divergence free flow ($\vec{\nabla}\cdot\vec{\Omega}\phi = 0$ and $\phi_{i+1} = \phi_i$), equation (A.12) reduces to $\Omega\phi = S$. Then it follows that

$$\alpha_{m+\frac{1}{2}} - \alpha_{m-\frac{1}{2}} = w_m \mu_m (A_{i+1} - A_i) \qquad (A.14)$$

With $\alpha_{\frac{1}{2}} = 0$, equation (A.14) provides a recursion relationship for the α's. In the case of plane geometry $A_{i+1} = A_i$; therefore, equation (A.14) shows that for this case all the α's are equal to zero. This result follows from the fact that there is no angular redistribution in plane geometry. In curvilinear coordinates A_{i+1} does not equal A_i; however, it follows from equation (A.13) that the m sum of equation (A.14) with the first and last α's equaling zero must vanish. This implies that

$$\sum_{m=1}^{MM} w_m \mu_m = 0 \qquad (A.15)$$

Equation (A.15) represents a constraint which the quadrature set used to specify the set of discrete directions Ω_m must satisfy. This is another way of saying that the quadrature set used must correctly integrrate over the solid angle Ω.

A.1.4. Equivalence of the Discrete Transport Equation with the Boltzmann Transport Equation

It is now necessary to show that the discrete ordinates form of the transport equation approaches the analytic form of the Boltzmann equation as the finite-difference phase space cell approaches differential size. Dividing equation (A.12) by w V gives

$$\frac{\mu(A_{i+1}\ \Phi_{i+1} - A_i\ \Phi_i)}{V} + \frac{\alpha_{m+\frac{1}{2}}\Phi_{m+\frac{1}{2}} - \alpha_{m-\frac{1}{2}}\Phi_{m-\frac{1}{2}}}{w\ V}$$

$$+ \Sigma\Phi = S \ . \qquad \text{(A.16)}$$

In plane geometry as the space and angular mesh intervals approach differential size the variables $w \to d\mu$ and $V \to dx$. Then equation (A.16) becomes

$$\mu\ \frac{\partial\Phi}{\partial x} + \Sigma\ \Phi = S \qquad \text{(A.17)}$$

which is the form of the Boltzmann transport equation for one-dimensional plane geometry.

In spherical geometry as the space and angular mesh intervals approach differential size, $w \to d\mu$, $V \to 4\pi r^2\ dr$, and $A \to 4\pi r^2$. The first term in equation (A.16) then becomes

$$\mu\ \frac{(4\pi r^2_{i+1}\ \Phi_{i+1} - 4\pi r^2_i\ \Phi_i)}{4\pi r^2\ dr} \to \frac{\mu}{r^2}\ \frac{\partial(r^2\ \Phi)}{\partial r} \qquad \text{(A.18)}$$

A relationship for the change in α with respect to $d\mu$ is given by dividing equation (A.14) by w V. The result is

$$\frac{\alpha_{m+\frac{1}{2}} - \alpha_{m-\frac{1}{2}}}{w\ V} = \frac{\mu(A_{i+1} - A_i)}{V} \quad . \tag{A.19}$$

The limit of this equation as $w \to d\mu$ is

$$\frac{1}{V}\frac{\partial \alpha}{\partial \mu} = \frac{2\mu}{r} \tag{A.20}$$

Integrating equation (A.20) with respect to μ yields

$$\frac{\alpha}{V} = -\frac{\mu^2}{r} + C \tag{A.21}$$

where C is the constant of integration. Because α vanishes at the ends of the μ interval ($\alpha_{MM+\frac{1}{2}} = \alpha_{\frac{1}{2}} = 0$) where $\mu = \pm 1$, the constant C evaluates to $1/r$.

After multiplying equation (A.21) by ϕ and then taking the derivative with respect to μ, the resulting expressions are

$$\frac{\alpha\phi}{V} = \frac{1}{r}(1 - \mu^2)\ \phi,$$

and

$$\frac{1}{V}\frac{\partial(\alpha\phi)}{\partial\mu} = \frac{1}{r}\frac{\partial}{\partial\mu}[(1 - \mu^2)\ \phi] \quad . \tag{A.22}$$

The left side of equation (A.22) is just the differential form of the second term in equation (A.16). Therefore, using equation (A.22), it is seen that

$$\frac{\alpha_{m+\frac{1}{2}} - \alpha_{m-\frac{1}{2}}\ \phi_{m-\frac{1}{2}}}{wV} \to \frac{1}{r}\frac{\partial}{\partial\mu}[(1 - \mu^2)\ \phi] \quad . \tag{A.23}$$

Thus, equation (A.16) becomes

$$\frac{\mu}{r^2}\frac{\partial(r^2\phi)}{\partial r} + \frac{1}{r}\frac{\partial}{\partial\mu}[(1-\mu^2)\phi] + \Sigma\phi = S. \qquad (A.24)$$

This is the analytic (short) form of the Boltzmann equation in spherical geometry, where the source term S has yet to be evaluated.

A.1.5. Evaluation of the Source Term

The source term is in actuality three separate source terms as follows:

$$S_{g,i+\frac{1}{2},m} = S\ (\text{inscattering})/_{g,i+\frac{1}{2},m} + S\ (\text{independent})/_{g,i+\frac{1}{2},m} + S\ (\text{fission})/_{g,i+\frac{1}{2},m} \ . \qquad (A.25)$$

The analytic form of the inscattering source term is

$$\int_{E'}\int_{\Omega'} \Sigma_s(\vec{r},E'\to E,\vec{\Omega}'\to\Omega)\ \phi(\vec{r},E',\vec{\Omega}')\ dE'\ d\Omega'/_{g,i+\frac{1}{2},m}. \qquad (A.26)$$

where $\Sigma_s(\vec{r},E'\to E\vec{\Omega}'\to\Omega)$ is the scattering cross section for changing the incoming energy and direction $E',\vec{\Omega}'$ to the outgoing energy and direction $E,\vec{\Omega}$. The integration is over the incoming directions and energies. The fundamental assumption in the discrete ordinates method is that this inscattering integral can be approximated by a quadrature

scheme which evaluates the integral as the sum of a discrete distribution. In one dimensional geometries a Gaussian quadrature scheme can be used to provide the discrete distribution, with discrete direction cosines corresponding to the Gaussian zeros.

The differential scattering cross section can be approximated by a truncated Legendre series expansion in the cosine of the scattering angle μ_o. That is

$$\Sigma_s(\vec{r},E'\to E,\vec{\Omega}'\to\Omega) = \sum_{\ell=o}^{L} \frac{2\ \ell+1}{4\pi}\ \sigma_{s\ell}(\vec{r},E'\to E)\ P_\ell(\mu_o), \qquad (A.27)$$

where the Legendre expansion coefficients, $\sigma_{s\ell}(\vec{r},E'\to E)$, are given by

$$\sigma_{s\ell}(\vec{r},E'\to E) = \int_{-1}^{1} \Sigma_s(\vec{r},E'\to E,\vec{\Omega}'\to\Omega)\ P_\ell(\mu_o)\ d\mu_o \ . \qquad (A.28)$$

The scattering angle μ_o is related to the initial and final angles μ' and μ by the addition theorem for Legendre Polynomials. For one-dimensional plane and spherical geometries the relationship is simply

$$P_\ell(\mu_o) = P_\ell(\mu')\ P_\ell(\mu) \ . \qquad (A.29)$$

Substituting equations (A.27) and (A.29) into expression (A.26) gives

$$\sum_{\ell=o}^{L} \frac{2\ \ell+1}{2}\ P_\ell(\mu) \int_{E'} \sigma_{s\ell}(\vec{r},E'\to E) \int_{-1}^{1} \phi(\vec{r},E',\mu')\ P_\ell(\mu')\ dE'\ d\mu'/_{g,i+\frac{1}{2},m} \ . \qquad (A.30)$$

The multigroup transfer cross section is now defined as

$$\sigma_{s\ell}^{h\to g}(\vec{r},E) = \frac{\int_{E_h}^{E_{h-1}} \sigma_{s\ell}(\vec{r},E'\to E) \int_{-1}^{1} \phi(\vec{r},E',\mu')\, P_\ell(\mu')\, dE'\, d\mu'}{\int_{E_h}^{E_{h-1}} \int \phi(\vec{r},E',\mu')\, P_\ell(\mu')\, dE'\, d\mu'} \tag{A.31}$$

Substituting this definition into equation (A.30) and representing the integration over E' by a summation of group integrals having the form

$$\phi_h(\vec{r},\mu') = \int_{E_h}^{E_{h-1}} \phi(\vec{r},E',\mu')\, dE' \quad , \tag{A.32}$$

yields

$$\sum_{\ell}^{L} \frac{2\ \ell+1}{2} P_\ell(\mu) \sum_{h=1}^{g} \sigma_{s\ell}^{h\to g}(\vec{r},E) \int_{-1}^{1} \phi_h(\vec{r},\mu')\, P_\ell(\mu')\, d\mu' /_{g,i+\frac{1}{2},m} \tag{A.33}$$

The generalized Gaussian quadrature formulas, as presented in Reference [41], can now be used to approximate the integral in equation (A.33) as the weighted sum of a discrete distribution. More precisely,

$$\int_{-1}^{1} \phi_h(r,\mu')\, P_\ell(\mu')\, d\mu' \sim \sum_{m'=1}^{N} \phi_h(\mu_{m'})\, P_\ell(\mu_{m'})\, w_{m'}, \tag{A.34}$$

where the direction cosines μ_m correspond to the roots of the orthogonal polynomials used to generate the discrete weights w_m and the index N represents the order of angular quadrature (S_N), i.e., the number of discrete directions. The discrete ordinates form of the inscattering integral is obtained by substituting the quadrature formula given by equation (A.34) into equation (A.33) and then performing the integrations which correspond to the subscripts $g, i+\frac{1}{2}$, and m. The result is

$$\sum_{\ell=0}^{L} \frac{2\ell+1}{2} P_\ell(\mu_m) \sum_{h=1}^{g} \sigma_{s\ell,i+\frac{1}{2}}^{h\to g} \sum_{m'=1}^{N} w_{m'} P_\ell(\mu_{m'}) \psi_{h,i+\frac{1}{2},m'}. \tag{A.35}$$

APPENDIX B

B.1. The Relation between the Lattice Model and the Integral Transport Equation*

The exact relation between Boltzmann equation and recurrence relations which define random walks is given by E. Guth and E. Inonu.[75] In Appendix 2 of the article[76] a discussion of the transport equation for particle collision density is presented. Here we try to formulate the problem of gamma-ray transport through matter considering the probabilistic model on which we have based our sampling.

It is usual to assume that particle-particle interaction may be ignored. This is a good assumption in most radiation transport problems. It leads to a linear equation and allows us to discuss one particle at a time in our formulation. The random walk performed by each photon is described in terms of its collision with atomic electrons and nuclei. Between successive collisions it is assumed that the gamma-ray travel in straight line with constant energy. It is further assumed that the expected number of collision per unit distance is constant. This constant, called linear attenuation coefficient, depends only on the energy of photon and the material through which the photon is travelling.

*Reproduced directly from Appendix A of Reference [55].

For this analysis we will be concerned only with the steady state condition of photon transport, i.e., time independent problem where no transient conditions exist.

In the model considered, the space is assumed to be filled with a cubic lattice and gamma rays are sampled at the lattice points.[54] There are all together 26 allowed directions of motion for gamma rays. We define the location of any lattice point by a vector $\bar{r}_{ijk}$, the direction of the motion of photons by $\bar{\Omega}_m$, and its energy by E. The motion of photons can be described by the following quantities.

$\psi_n(\bar{r}_{ijk}, \bar{\Omega}_m, E)$ = Expected angular density of photons entering their n^{th} collision at $\bar{r}_{ijk}$ per unit volume per unit energy at E, moving in direction, $\bar{\Omega}_m$, per unit solid angle.

$\chi_n(\bar{r}_{ijk}, \bar{\Omega}_m, E)$ = Expected angular density of photons leaving their n^{th} collision at $\bar{r}_{ijk}$ per unit volume per unit energy at E, moving in direction, $\bar{\Omega}_m$, per unit solid angle.

It should be pointed out that the energies and directions of the χ_n are in general not the same as for the ψ_n.

The random walk of photon consists of a succession of collisions and subsequent traversal of a free path. We denote by $P(\bar{r}_{i'j'k'} \to \bar{r}_{ijk}, \bar{\Omega}_{m'} \to \bar{\Omega}_m, E' \to E)$, the probability density that a step changes the state of $(\bar{r}_{i'j'k'}, \bar{\Omega}_{m'}, E')$ into a unit interval at $(\bar{r}_{ijk}, \bar{\Omega}_m, E)$. It is convenient to factor the above kernel into two functions, one dealing with

changes in the spatial coordinate, the other with changes in the energy and direction coordinates.

$$P(\bar{r}_{i'j'k'} \to \bar{r}_{ijk}, \bar{\Omega}_{m'} \to \bar{\Omega}_m, E' \to E) = K(\bar{r}_{i'j'k'}, \bar{\Omega}_{m'} \to \bar{\Omega}_m, E' \to E)$$

$$\cdot \mathrm{Exp}\left[- \sum_{q=0}^{|\bar{r}_{ijk} - \bar{r}_{i'j'k'}|/d_m} \mu(\bar{r}_{i'j'k'} + \bar{\Omega}_m d_m, E) d_m \right]$$

$$\cdot \delta \left(\frac{\bar{r}_{ijk} - \bar{r}_{i'j'k'}}{|\bar{r}_{ijk} - \bar{r}_{i'j'k'}|} - \bar{\Omega}_m \right) \qquad (A.1)$$

where $K(\bar{r}_{i'j'k'}, \bar{\Omega}_{m'} \to \bar{\Omega}_m, E' \to E)$, the Klein-Nishina formula equation (2.2), is the probability at $\bar{r}_{i'j'k'}$ of a gamma ray scattering from $(\bar{\Omega}_{m'}, E')$ to $(\bar{\Omega}_m, E)$ per unit interval at $(\bar{\Omega}_m, E)$. The exponential function represents simply the probability that photon reaches $\bar{r}_{ijk}$ from $\bar{r}_{i'j'k'}$ without any collision. d_m is the lattice spacing in the direction of motion, m. The δ-function represents the fact that photons travel in straight line between any two successive collisions, with no change in direction and energy.

In calculations the sampling is made from the normalized probability distribution. Let us define the collision kernel $C(\bar{r}_{i'j'k'}, \bar{\Omega}_{m'} \to \bar{\Omega}_m, E' \to E)$ as the expected number of photons leaving the collision per unit solid angle at $\bar{\Omega}_m$, and unit energy at E for a photon entering a collision at $(\bar{r}_{i'j'k'}, \bar{\Omega}_{m'}, E')$. The relation between the collision kernel and the Klein-Nishina formula is

$$C(\bar{r}_{i'j'k'},\bar{\Omega}_{m'}\rightarrow\bar{\Omega}_{m},E'\rightarrow E) = \frac{\mu_s(\bar{r}_{i'j'k'},E')}{\mu(\bar{r}_{i'j'k'},E')}$$

$$\cdot \frac{K(\bar{r}_{i'j'k'},\bar{\Omega}_{m'}\rightarrow\bar{\Omega}_{m},E'\rightarrow E)}{\mu_s(\bar{r}_{i'j'k'},E')} \qquad (A.2)$$

The first term of equation (A.2) represents the probability that a scattering collision has occurred and the second term is the normalized probability distribution for scattering. Similarly, we can define the transport kernel $T(\bar{r}_{i'j'k'},\rightarrow\bar{\Omega}_{ijk},\bar{\Omega}_{m},E)$ as the expected number of the next collision per unit volume at $\bar{r}_{ijk}$ for a photon leaving a source or a collision at $(\bar{r}_{i'j'k'},\bar{\Omega}_{m},E)$. $T(\bar{r}_{i'j'k'}\rightarrow\bar{r}_{ijk},\bar{\Omega}_{m},E)$ is the normalized transport probability distribution and can be found simply by multiplying the second term of equation (A.1) by the linear attenuation coefficient, $\mu(\bar{r}_{ijk},E)$.

$$T(\bar{r}_{i'j'k'}\rightarrow\bar{r}_{ijk},\bar{\Omega}_{m},E) = \mu(\bar{r}_{ijk},E)\ \mathrm{Exp}\Big[-\sum_{q=0}^{|\bar{r}_{ijk}-\bar{r}_{i'j'k'}|/d_m} \mu(\bar{r}_{i'j'k'} + q\bar{\Omega}_{m}d_{m},E)d_{m}\Big]\ \delta\left(\frac{\bar{r}_{ijk}-\bar{r}_{i;j'k'}}{|\bar{r}_{ijk}-\bar{r}_{i'j'k'}|} - \bar{\Omega}_{m}\right) . \qquad (A.3)$$

From equations (A.1), (A.2), and (A.3) one obtains,

$$P(\bar{r}_{i'j'k'} \to \bar{r}_{ijk}, \bar{\Omega}_{m} \to \bar{\Omega}_{m}, E' \to E) = [\mu(\bar{r}_{i'j'k'}, E')$$

$$\cdot C(\bar{r}_{i'j'k'}, \bar{\Omega}_{m'} \to \bar{\Omega}_{m}, E' \to E)]$$

$$\cdot \left[\frac{T(\bar{r}_{i'j'k'} \to \bar{r}_{ijk}, \bar{\Omega}_{m}, E)}{\mu(\bar{r}_{ijk}, E)}\right. \qquad (A.4)$$

In a random walk problem we ask in general for the state $(\bar{r}_{ijk}, \bar{\Omega}_{m}, E)$ of photon reached after n steps. On the other hand the Boltzmann transport equation gives us the total collision density, $\psi(\bar{r}_{ijk}, \bar{\Omega}_{m}, E)$, regardless of the number of steps to reach that state. More precisely

$$\psi(\bar{r}_{ijk}, \bar{\Omega}_{m}, E) = \lim_{K \to \infty} \sum_{n=1}^{K} \psi_{n}(\bar{r}_{ijk}, \bar{\Omega}_{m}, E).$$

It is interesting to note that using Boltzmann theory, we lose some information, in that knowledge of ψ_n is more informative than the knowledge of ∇. It should also be pointed out that ψ is a quantity denoting the average behavior of photons in the medium, while from the random walks of photons we can obtain information as to the fluctuation and variation from the expected value. Similarly,

$$\chi(\bar{r}_{ijk}, \Omega_{m}, E) = \lim_{K \to \infty} \sum_{n=1}^{K} \chi_{n}(\bar{r}_{ijk}, \bar{\Omega}_{m}, E).$$

Where χ_n and ψ_n were previously defined. We note χ_o by the source $S(\bar{r}_{ijk},\bar{\Omega}_m,E)$. Considering the definition of ψ_n, χ_n, and denoting the lattice volume by v, for photons entering their $n+1^{st}$ scattering at position $\bar{r}_{ijk}$, one obtains

$$\psi_{n+1}(\bar{r}_{ijk},\bar{\Omega}_m,E) = \sum_{i'j'k'} \chi_n(\bar{r}_{i'j'k'},\bar{\Omega}_m,E)T(\bar{r}_{i'j'k'} \rightarrow \bar{\Omega}_{ijk},\bar{\Omega}_m,E)\Delta v \qquad (A.5)$$

for $n = 0, 1, 2, \ldots$

Similarly,

$$\chi(\bar{r}_{ijk},\bar{\Omega}_m,E) = \sum_{m'} \int_{E'} \psi_n(\bar{r}_{i'j'k'},\bar{\Omega}_{m'},E') \cdot C(\bar{r}_{ijk},\bar{\Omega}_{m'}\rightarrow\bar{\Omega}_m,E'\rightarrow E)\Delta\Omega_m, \Delta E' \quad , \qquad (A.6)$$

for $n = 0, 1, 2, \ldots$

By summation over all n, and using the definition of χ_o, ψ, and χ previously defined, one obtains

$$\psi(\bar{r}_{ijk},\bar{\Omega}_m,E) = \sum_{i'j'k'} \chi(\bar{r}_{i'j'k'},\bar{\Omega}_m,E)T(\bar{r}_{i'j'k'}\rightarrow\bar{r}_{ijk},\bar{\Omega}_m,E)\Delta v, \qquad (A.7)$$

and similarly,

$$\chi(\bar{r}_{ijk},\bar{\Omega}_m,E) = \sum_{m'} \int_{E'} \psi(\bar{r}_{ijk},\bar{\Omega}_{m'},E') \cdot C(\bar{r}_{ijk},\bar{\Omega}_{m'}\rightarrow\bar{\Omega}_m,E'\rightarrow E)\Delta\Omega_{m'}dE' + S(\bar{r}_{ijk},\bar{\Omega}_m,E). \qquad (A.8)$$

χ can be eliminated between the equations (A.7) and (A.8), to obtain

$$\psi(\bar{r}_{ijk},\bar{\Omega}_m,E) = \sum_{i'j'k'} \sum_{m'} \int_E \psi(\bar{r}_{i'j'k'},\bar{\Omega}_{m'},E')$$

$$\cdot C(\bar{r}_{i'j'k'},\bar{\Omega}_{m'}\to\bar{\Omega}_m,E'\to E)\cdot T(\bar{r}_{i'j'k'}\to\bar{r}_{ijk},\bar{\Omega}_m,E)dE'\Delta\Omega_m,\Delta v$$

$$+ \sum_{i'j'k'} S(\bar{r}_{i'j'k'},\bar{\Omega}_m,E)\cdot T(\bar{r}_{i'j'k'}\to\bar{r}_{ijk},\bar{\Omega}_m,E)\Delta v. \quad (A.9)$$

The photon flux, $\phi(\bar{r}_{ijk},\bar{\Omega}_m,E)$ is related to the collision density by a very simple relation,

$$\psi(\bar{r}_{ijk},\bar{\Omega}_m,E) = \mu(\bar{r}_{ijk},E)\ \phi(\bar{r}_{ijk},\bar{\Omega}_m,E) \quad (A.10)$$

The transport equation for flux, ϕ, can be easily obtained by substitution of (A.10) into (A.9) and using equation (A.3),

$$\phi(\bar{r}_{ijk},\bar{\Omega}_m,E) = \sum_{m'} \sum_{i'j'k'} \int_{E'} \phi(\bar{r}_{i'j'k'},\bar{\Omega}_{m'},E')$$

$$\cdot P(\bar{r}_{i'j'k'}\to\bar{r}_{ijk},\bar{\Omega}_{m'}\to\bar{\Omega}_m,E'\to E)dE'\Delta\Omega_{m'}\ \Delta v$$

$$+ \frac{1}{\mu(\bar{r}_{ijk},E)} \sum_{i'j'k'} S(\bar{r}_{ijk},\bar{\Omega}_m,E)T(\bar{r}_{i'j'k'}\to\bar{r}_{ijk},\bar{\Omega}_m,E)\Delta v$$

(A.11)

The integral form of the Boltzmann equation now can be written by substituting (A.1) and (A.3) into equation (A.11), after summation over the δ-function, as follows

$$\phi(\bar{r}_{ijk},\bar{\Omega}_m,E) = \sum_{s=0}^{\infty} d_m \Big[\sum_{m'} \int_{E'} \phi(\bar{r}_{ijk}-sd_m\bar{\Omega}_m,\bar{\Omega}_m,E')$$

$$\cdot K(\bar{r}_{ijk}-sd_m\bar{\Omega}_m\bar{\Omega}_{m'},\rightarrow\bar{\Omega}_m,E'\rightarrow E)dE'\Delta\Omega_{m'}$$

$$+ S(\bar{r}_{ijk}-sd_m\bar{\Omega}_m,\bar{\Omega}_m,E)\Big] \text{Exp}\Big[-\sum_{s'=0}^{s} \mu(\bar{r}_{ijk}-s'd_m\bar{\Omega}_m,E)d_m\Big]$$

(A.12)

It is interesting to note the similarity of the above equation to the familiar form of the integral transport equation[22], except for that in the equation developed space and direction of motion of photons are discrete quantities. This is the basic assumption of the model used in this work. In the limit, a lattice distance, $d_m \rightarrow 0$ and $\Delta\Omega_m \rightarrow 0$ implying that the number of lattice points and directions become infinite, the two equations should be equivalent.

APPENDIX C

C.1. Tables of Results

The tables in this appendix are arranged as follows:

Table C.1. Energy and Dose Buildup Factors and the Quantity $\bar{\mu}_{en}^{air}/\mu_{en}^{air}(E_o)$ for 1MeV Photons in Slabs of Iron Followed by Water.

ENERGY BUILDUP IRON-WATER,1MEV

B1	B2=1	B2=2	B2=3	B2=4	B2=5	B2=6	B2=7	B2=8
1	2.617E+00	3.560E+00	4.610E+00	5.758E+00	6.996E+00	8.330E+00	9.753E+00	1.125E+01
2	3.463E+00	4.549E+00	5.714E+00	6.967E+00	8.305E+00	9.720E+00	1.124E+01	1.284E+01
3	4.390E+00	5.613E+00	6.897E+00	8.263E+00	9.684E+00	1.119E+01	1.281E+01	1.456E+01
4	5.382E+00	6.748E+00	8.163E+00	9.619E+00	1.114E+01	1.280E+01	1.452E+01	1.633E+01
5	6.440E+00	7.963E+00	9.482E+00	1.105E+01	1.266E+01	1.443E+01	1.624E+01	1.813E+01

DOSE BUILDUP IRON-WATER,1MEV

B1	B2=1	B2=2	B2=3	B2=4	B2=5	B2=6	B2=7	B2=8
1	2.672E+00	3.656E+00	4.755E+00	5.955E+00	7.255E+00	8.653E+00	1.014E+01	1.171E+01
2	3.546E+00	4.682E+00	5.906E+00	7.222E+00	8.627E+00	1.011E+01	1.170E+01	1.338E+01
3	4.502E+00	5.788E+00	7.141E+00	8.579E+00	1.007E+01	1.166E+01	1.336E+01	1.519E+01
4	5.526E+00	6.967E+00	8.462E+00	9.995E+00	1.161E+01	1.335E+01	1.515E+01	1.705E+01
5	6.619E+00	8.230E+00	9.840E+00	1.150E+01	1.320E+01	1.506E+01	1.696E+01	1.895E+01

$\bar{\mu}_{en}^{air}/\mu_{en}^{air}(E_o)$ IRON-WATER,1MEV

B1	B2=1	B2=2	B2=3	B2=4	B2=5	B2=6	B2=7	B2=8
1	1.034E+00	1.037E+00	1.040E+00	1.042E+00	1.043E+00	1.044E+00	1.045E+00	1.045E+00
2	1.033E+00	1.038E+00	1.041E+00	1.043E+00	1.044E+00	1.045E+00	1.045E+00	1.046E+00
3	1.033E+00	1.038E+00	1.041E+00	1.043E+00	1.046E+00	1.046E+00	1.046E+00	1.046E+00
4	1.033E+00	1.038E+00	1.042E+00	1.044E+00	1.046E+00	1.046E+00	1.047E+00	1.047E+00
5	1.033E+00	1.038E+00	1.042E+00	1.045E+00	1.046E+00	1.047E+00	1.047E+00	1.048E+00

Table C.2. Energy and Dose Buildup Factors and the Quantity $\mu_{en}^{air}/\mu_{en}^{air}(E_o)$ for 1MeV Photons in Slabs of Tin Followed by Water.

ENERGY BUILDUP TIN-WATER,1MEV

B1	B2=1	B2=2	B2=3	B2=4	B2=5	B2=6	B2=7	B2=8
2	3.186E+00	4.285E+00	5.462E+00	6.710E+00	8.063E+00	9.500E+00	1.105E+01	0.
4	4.579E+00	5.969E+00	7.408E+00	8.830E+00	1.038E+01	1.198E+01	0.	0.

DOSE BUILDUP TIN-WATER,1MEV

B1	B2=1	B2=2	B2=3	B2=4	B2=5	B2=6	B2=7	B2=8
2	3.262E+00	4.410E+00	5.645E+00	6.945E+00	8.386E+00	9.902E+00	1.154E+01	0.
4	4.703E+00	6.159E+00	7.675E+00	9.156E+00	1.081E+01	1.251E+01	0.	0.

$\mu_{en}^{air}/\mu_{en}^{air}(E_o)$ TIN-WATER,1MEV

B1	B2=1	B2=2	B2=3	B2=4	B2=5	B2=6	B2=7	B2=8
2	1.035E+00	1.038E+00	1.041E+00	1.041E+00	1.045E+00	1.047E+00	1.049E+00	1.049E+00
4	1.035E+00	1.038E+00	1.042E+00	1.042E+00	1.046E+00	1.048E+00	1.050E+00	1.051E+00

Table C.3. Energy and Dose Buildup Factors and the Quantity $\bar{\mu}_{en}^{air}/\mu_{en}^{air}(E_o)$ for 1MeV Photons in Slabs of Lead Followed by Water.

ENERGY BUILDUP LEAD-WATER,1MEV

B1	B2=1	B2=2	B2=3	B2=4	B2=5	B2=6	B2=7	B2=8
1	2.275E+00	3.234E+00	4.288E+00	5.442E+00	6.640E+00	7.986E+00	9.375E+00	1.089E+01
2	2.474E+00	3.724E+00	4.830E+00	6.091E+00	7.408E+00	8.799E+00	1.031E+01	1.192E+01
3	3.030E+00	4.177E+00	5.402E+00	6.722E+00	8.123E+00	9.630E+00	1.125E+01	1.294E+01
4	3.359E+00	4.601E+00	5.914E+00	7.316E+00	8.795E+00	1.041E+01	1.209E+01	1.389E+01
5	3.667E+00	4.998E+00	6.399E+00	7.922E+00	9.427E+00	1.119E+01	1.295E+01	1.485E+01

DOSE BUILDUP LEAD-WATER,1MEV

B1	B2=1	B2=2	B2=3	B2=4	B2=5	B2=6	B2=7	B2=8
1	2.319E+00	3.317E+00	4.417E+00	5.625E+00	6.880E+00	8.290E+00	9.744E+00	1.133E+01
2	2.732E+00	3.824E+00	4.981E+00	6.301E+00	7.683E+00	9.141E+00	1.072E+01	1.241E+01
3	3.099E+00	4.294E+00	5.575E+00	6.959E+00	8.430E+00	1.001E+01	1.171E+01	1.348E+01
4	3.438E+00	4.732E+00	6.111E+00	7.578E+00	9.132E+00	1.083E+01	1.259E+01	1.447E+01
5	3.757E+00	5.143E+00	6.611E+00	8.210E+00	9.791E+00	1.164E+01	1.349E+01	1.548E+01

$\bar{\mu}_{en}^{air}/\mu_{en}^{air}(E_o)$ LEAD-WATER,1MEV

B1	B2=1	B2=2	B2=3	B2=4	B2=5	B2=6	B2=7	B2=8
1	1.035E+00	1.037E+00	1.039E+00	1.041E+00	1.043E+00	1.044E+00	1.044E+00	1.044E+00
2	1.034E+00	1.037E+00	1.039E+00	1.041E+00	1.043E+00	1.044E+00	1.044E+00	1.045E+00
3	1.034E+00	1.037E+00	1.039E+00	1.041E+00	1.043E+00	1.044E+00	1.045E+00	1.045E+00
4	1.034E+00	1.037E+00	1.039E+00	1.042E+00	1.043E+00	1.044E+00	1.045E+00	1.045E+00
5	1.034E+00	1.036E+00	1.039E+00	1.042E+00	1.043E+00	1.044E+00	1.045E+00	1.045E+00

Table C.4. Energy and Dose Buildup Factors and the Quantity $\mu_{en}^{air}/\mu_{en}^{air}(E_0)$ for 1MeV Photons in Slabs of Tin Followed by Aluminum.

ENERGY BUILDUP TIN-ALUM.,1MEV

B1	B2=1	B2=2	B2=3	B2=4	B2=5	B2=6	B2=7	B2=8
2	3.151E+00	4.172E+00	5.252E+00	6.425E+00	7.630E+00	8.880E+00	1.017E+01	1.155E+01
4	4.524E+00	5.793E+00	7.089E+00	8.390E+00	9.760E+00	1.120E+01	0.	0.

DOSE BUILDUP TIN-ALUM.,1MEV

B1	B2=1	B2=2	B2=3	B2=4	B2=5	B2=6	B2=7	B2=8
2	3.220E+00	4.262E+00	5.366E+00	6.570E+00	7.796E+00	9.069E+00	1.038E+01	1.179E+01
4	4.637E+00	5.928E+00	7.250E+00	8.586E+00	9.976E+00	1.144E+01	0.	0.

$\mu_{en}^{air}/\mu_{en}^{air}(E_0)$ TIN-ALUM.,1MEV

B1	B2=1	B2=2	B2=3	B2=4	B2=5	B2=6	B2=7	B2=8
2	1.032E+00	1.029E+00	1.027E+00	1.027E+00	1.025E+00	1.024E+00	1.023E+00	1.023E+00
4	1.032E+00	1.028E+00	1.026E+00	1.026E+00	1.025E+00	1.023E+00	1.023E+00	1.022E+00

Table C.5. Energy and Dose Buildup Factors and the Quantity $\mu_{en}^{air}/\rho_{en}^{air}(E_o)$ for 1MeV Photons in Slabs of Lead Followed by Aluminum.

ENERGY BUILDUP LEAD-ALUM.,1MEV

B1	B2=1	B2=2	B2=3	B2=4	B2=5	B2=6	B2=7	B2=8
2	2.546E+00	3.631E+00	4.675E+00	5.770E+00	6.995E+00	8.270E+00	9.520E+00	1.087E+01
4	3.315E+00	4.470E+00	5.677E+00	6.900E+00	8.269E+00	9.730E+00	1.125E+01	0.

DOSE BUILDUP LEAD-ALUM.,1MEV

B1	B2=1	B2=2	B2=3	B2=4	B2=5	B2=6	B2=7	B2=8
2	2.699E+00	3.708E+00	4.776E+00	5.900E+00	7.147E+00	8.446E+00	9.720E+00	1.110E+01
4	3.389E+00	4.570E+00	5.804E+00	7.060E+00	8.443E+00	9.940E+00	1.149E+01	0.

$\mu_{en}^{air}/\rho_{en}^{air}(E_o)$ LEAD-ALUM.,1MEV

B1	B2=1	B2=2	B2=3	B2=4	B2=5	B2=6	B2=7	B2=8
2	1.032E+00	1.029E+00	1.027E+00	1.027E+00	1.025E+00	1.024E+00	1.024E+00	1.023E+00
4	1.032E+00	1.029E+00	1.027E+00	1.027E+00	1.025E+00	1.024E+00	1.023E+00	1.023E+00

Table C.6. Energy and Dose Buildup Factors and the Quantity $\bar{\mu}_{en}^{air}/\mu_{en}^{air}(E_o)$ for 1MeV Photons in Slabs of Water Followed by Iron.

ENERGY BUILDUP WATER-IRON,1MEV

B1	B2=1	B2=2	B2=3	B2=4	B2=5	B2=6	B2=7	B2=8
1	2.477E+00	3.243E+00	4.070E+00	4.952E+00	5.880E+00	6.870E+00	7.901E+00	9.001E+00
2	3.272E+00	4.085E+00	4.967E+00	5.902E+00	6.896E+00	7.922E+00	9.015E+00	1.016E+01
3	4.135E+00	4.994E+00	5.924E+00	6.917E+00	7.945E+00	9.029E+00	1.017E+01	1.136E+01
4	5.066E+00	5.966E+00	6.946E+00	7.971E+00	9.053E+00	1.019E+01	1.137E+01	1.260E+01
5	6.064E+00	7.004E+00	8.012E+00	9.082E+00	1.021E+01	1.139E+01	1.263E+01	1.389E+01

DOSE BUILDUP WATER-IRON,1MEV

B1	B2=1	B2=2	B2=3	B2=4	B2=5	B2=6	B2=7	B2=8
1	2.531E+00	3.324E+00	4.181E+00	5.095E+00	6.065E+00	7.082E+00	8.150E+00	9.290E+00
2	3.353E+00	4.197E+00	5.110E+00	6.079E+00	7.110E+00	8.173E+00	9.305E+00	1.049E+01
3	4.246E+00	5.138E+00	6.102E+00	7.131E+00	8.196E+00	9.320E+00	1.050E+01	1.174E+01
4	5.209E+00	6.144E+00	7.161E+00	8.224E+00	9.346E+00	1.052E+01	1.175E+01	1.302E+01
5	6.242E+00	7.220E+00	8.265E+00	9.381E+00	1.054E+01	1.177E+01	1.305E+01	1.436E+01

$\bar{\mu}_{en}^{air}/\mu_{en}^{air}(E_o)$ WATER-IRON,1MEV

B1	B2=1	B2=2	B2=3	B2=4	B2=5	B2=6	B2=7	B2=8
1	1.037E+00	1.036E+00	1.036E+00	1.036E+00	1.036E+00	1.036E+00	1.036E+00	1.036E+00
2	1.036E+00	1.036E+00	1.036E+00	1.036E+00	1.036E+00	1.036E+00	1.036E+00	1.036E+00
3	1.035E+00	1.036E+00	1.036E+00	1.036E+00	1.036E+00	1.036E+00	1.036E+00	1.036E+00
4	1.035E+00	1.036E+00	1.036E+00	1.036E+00	1.036E+00	1.036E+00	1.036E+00	1.036E+00
5	1.035E+00	1.036E+00	1.036E+00	1.036E+00	1.036E+00	1.036E+00	1.036E+00	1.036E+00

Table C.7. Energy and Dose Buildup Factors and the Quantity $\bar{\mu}_{en}^{air}/\mu_{en}^{air}(E_o)$ for 1MeV Photons in Slabs of Lead Followed by Iron.

ENERGY BUILDUP LEAD-IRON,1MEV

B1	B2=1	B2=2	B2=3	B2=4	B2=5	B2=6	B2=7	B2=8
1	2.187E+00	2.963E+00	3.786E+00	4.658E+00	5.586E+00	6.567E+00	7.596E+00	8.690E+00
2	2.552E+00	3.395E+00	4.274E+00	5.200E+00	6.179E+00	7.217E+00	8.301E+00	9.440E+00
3	2.892E+00	3.805E+00	4.740E+00	5.715E+00	6.748E+00	7.840E+00	8.978E+00	1.016E+01
4	3.199E+00	4.177E+00	5.176E+00	6.201E+00	7.271E+00	8.424E+00	9.615E+00	1.084E+01
5	3.487E+00	4.532E+00	5.576E+00	6.623E+00	7.767E+00	8.965E+00	1.021E+01	1.148E+01

DOSE BUILDUP LEAD-IRON,1MEV

B1	B2=1	B2=2	B2=3	B2=4	B2=5	B2=6	B2=7	B2=8
1	2.231E+00	3.034E+00	3.886E+00	4.791E+00	5.751E+00	6.768E+00	7.834E+00	8.968E+00
2	2.608E+00	3.482E+00	4.392E+00	5.352E+00	6.367E+00	7.442E+00	8.565E+00	9.745E+00
3	2.960E+00	3.906E+00	4.875E+00	5.886E+00	6.954E+00	8.087E+00	9.267E+00	1.049E+01
4	3.278E+00	4.291E+00	5.329E+00	6.389E+00	7.497E+00	8.693E+00	9.927E+00	1.120E+01
5	3.576E+00	4.658E+00	5.740E+00	6.831E+00	8.011E+00	9.253E+00	1.054E+01	1.186E+01

$\bar{\mu}_{en}^{air}/\mu_{en}^{air}(E_o)$ LEAD-IRON,1MEV

B1	B2=1	B2=2	B2=3	B2=4	B2=5	B2=6	B2=7	B2=8
1	1.037E+00	1.036E+00	1.036E+00	1.036E+00	1.036E+00	1.036E+00	1.036E+00	1.036E+00
2	1.037E+00	1.036E+00	1.036E+00	1.036E+00	1.036E+00	1.036E+00	1.036E+00	1.036E+00
3	1.036E+00	1.036E+00	1.036E+00	1.036E+00	1.036E+00	1.036E+00	1.036E+00	1.036E+00
4	1.036E+00	1.036E+00	1.036E+00	1.036E+00	1.036E+00	1.036E+00	1.036E+00	1.036E+00
5	1.036E+00	1.036E+00	1.036E+00	1.036E+00	1.036E+00	1.036E+00	1.036E+00	1.036E+00

Table C.8. Energy and Dose Buildup Factors and the Quantity $\bar{\mu}_{en}^{air}/\mu_{en}^{air}(E_o)$ for 1MeV Photons in Slabs of Water Followed by Tin.

ENERGY BUILDUP WATER-TIN,1MEV

B1	B2=1	B2=2	B2=3	B2=4	B2=5	B2=6	B2=7	B2=8
2	2.805E+00	3.296E+00	3.816E+00	4.340E+00	4.882E+00	5.410E+00	5.950E+00	0.
4	4.160E+00	4.597E+00	5.040E+00	5.590E+00	6.150E+00	6.690E+00	0.	0.

DOSE BUILDUP WATER-TIN,1MEV

B1	B2=1	B2=2	B2=3	B2=4	B2=5	B2=6	B2=7	B2=8
2	2.878E+00	3.388E+00	3.928E+00	4.473E+00	5.037E+00	5.587E+00	6.148E+00	0.
4	4.288E+00	4.743E+00	5.203E+00	5.775E+00	6.358E+00	6.920E+00	0.	0.

$\bar{\mu}_{en}^{air}/\mu_{en}^{air}(E_o)$ WATER-TIN,1MEV

B1	B2=1	B2=2	B2=3	B2=4	B2=5	B2=6	B2=7	B2=8
2	1.040E+00	1.040E+00	1.040E+00	1.040E+00	1.040E+00	1.040E+00	1.040E+00	1.040E+00
4	1.041E+00	1.040E+00	1.040E+00	1.040E+00	1.040E+00	1.040E+00	1.040E+00	1.040E+00

Table C.9. Energy and Dose Buildup Factors and the Quantity $\mu_{en}^{-air}/\mu_{en}^{air}(E_o)$ for 1MeV Photons in Slabs of Water Followed by Lead.

ENERGY BUILDUP WATER-LEAD,1MEV

B1	B2=1	B2=2	B2=3	B2=4	B2=5	B2=6	B2=7	B2=8
1	1.789E+00	1.996E+00	2.200E+00	2.395E+00	2.583E+00	2.755E+00	2.929E+00	3.105E+00
2	2.220E+00	2.362E+00	2.530E+00	2.700E+00	2.866E+00	3.020E+00	3.178E+00	3.340E+00
3	2.670E+00	2.740E+00	2.860E+00	3.005E+00	3.146E+00	3.280E+00	3.422E+00	3.568E+00
4	3.140E+00	3.129E+00	3.210E+00	3.313E+00	3.430E+00	3.544E+00	3.667E+00	3.796E+00
5	3.627E+00	3.519E+00	3.557E+00	3.631E+00	3.719E+00	3.812E+00	3.913E+00	4.024E+00

DOSE BUILDUP WATER-LEAD,1MEV

B1	B2=1	B2=2	B2=3	B2=4	B2=5	B2=6	B2=7	B2=8
1	1.818E+00	2.031E+00	2.241E+00	2.442E+00	2.636E+00	2.813E+00	2.993E+00	3.174E+00
2	2.265E+00	2.410E+00	2.582E+00	2.757E+00	2.928E+00	3.087E+00	3.250E+00	3.417E+00
3	2.731E+00	2.801E+00	2.923E+00	3.072E+00	3.217E+00	3.355E+00	3.501E+00	3.652E+00
4	3.219E+00	3.203E+00	3.285E+00	3.390E+00	3.510E+00	3.627E+00	3.754E+00	3.887E+00
5	3.725E+00	3.607E+00	3.644E+00	3.719E+00	3.809E+00	3.904E+00	4.008E+00	4.123E+00

$\mu_{en}^{-air}/\mu_{en}^{air}(E_o)$ WATER-LEAD,1MEV

B1	B2=1	B2=2	B2=3	B2=4	B2=5	B2=6	B2=7	B2=8
1	1.037E+00	1.035E+00	1.035E+00	1.034E+00	1.034E+00	1.033E+00	1.033E+00	1.033E+00
2	1.037E+00	1.035E+00	1.034E+00	1.034E+00	1.033E+00	1.033E+00	1.033E+00	1.033E+00
3	1.037E+00	1.035E+00	1.034E+00	1.033E+00	1.033E+00	1.033E+00	1.033E+00	1.033E+00
4	1.037E+00	1.035E+00	1.034E+00	1.033E+00	1.033E+00	1.033E+00	1.033E+00	1.033E+00
5	1.037E+00	1.035E+00	1.034E+00	1.033E+00	1.033E+00	1.033E+00	1.033E+00	1.032E+00

Table C.10. Energy and Dose Buildup Factors and the Quantity $\bar{\mu}_{en}^{air}/\mu_{en}^{air}(E_o)$ for 1MeV Photons in Slabs of Iron Followed by Lead.

ENERGY BUILDUP IRON-LEAD,1MEV

B1	B2=1	B2=2	B2=3	B2=4	B2=5	B2=6	B2=7	B2=8
1	1.791E+00	2.003E+00	2.208E+00	2.403E+00	2.587E+00	2.758E+00	2.931E+00	3.106E+00
2	2.213E+00	2.360E+00	2.527E+00	2.697E+00	2.863E+00	3.015E+00	3.172E+00	3.333E+00
3	2.652E+00	2.727E+00	2.856E+00	2.999E+00	3.136E+00	3.272E+00	3.412E+00	3.555E+00
4	3.109E+00	3.108E+00	3.194E+00	3.299E+00	3.416E+00	3.532E+00	3.655E+00	3.778E+00
5	3.559E+00	3.502E+00	3.531E+00	3.608E+00	3.696E+00	3.792E+00	3.895E+00	4.005E+00

DOSE BUILDUP IRON-LEAD,1MEV

B1	B2=1	B2=2	B2=3	B2=4	B2=5	B2=6	B2=7	B2=8
1	1.820E+00	2.039E+00	2.249E+00	2.451E+00	2.641E+00	2.816E+00	2.995E+00	3.176E+00
2	2.258E+00	2.407E+00	2.579E+00	2.754E+00	2.926E+00	3.081E+00	3.243E+00	3.410E+00
3	2.712E+00	2.787E+00	2.919E+00	3.065E+00	3.206E+00	3.347E+00	3.491E+00	3.638E+00
4	3.187E+00	3.181E+00	3.268E+00	3.375E+00	3.494E+00	3.615E+00	3.742E+00	3.868E+00
5	3.653E+00	3.590E+00	3.617E+00	3.695E+00	3.785E+00	3.883E+00	3.989E+00	4.103E+00

$\bar{\mu}_{en}^{air}/\mu_{en}^{air}(E_o)$ IRON-LEAD,1MEV

B1	B2=1	B2=2	B2=3	B2=4	B2=5	B2=6	B2=7	B2=8
1	1.037E+00	1.035E+00	1.035E+00	1.034E+00	1.034E+00	1.033E+00	1.033E+00	1.033E+00
2	1.037E+00	1.035E+00	1.034E+00	1.034E+00	1.033E+00	1.033E+00	1.033E+00	1.033E+00
3	1.037E+00	1.035E+00	1.034E+00	1.033E+00	1.033E+00	1.033E+00	1.033E+00	1.033E+00
4	1.037E+00	1.035E+00	1.034E+00	1.033E+00	1.033E+00	1.033E+00	1.033E+00	1.033E+00
5	1.037E+00	1.035E+00	1.034E+00	1.033E+00	1.033E+00	1.033E+00	1.033E+00	1.032E+00

Table C.11. Energy and Dose Buildup Factors and the Quantity $\bar{\mu}_{en}^{air}/\mu_{en}^{air}(E_o)$ for 3MeV Photons in Slabs of Iron Followed by Water.

ENERGY BUILDUP IRON-WATER,3MEV

B1	B2=1	B2=2	B2=3	B2=4	B2=5	B2=6	B2=7	B2=8
1	1.964E+00	2.444E+00	2.930E+00	3.420E+00	3.911E+00	4.402E+00	4.887E+00	5.365E+00
2	2.424E+00	2.912E+00	3.400E+00	3.889E+00	4.381E+00	4.860E+00	5.339E+00	5.810E+00
3	2.903E+00	3.395E+00	3.882E+00	4.371E+00	4.847E+00	5.323E+00	5.793E+00	6.256E+00
4	3.402E+00	3.893E+00	4.379E+00	4.852E+00	5.324E+00	5.7[illegible]E+00	5.245E+00	6.700E+00
5	3.915E+00	4.406E+00	4.874E+00	5.342E+00	5.802E+00	6.255E+00	6.710E+00	7.145E+00

DOSE BUILDUP IRON-WATER,3MEV

B1	B2=1	B2=2	B2=3	B2=4	B2=5	B2=6	B2=7	B2=8
1	2.159E+00	2.738E+00	3.327E+00	3.917E+00	4.512E+00	5.105E+00	5.693E+00	6.271E+00
2	2.716E+00	3.300E+00	3.893E+00	4.486E+00	5.082E+00	5.663E+00	6.243E+00	6.813E+00
3	3.294E+00	3.889E+00	4.479E+00	5.072E+00	5.650E+00	6.227E+00	6.797E+00	7.358E+00
4	3.896E+00	4.493E+00	5.082E+00	5.657E+00	6.231E+00	6.796E+00	7.350E+00	7.901E+00
5	4.519E+00	5.118E+00	5.687E+00	6.255E+00	6.815E+00	7.365E+00	7.917E+00	8.445E+00

$\bar{\mu}_{en}^{air}/\mu_{en}^{air}(E_o)$ IRON-WATER,3MEV

B1	B2=1	B2=2	B2=3	B2=4	B2=5	B2=6	B2=7	B2=8
1	1.203E+00	1.204E+00	1.205E+00	1.205E+00	1.206E+00	1.207E+00	1.207E+00	1.207E+00
2	1.205E+00	1.206E+00	1.206E+00	1.207E+00	1.207E+00	1.208E+00	1.208E+00	1.209E+00
3	1.206E+00	1.206E+00	1.207E+00	1.208E+00	1.208E+00	1.209E+00	1.209E+00	1.210E+00
4	1.206E+00	1.208E+00	1.208E+00	1.209E+00	1.210E+00	1.210E+00	1.210E+00	1.211E+00
5	1.207E+00	1.209E+00	1.210E+00	1.210E+00	1.211E+00	1.211E+00	1.211E+00	1.212E+00

Table C.12. Energy and Dose Buildup Factors and the Quantity $\bar{\mu}_{en}^{air}/\mu_{en}^{air}(E_o)$ for 3MeV Photons in Slabs of Tin Followed by Water.

ENERGY BUILDUP TIN-WATER,3MEV

B1	B2=1	B2=2	B2=3	B2=4	B2=5	B2=6	B2=7	B2=8
2	2.331E+00	2.822E+00	3.310E+00	3.800E+00	4.289E+00	4.770E+00	5.259E+00	5.750E+00
4	3.234E+00	3.737E+00	4.224E+00	4.695E+00	5.164E+00	5.644E+00	0.	0.

DOSE BUILDUP TIN-WATER,3MEV

B1	B2=1	B2=2	B2=3	B2=4	B2=5	B2=6	B2=7	B2=8
2	2.599E+00	3.195E+00	3.785E+00	4.376E+00	4.971E+00	5.556E+00	6.150E+00	6.745E+00
4	3.689E+00	4.304E+00	4.896E+00	5.466E+00	6.038E+00	6.623E+00	0.	0.

$\bar{\mu}_{en}^{air}/\mu_{en}^{air}(E_o)$ TIN-WATER,3MEV

B1	B2=1	B2=2	B2=3	B2=4	B2=5	B2=6	B2=7	B2=8
2	1.202E+00	1.205E+00	1.206E+00	1.208E+00	1.207E+00	1.209E+00	1.209E+00	1.210E+00
4	1.204E+00	1.207E+00	1.209E+00	1.209E+00	1.210E+00	1.211E+00	1.211E+00	1.212E+00

Table C.13. Energy and Dose Buildup Factors and the Quantity $\bar{\mu}_{en}^{air}/\mu_{en}^{air}(E_o)$ for 3MeV Photons in Slabs of Lead Followed by Water.

ENERGY BUILDUP LEAD-WATER,3MEV

B1	B2=1	B2=2	B2=3	B2=4	B2=5	B2=6	B2=7	B2=8
1	1.837E+00	2.322E+00	2.809E+00	3.299E+00	3.791E+00	4.283E+00	4.770E+00	5.250E+00
2	2.159E+00	2.658E+00	3.151E+00	3.643E+00	4.134E+00	4.621E+00	5.100E+00	5.574E+00
3	2.489E+00	3.005E+00	3.503E+00	3.996E+00	4.489E+00	4.959E+00	5.431E+00	5.901E+00
4	2.831E+00	3.362E+00	3.866E+00	4.359E+00	4.834E+00	5.306E+00	5.777E+00	6.241E+00
5	3.184E+00	3.733E+00	4.239E+00	4.719E+00	5.192E+00	5.662E+00	6.134E+00	6.580E+00

DOSE BUILDUP LEAD-WATER,3MEV

B1	B2=1	B2=2	B2=3	B2=4	B2=5	B2=6	B2=7	B2=8
1	2.005E+00	2.590E+00	3.179E+00	3.771E+00	4.364E+00	4.961E+00	5.551E+00	6.131E+00
2	2.387E+00	2.994E+00	3.591E+00	4.188E+00	4.782E+00	5.373E+00	5.953E+00	6.526E+00
3	2.782E+00	3.412E+00	4.016E+00	4.616E+00	5.203E+00	5.785E+00	6.357E+00	6.926E+00
4	3.190E+00	3.842E+00	4.459E+00	5.050E+00	5.635E+00	6.209E+00	6.780E+00	7.342E+00
5	3.613E+00	4.291E+00	4.903E+00	5.495E+00	6.072E+00	6.643E+00	7.215E+00	7.757E+00

$\bar{\mu}_{en}^{air}/\mu_{en}^{air}(E_o)$ LEAD-WATER,3MEV

B1	B2=1	B2=2	B2=3	B2=4	B2=5	B2=6	B2=7	B2=8
1	1.200E+00	1.203E+00	1.204E+00	1.205E+00	1.206E+00	1.207E+00	1.207E+00	1.207E+00
2	1.198E+00	1.203E+00	1.205E+00	1.206E+00	1.207E+00	1.208E+00	1.208E+00	1.208E+00
3	1.197E+00	1.203E+00	1.205E+00	1.207E+00	1.208E+00	1.209E+00	1.209E+00	1.209E+00
4	1.196E+00	1.203E+00	1.206E+00	1.208E+00	1.209E+00	1.209E+00	1.210E+00	1.210E+00
5	1.196E+00	1.204E+00	1.207E+00	1.209E+00	1.210E+00	1.210E+00	1.211E+00	1.211E+00

Table C.14. Energy and Dose Buildup Factors and the Quantity $\bar{\mu}_{en}^{air}/\mu_{en}^{air}(E_o)$ for 3MeV Photons in Slabs of Tin Followed by Aluminum.

ENERGY BUILDUP TIN-ALUM.,3MEV

B1	B2=1	B2=2	B2=3	B2=4	B2=5	B2=6	B2=7	B2=8
2	2.324E+00	2.815E+00	3.309E+00	3.825E+00	4.321E+00	4.830E+00	5.340E+00	5.840E+00
4	3.234E+00	3.746E+00	4.250E+00	4.735E+00	5.239E+00	5.740E+00	0.	0.

DOSE BUILDUP TIN-ALUM.,3MEV

B1	B2=1	B2=2	B2=3	B2=4	B2=5	B2=6	B2=7	B2=8
2	2.586E+00	3.177E+00	3.772E+00	4.391E+00	4.992E+00	5.609E+00	6.226E+00	6.830E+00
4	3.681E+00	4.301E+00	4.910E+00	5.494E+00	6.107E+00	6.715E+00	0.	0.

$\bar{\mu}_{en}^{air}/\mu_{en}^{air}(E_o)$ TIN-ALUM.,3MEV

B1	B2=1	B2=2	B2=3	B2=4	B2=5	B2=6	B2=7	B2=8
2	1.198E+00	1.199E+00	1.200E+00	1.200E+00	1.202E+00	1.203E+00	1.204E+00	1.204E+00
4	1.200E+00	1.202E+00	1.203E+00	1.203E+00	1.205E+00	1.206E+00	1.206E+00	1.207E+00

Table C.15. Energy and Dose Buildup Factors and the Quantity $\mu_{en}^{air}/\mu_{en}^{air}(E_o)$ for 3MeV Photons in Slabs of Lead Followed by Aluminum.

ENERGY BUILDUP LEAD-ALUM.,3MEV

B1	B2=1	B2=2	B2=3	B2=4	B2=5	B2=6	B2=7	B2=8
2	2.150E+00	2.648E+00	3.146E+00	3.649E+00	4.155E+00	4.660E+00	5.163E+00	5.706E+00
4	2.828E+00	3.364E+00	3.883E+00	4.388E+00	4.891E+00	5.393E+00	5.894E+00	6.433E+00

DOSE BUILDUP LEAD-ALUM.,3MEV

B1	B2=1	B2=2	B2=3	B2=4	B2=5	B2=6	B2=7	B2=8
2	2.373E+00	2.974E+00	3.574E+00	4.177E+00	4.791E+00	5.403E+00	6.012E+00	6.668E+00
4	3.181E+00	3.833E+00	4.462E+00	5.069E+00	5.683E+00	6.295E+00	6.903E+00	7.556E+00

$\mu_{en}^{air}/\mu_{en}^{air}(E_o)$ LEAD-ALUM.,3MEV

B1	B2=1	B2=2	B2=3	B2=4	B2=5	B2=6	B2=7	B2=8
2	1.194E+00	1.198E+00	1.199E+00	1.199E+00	1.202E+00	1.203E+00	1.204E+00	1.204E+00
4	1.193E+00	1.199E+00	1.201E+00	1.201E+00	1.204E+00	1.205E+00	1.206E+00	1.207E+00

Table C.16. Energy and Dose Buildup Factors and the Quantity $\mu_{en}^{-air} / \mu_{en}^{air}(E_o)$ for 3MeV Photons in Slabs of Water Followed by Iron.

ENERGY BUILDUP WATER-IRON,3MEV

B1	B2=1	B2=2	B2=3	B2=4	B2=5	B2=6	B2=7	B2=8
1	1.953E+00	2.421E+00	2.905E+00	3.407E+00	3.927E+00	4.460E+00	4.998E+00	5.547E+00
2	2.436E+00	2.923E+00	3.430E+00	3.953E+00	4.488E+00	5.026E+00	5.576E+00	6.127E+00
3	2.923E+00	3.430E+00	3.958E+00	4.498E+00	5.036E+00	5.592E+00	6.145E+00	6.707E+00
4	3.435E+00	3.965E+00	4.515E+00	5.063E+00	5.621E+00	6.176E+00	6.740E+00	7.316E+00
5	3.906E+00	4.452E+00	5.003E+00	5.561E+00	6.124E+00	6.680E+00	7.256E+00	7.834E+00

DOSE BUILDUP WATER-IRON,3MEV

B1	B2=1	B2=2	B2=3	B2=4	B2=5	B2=6	B2=7	B2=8
1	2.144E+00	2.606E+00	3.284E+00	3.890E+00	4.519E+00	5.161E+00	5.810E+00	6.472E+00
2	2.719E+00	3.305E+00	3.919E+00	4.548E+00	5.199E+00	5.847E+00	6.512E+00	7.177E+00
3	3.303E+00	3.914E+00	4.553E+00	5.207E+00	5.861E+00	6.534E+00	7.203E+00	7.883E+00
4	3.917E+00	4.559E+00	5.225E+00	5.899E+00	6.569E+00	7.243E+00	7.928E+00	8.624E+00
5	4.484E+00	5.146E+00	5.815E+00	6.495E+00	7.181E+00	7.857E+00	8.558E+00	9.256E+00

$\mu_{en}^{-air} / \mu_{en}^{air}(E_o)$ WATER-IRON,3MEV

B1	B2=1	B2=2	B2=3	B2=4	B2=5	B2=6	B2=7	B2=8
1	1.198E+00	1.131E+00	1.199E+00	1.200E+00	1.202E+00	1.203E+00	1.203E+00	1.203E+00
2	1.197E+00	1.199E+00	1.200E+00	1.201E+00	1.203E+00	1.204E+00	1.205E+00	1.205E+00
3	1.197E+00	1.199E+00	1.201E+00	1.203E+00	1.204E+00	1.205E+00	1.206E+00	1.206E+00
4	1.198E+00	1.200E+00	1.202E+00	1.204E+00	1.205E+00	1.206E+00	1.207E+00	1.207E+00
5	1.199E+00	1.201E+00	1.203E+00	1.205E+00	1.206E+00	1.207E+00	1.208E+00	1.208E+00

Table C.17. Energy and Dose Buildup Factors and the Quantity $\mu_{en}^{air}/\rho_{en}^{air}(E_0)$ for 3MeV Photons in Slabs of Lead Followed by Iron.

ENERGY BUILDUP LEAD-IRON,3MEV

B1	B2=1	B2=2	B2=3	B2=4	B2=5	B2=6	B2=7	B2=8
1	1.801E+00	2.264E+00	2.749E+00	3.242E+00	3.753E+00	4.279E+00	4.815E+00	5.354E+00
2	2.126E+00	2.614E+00	3.111E+00	3.622E+00	4.147E+00	4.676E+00	5.214E+00	5.757E+00
3	2.461E+00	2.974E+00	3.488E+00	4.015E+00	4.547E+00	5.081E+00	5.626E+00	6.167E+00
4	2.803E+00	3.344E+00	3.874E+00	4.408E+00	4.947E+00	5.491E+00	6.040E+00	6.579E+00
5	3.166E+00	3.731E+00	4.273E+00	4.815E+00	5.359E+00	5.910E+00	6.459E+00	7.000E+00

DOSE BUILDUP LEAD-IRON,3MEV

B1	B2=1	B2=2	B2=3	B2=4	B2=5	B2=6	B2=7	B2=8
1	1.958E+00	2.514E+00	3.092E+00	3.691E+00	4.310E+00	4.942E+00	5.589E+00	6.238E+00
2	2.344E+00	2.932E+00	3.532E+00	4.149E+00	4.784E+00	5.424E+00	6.074E+00	6.728E+00
3	2.742E+00	3.363E+00	3.986E+00	4.623E+00	5.269E+00	5.916E+00	6.575E+00	7.229E+00
4	3.155E+00	3.809E+00	4.450E+00	5.100E+00	5.754E+00	6.414E+00	7.080E+00	7.732E+00
5	3.582E+00	4.274E+00	4.933E+00	5.593E+00	6.256E+00	6.925E+00	7.590E+00	8.247E+00

$\mu_{en}^{air}/\rho_{en}^{air}(E_0)$ LEAD-IRON,3MEV

B1	B2=1	B2=2	B2=3	B2=4	B2=5	B2=6	B2=7	B2=8
1	1.196E+00	1.198E+00	1.199E+00	1.200E+00	1.201E+00	1.202E+00	1.203E+00	1.203E+00
2	1.194E+00	1.197E+00	1.199E+00	1.201E+00	1.202E+00	1.203E+00	1.204E+00	1.204E+00
3	1.192E+00	1.197E+00	1.200E+00	1.202E+00	1.204E+00	1.205E+00	1.205E+00	1.206E+00
4	1.192E+00	1.198E+00	1.201E+00	1.203E+00	1.205E+00	1.206E+00	1.206E+00	1.207E+00
5	1.192E+00	1.199E+00	1.202E+00	1.204E+00	1.206E+00	1.207E+00	1.207E+00	1.208E+00

Table C.18. Energy and Dose Buildup Factors and the Quantity $\mu_{en}^{air}/\mu_{en}^{air}(E_o)$ for 3MeV Photons in Slabs of Water Followed by Tin.

ENERGY BUILDUP WATER-TIN,3MEV

B1	B2=1	B2=2	B2=3	B2=4	B2=5	B2=6	B2=7	B2=8
2	2.340E+00	2.782E+00	3.252E+00	3.735E+00	4.254E+00	4.780E+00	5.325E+00	5.895E+00
4	3.302E+00	3.800E+00	4.330E+00	4.865E+00	5.429E+00	6.010E+00	0.	0.

DOSE BUILDUP WATER-TIN,3MEV

B1	B2=1	B2=2	B2=3	B2=4	B2=5	B2=6	B2=7	B2=8
2	2.592E+00	3.118E+00	3.690E+00	4.295E+00	4.894E+00	5.519E+00	6.176E+00	6.862E+00
4	3.735E+00	4.331E+00	4.968E+00	5.606E+00	6.294E+00	7.003E+00	0.	0.

$\mu_{en}^{air}/\mu_{en}^{air}(E_o)$ WATER-TIN,3MEV

B1	B2=1	B2=2	B2=3	B2=4	B2=5	B2=6	B2=7	B2=8
2	1.188E+00	1.189E+00	1.190E+00	1.190E+00	1.193E+00	1.196E+00	1.197E+00	1.198E+00
4	1.189E+00	1.190E+00	1.192E+00	1.192E+00	1.196E+00	1.193E+00	1.200E+00	1.200E+00

Table C.18. Energy and Dose Buildup Factors and the Quantity $\mu_{en}^{air}/\mu_{en}^{air}(E_o)$ for 3MeV Photons in Slabs of Water Followed by Tin.

ENERGY BUILDUP WATER-TIN,3MEV

B1	B2=1	B2=2	B2=3	B2=4	B2=5	B2=6	B2=7	B2=8
2	2.340E+00	2.782E+00	3.252E+00	3.735E+00	4.254E+00	4.780E+00	5.325E+00	5.895E+00
4	3.302E+00	3.800E+00	4.330E+00	4.865E+00	5.429E+00	6.010E+00	0.	0.

DOSE BUILDUP WATER-TIN,3MEV

B1	B2=1	B2=2	B2=3	B2=4	B2=5	B2=6	B2=7	B2=8
2	2.592E+00	3.118E+00	3.690E+00	4.255E+00	4.834E+00	5.519E+00	6.176E+00	6.862E+00
4	3.735E+00	4.331E+00	4.968E+00	5.606E+00	6.294E+00	7.003E+00	0.	0.

$\mu_{en}^{air}/\mu_{en}^{air}(E_o)$ WATER-TIN,3MEV

B1	B2=1	B2=2	B2=3	B2=4	B2=5	B2=6	B2=7	B2=8
2	1.188E+00	1.189E+00	1.190E+00	1.190E+00	1.193E+00	1.196E+00	1.197E+00	1.198E+00
4	1.188E+00	1.190E+00	1.192E+00	1.192E+00	1.196E+00	1.193E+00	1.200E+00	1.200E+00

Table C.19. Energy and Dose Buildup Factors and the Quantity $\mu_{en}^{air}/\rho_{en}^{air}(E_0)$ for 3MeV Photons in Slabs of Aluminum Followed by Tin.

ENERGY BUILDUP ALUM.-TIN,3MEV

B1	B2=1	B2=2	B2=3	B2=4	B2=5	B2=6	B2=7	B2=8
2	2.327E+00	2.764E+00	3.234E+00	3.724E+00	4.232E+00	4.760E+00	5.310E+00	5.880E+00
4	3.274E+00	3.766E+00	4.284E+00	4.815E+00	5.374E+00	5.950E+00	0.	0.

DOSE BUILDUP ALUM.-TIN,3MEV

B1	B2=1	B2=2	B2=3	B2=4	B2=5	B2=6	B2=7	B2=8
2	2.577E+00	3.098E+00	3.660E+00	4.242E+00	4.857E+00	5.495E+00	6.158E+00	6.844E+00
4	3.705E+00	4.293E+00	4.916E+00	5.549E+00	6.231E+00	6.931E+00	0.	0.

$\mu_{en}^{air}/\rho_{en}^{air}(E_0)$ ALUM.-TIN,3MEV

B1	B2=1	B2=2	B2=3	B2=4	B2=5	B2=6	B2=7	B2=8
2	1.189E+00	1.189E+00	1.190E+00	1.190E+00	1.194E+00	1.196E+00	1.197E+00	1.198E+00
4	1.189E+00	1.190E+00	1.192E+00	1.192E+00	1.196E+00	1.198E+00	1.200E+00	1.200E+00

Table C.20. Energy and Dose Buildup Factors and the Quantity $\mu_{en}^{air}/\rho_{en}^{air}(E_o)$ for 3MeV Photons in Slabs of Water Followed by Lead.

ENERGY BUILDUP WATER-LEAD,3MEV

B1	B2=1	B2=2	B2=3	B2=4	B2=5	B2=6	B2=7	B2=8
1	1.752E+00	2.029E+00	2.324E+00	2.634E+00	2.957E+00	3.286E+00	3.626E+00	3.972E+00
2	2.147E+00	2.464E+00	2.762E+00	3.096E+00	3.424E+00	3.765E+00	4.114E+00	4.472E+00
3	2.566E+00	2.871E+00	3.201E+00	3.541E+00	3.887E+00	4.235E+00	4.592E+00	4.960E+00
4	2.985E+00	3.294E+00	3.640E+00	3.983E+00	4.343E+00	4.702E+00	5.068E+00	5.448E+00
5	3.406E+00	3.725E+00	4.071E+00	4.429E+00	4.797E+00	5.170E+00	5.545E+00	5.936E+00

DOSE BUILDUP WATER-LEAD,3MEV

B1	B2=1	B2=2	B2=3	B2=4	B2=5	B2=6	B2=7	B2=8
1	1.880E+00	2.200E+00	2.543E+00	2.904E+00	3.281E+00	3.664E+00	4.061E+00	4.465E+00
2	2.340E+00	2.683E+00	3.033E+00	3.431E+00	3.829E+00	4.224E+00	4.632E+00	5.050E+00
3	2.828E+00	3.180E+00	3.564E+00	3.961E+00	4.367E+00	4.774E+00	5.192E+00	5.622E+00
4	3.318E+00	3.673E+00	4.076E+00	4.479E+00	4.900E+00	5.322E+00	5.750E+00	6.195E+00
5	3.810E+00	4.177E+00	4.580E+00	5.000E+00	5.438E+00	5.871E+00	6.310E+00	6.768E+00

$\mu_{en}^{air}/\rho_{en}^{air}(E_o)$ WATER-LEAD,3MEV

B1	B2=1	B2=2	B2=3	B2=4	B2=5	B2=6	B2=7	B2=8
1	1.170E+00	1.167E+00	1.165E+00	1.165E+00	1.165E+00	1.165E+00	1.166E+00	1.166E+00
2	1.169E+00	1.165E+00	1.165E+00	1.165E+00	1.166E+00	1.166E+00	1.166E+00	1.166E+00
3	1.168E+00	1.165E+00	1.165E+00	1.165E+00	1.166E+00	1.167E+00	1.167E+00	1.167E+00
4	1.168E+00	1.165E+00	1.165E+00	1.166E+00	1.167E+00	1.167E+00	1.168E+00	1.168E+00
5	1.168E+00	1.166E+00	1.166E+00	1.167E+00	1.167E+00	1.168E+00	1.168E+00	1.169E+00

Table C.21. Energy and Dose Buildup Factors and the Quantity $\bar{\mu}_{en}^{air}/\mu_{en}^{air}(E_0)$ for 3MeV Photons in Slabs of Iron Followed by Lead.

ENERGY BUILDUP IRON-LEAD,3MEV

B1	B2=1	B2=2	B2=3	B2=4	B2=5	B2=6	B2=7	B2=8
1	1.709E+00	1.996E+00	2.295E+00	2.607E+00	2.924E+00	3.256E+00	3.595E+00	3.940E+00
2	2.109E+00	2.405E+00	2.715E+00	3.039E+00	3.374E+00	3.711E+00	4.064E+00	4.420E+00
3	2.525E+00	2.829E+00	3.145E+00	3.484E+00	3.822E+00	4.168E+00	4.525E+00	4.891E+00
4	2.953E+00	3.257E+00	3.591E+00	3.929E+00	4.280E+00	4.632E+00	4.995E+00	5.370E+00
5	3.393E+00	3.702E+00	4.034E+00	4.384E+00	4.746E+00	5.100E+00	5.478E+00	5.860E+00

DOSE BUILDUP IRON-LEAD,3MEV

B1	B2=1	B2=2	B2=3	B2=4	B2=5	B2=6	B2=7	B2=8
1	1.830E+00	2.163E+00	2.510E+00	2.872E+00	3.244E+00	3.630E+00	4.025E+00	4.427E+00
2	2.297E+00	2.638E+00	2.998E+00	3.376E+00	3.767E+00	4.162E+00	4.574E+00	4.990E+00
3	2.783E+00	3.129E+00	3.501E+00	3.890E+00	4.292E+00	4.698E+00	5.117E+00	5.543E+00
4	3.285E+00	3.634E+00	4.022E+00	4.418E+00	4.830E+00	5.243E+00	5.668E+00	6.106E+00
5	3.802E+00	4.156E+00	4.542E+00	4.952E+00	5.375E+00	5.793E+00	6.236E+00	6.683E+00

$\bar{\mu}_{en}^{air}/\mu_{en}^{air}(E_0)$ IRON-LEAD,3MEV

B1	B2=1	B2=2	B2=3	B2=4	B2=5	B2=6	B2=7	B2=8
1	1.171E+00	1.167E+00	1.166E+00	1.165E+00	1.165E+00	1.166E+00	1.166E+00	1.166E+00
2	1.159E+00	1.166E+00	1.165E+00	1.165E+00	1.166E+00	1.166E+00	1.166E+00	1.167E+00
3	1.163E+00	1.166E+00	1.166E+00	1.166E+00	1.167E+00	1.167E+00	1.167E+00	1.168E+00
4	1.170E+00	1.167E+00	1.167E+00	1.167E+00	1.168E+00	1.168E+00	1.169E+00	1.169E+00
5	1.171E+00	1.168E+00	1.167E+00	1.166E+00	1.168E+00	1.169E+00	1.169E+00	1.169E+00

Table C.22. Energy and Dose Buildup Factors and the Quantity $\mu_{en}^{air}/\mu_{en}^{air}(E_o)$ for 6MeV Photons in Slabs of Iron Followed by Water.

ENERGY BUILDUP IRON-WATER,6MEV

B1	B2=1	B2=2	B2=3	B2=4	B2=5	B2=6	B2=7	B2=8
1	1.533E+00	1.940E+00	2.246E+00	2.546E+00	2.833E+00	3.122E+00	3.396E+00	3.650E+00
2	1.899E+00	2.195E+00	2.491E+00	2.781E+00	3.063E+00	3.336E+00	3.599E+00	3.852E+00
3	2.176E+00	2.459E+00	2.741E+00	3.019E+00	3.295E+00	3.549E+00	3.800E+00	4.042E+00
4	2.466E+00	2.730E+00	2.997E+00	3.265E+00	3.514E+00	3.764E+00	4.003E+00	4.233E+00
5	2.759E+00	3.039E+00	3.257E+00	3.502E+00	3.745E+00	3.980E+00	4.206E+00	4.423E+00

DOSE BUILDUP IRON-WATER,6MEV

B1	B2=1	B2=2	B2=3	B2=4	B2=5	B2=6	B2=7	B2=8
1	1.305E+00	2.189E+00	2.570E+00	2.943E+00	3.307E+00	3.662E+00	4.004E+00	4.335E+00
2	2.141E+00	2.508E+00	2.876E+00	3.238E+00	3.592E+00	3.936E+00	4.268E+00	4.589E+00
3	2.494E+00	2.841E+00	3.192E+00	3.537E+00	3.874E+00	4.198E+00	4.512E+00	4.815E+00
4	2.853E+00	3.186E+00	3.515E+00	3.842E+00	4.160E+00	4.469E+00	4.767E+00	5.055E+00
5	3.209E+00	3.541E+00	3.845E+00	4.145E+00	4.442E+00	4.741E+00	5.023E+00	5.295E+00

$\mu_{en}^{air}/\mu_{en}^{air}(E_o)$ IRON-WATER,6MEV

B1	B2=1	B2=2	B2=3	B2=4	B2=5	B2=6	B2=7	B2=8
1	1.273E+00	1.254E+00	1.260E+00	1.257E+00	1.255E+00	1.255E+00	1.254E+00	1.254E+00
2	1.271E+00	1.263E+00	1.259E+00	1.257E+00	1.255E+00	1.254E+00	1.254E+00	1.254E+00
3	1.270E+00	1.262E+00	1.259E+00	1.257E+00	1.255E+00	1.255E+00	1.254E+00	1.254E+00
4	1.271E+00	1.263E+00	1.259E+00	1.257E+00	1.255E+00	1.255E+00	1.255E+00	1.254E+00
5	1.272E+00	1.255E+00	1.261E+00	1.258E+00	1.255E+00	1.255E+00	1.255E+00	1.254E+00

Table C.23. Energy and Dose Buildup Factors and the Quantity $\bar{\mu}_{en}^{air}/\mu_{en}^{air}(E_o)$ for 6MeV Photons in Slabs of Tin Followed by Water.

ENERGY BUILDUP TIN-WATER,6MEV

B1	B2=1	B2=2	B2=3	B2=4	B2=5	B2=6	B2=7	B2=8
2	1.300E+00	2.045E+00	2.391E+00	2.680E+00	2.960E+00	3.240E+00	3.500E+00	3.750E+00
4	2.307E+00	2.561E+00	2.824E+00	3.0[illegible]E+00	3.342E+00	3.590E+00	3.830E+00	4.060E+00

DOSE BUILDUP TIN-WATER,6MEV

B1	B2=1	B2=2	B2=3	B2=4	B2=5	B2=6	B2=7	B2=8
2	2.020E+00	2.[illegible]E+00	2.7[illegible]E+00	3.117E+00	3.46[illegible]E+00	3.807E+00	4.129E+00	4.440E+00
4	2.573E+00	2.[illegible]E+00	3.30[illegible]E+00	3.623E+00	3.[illegible]E+00	4.24[illegible]E+00	4.543E+00	4.828E+00

$\bar{\mu}_{en}^{air}/\mu_{en}^{air}(E_o)$ TIN-WATER,6MEV

B1	B2=1	B2=2	B2=3	B2=4	B2=5	B2=6	B2=7	B2=8
2	1.275E+00	1.265E+00	1.260E+00	1.260E+00	1.256E+00	1.253E+00	1.252E+00	1.251E+00
4	1.[illegible]E+00	1.249E+00	1.24[illegible]E+00	1.263E+00	1.257E+00	1.254E+00	1.252E+00	1.251E+00

Table C.24. Energy and Dose Buildup Factors and the Quantity $\mu_{en}^{-air}/\mu_{en}^{air}(E_o)$ for 6MeV Photons in Slabs of Lead Followed by Water.

ENERGY BUILDUP LEAD-WATER,6MEV

B1	B2=1	B2=2	B2=3	B2=4	B2=5	B2=6	B2=7	B2=8
1	1.534E+00	1.843E+00	2.152E+00	2.457E+00	2.747E+00	3.033E+00	3.309E+00	3.577E+00
2	1.701E+00	2.002E+00	2.302E+00	2.596E+00	2.882E+00	3.159E+00	3.427E+00	3.688E+00
3	1.885E+00	2.174E+00	2.462E+00	2.746E+00	3.023E+00	3.289E+00	3.549E+00	3.802E+00
4	2.086E+00	2.359E+00	2.633E+00	2.904E+00	3.163E+00	3.424E+00	3.674E+00	3.913E+00
5	2.307E+00	2.560E+00	2.815E+00	3.068E+00	3.320E+00	3.564E+00	3.802E+00	4.036E+00

DOSE BUILDUP LEAD-WATER,6MEV

B1	B2=1	B2=2	B2=3	B2=4	B2=5	B2=6	B2=7	B2=8
1	1.531E+00	2.058E+00	2.450E+00	2.827E+00	3.194E+00	3.551E+00	3.896E+00	4.231E+00
2	1.692E+00	2.258E+00	2.640E+00	3.007E+00	3.364E+00	3.710E+00	4.045E+00	4.371E+00
3	2.125E+00	2.485E+00	2.844E+00	3.197E+00	3.541E+00	3.874E+00	4.199E+00	4.514E+00
4	2.334E+00	2.723E+00	3.062E+00	3.396E+00	3.725E+00	4.045E+00	4.357E+00	4.661E+00
5	2.559E+00	2.982E+00	3.295E+00	3.608E+00	3.920E+00	4.221E+00	4.519E+00	4.812E+00

$\mu_{en}^{-air}/\mu_{en}^{air}(E_o)$ LEAD-WATER,6MEV

B1	B2=1	B2=2	B2=3	B2=4	B2=5	B2=6	B2=7	B2=8
1	1.275E+00	1.266E+00	1.261E+00	1.258E+00	1.256E+00	1.255E+00	1.254E+00	1.254E+00
2	1.273E+00	1.265E+00	1.260E+00	1.258E+00	1.256E+00	1.255E+00	1.254E+00	1.254E+00
3	1.273E+00	1.266E+00	1.261E+00	1.258E+00	1.256E+00	1.255E+00	1.255E+00	1.254E+00
4	1.276E+00	1.268E+00	1.263E+00	1.259E+00	1.257E+00	1.256E+00	1.255E+00	1.255E+00
5	1.279E+00	1.270E+00	1.265E+00	1.261E+00	1.259E+00	1.257E+00	1.256E+00	1.255E+00

Table C.25. Energy and Dose Buildup Factors and the Quantity $\mu_{en}^{air}/\mu_{en}^{air}(E_o)$ for 6MeV Photons in Slabs of Tin Followed by Aluminum.

ENERGY BUILDUP TIN-ALUM.,6MEV

B1	B2=1	B2=2	B2=3	B2=4	B2=5	B2=6	B2=7	B2=8
2	1.001E+00	2.097E+00	2.[illegible]E+00	2.700E+00	2.934E+00	3.300E+00	3.590E+00	3.860E+00
4	2.334E+00	2.603E+00	2.[illegible]E+00	3.170E+00	3.465E+00	3.720E+00	-0.	-0.

DOSE BUILDUP TIN-ALUM.,6MEV

B1	B2=1	B2=2	B2=3	B2=4	B2=5	B2=6	B2=7	B2=8
2	2.022E+00	2.395E+00	2.772E+00	3.165E+00	3.522E+00	3.906E+00	4.270E+00	4.609E+00
4	2.715E+00	3.055E+00	3.[illegible]E+00	3.756E+00	4.103E+00	4.443E+00	0.	0.

$\mu_{en}^{air}/\mu_{en}^{air}(E_o)$ TIN-ALUM.,6MEV

B1	B2=1	B2=2	B2=3	B2=4	B2=5	B2=6	B2=7	B2=8
2	1.260E+00	1.272E+00	1.[illegible]E+00	1.268E+00	1.265E+00	1.263E+00	1.262E+00	1.262E+00
4	1.283E+00	1.276E+00	1.271E+00	1.271E+00	1.268E+00	1.266E+00	1.264E+00	1.264E+00

Table C.26. Energy and Dose Buildup Factors and the Quantity $\mu_{en}^{air}/\rho_{en}^{air}(E_o)$ for 6MeV Photons in Slabs of Lead Followed by Aluminum.

ENERGY BUILDUP LEAD-ALUM.,6MEV

B1	B2=1	B2=2	B2=3	B2=4	B2=5	B2=6	B2=7	B2=8
2	1.697E+00	1.997E+00	2.2[illegible]E+00	2.605E+00	2.901E+00	3.195E+00	3.490E+00	3.780E+00
4	2.102E+00	2.[illegible]E+00	2.[illegible]E+00	2.965E+00	3.247E+00	3.528E+00	3.808E+00	4.093E+00

DOSE BUILDUP LEAD-ALUM.,6MEV

B1	B2=1	B2=2	B2=3	B2=4	B2=5	B2=6	B2=7	B2=8
2	1.8[illegible]E+00	2.267E+00	2.64[illegible]E+00	3.035E+00	3.403E+00	3.774E+00	4.143E+00	4.507E+00
4	2.4[illegible]E+00	2.77[illegible]E+00	3.12[illegible]E+00	3.49[illegible]E+00	3.84[illegible]E+00	4.199E+00	4.550E+00	4.[illegible]04E+00

$\mu_{en}^{air}/\rho_{en}^{air}(E_o)$ LEAD-ALUM.,6MEV

B1	B2=1	B2=2	B2=3	B2=4	B2=5	B2=6	B2=7	B2=8
2	1.27[illegible]E+00	1.271E+00	1.2[illegible]E+00	1.268E+00	1.265E+00	1.263E+00	1.262E+00	1.262E+00
4	1.27[illegible]E+00	1.27[illegible]E+00	1.[illegible]E+00	1.271E+00	1.26[illegible]E+00	1.265E+00	1.264E+00	1.263E+00

Table C.27. Energy and Dose Buildup Factors and the Quantity $\bar{\mu}_{en}^{air}/\mu_{en}^{air}(E_o)$ for 6MeV Photons in Slabs of Water Followed by Iron.

ENERGY BUILDUP WATER-IRON,6MEV

B1	B2=1	B2=2	B2=3	B2=4	B2=5	B2=6	B2=7	B2=8
1	1.530E+00	1.939E+00	2.307E+00	2.644E+00	2.98[illegible]E+00	3.348E+00	3.715E+00	4.090E+00
2	2.[illegible]23E+00	2.366E+00	2.705E+00	3.05[illegible]+00	3.421E+00	3.7[illegible]E+00	4.170E+00	4.55[illegible]E+00
3	2.3[illegible]4E+00	2.721E+00	3.0[illegible]E+00	3.461E+00	3.83[illegible]E+00	4.22[illegible]E+00	4.613E+00	5.007E+00
4	2.6[illegible]6E+00	3.076E+00	3.462E+00	3.850E+00	4.242E+00	4.64[illegible]E+00	5.040E+00	5.442E+00
5	3.01[illegible]E+00	3.42[illegible]E+00	3.823E+00	4.22[illegible]E+00	4.633E+00	5.04[illegible]E+00	5.450E+00	5.85[illegible]E+00

DOSE BUILDUP WATER-IRON,6MEV

B1	B2=1	B2=2	B2=3	B2=4	B2=5	B2=6	B2=7	B2=8
1	1.875E+00	2.270E+00	2.63[illegible]E+00	3.113E+00	3.55[illegible]E+00	4.022E+00	4.497E+00	4.980E+00
2	2.30[illegible]E+00	2.737E+00	3.19[illegible]E+00	3.644E+00	4.115E+00	4.596E+00	5.087E+00	5.585E+00
3	2.73[illegible]E+00	3.13[illegible]E+00	3.57[illegible]E+00	4.160E+00	4.65[illegible]E+00	5.154E+00	5.661E+00	5.173E+00
4	3.15[illegible]E+00	3.54[illegible]E+00	4.15[illegible]E+00	4.66[illegible]E+00	5.17[illegible]E+00	5.69[illegible]E+00	6.215E+00	6.73[illegible]E+00
5	3.5[illegible]E+00	4.03[illegible]E+00	4.61[illegible]E+00	5.14[illegible]E+00	5.68[illegible]E+00	6.21[illegible]E+00	6.749E+00	7.281E+00

$\bar{\mu}_{en}^{air}/\mu_{en}^{air}(E_o)$ WATER-IRON,6MEV

B1	B2=1	B2=2	B2=3	B2=4	B2=5	B2=6	B2=7	B2=8
1	1.233E+00	1.286E+00	1.29[illegible]E+00	1.285E+00	1.287E+00	1.287E+00	1.288E+00	1.288E+00
2	1.273E+00	1.281E+00	1.282E+00	1.285E+00	1.287E+00	1.288E+00	1.289E+00	1.290E+00
3	1.272E+00	1.278E+00	1.281E+00	1.284E+00	1.287E+00	1.289E+00	1.290E+00	1.291E+00
4	1.269E+00	1.276E+00	1.28[illegible]E+00	1.284E+00	1.28[illegible]E+00	1.290E+00	1.291E+00	1.292E+00
5	1.267E+00	1.276E+00	1.28[illegible]E+00	1.284E+00	1.28[illegible]E+00	1.290E+00	1.292E+00	1.292E+00

Table C.28. Energy and Dose Buildup Factors and the Quantity $\bar{\mu}_{en}^{air}/\mu_{en}^{air}(E_o)$ for 6MeV Photons in Slabs of Lead Followed by Iron.

ENERGY BUILDUP LEAD-IRON,6MEV

B1	B2=1	B2=2	B2=3	B2=4	B2=5	B2=6	B2=7	B2=8
1	1.500E+00	1.730E+00	2.097E+00	2.41[illegible]E+00	2.758E+00	3.100E+00	3.457E+00	3.824E+00
2	1.6[illegible]8E+00	1.959E+00	2.303E+00	2.631E+00	2.971E+00	3.323E+00	3.683E+00	4.054E+00
3	1.8[illegible]6E+00	2.206E+00	2.527E+00	2.861E+00	3.205E+00	3.560E+00	3.925E+00	4.295E+00
4	2.125E+00	2.444E+00	2.771E+00	3.104E+00	3.450E+00	3.812E+00	4.179E+00	4.551E+00
5	2.379E+00	2.704E+00	3.045E+00	3.374E+00	3.724E+00	4.082E+00	4.449E+00	4.820E+00

DOSE BUILDUP LEAD-IRON,6MEV

B1	B2=1	B2=2	B2=3	B2=4	B2=5	B2=6	B2=7	B2=8
1	1.550E+00	2.020E+00	2.412E+00	2.824E+00	3.25[illegible]E+00	3.702E+00	4.152E+00	4.605E+00
2	1.[illegible]9E+00	2.27[illegible]E+00	2.67[illegible]E+00	3.100E+00	3.53[illegible]E+00	3.[illegible]93E+00	4.458E+00	4.937E+00
3	2.157E+00	2.555E+00	2.9[illegible]E+00	3.400E+00	3.84[illegible]E+00	4.305E+00	4.775E+00	5.257E+00
4	2.453E+00	2.855E+00	3.287E+00	3.724E+00	4.17[illegible]E+00	4.63[illegible]E+00	5.113E+00	5.59[illegible]E+00
5	2.733E+00	3.2[illegible]E+00	3.6[illegible]E+00	4.07[illegible]E+00	4.53[illegible]E+00	4.[illegible]05E+00	5.472E+00	5.953E+00

$\bar{\mu}_{en}^{air}/\mu_{en}^{air}(E_o)$ LEAD-IRON,6MEV

B1	B2=1	B2=2	B2=3	B2=4	B2=5	B2=6	B2=7	B2=8
1	1.300E+00	1.291E+00	1.287E+00	1.286E+00	1.287E+00	1.287E+00	1.287E+00	1.287E+00
2	1.293E+00	1.289E+00	1.2[illegible]E+00	1.287E+00	1.28[illegible]E+00	1.289E+00	1.289E+00	1.289E+00
3	1.291E+00	1.290E+00	1.289E+00	1.289E+00	1.29[illegible]E+00	1.291E+00	1.291E+00	1.291E+00
4	1.291E+00	1.292E+00	1.292E+00	1.292E+00	1.293E+00	1.293E+00	1.294E+00	1.294E+00
5	1.293E+00	1.295E+00	1.296E+00	1.296E+00	1.296E+00	1.296E+00	1.297E+00	1.297E+00

Table C.29. Energy and Dose Buildup Factors and the Quantity $\mu_{en}^{-air}/\mu_{en}^{air}(E_o)$ for 6MeV Photons in Slabs of Water Followed by Tin.

ENERGY BUILDUP WATER-TIN,6MEV

B1	B2=1	B2=2	B2=3	B2=4	B2=5	B2=6	B2=7	B2=8
2	1.[illegible]E+00	2.330E+00	2.[illegible]E+00	3.100E+00	3.51[illegible]E+00	3.9[illegible]E+00	4.460E+00	4.96[illegible]E+00
4	2.6[illegible]E+00	3.122E+00	3.[illegible]E+00	4.0[illegible]E+00	4.56[illegible]E+00	5.0[illegible]E+00	-0.	-0.

DOSE BUILDUP WATER-TIN,6MEV

B1	B2=1	B2=2	B2=3	B2=4	B2=5	B2=6	B2=7	B2=8
2	2.27[illegible]E+00	2.711E+00	3.1[illegible]E+00	3.712E+00	4.28[illegible]E+00	4.90[illegible]E+00	5.546E+00	6.213E+00
4	3.15[illegible]E+00	3.71[illegible]E+00	4.31[illegible]E+00	4.93[illegible]E+00	5.6[illegible]E+00	6.35[illegible]E+00	0.	0.

$\mu_{en}^{-air}/\mu_{en}^{air}(E_o)$ WATER-TIN,6MEV

B1	B2=1	B2=2	B2=3	B2=4	B2=5	B2=6	B2=7	B2=8
2	1.280E+00	1.287E+00	1.292E+00	1.292E+00	1.30[illegible]E+00	1.310E+00	1.314E+00	1.316E+00
4	1.270E+00	1.281E+00	1.29[illegible]E+00	1.296E+00	1.30[illegible]E+00	1.315E+00	1.320E+00	1.324E+00

Table C.30. Energy and Dose Buildup Factors and the Quantity $\mu_{en}^{-air}/\mu_{en}^{air}(E_0)$ for 6MeV Photons in Slabs of Aluminum Followed by Tin.

ENERGY BUILDUP ALUM.-TIN,6MEV

B1	B2=1	B2=2	B2=3	B2=4	B2=5	B2=6	B2=7	B2=8
2	1.[illegible]+00	2.[illegible]+00	2.[illegible]+00	3.[illegible]+00	3.44[illegible]+00	3.9[illegible]+00	4.3[illegible]+00	3.[illegible]+00
4	[illegible]	[illegible]	[illegible]	[illegible]	[illegible]	[illegible]+00	-0.	-0.

DOSE BUILDUP ALUM.-TIN,6MEV

B1	B2=1	B2=2	B2=3	B2=4	B2=5	B2=6	B2=7	B2=8
2	2.[illegible]+00	2.[illegible]+00	3.[illegible]+00	3.[illegible]+00	4.[illegible]+00	4.[illegible]+00	5.441[illegible]+00	4.[illegible]+00
4	[illegible]	[illegible]	[illegible]	[illegible]	[illegible]	[illegible]	0.	0.

$\mu_{en}^{-air}/\mu_{en}^{air}(E_0)$ ALUM.-TIN,6MEV

B1	B2=1	B2=2	B2=3	B2=4	B2=5	B2=6	B2=7	B2=8
2	1.[illegible]E+00	1.[illegible]E+00	1.[illegible]E+00	1.[illegible]E+00	1.304E+00	1.310E+00	1.314E+00	1.316E+00
4	1.[illegible]E+00	1.[illegible]E+00	1.[illegible]E+00	1.[illegible]E+00	1.307E+00	1.316E+00	1.321E+00	1.324E+00

Table C.31. Energy and Dose Buildup Factors and the Quantity $\mu_{en}^{-air}/\mu_{en}^{air}(E_o)$ for 6MeV Photons in Slabs of Water Followed by Lead.

ENERGY BUILDUP WATER-LEAD,6MEV

B1	B2=1	B2=2	B2=3	B2=4	B2=5	B2=6	B2=7	B2=8
1	1.55[illegible]E+00	1.772E+00	2.00[illegible]E+00	2.26[illegible]E+00	2.554E+00	2.870E+00	3.21[illegible]E+00	3.59[illegible]E+00
2	1.90[illegible]E+00	2.155E+00	2.440E+00	2.74[illegible]E+00	3.0[illegible]7E+00	3.461E+00	3.87[illegible]E+00	4.312E+00
3	2.237E+00	2.532E+00	2.86[illegible]E+00	3.214[illegible]E+00	3.604E+00	4.0[illegible]3E+00	4.49[illegible]E+00	4.99[illegible]E+00
4	2.59[illegible]E+00	2.90[illegible]E+00	3.26[illegible]E+00	3.66[illegible]E+00	4.10[illegible]E+00	4.5[illegible]E+00	5.10[illegible]E+00	5.66[illegible]E+00
5	2.3[illegible]E+00	3.25[illegible]E+00	3.65[illegible]E+00	4.10[illegible]E+00	4.59[illegible]E+00	5.12[illegible]E+00	5.69[illegible]E+00	6.31[illegible]E+00

DOSE BUILDUP WATER-LEAD,6MEV

B1	B2=1	B2=2	B2=3	B2=4	B2=5	B2=6	B2=7	B2=8
1	1.70[illegible]E+00	1.97[illegible]E+00	2.27[illegible]E+00	2.61[illegible]E+00	2.97[illegible]E+00	3.3[illegible]E+00	3.83[illegible]E+00	4.31[illegible]E+00
2	2.13[illegible]E+00	2.454E+00	2.820E+00	3.21[illegible]E+00	3.65[illegible]E+00	4.142E+00	4.57[illegible]E+00	5.23[illegible]E+00
3	2.54[illegible]E+00	2.92[illegible]E+00	3.34[illegible]E+00	3.80[illegible]E+00	4.31[illegible]E+00	4.87[illegible]E+00	5.47[illegible]E+00	6.12[illegible]E+00
4	2.95[illegible]E+00	3.38[illegible]E+00	3.85[illegible]E+00	4.38[illegible]E+00	4.96[illegible]E+00	5.59[illegible]E+00	6.26[illegible]E+00	6.99[illegible]E+00
5	3.34[illegible]E+00	3.82[illegible]E+00	4.35[illegible]E+00	4.93[illegible]E+00	5.58[illegible]E+00	6.28[illegible]E+00	7.02[illegible]E+00	7.82[illegible]E+00

$\mu_{en}^{-air}/\mu_{en}^{air}(E_o)$ WATER-LEAD,6MEV

B1	B2=1	B2=2	B2=3	B2=4	B2=5	B2=6	B2=7	B2=8
1	1.259E+00	1.266E+00	1.267E+00	1.269[illegible]E+00	1.273E+00	1.275E+00	1.276E+00	1.277E+00
2	1.2[illegible]6E+00	1.2[illegible]E+00	1.264E+00	1.26[illegible]E+00	1.27[illegible]E+00	1.277E+00	1.27[illegible]E+00	1.28[illegible]E+00
3	1.25[illegible]E+00	1.25[illegible]E+00	1.2[illegible]E+00	1.2[illegible]E+00	1.274E+00	1.27[illegible]E+00	1.28[illegible]E+00	1.282[illegible]E+00
4	1.247E+00	1.25[illegible]E+00	1.26[illegible]E+00	1.26[illegible]E+00	1.27[illegible]E+00	1.27[illegible]E+00	1.28[illegible]E+00	1.28[illegible]E+00
5	1.245E+00	1.252E+00	1.26[illegible]E+00	1.26[illegible]E+00	1.27[illegible]E+00	1.28[illegible]E+00	1.28[illegible]E+00	1.285E+00

Table C.32. Energy and Dose Buildup Factors and the Quantity $\bar{\mu}_{en}^{air}/\mu_{en}^{air}(E_o)$ for 6MeV Photons in Slabs of Iron Followed by Lead.

ENERGY BUILDUP IRON-LEAD,6MEV

B1	B2=1	B2=2	B2=3	B2=4	B2=5	B2=6	B2=7	B2=8
1	1.485E+00	1.639E+00	1.814E+00	2.164E+00	2.437E+00	2.742E+00	3.075E+00	3.441E+00
2	1.793E+00	2.022E+00	2.261E+00	2.571E+00	2.882E+00	3.237E+00	3.629E+00	4.035E+00
3	2.097E+00	2.359E+00	2.660E+00	2.996E+00	3.357E+00	3.753E+00	4.185E+00	4.655E+00
4	2.426E+00	2.730E+00	3.068E+00	3.436E+00	3.846E+00	4.292E+00	4.777E+00	5.303E+00
5	2.767E+00	3.105E+00	3.484E+00	3.897E+00	4.352E+00	4.854E+00	5.390E+00	5.973E+00

DOSE BUILDUP IRON-LEAD,6MEV

B1	B2=1	B2=2	B2=3	B2=4	B2=5	B2=6	B2=7	B2=8
1	1.521E+00	1.876E+00	2.150E+00	2.479E+00	2.833E+00	3.221E+00	3.643E+00	4.116E+00
2	1.993E+00	2.292E+00	2.625E+00	2.998E+00	3.407E+00	3.860E+00	4.354E+00	4.890E+00
3	2.336E+00	2.730E+00	3.113E+00	3.542E+00	4.013E+00	4.533E+00	5.091E+00	5.699E+00
4	2.803E+00	3.139E+00	3.623E+00	4.113E+00	4.647E+00	5.231E+00	5.863E+00	6.543E+00
5	3.233E+00	3.659E+00	4.162E+00	4.704E+00	5.305E+00	5.959E+00	6.665E+00	7.424E+00

$\bar{\mu}_{en}^{air}/\mu_{en}^{air}(E_o)$ IRON-LEAD,6MEV

B1	B2=1	B2=2	B2=3	B2=4	B2=5	B2=6	B2=7	B2=8
1	1.277E+00	1.270E+00	1.269E+00	1.271E+00	1.273E+00	1.275E+00	1.276E+00	1.277E+00
2	1.267E+00	1.265E+00	1.268E+00	1.272E+00	1.276E+00	1.279E+00	1.280E+00	1.281E+00
3	1.263E+00	1.265E+00	1.269E+00	1.274E+00	1.279E+00	1.282E+00	1.284E+00	1.285E+00
4	1.263E+00	1.266E+00	1.271E+00	1.276E+00	1.280E+00	1.283E+00	1.287E+00	1.289E+00
5	1.263E+00	1.267E+00	1.273E+00	1.279E+00	1.285E+00	1.289E+00	1.290E+00	1.292E+00

Table C.33. Scattered Energy Buildup Factors, $B_E^S(b_1,b_2)$, for 1MeV Photons in Two-Layered Slabs of Iron-Water and Lead-Water.

	$B_E^S(b_1,b_2)$ Iron-Water 1MeV						
b_2 \ b_1	1	2	3	4	5	6	7
1	2.209	2.158	2.165	2.169	2.154	2.176	2.198
2	3.302	3.323	3.348	3.366	3.357	3.397	3.435
3	4.670	4.678	4.713	4.748	4.720	4.750	4.780
4	6.084	6.143	6.218	6.243	6.223	6.260	6.290
5	7.770	7.821	7.878	7.937	7.898	7.920	7.940
6	9.472	9.550	9.666	9.859	9.831	9.871	9.905
7	11.60	11.62	11.77	12.00	11.96	12.00	12.03
8	13.78	13.88	14.20	14.35	14.25	14.29	14.33

	$B_E^S(b_1,b_2)$ Lead-Water 1MeV						
b_2 \ b_1	1	2	3	4	5	6	7
1	2.068	2.015	1.962	1.937	1.897	1.865	1.833
2	3.204	3.074	2.998	2.963	2.899	2.867	2.838
3	4.733	4.311	4.279	4.229	4.110	4.060	4.010
4	6.364	5.889	5.724	5.659	5.607	5.540	5.493
5	7.956	7.647	7.423	7.333	7.148	7.060	7.004
6	9.993	9.392	9.309	9.287	9.201	9.080	8.980
7	12.13	11.72	11.66	11.53	11.40	11.29	11.20
8	14.84	14.34	14.17	14.12	13.99	13.88	13.79

Table C.34. Scattered Energy Buildup Factors, $B_E^S(b_1,b_2)$, for 1MeV Photons in Two-Layered Slabs of Water-Iron and Lead-Iron.

	$B_E^S(b_1,b_2)$ Water-Iron 1MeV						
b_2 \ b_1	1	2	3	4	5	6	7
1	1.967	1.984	1.958	1.964	1.963	1.950	1.939
2	2.857	2.856	2.839	2.840	2.848	2.814	2.796
3	3.798	3.795	3.793	3.794	3.796	3.770	3.746
4	4.795	4.820	4.839	4.835	4.848	4.826	4.798
5	5.973	6.000	5.981	5.993	6.005	5.980	5.954
6	7.233	7.237	7.255	7.272	7.301	7.270	7.240
7	8.633	8.668	8.655	8.677	8.720	8.700	8.670
8	10.10	10.12	10.14	10.15	10.18	10.16	10.13

	$B_E^S(b_1,b_2)$ Lead-Iron 1MeV						
b_2 \ b_1	1	2	3	4	5	6	7
1	1.916	1.873	1.865	1.851	1.844	1.835	1.825
2	2.785	2.719	2.707	2.683	2.674	2.664	2.655
3	3.693	3.630	3.619	3.612	3.584	3.574	3.564
4	4.664	4.628	4 623	4.616	4.556	4.548	4.540
5	5.852	5.813	5.811	5.771	5.752	5.740	5.735
6	7.233	7.190	7.190	7.167	7.127	7.115	7.100
7	8.781	8.729	8.726	8.706	8.675	8.665	8.650
8	10.35	10.29	10.29	10.28	10.25	10.24	10.22

Table C.35. Scattered Energy Buildup Factors, $B_E^S(b_1,b_2)$, for 1MeV Photons in Two-Layered Slabs of Water-Lead and Iron-Lead.

	$B_E^S(b_1,b_2)$ Water-Lead 1MeV						
b_2 \ b_1	1	2	3	4	5	6	7
1	1.424	1.403	1.401	1.394	1.385	1.365	1.346
2	1.692	1.656	1.657	1.648	1.628	1.608	1.588
3	1.944	1.899	1.884	1.885	1.867	1.852	1.840
4	2.160	2.118	2.110	2.093	2.083	2.068	2.058
5	2.341	2.303	2.295	2.282	2.268	2.248	2.240
6	2.509	2.476	2.466	2.456	2.444	2.420	2.410
7	2.657	2.630	2.622	2.609	2.590	2.570	2.560
8	2.790	2.766	2.756	2.739	2.718	2.700	2.690

	$B_E^S(b_1,b_2)$ Iron-Lead 1MeV						
b_2 \ b_1	1	2	3	4	5	6	7
1	1.456	1.419	1.404	1.395	1.374	1.367	1.360
2	1.752	1.684	1.658	1.647	1.643	1.628	1.605
3	2.016	1.926	1.897	1.886	1.869	1.852	1.840
4	2.247	2.147	2.117	2.092	2.082	2.067	2.056
5	2.408	2.334	2.289	2.275	2.264	2.240	2.230
6	2.568	2.497	2.465	2.451	2.439	2.418	2.408
7	2.714	2.642	2.613	2.599	2.584	2.566	2.556
8	2.834	2.773	2.730	2.708	2.705	2.680	2.670

Table C.36. Scattered Energy Buildup Factors, $B_E^S(b_1,b_2)$, for 3MeV Photons in Two-Layered Slabs of Iron-Water and Lead-Water.

	$B_E^S(b_1,b_2)$ Iron-Water 3MeV						
b_2 \ b_1	1	2	3	4	5	6	7
1	1.662	1.703	1.721	1.733	1.746	1.748	1.749
2	2.212	2.270	2.296	2.313	2.326	2.328	2.330
3	2.781	2.849	2.882	2.908	2.909	2.910	2.917
4	3.362	3.443	3.488	3.500	3.509	3.510	3.518
5	3.940	4.053	4.076	4.103	4.113	4.120	4.123
6	4.514	4.622	4.650	4.677	4.706	4.712	4.717
7	5.073	5.212	5.264	5.290	5.299	5.310	5.320
8	5.647	5.799	5.859	5.887	5.898	5.908	5.928

	$B_E^S(b_1,b_2)$ Lead-Water 3MeV						
b_2 \ b_1	1	2	3	4	5	6	7
1	1.592	1.638	1.657	1.667	1.674	1.679	1.683
2	2.142	2.212	2.239	2.256	2.273	2.277	2.280
3	2.712	2.793	2.833	2.863	2.870	2.874	2.877
4	3.284	3.388	3.436	3.459	3.478	3.482	3.485
5	3.852	3.982	4.027	4.060	4.081	4.086	4.091
6	4.420	4.541	4.606	4.650	4.689	4.698	4.708
7	4.975	5.120	5.175	5.238	5.281	5.301	5.315
8	5.557	5.699	5.768	5.859	5.894	5.920	5.940

Table C.37. Scattered Energy Buildup Factors, $B_E^S(b_1,b_2)$, for 3MeV Photons in Two-Layered Slabs of Water-Iron and Lead-Iron.

	$B_E^S(b_1,b_2)$ Water-Iron 3MeV						
b_2 \ b_1	1	2	3	4	5	6	7
1	1.572	1.609	1.624	1.644	1.638	1.639	1.640
2	2.068	2.121	2.141	2.173	2.167	2.162	2.158
3	2.609	2.685	2.708	2.753	2.728	2.720	2.710
4	3.175	3.268	3.304	3.345	3.316	3.302	3.280
5	3.758	3.875	3.896	3.965	3.923	3.908	3.883
6	4.356	4.472	4.523	4.590	4.539	4.521	4.495
7	4.953	5.110	5.158	5.240	5.184	5.160	5.135
8	5.621	5.752	5.825	5.935	5.875	5.840	5.810

	$B_E^S(b_1,b_2$ Lead-Iron 3MeV						
b_2 \ b_1	1	2	3	4	5	6	7
1	1.511	1.562	1.582	1.593	1.600	1.604	1.608
2	2.000	2.079	2.109	2.126	2.143	2.145	2.146
3	2.555	2.641	2.676	2.706	2.712	2.714	2.715
4	3.113	3.223	3.276	3.291	3.308	3.313	3.317
5	3.667	3.820	3.879	3.899	3.916	3.925	3.930
6	4.234	4.413	4.485	4.520	4.555	4.568	4.578
7	4.790	4.991	5.081	5.119	5.141	5.153	5.163
8	5.365	5.595	5.702	5.752	5.771	5.784	5.794

Table C.38. Scattered Energy Buildup Factors, $B_E^S(b_1,b_2)$, for 3MeV Photons in Two-Layered Slabs of Water-Lead and Iron-Lead.

$B_E^S(b_1,b_2)$	Water-Lead				3MeV		
b_2 \ b_1	1	2	3	4	5	6	7
1	1.333	1.310	1.322	1.328	1.332	1.330	1.328
2	1.575	1.587	1.601	1.605	1.614	1.610	1.606
3	1.835	1.885	1.902	1.911	1.910	1.905	1.900
4	2.118	2.187	2.215	2.216	2.223	2.216	2.209
5	2.432	2.513	2.538	2.542	2.547	2.533	2.522
6	2.731	2.830	2.851	2.862	2.875	2.860	2.848
7	3.043	3.150	3.171	3.184	3.202	3.192	3.182
8	3.369	3.487	3.510	3.530	3.550	3.540	3.530

$B_E^S(b_1,b_2)$	Iron-Lead				3MeV		
b_2 \ b_1	1	2	3	4	5	6	7
1	1.267	1.305	1.324	1.331	1.336	1.335	1.334
2	1.544	1.587	1.607	1.613	1.621	1.615	1.610
3	1.819	1.874	1.900	1.916	1.917	1.913	1.909
4	2.113	2.181	2.218	2.221	2.227	2.217	2.210
5	2.414	2.507	2.532	2.543	2.551	2.541	2.532
6	2.723	2.816	2.850	2.859	2.865	2.857	2.852
7	3.033	3.152	3.177	3.184	3.198	3.188	3.178
8	3.354	3.505	3.516	3.526	3.545	3.515	3.525

Table C.39. Scattered Energy Buildup Factors, $B_E^S(b_1,b_2)$, for 6MeV Photons in Two-Layered Slabs of Iron-Water and Lead-Water.

	$B_E^S(b_1,b_2)$ Iron-Water 6MeV						
b_2 \ b_1	1	2	3	4	5	6	7
1	1.436	1.485	1.506	1.520	1.530	1.533	1.535
2	1.808	1.865	1.891	1.908	1.920	1.912	1.910
3	2.188	2.253	2.282	2.300	2.310	2.308	2.305
4	2.563	2.637	2.667	2.686	2.692	2.694	2.696
5	2.925	3.007	3.037	3.056	3.067	3.073	3.080
6	3.248	3.345	3.375	3.398	3.414	3.420	3.425
7	3.570	3.663	3.694	3.720	3.734	3.739	3.744
8	3.841	3.945	3.979	4.003	4.020	4.025	4.030

	$B_E^S(b_1,b_2)$ Lead-Water 6MeV						
b_2 \ b_1	1	2	3	4	5	6	7
1	1.363	1.437	1.473	1.496	1.517	1.525	1.531
2	1.720	1.809	1.854	1.884	1.911	1.909	1.904
3	2.072	2.175	2.227	2.262	2.291	2.291	2.292
4	2.417	2.530	2.588	2.624	2.650	2.655	2.660
5	2.741	2.863	2.923	2.959	2.991	2.997	3.005
6	3.009	3.143	3.207	3.248	3.278	3.284	3.290
7	3.267	3.407	3.478	3.520	3.553	3.558	3.565
8	3.506	3.648	3.721	3.766	3.800	3.805	3.810

Table C.40. Scattered Energy Buildup Factors, $B_E^S(b_1,b_2)$, for 6MeV Photons in Two-Layered Slabs of Water-Iron and Lead-Iron.

	$B_E^S(b_1,b_2)$ Water-Iron 6MeV						
b_2 \ b_1	1	2	3	4	5	6	7
1	1.374	1.404	1.416	1.423	1.427	1.430	1.434
2	1.738	1.765	1.780	1.792	1.797	1.800	1.804
3	2.121	2.178	2.192	2.203	2.206	2.209	2.212
4	2.554	2.609	2.626	2.639	2.642	2.647	2.652
5	2.988	3.060	3.083	3.098	3.104	3.109	3.114
6	3.459	3.529	3.560	3.578	3.579	3.585	3.590
7	3.947	4.019	4.047	4.069	4.071	4.077	4.083
8	4.442	4.515	4.545	4.568	4.569	4.575	4.581

	$B_E^S(b_1,b_2)$ Lead-Iron 6MeV						
b_2 \ b_1	1	2	3	4	5	6	7
1	1.326	1.383	1.411	1.429	1.443	1.454	1.464
2	1.666	1.742	1.781	1.808	1.829	1.836	1.844
3	2.031	2.126	2.177	2.212	2.238	2.248	2.259
4	2.417	2.533	2.595	2.636	2.665	2.680	2.695
5	2.815	2.955	3.027	3.076	3.112	3.132	3.162
6	3.234	3.393	3.475	3.530	3.572	3.593	3.614
7	3.669	3.836	3.942	4.004	4.050	4.073	4.096
8	4.123	4.307	4.409	4.475	4.523	4.548	4.573

Table C.41. Scattered Energy Buildup Factors, $B_E^S(b_1,b_2)$, for 6MeV Photons in Two-Layered Slabs of Water-Lead and Iron-Lead.

$B_E^S(b_1,b_2)$ Water-Lead 6MeV							
b_2 \ b_1	1	2	3	4	5	6	7
1	1.179	1.204	1.214	1.220	1.221	1.224	1.227
2	1.383	1.409	1.423	1.430	1.432	1.435	1.437
3	1.615	1.660	1.673	1.679	1.680	1.683	1.685
4	1.883	1.926	1.942	1.950	1.952	1.956	1.958
5	2.159	2.220	2.239	2.247	2.250	2.254	2.257
6	2.468	2.538	2.559	2.567	2.569	2.573	2.576
7	2.803	2.878	2.898	2.906	2.910	2.914	2.918
8	3.142	3.222	3.243	3.254	3.258	3.262	3.266

$B_E^S(b_1,b_2)$ Iron-Lead 6MeV							
b_2 \ b_1	1	2	3	4	5	6	7
1	1.174	1.207	1.221	1.229	1.234	1.238	1.242
2	1.376	1.416	1.433	1.441	1.448	1.451	1.455
3	1.607	1.656	1.675	1.689	1.696	1.703	1.710
4	1.867	1.926	1.947	1.961	1.967	1.979	1.990
5	2.138	2.212	2.238	2.254	2.263	2.275	2.288
6	2.449	2.522	2.552	2.569	2.581	2.593	2.604
7	2.774	2.855	2.883	2.903	2.917	2.928	2.937
8	3.109	3.194	3.226	3.248	3.263	3.274	3.285

Table C.42. Energy Fluxes, $I_n^{su}(b_1+b_2)$, for 1MeV Photons in Two-Layered Slabs of Iron-Water and Lead-Water.

$I_n^{su}(b_1+b_2)$	Iron-Water			1MeV	
b_2 \ b_1	1	2	3	4	5
1	1.392(-1)	1.554(-1)	1.611(-1)	1.638(-1)	1.647(-1)
2	3.706(-2)	4.144(-2)	4.301(-2)	4.368(-2)	4.382(-2)
3	1.093(-2)	1.218(-2)	1.259(-2)	1.274(-2)	1.274(-2)
4	3.362(-3)	3.730(-3)	3.841(-3)	3.875(-3)	3.863(-3)
5	1.063(-3)	1.174(-3)	1.205(-3)	1.211(-3)	1.204(-3)
6	3.419(-4)	3.762(-4)	3.849(-4)	3.858(-4)	3.827(-4)
7	1.116(-4)	1.224(-4)	1.248(-4)	1.248(-4)	1.234(-4)
8	3.681(-5)	4.024(-5)	4.096(-5)	4.086(-5)	4.034(-5)

$I_n^{su}(b_1+b_2)$	Lead-Water			1MeV	
b_2 \ b_1	1	2	3	4	5
1	1.597(-1)	1.919(-1)	2.098(-1)	2.202(-1)	2.301(-1)
2	4.441(-2)	5.498(-2)	6.100(-2)	6.471(-2)	6.814(-2)
3	1.345(-2)	1.681(-2)	1.877(-2)	2.000(-2)	2.124(-2)
4	4.202(-3)	5.278(-3)	5.917(-3)	6.310(-3)	6.682(-3)
5	1.340(-3)	1.688(-3)	1.897(-3)	2.025(-3)	2.148(-3)
6	4.343(-4)	5.479(-4)	6.165(-4)	6.585(-4)	6.992(-4)
7	1.424(-4)	1.798(-4)	2.026(-4)	2.164(-4)	2.300(-4)
8	4.717(-5)	5.960(-5)	6.724(-5)	7.178(-5)	7.634(-5)

Table C.43. Energy Fluxes, $I_n^{su}(b_1+b_2)$, for 1MeV Photons in Two-Layered Slabs of Water-Iron and Lead-Iron.

$I_n^{su}(b_1+b_2)$	Water-Iron			1MeV	
b_2 \ b_1	1	2	3	4	5
1	1.374(-1)	1.445(-1)	1.480(-1)	1.472(-1)	1.464(-1)
2	3.691(-2)	3.912(-2)	3.964(-2)	3.938(-2)	3.892(-2)
3	1.088(-2)	1.153(-2)	1.158(-2)	1.148(-2)	1.129(-2)
4	3.352(-3)	3.536(-3)	3.536(-3)	3.485(-3)	3.417(-3)
5	1.059(-3)	1.113(-3)	1.109(-3)	1.089(-3)	1.064(-3)
6	3.410(-4)	3.570(-4)	3.542(-4)	3.468(-4)	3.381(-4)
7	1.113(-4)	1.161(-4)	1.149(-4)	1.122(-4)	1.091(-4)
8	3.671(-5)	3.819(-5)	3.768(-5)	3.671(-5)	3.564(-5)

$I_n^{su}(b_1+b_2)$	Lead-Iron			1MeV	
b_2 \ b_1	1	2	3	4	5
1	1.738(-1)	2.038(-1)	2.175(-1)	2.264(-1)	2.325(-1)
2	4.944(-2)	5.937(-2)	6.421(-2)	6.746(-2)	6.972(-2)
3	1.497(-2)	1.816(-2)	1.976(-2)	2.085(-2)	2.161(-2)
4	4.678(-3)	5.704(-3)	6.227(-3)	6.586(-3)	6.839(-3)
5	1.492(-3)	1.825(-3)	1.997(-3)	2.115(-3)	2.198(-3)
6	4.835(-4)	5.923(-4)	6.487(-4)	6.879(-4)	7.157(-4)
7	1.585(-4)	1.944(-4)	2.132(-4)	2.262(-4)	2.359(-4)
8	5.249(-5)	6.442(-5)	7.068(-5)	7.503(-5)	7.814(-5)

Table C.44. Energy Fluxes, $I_n^{su}(b_1+b_2)$, for 1MeV Photons in Two-Layered Slabs of Water-Lead and Iron-Lead.

	$I_n^{su}(b_1+b_2)$ Water-Lead 1MeV				
b_2 \ b_1	1	2	3	4	5
1	1.301(-1)	1.300(-1)	1.282(-1)	1.248(-1)	1.218(-1)
2	3.470(-2)	3.465(-2)	3.389(-2)	3.279(-2)	3.182(-2)
3	1.016(-2)	1.009(-2)	9.822(-3)	9.457(-3)	9.137(-3)
4	3.109(-3)	3.076(-3)	2.982(-3)	2.860(-3)	2.754(-3)
5	9.792(-4)	9.655(-4)	9.329(-4)	8.918(-14)	8.563(-4)
6	3.147(-4)	3.094(-4)	2.982(-4)	2.843(-4)	2.724(-4)
7	1.027(-4)	1.007(-4)	9.689(-5)	9.220(-5)	8.819(-5)
8	3.396(-5)	3.324(-5)	3.191(-5)	3.031(-5)	2.895(-5)

	$I_n^{su}(b_1+b_2)$ Iron-Lead 1MeV				
b_2 \ b_1	1	2	3	4	5
1	1.375(-1)	1.450(-1)	1.465(-1)	1.463(-1)	1.453(-1)
2	3.676(-2)	3.863(-2)	3.886(-2)	3.860(-2)	3.815(-2)
3	1.077(-2)	1.126(-2)	1.128(-2)	1.115(-2)	1.097(-2)
4	3.299(-3)	3.434(-3)	3.426(-3)	3.376(-3)	3.311(-3)
5	1.039(-3)	1.078(-3)	1.072(-3)	1.053(-3)	1.030(-3)
6	3.342(-4)	3.456(-4)	3.429(-4)	3.361(-4)	3.281(-4)
7	1.091(-4)	1.126(-4)	1.114(-4)	1.091(-4)	1.063(-4)
8	3.609(-5)	3.714(-5)	3.674(-5)	3.587(-5)	3.490(-5)

Table C.45. Energy Fluxes, $I_n^{su}(b_1+b_2)$, for 3MeV Photons in Two-Layered Slabs of Iron-Water and Lead-Water.

	$I_n^{su}(b_1+b_2)$	Iron-Water		3MeV	
b_2 \ b_1	1	2	3	4	5
1	1.791(-1)	1.903(-1)	1.937(-1)	1.947(-1)	1.944(-1)
2	5.024(-2)	5.325(-2)	5.399(-2)	5.406(-2)	5.399(-2)
3	1.495(-2)	1.577(-2)	1.592(-2)	1.588(-2)	1.581(-2)
4	4.586(-3)	4.818(-3)	4.847(-3)	4.820(-3)	4.785(-3)
5	1.437(-3)	1.505(-3)	1.509(-3)	1.497(-3)	1.482(-3)
6	4.582(-4)	4.779(-4)	4.803(-4)	4.758(-4)	4.681(-4)
7	1.478(-4)	1.537(-4)	1.536(-4)	1.518(-4)	1.505(-4)
8	4.837(-5)	5.017(-5)	5.004(-5)	4.939(-5)	4.870(-5)

	$I_n^{su}(b_1+b_2)$	Lead-Water		3MeV	
b_2 \ b_1	1	2	3	4	5
1	2.004(-1)	3.176(-1)	2.224(-1)	2.277(-1)	2.296(-1)
2	5.676(-2)	6.174(-2)	6.366(-2)	6.452(-2)	6.492(-2)
3	1.691(-2)	1.837(-2)	1.888(-2)	1.908(-2)	1.915(-2)
4	5.192(-3)	5.621(-3)	5.760(-3)	5.807(-3)	5.812(-3)
5	1.627(-3)	1.756(-3)	1.795(-3)	1.806(-3)	1.803(-3)
6	5.189(-4)	5.610(-4)	5.693(-4)	5.709(-4)	5.695(-4)
7	1.673(-4)	1.795(-4)	1.827(-4)	1.835(-4)	1.838(-4)
8	5.470(-4)	5.858(-4)	5.952(-4)	5.953(-4)	5.929(-4)

Table C.46. Energy Fluxes, $I_n^{su}(b_1+b_2)$, for 3MeV Photons in Two-Layered Slabs of Water-Iron and Lead-Iron.

$I_n^{su}(b_1+b_2)$	Water-Iron		3MeV		
b_2 \ b_1	1	2	3	4	5
1	1.914(-1)	2.015(-1)	2.046(-1)	2.057(-1)	2.061(-1)
2	5.577(-2)	5.868(-2)	5.948(-2)	5.969(-2)	5.965(-2)
3	1.707(-2)	1.790(-2)	1.810(-2)	1.811(-2)	1.807(-2)
4	5.363(-3)	5.609(-3)	5.655(-3)	5.650(-3)	5.627(-3)
5	1.717(-3)	1.790(-3)	1.802(-3)	1.797(-3)	1.788(-3)
6	5.609(-4)	5.819(-4)	5.844(-4)	5.809(-4)	5.767(-4)
7	1.833(-4)	1.902(-4)	1.908(-4)	1.898(-4)	1.893(-4)
8	6.083(-5)	6.300(-5)	6.311(-5)	6.271(-5)	6.216(-5)

$I_n^{su}(b_1+b_2)$	Lead-Iron		3MeV		
b_2 \ b_1	1	2	3	4	5
1	2.185(-1)	2.353(-1)	2.419(-1)	2.452(-1)	2.470(-1)
2	6.417(-2)	6.932(-2)	7.127(-2)	7.221(-2)	7.264(-2)
3	1.966(-2)	2.119(-2)	2.175(-2)	2.198(-2)	2.207(-2)
4	6.179(-3)	6.637(-3)	6.799(-3)	6.857(-3)	6.869(-3)
5	1.977(-3)	2.119(-3)	2.164(-3)	2.177(-3)	2.179(-3)
6	6.419(-4)	6.860(-4)	6.993(-4)	7.029(-4)	7.013(-4)
7	2.108(-4)	2.247(-4)	2.295(-4)	2.307(-4)	2.294(-4)
8	6.990(-5)	7.440(-5)	7.559(-5)	7.571(-5)	7.572(-5)

Table C.47. Energy Fluxes, $I_n^{su}(b_1+b_2)$, for 3MeV Photons in Two-Layered Slabs of Water-Lead and Iron-Lead.

$I_n^{su}(b_1+b_2)$	Water-Lead		3MeV		
b_2 \ b_1	1	2	3	4	5
1	2.202(-1)	2.283(-1)	2.305(-1)	2.311(-1)	2.311(-1)
2	6.843(-2)	7.099(-2)	7.161(-2)	7.170(-2)	7.159(-2)
3	2.197(-2)	2.275(-2)	2.290(-2)	2.290(-2)	2.285(-2)
4	7.188(-3)	7.427(-3)	7.465(-3)	7.451(-3)	7.422(-3)
5	2.385(-3)	2.460(-3)	2.468(-3)	2.460(-3)	2.448(-3)
6	8.000(-4)	8.231(-4)	8.250(-4)	8.216(-4)	8.168(-4)
7	2.707(-4)	2.782(-4)	2.784(-4)	2.771(-4)	2.752(-4)
8	9.234(-5)	9.472(-5)	9.472(-5)	9.417(-5)	9.348(-5)

$I_n^{su}(b_1+b_2)$	Iron-Lead		3MeV		
b_2 \ b_1	1	2	3	4	5
1	2.247(-1)	2.339(-1)	2.364(-1)	2.369(-1)	2.368(-1)
2	6.970(-2)	7.248(-2)	7.309(-2)	7.310(-2)	7.288(-2)
3	2.235(-2)	2.318(-2)	2.332(-2)	2.326(-2)	2.315(-2)
4	7.307(-3)	7.557(-3)	7.584(-3)	7.552(-3)	7.504(-3)
5	2.423(-3)	2.499(-3)	2.503(-3)	2.489(-3)	2.469(-3)
6	8.123(-4)	8.360(-4)	8.357(-4)	8.298(-4)	8.224(-4)
7	2.748(-4)	2.823(-4)	2.818(-4)	2.794(-4)	2.769(-4)
8	9.369(-5)	9.608(-5)	9.579(-5)	9.486(-5)	9.381(-5)

Table C.48. Energy Fluxes, $I_n^{su}(b_1+b_2)$, for 6MeV Photons in Two-Layered Slabs of Iron-Water and Lead-Water.

$I_n^{su}(b_1+b_2)$	Iron-Water		6MeV		
b_2 \ b_1	1	2	3	4	5
1	1.788(-1(	1.953(-1)	2.009(-1)	2.029(-1)	2.033(-1)
2	5.089(-2)	5.529(-2)	5.649(-2)	5.669(-2)	5.647(-2)
3	1.509(-2)	1.630(-2)	1.657(-2)	1.655(-2)	1.642(-2)
4	4.596(-3)	4.945(-3)	5.005(-3)	4.981(-3)	4.925(-3)
5	1.430(-3)	1.533(-3)	1.547(-3)	1.535(-3)	1.514(-3)
6	4.523(-4)	4.836(-4)	4.868(-4)	4.821(-4)	4.745(-4)
7	1.451(-4)	1.548(-4)	1.555(-4)	1.537(-4)	1.511(-4)
8.	4.713(-5)	5.017(-5)	5.031(-5)	4.966(-5)	4.873(-5)

$I_n^{su}(b_1+b_2)$	Lead-Water		6MeV		
b_2 \ b_1	1	2	3	4	5
1	1.797(-1)	2.016(-1)	2.086(-1)	2.110(-1)	2.112(-1)
2	5.076(-2)	5.656(-2)	5.798(-2)	5.805(-2)	5.759(-2)
3	1.499(-2)	1.659(-2)	1.687(-2)	1.677(-2)	1.651(-2)
4	4.553(-3)	5.010(-3)	5.066(-3)	5.007(-3)	4.901(-3)
5	1.413(-3)	1.548(-3)	1.559(-3)	1.533(-3)	1.495(-3)
6	4.463(-4)	4.873(-4)	4.887(-4)	4.790(-4)	4.654(-4)
7	1.430(-4)	1.557(-4)	1.557(-4)	1.521(-4)	1.474(-4)
8	4.638(-5)	5.037(-5)	5.024(-5)	4.898(-5)	4.735(-5)

Table C.49. Energy Fluxes, $I_n^{su}(b_1+b_2)$, for 6MeV Photons in Two-Layered Slabs of Water-Iron and Lead-Iron.

	$I_n^{su}(b_1+b_2)$	Water-Iron		6MeV	
b_2 \ b_1	1	2	3	4	5
1	2.232(-1)	2.427(-1)	2.498(-1)	2.531(-1)	2.550(-1)
2	6.974(-2)	7.612(-2)	7.835(-2)	7.919(-2)	7.969(-2)
3	2.222(-2)	2.422(-2)	2.489(-2)	2.512(-2)	2.526(-2)
4	7.174(-3)	7.808(-3)	8.016(-3)	8.081(-3)	8.119(-3)
5	2.344(-3)	2.548(-3)	2.613(-3)	2.632(-3)	2.643(-3)
6	7.740(-4)	8.401(-4)	8.608(-4)	8.664(-4)	8.695(-4)
7	2.578(-4)	2.795(-4)	2.862(-4)	2.879(-4)	2.888(-4)
8	8.655(-5)	9.375(-5)	9.593(-5)	9.643(-5)	9.671(-5)

	$I_n^{su}(b_1+b_2)$	Lead-Iron		6MeV	
b_2 \ b_1	1	2	3	4	5
1	2.040(-1)	2.334(-1)	2.441(-1)	2.488(-1)	2.509(-1)
2	6.271(-2)	7.168(-2)	7.460(-2)	7.564(-2)	7.585(-2)
3	1.982(-2)	2.255(-2)	2.334(-2)	2.354(-2)	2.349(-2)
4	6.367(-3)	7.211(-3)	7.431(-3)	7.465(-3)	7.419(-3)
5	2.072(-3)	2.338(-3)	2.401(-3)	2.403(-3)	2.380(-3)
6	6.820(-4)	7.669(-4)	7.850(-4)	7.833(-4)	7.736(-4)
7	2.266(-4)	2.541(-4)	2.593(-4)	2.581(-4)	2.542(-4)
8	7.587(-5)	8.487(-5)	8.643(-5)	8.583(-5)	8.435(-5)

Table C.50. Energy Fluxes, $I_n^{su}(b_1+b_2)$, for 6MeV Photons in Two-Layered Slabs of Water-Lead and Iron-Lead.

	$I_n^{su}(b_1+b_2)$	Water-Lead		6MeV	
b_2 \ b_1	1	2	3	4	5
1	2.709(-1)	2.921(-1)	2.993(-1)	3.026(-1)	3.042(-1)
2	9.492(-2)	1.026(-1)	1.051(-1)	1.062(-1)	1.067(-1)
3	3.327(-2)	3.594(-2)	3.680(-2)	3.716(-2)	3.732(-2)
4	1.172(-2)	1.265(-2)	1.295(-2)	1.307(-2)	1.312(-2)
5	4.154(-3)	4.482(-3)	4.583(-3)	4.625(-3)	4.641(-3)
6	1.481(-3)	1.597(-3)	1.633(-3)	1.647(-3)	1.653(-3)
7	5.312(-4)	5.724(-4)	5.849(-4)	5.900(-4)	5.918(-4)
8	1.914(-4)	2.062(-4)	2.106(-4)	2.124(-4)	2.131(-4)

	$I_n^{su}(b_1+b_2)$	Iron-Lead		6MeV	
b_2 \ b_1	1	2	3	4	5
1	2.523(-1)	2.774(-1)	2.865(-1)	2.905(-1)	2.926(-1)
2	8.779(-2)	9.658(-2)	9.960(-2)	1.009(-1)	1.015(-1)
3	3.068(-2)	3.371(-2)	3.473(-2)	3.513(-2)	3.532(-2)
4	1.079(-2)	1.184(-2)	1.219(-2)	1.232(-2)	1.238(-2)
5	3.823(-3)	4.190(-3)	4.309(-3)	4.353(-3)	4.373(-3)
6	1.362(-3)	1.492(-3)	1.533(-3)	1.549(-3)	1.555(-3)
7	4.884(-4)	5.345(-4)	5.491(-4)	5.544(-4)	5.566(-4)
8	1.760(-4)	1.925(-4)	1.977(-4)	1.996(-4)	2.008(-4)

Table C.51. Interface Energy Buildup Factors, $B_E(b_1,b_2)$, for 1MeV Photons in Two-Layered Slabs.

	Iron-Water			Lead-Water		
b_1	$B_E(b_1)$	$B_E(b_1,1)$	$B_E(b_1,2)$	$B_E(b_1)$	$B_E(b_1,1)$	$B_E(b_1,2)$
1	1.744	1.977	1.994	1.370	1.529	1.546
2	2.460	2.825	2.856	1.635	1.832	1.852
3	3.236	3.732	3.775	1.870	2.099	2.123
4	4.070	4.709	4.763	2.090	2.344	2.370
5	4.945	5.811	5.878	2.300	2.574	2.602
7	6.842	8.024	8.085	2.680	3.010	3.040
	Water-Iron			Lead-Iron		
1	1.800	1.998	2.005	1.370	1.489	1.494
2	2.660	2.960	2.969	1.635	1.778	1.784
3	3.590	4.035	4.047	1.870	2.041	2.047
4	4.645	5.226	5.241	2.090	2.277	2.284
5	5.776	6.531	6.548	2.300	2.496	2.504
7	8.341	9.468	9.504	2.680	2.901	2.911
	Water-Lead			Iron-Lead		
1	1.800	1.832	1.832	1.744	1.774	1.774
2	2.660	2.715	2.715	2.460	2.508	2.508
3	3.590	3.663	3.663	3.236	3.293	3.293
4	4.645	4.742	4.742	4.070	4.135	4.135
5	5.776	5.922	5.922	4.945	5.033	5.033
7	8.341	8.553	8.555	6.842	6.998	6.998

Table C.52. Interface Energy Buildup Factors, $B_E(b_1,b_2)$, for 3MeV Photons in Two-Layered Slabs.

	Iron-Water			Lead-Water		
b_1	$B_E(b_1)$	$B_E(b_1,1)$	$B_E(b_1,2)$	$B_E(b_1)$	$B_E(b_1,1)$	$B_E(b_1,2)$
1	1.485	1.543	1.545	1.327	1.362	1.363
2	1.930	2.022	2.025	1.604	1.654	1.656
3	2.390	2.524	2.528	1.893	1.955	1.958
4	2.872	3.048	3.053	2.191	2.267	2.270
5	3.376	3.592	3.597	2.498	2.589	2.593
7	4.425	4.743	4.749	3.144	3.271	3.276
	Water-Iron			Lead-Iron		
1	1.524	1.575	1.576	1.327	1.352	1.353
2	1.996	2.079	2.080	1.604	1.641	1.642
3	2.475	2.593	2.594	1.893	1.939	1.940
4	2.961	3.121	3.123	2.191	2.246	2.247
5	3.453	3.638	3.640	2.498	2.565	2.566
7	4.439	4.690	4.692	3.144	3.240	3.241
	Water-Lead			Iron-Lead		
1	1.525	1.533	1.533	1.485	1.493	1.493
2	1.996	2.010	2.010	1.930	1.942	1.942
3	2.475	2.495	2.495	2.390	2.408	2.408
4	2.961	2.988	2.988	2.872	2.897	2.897
5	3.453	3.485	3.485	3.376	3.403	3.403
7	4.439	4.484	4.484	4.425	4.462	4.462

Table C.53. Interface Energy Buildup Factors, $B_E(b_1,b_2)$, for 6MeV Photons in Two-Layered Slabs.

	Iron-Water			Lead-Water		
b_1	$B_E(b_1)$	$B_E(b_1,1)$	$B_E(b_1,2)$	$B_E(b_1)$	$B_E(b_1,1)$	$B_E(b_1,2)$
1	1.328	1.356	1.357	1.204	1.226	1.226
2	1.609	1.652	1.652	1.377	1.403	1.403
3	1.907	1.963	1.964	1.567	1.599	1.600
4	2.222	2.291	2.292	1.779	1.818	1.819
5	2.550	2.636	2.637	2.013	2.059	2.060
7	3.244	3.369	3.370	2.555	2.624	2.625
	Water-Iron			Lead-Iron		
1	1.384	1.422	1.423	1.204	1.234	1.234
2	1.698	1.752	1.752	1.377	1.411	1.411
3	2.010	2.077	2.078	1.567	1.607	1.608
4	2.317	2.397	2.398	1.779	1.825	1.826
5	2.617	2.710	2.711	2.013	2.067	2.068
7	3.193	3.308	3.310	2.555	2.629	2.630
	Water-Lead			Iron-Lead		
1	1.384	1.407	1.407	1.328	1.350	1.350
2	1.698	1.728	1.728	1.609	1.636	1.636
3	2.010	2.045	2.045	1.907	1.939	1.939
4	2.317	2.357	2.357	2.222	2.259	2.259
5	2.617	2.665	2.665	2.550	2.593	2.593
7	3.193	3.250	3.250	3.244	3.296	3.296

Table C.54. Single-Medium Energy Buildup Factors, $B_E(b)$.

Material	Energy MeV	Distance in Mean Free Paths								
		1.0	2.0	3.0	4.0	5.0	6.0	7.0	8.0	10.0
Water	1	1.800	2.660	3.590	4.645	5.776	7.030	8.341	9.750	12.870
	3	1.524	1.996	2.475	2.961	3.453	3.947	4.439	4.921	5.871
	6	1.379	1.698	2.010	2.317	2.617	2.910	3.193	3.467	3.985
Aluminum	1	1.780	2.590	3.490	4.460	5.510	6.670	7.890	9.160	
	3	1.511	1.976	2.451	2.936	3.439	3.945	4.454	4.970	5.964
	6	1.363	1.666	1.972	2.280	2.589	2.895	3.197	3.500	4.070
Iron	1	1.744	2.460	3.236	4.070	4.945	5.870	6.842	7.890	10.120
	3	1.485	1.930	2.390	2.872	3.376	3.892	4.425	4.960	6.054
	6	1.328	1.609	1.907	2.222	2.550	2.891	3.244	3.606	4.354
Tin	1	1.560	2.100	2.635	3.150	3.691	4.230	4.770	5.312	
	3	1.421	1.803	2.213	2.642	3.103	3.590	4.085	4.620	5.690
	6	1.272	1.507	1.769	2.065	2.390	2.750	3.130	3.570	3.490
Lead	1	1.370	1.635	1.870	2.090	2.300	2.490	2.680	2.870	3.210
	3	1.327	1.604	1.893	2.191	2.498	2.816	3.144	3.478	4.164
	6	1.206	1.377	1.567	1.779	2.012	2.271	2.555	2.870	3.593

Table C.55. Unscattered Energy Flux Albedos, $\alpha_{\phi}^{u}(b)$.

Material	Energy MeV	$\alpha_{\phi}^{u}(1)$	$\alpha_{\phi}^{u}(2)$	$\alpha_{\phi}^{u}(\infty)$
	1	0.0890	0.0994	0.1002
Water	3	0.0238	0.0249	0.0250
	6	0.0132	0.0133	0.0133
	1	0.0840	0.0916	0.0920
Aluminum	3	0.0222	0.0229	0.0230
	6	0.0164	0.0166	0.0166
	1	0.0650	0.0697	0.0701
Iron	3	0.0183	0.0184	0.0184
	6	0.0205	0.0208	0.0208
	1	0.0280	0.0290	0.0290
Tin	3	0.0103	0.0104	0.0104
	6	0.0188	0.0188	0.0188
	1	0.0110	0.0110	0.0110
Lead	3	0.0055	0.0055	0.0055
	6	0.0154	0.0154	0.0154

Table C.56. Scattered Energy Flux Albedos, $\alpha_\phi^s(b_1,b_2)$, for 1MeV Photons in Two-Layered Slabs.

	Iron-Water				Lead-Water			
	$\alpha_\phi^s(b_1,b_2)$		$\alpha_\phi^s/\alpha_\phi^u$		$\alpha_\phi^s(b_1,b_2)$		$\alpha_\phi^s/\alpha_\phi^u$	
b_1	b_2=1	b_2=2	b_2=1	b_2=2	b_2=1	b_2=2	b_2=1	b_2=2
1	0.193	0.203	2.16	2.03	0.189	0.205	2.12	2.05
2	0.189	0.203	2.12	2.03	0.170	0.184	1.91	1.84
3	0.182	0.196	2.04	1.96	0.161	0.175	1.81	1.75
4	0.179	0.193	2.01	1.93	0.151	0.165	1.70	1.65
5	0.197	0.211	2.21	2.11	0.142	0.155	1.60	1.55
7	0.187	0.196	2.10	1.96	0.142	0.155	1.60	1.55
	Water-Iron				Lead-Iron			
1	0.166	0.169	2.55	2.41	0.145	0.146	2.23	2.09
2	0.141	0.144	2.17	2.06	0.123	0.124	1.89	1.77
3	0.147	0.149	2.26	2.13	0.122	0.123	1.88	1.76
4	0.142	0.144	2.18	2.06	0.112	0.114	1.72	1.63
5	0.144	0.147	2.22	2.10	0.101	0.103	1.55	1.47
7	0.145	0.149	2.23	2.13	0.093	0.096	1.43	1.37
	Water-Lead				Iron-Lead			
1	0.026	0.026	2.36	2.36	0.026	0.026	2.36	2.36
2	0.026	0.026	2.36	2.36	0.025	0.025	2.27	2.27
3	0.024	0.024	2.18	2.18	0.021	0.021	1.91	1.91
4	0.023	0.023	2.09	2.09	0.018	0.018	1.64	1.64
5	0.028	0.028	2.54	2.54	0.020	0.020	1.82	1.82
7	0.028	0.028	2.54	2.54	0.025	0.025	2.27	2.27

Table C.57. Scattered Energy Flux Albedos, $\alpha_\phi^s(b_1,b_2)$, for 3MeV Photons in Two-Layered Slabs.

	Iron-Water				Lead-Water			
	$\alpha_\phi^s(b_1,b_2)$		$\alpha_\phi^s/\alpha_\phi^u$		$\alpha_\phi^s(b_1,b_2)$		$\alpha_\phi^s/\alpha_\phi^u$	
b_1	b_2=1	b_2=2	b_2=1	b_2=2	b_2=1	b_2=2	b_2=1	b_2=2
1	0.0713	0.0732	3.00	2.94	0.0423	0.0438	1.78	1.76
2	0.0733	0.0755	3.08	3.03	0.0435	0.0453	1.83	1.82
3	0.0792	0.0813	3.33	3.26	0.0425	0.0438	1.79	1.76
4	0.0810	0.0833	3.40	3.35	0.0435	0.0454	1.83	1.82
5	0.0811	0.0836	3.41	3.36	0.0450	0.0467	1.89	1.88
7	0.0858	0.0888	3.61	3.57	0.0485	0.0500	2.04	2.01
	Water-Iron				Lead-Iron			
1	0.0622	0.0640	3.40	3.48	0.0302	0.0318	1.65	1.73
2	0.0649	0.0661	3.55	3.59	0.0316	0.0325	1.73	1.77
3	0.0675	0.0685	3.69	3.72	0.0302	0.0310	1.65	1.68
4	0.0723	0.0735	3.95	3.99	0.0309	0.0318	1.69	1.73
5	0.0680	0.0693	3.72	3.77	0.0325	0.0334	1.78	1.82
7	0.0677	0.0690	3.70	3.75	0.0360	0.0370	1.97	2.01
	Water-Lead				Iron-Lead			
1	0.0071	0.0071	1.29	1.29	0.0060	0.0060	1.09	1.09
2	0.0080	0.0080	1.45	1.45	0.0073	0.0073	1.33	1.33
3	0.0102	0.0102	1.85	1.85	0.0089	0.0089	1.62	1.62
4	0.0109	0.0109	1.98	1.98	0.0106	0.0106	1.93	1.93
5	0.0107	0.0107	1.95	1.95	0.0093	0.0093	1.69	1.69
7	0.0115	0.0115	2.09	2.09	0.0093	0.0093	1.69	1.69

Table C.58. Scattered Energy Flux Albedos, $\alpha_{\phi}^{s}(b_1,b_2)$, for 6MeV Photons in Two-Layered Slabs.

	Iron-Water				Lead-Water			
	$\alpha_{\phi}^{s}(b_1,b_2)$		$\alpha_{\phi}^{s}/\alpha_{\phi}^{u}$		$\alpha_{\phi}^{s}(b_1,b_2)$		$\alpha_{\phi}^{s}/\alpha_{\phi}^{u}$	
b_1	b_2=1	b_2=2	b_2=1	b_2=2	b_2=1	b_2=2	b_2=1	b_2=2
1	0.0457	0.0464	3.46	3.49	0.0296	0.0305	2.24	2.29
2	0.0477	0.0482	3.61	3.62	0.0324	0.0331	2.45	2.49
3	0.0470	0.0475	3.56	3.57	0.0330	0.0336	2.50	2.53
4	0.0463	0.0468	3.51	3.52	0.0334	0.0340	2.53	2.56
5	0.0473	0.0477	3.58	3.59	0.0339	0.0345	2.57	2.59
7	0.0502	0.0507	3.80	3.81	0.0360	0.0365	2.72	2.74
	Water-Iron				Lead-Iron			
1	0.0450	0.0468	2.20	2.25	0.0325	0.0344	1.59	1.65
2	0.0480	0.0487	2.34	2.34	0.0339	0.0352	1.65	1.69
3	0.0468	0.0476	2.28	2.29	0.0336	0.0347	1.64	1.67
4	0.0457	0.0466	2.23	2.24	0.0329	0.0336	1.60	1.62
5	0.0448	0.0455	2.18	2.19	0.0337	0.0345	1.64	1.66
7	0.0433	0.0441	2.11	2.12	0.0342	0.0352	1.67	1.69
	Water-Lead				Iron-Lead			
1	0.0190	0.0190	1.23	1.23	0.0191	0.0191	1.24	1.24
2	0.0211	0.0211	1.32	1.32	0.0190	0.0190	1.23	1.23
3	0.0201	0.0201	1.30	1.30	0.0181	0.0181	1.18	1.18
4	0.0191	0.0191	1.24	1.24	0.0181	0.0181	1.18	1.18
5	0.0199	0.0199	1.29	1.29	0.0176	0.0176	1.14	1.14
7	0.0190	0.0190	1.23	1.23	0.0165	0.0165	1.07	1.07

Table C.59. The Mass Energy-Absorption Coefficient of Air in the Energy Group Structure of the Calculated Results for a 1MeV Source.

Group	E_i(MeV)	ΔE_i(MeV)	$(\frac{\mu_{en}}{\rho})_{air}$ cm^2/gm
1	0.995	0.01	0.0278
2	0.945	0.09	0.0281
3	0.850	0.10	0.0286
4	0.750	0.10	0.0291
5	0.650	0.10	0.0294
6	0.550	0.10	0.02955
7	0.450	0.10	0.02955
8	0.350	0.10	0.0292
9	0.250	0.10	0.0278
10	0.175	0.05	0.0259
11	0.125	0.05	0.0241
12	0.095	0.01	0.0236
13	0.085	0.01	0.0241
14	0.075	0.01	0.0258
15	0.065	0.01	0.02895
16	0.055	0.01	0.03555
17	0.045	0.01	0.05375
18	0.035	0.01	0.10745
19	0.025	0.01	0.3295
20	0.015	0.01	1.915

Table C.60. The Mass Energy-Absorption Coefficient of Air in the Energy Group Structure of the Calculated Results for a 3MeV Source.

Group	E_i(MeV)	ΔE_i(MeV)	$(\frac{\mu_{en}}{\rho})_{air}$ cm^2/gm
1	2.995	0.01	.0205
2	2.895	0.19	.0208
3	2.700	0.20	.02135
4	2.500	0.20	.02195
5	2.300	0.20	.02254
6	2.100	0.20	.0231
7	1.900	0.20	.0238
8	1.700	0.20	.0246
9	1.500	0.20	.0254
10	1.300	0.20	.02635
11	1.100	0.20	.0273
12	0.900	0.20	.02835
13	0.700	0.20	.0292
14	0.500	0.20	.02955
15	0.300	0.20	.0285
16	0.150	0.10	.0250
17	0.090	0.02	.02385
18	0.070	0.02	.02735
19	0.050	0.02	.04465
20	0.030	0.02	.165

Table C.61. The Mass Energy-Absorption Coefficient of Air in the Energy Group Structure of the Calculated Results for a 6MeV Source.

Group	E_i(MeV)	ΔE_i(MeV)	$(\frac{\mu_{en}}{\rho})^{air}$ cm^2/gm
1	5.995	0.01	0.0164
2	5.695	0.39	0.0166
3	5.400	0.40	0.0170
4	5.000	0.40	0.0174
5	4.600	0.40	0.0179
6	4.200	0.40	0.0184
7	3.800	0.40	0.0190
8	3.400	0.40	0.0198
9	3.000	0.40	0.0206
10	2.600	0.40	0.0217
11	2.200	0.40	0.0228
12	1.800	0.40	0.0242
13	1.400	0.40	0.0259
14	1.000	0.40	0.0278
15	0.700	0.20	0.0292
16	0.500	0.20	0.0296
17	0.300	0.20	0.0285
18	0.150	0.10	0.0250
19	0.080	0.04	0.0256
20	0.040	0.04	0.1317

Table C.62. Scattered Energy Flux Spectra, $I^S(b_1+b_2,E_i)/I^S(b_1+b_2)$, for 1MeV Photons in Slabs of Iron Followed by Water.

IRON-WATER, 1MEV, B1=1

GRP.	B2=1	B2=2	B2=3	B2=4	B2=5
1	1.5832E+00	1.4751E+00	1.3874E+00	1.3C75E+C0	1.2335E+00
2	1.5148E+00	1.4193E+00	1.3411E+00	1.2707E+C0	1.2064E+00
3	1.3847E+00	1.3134E+0C	1.2531E+0C	1.2CC9E+C0	1.155CE+00
4	1.2945E+00	1.2317E+0C	1.1820E+CC	1.1424E+00	1.1098E+00
5	1.2414E+00	1.1767E+0C	1.1343E+0C	1.1C47E+C0	1.0829E+00
6	1.1859E+00	1.1216E+00	1.0898E+CC	1.0725E+C0	1.0625E+00
7	1.0626E+00	1.0221E+0C	1.0137E+CC	1.C162E+C0	1.0226E+00
8	8.1912E-01	8.4228E-01	8.7342E-01	9.C342E-01	9.3042E-01
9	6.0592E-01	6.8160E-01	7.3876E-01	7.E487E-01	8.2336E-01
10	6.0790E-01	6.9183E-01	7.5C41E-C1	7.9679E-01	8.3541E-01
11	6.3928E-01	8.0466E-01	9.0185E-01	9.7217E-01	1.0282E+00
12	5.7424E-01	7.9535E-01	9.2059E-01	1.CC89E+C0	1.0782E+00
13	5.2743E-01	7.7721E-01	9.1903E-01	1.C18CE+C0	1.0953E+00
14	4.7917E-01	7.6214E-01	9.2423E-01	1.C363E+C0	1.1231E+00
15	4.2077E-01	7.3412E-01	9.1716E-01	1.C428E+C0	1.1394E+00
16	3.2993E-01	6.5C10E-01	8.4452E-01	9.7769E-01	1.0795E+00
17	2.0559E-01	4.7345E-01	6.4594E-01	7.E468E-01	8.5508E-01
18	6.6312E-02	1.7395E-01	2.4641E-01	2.9654E-01	3.3462E-01
19	3.4749E-03	9.4008E-03	1.341CE-02	1.6184E-02	1.8291E-02
20	7.8386E-06	2.1099E-05	3.0059E-05	3.6251E-05	4.0971E-05

IRON-WATER, 1MEV, B1=2

GRP.	B2=1	B2=2	B2=3	B2=4	B2=5
1	1.5298E+00	1.4108E+00	1.3131E+C0	1.24C1E+C0	1.1694E+00
2	1.4711E+00	1.3629E+0C	1.2812E+CC	1.2122E+C0	1.1512E+00
3	1.3596E+00	1.2717E+00	1.2C93E+CC	1.1592E+C0	1.1168E+00
4	1.2735E+00	1.1987E+00	1.149EE+CC	1.1134E+C0	1.0844E+00
5	1.2147E+00	1.1493E+C0	1.1113E+CC	1.C86CE+C0	1.0678E+00
6	1.1553E+00	1.1030E+C0	1.0782E+CC	1.C651E+C0	1.0578E+00
7	1.0487E+00	1.0241E+00	1.0204E+CC	1.C244E+C0	1.0311E+00
8	8.5597E-01	8.7845E-01	9.0497E-01	9.3C67E-01	9.5421E-01
9	6.7122E-01	7.3399E-01	7.8184E-01	8.2126E-01	8.5460E-01
10	6.5170E-01	7.3537E-01	7.8956E-C1	8.3152E-01	8.6600E-01
11	6.7580E-01	8.5598E-01	9.5275E-01	1.C191E+C0	1.0703E+00
12	6.1485E-01	8.5664E-01	9.8264E-01	1.CE51E+C0	1.1295E+00
13	5.6738E-01	8.4256E-01	9.8667E-01	1.C809E+C0	1.1519E+00
14	5.1606E-01	8.3036E-01	9.9740E-01	1.1C54E+C0	1.1857E+00
15	4.5272E-01	8.0317E-01	9.9479E-01	1.1176E+C0	1.2077E+00
16	3.5525E-01	7.1560E-01	9.2217E-01	1.C542E+C0	1.1501E+00
17	2.2124E-01	5.2424E-01	7.1034E-01	8.3C13E-01	9.1638E-01
18	7.1275E-02	1.9337E-01	2.7230E-01	3.2342E-01	3.6006E-01
19	3.7334E-03	1.0459E-02	1.4832E-02	1.7666E-02	1.9696E-02
20	8.4225E-06	2.3469E-05	3.3243E-05	3.9575E-05	4.4111E-05

Table C.62. Continued.

IRON-WATER, 1MEV, B1=3

GRP.	B2=1	B2=2	B2=3	B2=4	B2=5
1	1.4732E+00	1.3473E+00	1.2543E+00	1.1773E+00	1.1102E+00
2	1.4225E+00	1.3078E+00	1.2253E+00	1.1584E+00	1.1006E+00
3	1.3260E+00	1.2326E+00	1.1704E+00	1.1226E+00	1.0831E+00
4	1.2482E+00	1.1710E+00	1.1234E+00	1.0896E+00	1.0632E+00
5	1.1944E+00	1.1305E+00	1.0950E+00	1.0723E+00	1.0562E+00
6	1.1433E+00	1.0953E+00	1.0730E+00	1.0616E+00	1.0555E+00
7	1.0557E+00	1.0338E+00	1.0302E+00	1.0337E+00	1.0398E+00
8	8.9438E-01	9.1119E-01	9.3272E-01	9.5463E-01	9.7509E-01
9	7.1978E-01	7.7481E-01	8.1676E-01	8.5152E-01	8.8112E-01
10	6.8522E-01	7.6932E-01	8.2137E-01	8.6038E-01	8.9159E-01
11	7.0479E-01	8.9446E-01	9.9324E-01	1.0577E+00	1.1059E+00
12	6.4636E-01	9.0256E-01	1.0314E+00	1.1129E+00	1.1726E+00
13	5.9846E-01	8.9123E-01	1.0396E+00	1.1321E+00	1.1933E+00
14	5.4497E-01	8.8069E-01	1.0544E+00	1.1615E+00	1.2380E+00
15	4.7811E-01	8.5386E-01	1.0549E+00	1.1781E+00	1.2647E+00
16	3.7573E-01	7.6332E-01	9.8198E-01	1.1158E+00	1.2025E+00
17	2.3428E-01	5.6106E-01	7.5978E-01	8.8267E-01	9.6726E-01
18	7.5522E-02	2.0741E-01	2.9212E-01	3.4497E-01	3.8116E-01
19	3.9570E-03	1.1223E-02	1.5921E-02	1.8853E-02	2.0850E-02
20	8.9267E-06	2.5183E-05	3.5680E-05	4.2231E-05	4.6714E-05

IRON-WATER, 1MEV, B1=4

GRP.	B2=1	B2=2	B2=3	B2=4	B2=5
1	1.4143E+00	1.2857E+00	1.1935E+00	1.1194E+00	1.0559E+00
2	1.3721E+00	1.2552E+00	1.1736E+00	1.1093E+00	1.0549E+00
3	1.2920E+00	1.1971E+00	1.1259E+00	1.0903E+00	1.0533E+00
4	1.2255E+00	1.1479E+00	1.1016E+00	1.0696E+00	1.0451E+00
5	1.1806E+00	1.1174E+00	1.0831E+00	1.0619E+00	1.0471E+00
6	1.1403E+00	1.0930E+00	1.0712E+00	1.0603E+00	1.0546E+00
7	1.0694E+00	1.0460E+00	1.0402E+00	1.0431E+00	1.0493E+00
8	9.2908E-01	9.3996E-01	9.5710E-01	9.7563E-01	9.9364E-01
9	7.5817E-01	8.0809E-01	8.4586E-01	8.7724E-01	9.0404E-01
10	7.1242E-01	7.7713E-01	8.4743E-01	8.8493E-01	9.1449E-01
11	7.2872E-01	9.2618E-01	1.0269E+00	1.0903E+00	1.1364E+00
12	6.7176E-01	9.3953E-01	1.0715E+00	1.1521E+00	1.2095E+00
13	6.2332E-01	9.3022E-01	1.0830E+00	1.1751E+00	1.2398E+00
14	5.6801E-01	9.2089E-01	1.1009E+00	1.2084E+00	1.2826E+00
15	4.9830E-01	8.9413E-01	1.1039E+00	1.2285E+00	1.3132E+00
16	3.9197E-01	8.0109E-01	1.0306E+00	1.1672E+00	1.2598E+00
17	2.4452E-01	5.9010E-01	7.9984E-01	9.2639E-01	1.0105E+00
18	7.8877E-02	2.1845E-01	3.0816E-01	3.6286E-01	3.9908E-01
19	4.1322E-03	1.1825E-02	1.6802E-02	1.9833E-02	2.1849E-02
20	9.3243E-06	2.6530E-05	3.7651E-05	4.4437E-05	4.8925E-05

Table C.62. Continued.

IRON-WATER, 1MEV, B1=5

GRP.	B2=1	B2=2	B2=3	B2=4	B2=5
1	1.3556E+00	1.2270E+00	1.1367E+00	1.0654E+00	1.0072E+00
2	1.3226E+00	1.2056E+00	1.1258E+00	1.0640E+00	1.0140E+00
3	1.2599E+00	1.1650E+00	1.1050E+00	1.0614E+00	1.0268E+00
4	1.2061E+00	1.1286E+00	1.0832E+00	1.0525E+00	1.0296E+00
5	1.1713E+00	1.1031E+00	1.0743E+00	1.0537E+00	1.0393E+00
6	1.1418E+00	1.0937E+00	1.0714E+00	1.0604E+00	1.0546E+00
7	1.0848E+00	1.0564E+00	1.0514E+00	1.0523E+00	1.0562E+00
8	9.5960E-01	9.6530E-01	9.7855E-01	9.9439E-01	1.0099E+00
9	7.8980E-01	8.3603E-01	8.7071E-01	9.0954E-01	9.2381E-01
10	7.3531E-01	8.2067E-01	8.7065E-01	9.0627E-01	9.3391E-01
11	7.4912E-01	9.5301E-01	1.0555E+00	1.1136E+00	1.1627E+00
12	6.9309E-01	9.7049E-01	1.1056E+00	1.1861E+00	1.2412E+00
13	6.4410E-01	9.6275E-01	1.1197E+00	1.2121E+00	1.2745E+00
14	5.8722E-01	9.5435E-01	1.1402E+00	1.2487E+00	1.3207E+00
15	5.1512E-01	9.2758E-01	1.1452E+00	1.2719E+00	1.3548E+00
16	4.0545E-01	8.3238E-01	1.0714E+00	1.2112E+00	1.3015E+00
17	2.5313E-01	6.1410E-01	8.3347E-01	9.6381E-01	1.0474E+00
18	8.1653E-02	2.2756E-01	3.2160E-01	3.7815E-01	4.1432E-01
19	4.2791E-03	1.2320E-02	1.7540E-02	2.0683E-02	2.2689E-02
20	9.6531E-05	2.7642E-05	3.9303E-05	4.6327E-05	5.0805E-05

Table C.63. Scattered Energy Flux Spectra, $I^S(b_1+b_2,E_i)/I^S(b_1+b_2)$, for 1MeV Photons in Slabs of Tin Followed by Water.

TIN-WATER, 1MEV, B1=2

GRP.	B2=1	B2=2	B2=3	B2=4	B2=5
1	1.6728E+00	1.4904E+00	1.3715E+00	1.3715E+00	1.1998E+00
2	1.5986E+00	1.4338E+00	1.3230E+00	1.3280E+00	1.1785E+00
3	1.4576E+00	1.3265E+00	1.2454E+00	1.2454E+00	1.1380E+00
4	1.3447E+00	1.2408E+00	1.1789E+00	1.1789E+00	1.1033E+00
5	1.2613E+00	1.1795E+00	1.1332E+00	1.1332E+00	1.0829E+00
6	1.1791E+00	1.1215E+00	1.0925E+00	1.0925E+00	1.0686E+00
7	1.0421E+00	1.0224E+00	1.0139E+00	1.0139E+00	1.0299E+00
8	7.9367E-01	8.3510E-01	8.6745E-01	8.6745E-01	9.1975E-01
9	5.6066E-01	6.6845E-01	7.3261E-01	7.3261E-01	8.1535E-01
10	5.3544E-01	6.8697E-01	7.6871E-01	7.6871E-01	8.5621E-01
11	5.3193E-01	7.0472E-01	8.9231E-01	8.9231E-01	1.0280E+00
12	4.9250E-01	8.0273E-01	9.6783E-01	9.6783E-01	1.1491E+00
13	4.5840E-01	7.9297E-01	9.7736E-01	9.7739E-01	1.1811E+00
14	4.1136E-01	7.7205E-01	9.7799E-01	9.7799E-01	1.2065E+00
15	3.5299E-01	7.3482E-01	9.6314E-01	9.6314E-01	1.2177E+00
16	2.7092E-01	6.3892E-01	8.7251E-01	8.7251E-01	1.1363E+00
17	1.6448E-01	4.5160E-01	6.4753E-01	6.4753E-01	8.7323E-01
18	5.5029E-02	1.7019E-01	2.5263E-01	2.5263E-01	3.4887E-01
19	4.7079E-03	1.5146E-02	2.2702E-02	2.2702E-02	3.1547E-02
20	8.7113E-06	2.7857E-05	4.1691E-05	4.1691E-05	5.7876E-05

TIN-WATER, 1MEV, B1=4

GRP.	B2=1	B2=2	B2=3	B2=4	B2=5
1	1.6692E+00	1.4433E+00	1.3021E+00	1.3021E+00	1.1182E+00
2	1.5983E+00	1.3951E+00	1.2702E+00	1.2702E+00	1.1105E+00
3	1.4638E+00	1.3035E+00	1.2094E+00	1.2094E+00	1.0958E+00
4	1.3457E+00	1.2258E+00	1.1573E+00	1.1573E+00	1.0793E+00
5	1.2531E+00	1.1693E+00	1.1222E+00	1.1222E+00	1.0725E+00
6	1.1667E+00	1.1187E+00	1.0926E+00	1.0926E+00	1.0703E+00
7	1.0373E+00	1.0326E+00	1.0331E+00	1.0331E+00	1.0444E+00
8	8.0754E-01	8.6105E-01	8.9577E-01	8.9577E-01	9.4618E-01
9	5.7401E-01	6.9371E-01	7.6257E-01	7.6257E-01	8.4599E-01
10	5.2935E-01	7.0122E-01	7.9361E-01	7.9361E-01	8.9696E-01
11	5.2423E-01	7.5502E-01	9.2211E-01	9.2211E-01	1.0669E+00
12	4.8870E-01	8.2448E-01	1.0072E+00	1.0072E+00	1.1998E+00
13	4.5665E-01	8.1708E-01	1.0206E+00	1.0206E+00	1.2372E+00
14	4.1014E-01	7.9710E-01	1.0241E+00	1.0241E+00	1.2675E+00
15	3.5116E-01	7.5967E-01	1.0111E+00	1.0111E+00	1.2833E+00
16	2.6976E-01	6.6214E-01	9.1916E-01	9.1916E-01	1.2022E+00
17	1.6389E-01	4.6912E-01	6.8456E-01	6.8456E-01	9.2780E-01
18	5.4953E-02	1.7706E-01	2.6768E-01	2.6768E-01	3.7163E-01
19	4.6935E-03	1.5763E-02	2.4070E-02	2.4070E-02	3.3630E-02
20	8.6845E-06	2.8092E-05	4.4159E-05	4.4159E-05	6.1691E-05

Table C.64. Scattered Energy Flux Spectra, $I^S(b_1+b_2,E_i)/I^S(b_1+b_2)$, for 1MeV Photons in Slabs of Lead Followed by Water.

LEAD-WATER, 1MEV, B1=1

GRP.	B2=1	B2=2	B2=3	B2=4	B2=5
1	1.7592E+00	1.5614E+00	1.4431E+00	1.3477E+00	1.2661E+00
2	1.6633E+00	1.4941E+00	1.3899E+00	1.3059E+00	1.2349E+00
3	1.4811E+00	1.3663E+00	1.2885E+00	1.2266E+00	1.1756E+00
4	1.3494E+00	1.2569E+00	1.2067E+00	1.1602E+00	1.1239E+00
5	1.2697E+00	1.1939E+00	1.1511E+00	1.1168E+00	1.0922E+00
6	1.1994E+00	1.1353E+00	1.0991E+00	1.0786E+00	1.0567E+00
7	1.0601E+00	1.0215E+00	1.0118E+00	1.0138E+00	1.0199E+00
8	7.7255E-01	8.1464E-01	8.5445E-01	8.8942E-01	9.1906E-01
9	5.0364E-01	6.3005E-01	7.0672E-01	7.6283E-01	8.0633E-01
10	4.9640E-01	6.3668E-01	7.1642E-01	7.7355E-01	8.1752E-01
11	5.0481E-01	7.3125E-01	8.5488E-01	9.3956E-01	1.0031E+00
12	4.3423E-01	7.0934E-01	8.6384E-01	9.6514E-01	1.0475E+00
13	3.9394E-01	6.8662E-01	8.5716E-01	9.7417E-01	1.0613E+00
14	3.5196E-01	6.6649E-01	8.5649E-01	9.8758E-01	1.0852E+00
15	3.0288E-01	6.3495E-01	8.4400E-01	9.8931E-01	1.0974E+00
16	2.3276E-01	5.5505E-01	7.7042E-01	9.2232E-01	1.0356E+00
17	1.4233E-01	3.9873E-01	5.8347E-01	7.1660E-01	8.1650E-01
18	4.5332E-02	1.4511E-01	2.2100E-01	2.7659E-01	3.1847E-01
19	2.3667E-03	7.8255E-03	1.2012E-02	1.5082E-02	1.7398E-02
20	5.3414E-06	1.7568E-05	2.6933E-05	3.3797E-05	3.9374E-05

LEAD-WATER, 1MEV, B1=2

GRP.	B2=1	B2=2	B2=3	B2=4	B2=5
1	1.8972E+00	1.6156E+00	1.4546E+00	1.3420E+00	1.2439E+00
2	1.7795E+00	1.5372E+00	1.3973E+00	1.2997E+00	1.2195E+00
3	1.5560E+00	1.3832E+00	1.2885E+00	1.2194E+00	1.1636E+00
4	1.3743E+00	1.2690E+00	1.2068E+00	1.1528E+00	1.1151E+00
5	1.2487E+00	1.1873E+00	1.1416E+00	1.1101E+00	1.0863E+00
6	1.1479E+00	1.1156E+00	1.0900E+00	1.0744E+00	1.0644E+00
7	1.0029E+00	1.0045E+00	1.0075E+00	1.0141E+00	1.0224E+00
8	7.3897E-01	8.0920E-01	8.5851E-01	8.9594E-01	9.2740E-01
9	4.8725E-01	6.2824E-01	7.1320E-01	7.7105E-01	8.1666E-01
10	4.6903E-01	6.2567E-01	7.1941E-01	7.7966E-01	8.2667E-01
11	4.7671E-01	7.2231E-01	8.5591E-01	9.4846E-01	1.0159E+00
12	4.1115E-01	7.0271E-01	8.7178E-01	9.8035E-01	1.0636E+00
13	3.7317E-01	6.8093E-01	8.6652E-01	9.8729E-01	1.0791E+00
14	3.3324E-01	6.6137E-01	8.6708E-01	1.0021E+00	1.1049E+00
15	2.8642E-01	6.3024E-01	8.5502E-01	1.0050E+00	1.1190E+00
16	2.1997E-01	5.5130E-01	7.8252E-01	9.3944E-01	1.0579E+00
17	1.3437E-01	3.9624E-01	5.9384E-01	7.3034E-01	8.3570E-01
18	4.2752E-02	1.4424E-01	2.2527E-01	2.8222E-01	3.2641E-01
19	2.2314E-03	7.7790E-03	1.2246E-02	1.5393E-02	1.7836E-02
20	5.0363E-06	1.7464E-05	2.7455E-05	3.4491E-05	3.9954E-05

Table C.64. Continued.

LEAD-WATER, 1MEV, B1=3

GRP.	B2=1	B2=2	B2=3	B2=4	B2=5
1	2.0152E+00	1.6666E+00	1.4741E+00	1.3411E+00	1.2381E+00
2	1.8731E+00	1.5764E+00	1.4116E+00	1.2978E+00	1.2098E+00
3	1.6030E+00	1.4050E+00	1.2929E+00	1.2154E+00	1.1560E+00
4	1.3808E+00	1.2685E+00	1.1980E+00	1.1478E+00	1.1093E+00
5	1.2277E+00	1.1768E+00	1.1359E+00	1.1055E+00	1.0826E+00
6	1.1127E+00	1.1013E+00	1.0838E+00	1.0713E+00	1.0630E+00
7	9.6682E-01	9.9168E-01	1.0033E+00	1.0139E+00	1.0240E+00
8	7.1707E-01	8.0343E-01	8.5854E-01	8.9981E-01	9.3281E-01
9	4.7493E-01	6.2485E-01	7.1387E-01	7.7593E-01	8.2314E-01
10	4.5177E-01	6.2176E-01	7.1778E-01	7.8311E-01	8.3224E-01
11	4.5942E-01	7.1480E-01	8.5823E-01	9.5354E-01	1.0238E+00
12	3.9696E-01	6.9670E-01	8.7138E-01	9.8797E-01	1.0737E+00
13	3.6047E-01	6.7566E-01	8.6662E-01	9.9538E-01	1.0904E+00
14	3.2192E-01	6.5651E-01	8.5749E-01	1.0111E+00	1.1174E+00
15	2.7664E-01	6.2583E-01	8.5626E-01	1.0149E+00	1.1326E+00
16	2.1251E-01	5.4780E-01	7.8342E-01	9.4875E-01	1.0720E+00
17	1.2984E-01	3.9396E-01	5.9474E-01	7.3925E-01	8.4790E-01
18	4.1312E-02	1.4347E-01	2.2565E-01	2.8588E-01	3.3146E-01
19	2.1563E-03	7.7383E-03	1.2268E-02	1.5595E-02	1.8115E-02
20	4.8668E-06	1.7372E-05	2.7504E-05	3.4944E-05	4.0577E-05

LEAD-WATER, 1MEV, B1=4

GRP.	B2=1	B2=2	B2=3	B2=4	B2=5
1	2.1108E+00	1.7108E+00	1.4911E+00	1.3426E+00	1.2309E+00
2	1.9465E+00	1.6097E+00	1.4238E+00	1.2980E+00	1.2033E+00
3	1.6343E+00	1.4177E+00	1.2960E+00	1.2131E+00	1.1508E+00
4	1.3813E+00	1.2672E+00	1.1955E+00	1.1442E+00	1.1052E+00
5	1.2108E+00	1.1685E+00	1.1312E+00	1.1022E+00	1.0801E+00
6	1.0880E+00	1.0905E+00	1.0784E+00	1.0690E+00	1.0620E+00
7	9.4206E-01	9.8195E-01	9.9985E-01	1.0134E+00	1.0251E+00
8	7.0160E-01	7.9844E-01	8.5833E-01	9.0223E-01	9.3656E-01
9	4.6564E-01	6.2135E-01	7.1431E-01	7.7894E-01	8.2762E-01
10	4.3969E-01	6.1602E-01	7.1664E-01	7.8508E-01	8.3503E-01
11	4.4732E-01	7.0853E-01	8.5739E-01	9.5674E-01	1.0293E+00
12	3.8695E-01	6.9143E-01	8.7159E-01	9.9243E-01	1.0808E+00
13	3.5148E-01	6.7096E-01	8.6732E-01	1.0005E+00	1.0932E+00
14	3.1390E-01	6.5203E-01	8.6858E-01	1.0169E+00	1.1261E+00
15	2.6972E-01	6.2170E-01	8.5769E-01	1.0213E+00	1.1422E+00
16	2.0723E-01	5.4440E-01	7.8519E-01	9.5545E-01	1.0819E+00
17	1.2662E-01	3.9167E-01	5.9644E-01	7.4509E-01	8.5555E-01
18	4.0290E-02	1.4267E-01	2.2639E-01	2.8830E-01	3.3504E-01
19	2.1030E-03	7.6956E-03	1.2309E-02	1.5728E-02	1.8312E-02
20	4.7464E-06	1.7276E-05	2.7595E-05	3.5242E-05	4.1018E-05

Table C.64. Continued.

LEAD-WATER, 1MEV, B1=5

GRP.	B2=1	B2=2	B2=3	B2=4	B2=5
1	2.1881E+00	1.7478E+00	1.5058E+00	1.3426E+00	1.2274E+00
2	2.0046E+00	1.6373E+00	1.4343E+00	1.2980E+00	1.1976E+00
3	1.6560E+00	1.4272E+00	1.2585E+00	1.2131E+00	1.1470E+00
4	1.3798E+00	1.2652E+00	1.1634E+00	1.1442E+00	1.1022E+00
5	1.1977E+00	1.1621E+00	1.1275E+00	1.1022E+00	1.0781E+00
6	1.0697E+00	1.0621E+00	1.0745E+00	1.0690E+00	1.0610E+00
7	9.2393E-01	9.7429E-01	9.9701E-01	1.0134E+00	1.0257E+00
8	6.9029E-01	7.9430E-01	8.5763E-01	9.0223E-01	9.3925E-01
9	4.5849E-01	6.1826E-01	7.1434E-01	7.7894E-01	8.3075E-01
10	4.3076E-01	6.1139E-01	7.1554E-01	7.8508E-01	8.3860E-01
11	4.3840E-01	7.0342E-01	8.5650E-01	9.5674E-01	1.0331E+00
12	3.7954E-01	6.8705E-01	8.7150E-01	9.9243E-01	1.0857E+00
13	3.4481E-01	6.6683E-01	8.6760E-01	1.0000E+00	1.1038E+00
14	3.0795E-01	6.4825E-01	8.6916E-01	1.0169E+00	1.1323E+00
15	2.6459E-01	6.1820E-01	8.5854E-01	1.0213E+00	1.1490E+00
16	2.0330E-01	5.4149E-01	7.8633E-01	9.5545E-01	1.0810E+00
17	1.2423E-01	3.8973E-01	5.9760E-01	7.4509E-01	8.6270E-01
18	3.9529E-02	1.4199E-01	2.2690E-01	2.8830E-01	3.3760E-01
19	2.0633E-03	7.6584E-03	1.2357E-02	1.5723E-02	1.8453E-02
20	4.6569E-06	1.7193E-05	2.7659E-05	3.5242E-05	4.1333E-05

Table C.65. Scattered Energy Flux Spectra, $I^S(b_1+b_2,E_i)/I^S(b_1+b_2)$, for 1MeV Photons in Slabs of Tin Followed by Aluminum.

TIN-ALUM.,1MEV,B1=2

GRP.	B2=1	B2=2	B2=3	B2=4	B2=5
1	1.7004E+00	1.5441E+00	1.4394E+00	1.4394E+00	1.2790E+00
2	1.6248E+00	1.4854E+00	1.3936E+00	1.3936E+00	1.2562E+00
3	1.4812E+00	1.3739E+00	1.3066E+00	1.3066E+00	1.2127E+00
4	1.3658E+00	1.2841E+00	1.2356E+00	1.2356E+00	1.1741E+00
5	1.2809E+00	1.2205E+00	1.1875E+00	1.1875E+00	1.1521E+00
6	1.1956E+00	1.1582E+00	1.1421E+00	1.1421E+00	1.1337E+00
7	1.0535E+00	1.0516E+00	1.0602E+00	1.0602E+00	1.0664E+00
8	8.0536E-01	8.6261E-01	9.0664E-01	9.0664E-01	9.7461E-01
9	5.5904E-01	6.7538E-01	7.4683E-01	7.4683E-01	8.3972E-01
10	5.2657E-01	6.8082E-01	7.6627E-01	7.6627E-01	8.6938E-01
11	4.8814E-01	6.9490E-01	7.9999E-01	7.9999E-01	9.1681E-01
12	3.9014E-01	6.0760E-01	7.1836E-01	7.1836E-01	8.3975E-01
13	3.2469E-01	5.2242E-01	6.2381E-01	6.2381E-01	7.3486E-01
14	2.4260E-01	4.0609E-01	4.8974E-01	4.8974E-01	5.8080E-01
15	1.5163E-01	2.6454E-01	3.2195E-01	3.2195E-01	3.8374E-01
16	6.5836E-02	1.1345E-01	1.4514E-01	1.4514E-01	1.7376E-01
17	1.3445E-02	2.4654E-02	3.0335E-02	3.0335E-02	3.6417E-02
18	5.5049E-04	1.0103E-03	1.2433E-03	1.2433E-03	1.4926E-03
19	4.9819E-06	9.1455E-06	1.1255E-05	1.1255E-05	1.3513E-05
20	2.9261E-09	5.3711E-09	6.6104E-09	6.6104E-09	7.9345E-09

TIN-ALUM.,1MEV,B1=4

GRP.	B2=1	B2=2	B2=3	B2=4	B2=5
1	1.6972E+00	1.4968E+00	1.3708E+00	1.3708E+00	1.1976E+00
2	1.6249E+00	1.4469E+00	1.3369E+00	1.3369E+00	1.1889E+00
3	1.4874E+00	1.3520E+00	1.2724E+00	1.2724E+00	1.1724E+00
4	1.3666E+00	1.2703E+00	1.2162E+00	1.2162E+00	1.1531E+00
5	1.2725E+00	1.2116E+00	1.1790E+00	1.1790E+00	1.1454E+00
6	1.1829E+00	1.1567E+00	1.1451E+00	1.1451E+00	1.1396E+00
7	1.0480E+00	1.0632E+00	1.0773E+00	1.0773E+00	1.1053E+00
8	8.1936E-01	8.9055E-01	9.3844E-01	9.3844E-01	1.0061E+00
9	5.7226E-01	7.0155E-01	7.7878E-01	7.7878E-01	8.7360E-01
10	5.2056E-01	6.9554E-01	7.9227E-01	7.9227E-01	9.0222E-01
11	4.8094E-01	7.0878E-01	8.2684E-01	8.2684E-01	9.5193E-01
12	3.8706E-01	6.2374E-01	7.4685E-01	7.4685E-01	8.7592E-01
13	3.2291E-01	5.3767E-01	6.5008E-01	6.5008E-01	7.6792E-01
14	2.4139E-01	4.1840E-01	5.1109E-01	5.1109E-01	6.0765E-01
15	1.5070E-01	2.7259E-01	3.3613E-01	3.3613E-01	4.0176E-01
16	6.5480E-02	1.2217E-01	1.5168E-01	1.5168E-01	1.8207E-01
17	1.3379E-02	2.5445E-02	3.1723E-02	3.1723E-02	3.8179E-02
18	5.4776E-04	1.0427E-03	1.3002E-03	1.3002E-03	1.5649E-03
19	4.9573E-06	9.4389E-06	1.1771E-05	1.1771E-05	1.4167E-05
20	2.9116E-09	5.5362E-09	6.8999E-09	6.8999E-09	1.2678E-08

Table C.66. Scattered Energy Flux Spectra, $I^S(b_1+b_2,E_i)/I^S(b_1+b_2)$, for 1MeV Photons in Slabs of Lead Followed by Aluminum.

LEAD-ALUM.,1MEV,B1=2

GRP.	B2=1	B2=2	B2=3	B2=4	B2=5
1	1.9262E+00	1.6691E+00	1.5275E+00	1.5275E+00	1.3337E+00
2	1.8064E+00	1.5880E+00	1.4667E+00	1.4667E+00	1.3018E+00
3	1.5787E+00	1.4339E+00	1.3513E+00	1.3513E+00	1.2412E+00
4	1.3950E+00	1.3113E+00	1.2593E+00	1.2593E+00	1.1902E+00
5	1.2676E+00	1.2268E+00	1.1970E+00	1.1970E+00	1.1592E+00
6	1.1627E+00	1.1503E+00	1.1395E+00	1.1395E+00	1.1322E+00
7	1.0083E+00	1.0272E+00	1.0424E+00	1.0424E+00	1.0748E+00
8	7.3364E-01	8.1497E-01	8.7107E-01	8.7107E-01	9.5274E-01
9	4.7680E-01	6.2007E-01	7.0509E-01	7.0509E-01	8.1386E-01
10	4.6760E-01	6.3287E-01	7.2644E-01	7.2644E-01	8.4276E-01
11	4.4061E-01	6.4850E-01	7.5839E-01	7.5839E-01	8.8847E-01
12	3.4590E-01	5.6107E-01	6.7667E-01	6.7667E-01	8.1087E-01
13	2.8579E-01	4.8016E-01	5.8577E-01	5.8577E-01	7.0851E-01
14	2.1289E-01	3.7229E-01	4.5904E-01	4.5904E-01	5.5930E-01
15	1.3310E-01	2.4228E-01	3.0142E-01	3.0142E-01	3.6936E-01
16	5.7624E-02	1.0826E-01	1.3569E-01	1.3569E-01	1.6712E-01
17	1.1744E-02	2.2505E-02	2.8336E-02	2.8336E-02	3.5011E-02
18	4.8083E-04	9.2221E-04	1.1613E-03	1.1613E-03	1.4350E-03
19	4.3513E-06	8.3479E-06	1.0513E-05	1.0513E-05	1.2991E-05
20	2.5557E-09	4.9027E-09	6.1744E-09	6.1744E-09	7.6659E-09

LEAD-ALUM.,1MEV,B1=4

GRP.	B2=1	B2=2	B2=3	B2=4	B2=5
1	2.1417E+00	1.7682E+00	1.5634E+00	1.5634E+00	1.3177E+00
2	1.9745E+00	1.6633E+00	1.4925E+00	1.4925E+00	1.2873E+00
3	1.6567E+00	1.4642E+00	1.3579E+00	1.3579E+00	1.2296E+00
4	1.4013E+00	1.3093E+00	1.2535E+00	1.2535E+00	1.1813E+00
5	1.2287E+00	1.2078E+00	1.1850E+00	1.1850E+00	1.1545E+00
6	1.1015E+00	1.1243E+00	1.1280E+00	1.1280E+00	1.1314E+00
7	9.4603E-01	1.0032E+00	1.0348E+00	1.0348E+00	1.0798E+00
8	6.9555E-01	8.0269E-01	8.7162E-01	8.7162E-01	9.6285E-01
9	4.5511E-01	6.1189E-01	7.0744E-01	7.0744E-01	8.2517E-01
10	4.3808E-01	6.1908E-01	7.2530E-01	7.2530E-01	8.5291E-01
11	4.1281E-01	6.3447E-01	7.5800E-01	7.5800E-01	8.9953E-01
12	3.2496E-01	5.5036E-01	6.7763E-01	6.7763E-01	8.2287E-01
13	2.6870E-01	4.7141E-01	5.8719E-01	5.8719E-01	7.1964E-01
14	2.0018E-01	3.6564E-01	4.6041E-01	4.6041E-01	5.6850E-01
15	1.2509E-01	2.3796E-01	3.0240E-01	3.0240E-01	3.7550E-01
16	5.4171E-02	1.0637E-01	1.3615E-01	1.3615E-01	1.6997E-01
17	1.1042E-02	2.2117E-02	2.8449E-02	2.8449E-02	3.5617E-02
18	4.5209E-04	9.0631E-04	1.1660E-03	1.1660E-03	1.4593E-03
19	4.0912E-06	8.2040E-06	1.0555E-05	1.0555E-05	1.3216E-05
20	2.4030E-09	4.8170E-09	6.1714E-09	6.1714E-09	1.1843E-08

Table C.67. Scattered Energy Flux Spectra, $I^S(b_1+b_2,E_i)/I^S(b_1+b_2)$, for 1MeV Photons in Slabs of Water Followed by Iron.

WATER-IRON, 1MEV, B1=1

GRP.	B2=1	B2=2	B2=3	B2=4	B2=5
1	1.7252E+00	1.6842E+00	1.6358E+CC	1.5778E+CO	1.5176E+00
2	1.6501E+00	1.6193E+CC	1.5782E+CC	1.529?E+CO	1.4?6CCE+CO
3	1.5074E+00	1.4961E+CC	1.4685E+CC	1.4385E+CO	1.4086E+00
4	1.4067E+00	1.3977E+00	1.3787E+CC	1.3604E+CO	1.3444E+CO
5	1.3442E+00	1.3278E+CO	1.3135E+CC	1.3042E+CC	1.3000E+00
6	1.2739E+00	1.2518E+00	1.2457E+CC	1.2484E+CO	1.2553E+00
7	1.1183E+00	1.1114E+CO	1.1242E+CC	1.1437E+CO	1.1646E+00
8	8.2624E-01	8.6650E-01	9.0781E-01	9.4588E-01	9.7986E-01
9	5.3995E-01	5.9140E-01	6.3271E-01	6.6696E-01	6.9587E-01
10	4.2574E-01	4.4080E-01	4.6012E-01	4.7782E-01	4.9339E-01
11	2.0919E-01	2.0569E-01	2.1172E-01	2.1792E-01	2.2357E-01
12	5.2171E-02	5.1974E-02	5.388?E-02	5.5722E-02	5.7361E-02
13	2.1855E-02	2.2045E-02	2.2915E-02	2.3732E-02	2.4457E-02
14	6.6035E-03	6.6647E-03	6.9230E-03	7.1665E-03	7.3832E-03
15	1.2650E-03	1.2603E-03	1.3042E-03	1.3469E-03	1.3853E-03
16	1.3688E-04	1.1881E-04	1.1402E-04	1.1223E-04	1.1163E-04
17	2.6556E-06	2.6349E-06	2.6968E-06	2.7669E-06	2.8336E-06
18	1.4173E-08	1.4113E-08	1.4487E-08	1.4887E-08	2.2295E-08
19	1.1761E-11	2.3113E-11	1.7990E-11	3.7317E-11	4.8367E-11
20	2.2221E-15	3.3327E-15	3.7304E-15	3.8923E-15	4.6097E-15

WATER-IRON, 1MEV, B1=2

GRP.	B2=1	B2=2	B2=3	B2=4	B2=5
1	1.6686E+00	1.6254E+00	1.5752E+CC	1.5160E+CO	1.4566E+00
2	1.6045E+00	1.5698E+CO	1.5272E+CC	1.4788E+CO	1.4299E+00
3	1.4827E+00	1.4641E+CC	1.4360E+CC	1.4071E+CO	1.3792E+00
4	1.3876E+00	1.3755E+00	1.3589E+CC	1.3435E+CO	1.3302E+00
5	1.3198E+00	1.3117E+CC	1.3037E+CC	1.2935E+CC	1.2975E+00
6	1.2465E+00	1.2453E+CC	1.2481E+CC	1.2552E+CO	1.2641E+00
7	1.1102E+00	1.1256E+00	1.1444E+CC	1.1652E+CO	1.1856E+00
8	8.7111E-01	9.1163E-01	9.4733E-01	9.8127E-01	1.0111E+CO
9	6.1052E-01	6.4046E-01	6.7040E-01	6.9769E-01	7.2190E-01
10	4.7243E-01	4.6841E-01	4.8064E-01	4.9466E-01	5.0785E-01
11	2.3042E-01	2.1510E-01	2.1896E-01	2.2401E-01	2.2893E-01
12	5.7966E-02	5.4713E-02	5.5979E-02	5.7481E-02	5.8902E-02
13	2.4210E-02	2.3186E-02	2.3771E-02	2.4436E-02	2.5058E-02
14	7.2987E-03	6.9859E-03	7.1584E-03	7.3567E-03	7.5421E-03
15	1.3989E-03	1.3159E-03	1.3445E-03	1.3794E-03	1.4124E-03
16	1.3073E-04	1.1508E-04	1.1221E-04	1.1141E-04	1.1139E-04
17	2.9126E-06	2.7312E-06	2.7077E-06	2.8298E-06	2.8891E-06
18	1.5667E-08	1.5016E-08	1.4921E-08	2.1553E-08	2.3571E-08
19	1.6536E-11	4.2491E-11	3.1[illegible]E-11	4.2847E-11	4.9412E-11
20	2.9125E-15	3.4546E-15	3.4C[illegible]E-15	4.4C86E-15	5.3645E-15

Table C.67. Continued.

WATER-IRON, 1MEV, B1=3

GRP.	B2=1	B2=2	B2=3	B2=4	B2=5
1	1.6068E+00	1.5634E+00	1.5120E+00	1.4543E+00	1.3974E+00
2	1.5515E+00	1.5171E+00	1.4745E+00	1.4276E+00	1.3816E+00
3	1.4464E+00	1.4292E+00	1.4034E+00	1.3770E+00	1.3516E+00
4	1.3616E+00	1.3539E+00	1.3410E+00	1.3288E+00	1.3178E+00
5	1.3004E+00	1.3006E+00	1.2978E+00	1.2966E+00	1.2967E+00
6	1.2375E+00	1.2468E+00	1.2546E+00	1.2639E+00	1.2737E+00
7	1.1235E+00	1.1458E+00	1.1662E+00	1.1865E+00	1.2058E+00
8	9.1757E-01	9.5312E-01	9.8439E-01	1.0133E+00	1.0394E+00
9	6.6663E-01	6.8157E-01	7.0294E-01	7.2469E-01	7.4495E-01
10	5.1140E-01	4.9268E-01	4.9901E-01	5.0981E-01	5.2088E-01
11	2.4807E-01	2.2371E-01	2.2548E-01	2.2960E-01	2.3383E-01
12	6.2729E-02	5.7157E-02	5.7871E-02	5.9075E-02	6.0280E-02
13	2.6136E-02	2.4262E-02	2.4607E-02	2.5139E-02	2.5656E-02
14	7.8517E-03	7.3078E-03	7.4082E-03	7.5665E-03	7.7244E-03
15	1.4999E-03	1.3734E-03	1.3888E-03	1.4168E-03	1.4450E-03
16	1.3062E-04	1.1410E-04	1.1192E-04	1.1161E-04	1.1938E-04
17	3.0931E-06	2.8339E-06	2.8482E-06	2.8678E-06	2.8974E-06
18	1.6795E-08	1.6224E-08	1.5433E-08	2.3039E-08	3.1192E-08
19	2.0404E-11	3.8954E-11	4.1564E-11	5.3502E-11	5.7460E-11
20	3.0483E-15	4.3582E-15	3.8222E-15	4.8367E-15	5.1320E-15

WATER-IRON, 1MEV, B1=4

GRP.	B2=1	B2=2	B2=3	B2=4	B2=5
1	1.5402E+00	1.4993E+00	1.4497E+00	1.3952E+00	1.3418E+00
2	1.4947E+00	1.4633E+00	1.4230E+00	1.3792E+00	1.3363E+00
3	1.4084E+00	1.3950E+00	1.3724E+00	1.3488E+00	1.3259E+00
4	1.3373E+00	1.3349E+00	1.3256E+00	1.3159E+00	1.3069E+00
5	1.2868E+00	1.2934E+00	1.2943E+00	1.2954E+00	1.2967E+00
6	1.2372E+00	1.2525E+00	1.2630E+00	1.2738E+00	1.2834E+00
7	1.1432E+00	1.1676E+00	1.1877E+00	1.2067E+00	1.2246E+00
8	9.6018E-01	9.9052E-01	1.0172E+00	1.0420E+00	1.0650E+00
9	7.1333E-01	7.1695E-01	7.3140E-01	7.4852E-01	7.6553E-01
10	5.4468E-01	5.1413E-01	5.1543E-01	5.2341E-01	5.3265E-01
11	2.6317E-01	2.3151E-01	2.3150E-01	2.3469E-01	2.3830E-01
12	6.6773E-02	5.9344E-02	5.9578E-02	6.0515E-02	6.1537E-02
13	2.7807E-02	2.5221E-02	2.5359E-02	2.5771E-02	2.6213E-02
14	8.3473E-03	7.5950E-03	7.6322E-03	7.7556E-03	7.8893E-03
15	1.5940E-03	1.4250E-03	1.4289E-03	1.4506E-03	1.4745E-03
16	1.3264E-04	1.1428E-04	1.1227E-04	1.1444E-04	1.1938E-04
17	3.2647E-06	2.9118E-06	2.9213E-06	2.9067E-06	2.9667E-06
18	1.7452E-08	1.9206E-08	1.5917E-08	2.3503E-08	3.2278E-08
19	2.1784E-11	4.0782E-11	4.4965E-11	5.2339E-11	5.9713E-11
20	3.3116E-15	4.8021E-15	4.2323E-15	4.7893E-15	5.6519E-15

Table C.67. Continued.

WATER-IRON, 1MEV, B1=5

GRP.	B2=1	B2=2	B2=3	B2=4	B2=5
1	1.4726E+00	1.4346E+00	1.3887E+00	1.3377E+00	1.2878E+00
2	1.4379E+00	1.4098E+00	1.3731E+00	1.3325E+00	1.2927E+00
3	1.3719E+00	1.3628E+00	1.3434E+00	1.3225E+00	1.3020E+00
4	1.3159E+00	1.3183E+00	1.3121E+00	1.3046E+00	1.2972E+00
5	1.2777E+00	1.2892E+00	1.2927E+00	1.2953E+00	1.2976E+00
6	1.2413E+00	1.2604E+00	1.2722E+00	1.2831E+00	1.2931E+00
7	1.1643E+00	1.1892E+00	1.2082E+00	1.2259E+00	1.2425E+00
8	9.9832E-01	1.0743E+00	1.0467E+00	1.0583E+00	1.0884E+00
9	7.5327E-01	7.4794E-01	7.5664E-01	7.6996E-01	7.8416E-01
10	5.7398E-01	5.3326E-01	5.3022E-01	5.3584E-01	5.4342E-01
11	2.7626E-01	2.3859E-01	2.3700E-01	2.3939E-01	2.4243E-01
12	7.0255E-02	6.1310E-02	6.1126E-02	6.1834E-02	6.2695E-02
13	2.9246E-02	2.6082E-02	2.6039E-02	2.6350E-02	2.6726E-02
14	8.7750E-03	7.8528E-03	7.8362E-03	7.9287E-03	8.0410E-03
15	1.6752E-03	1.4715E-03	1.4654E-03	1.4816E-03	1.5018E-03
16	1.3524E-04	1.1498E-04	1.1297E-04	1.1013E-04	1.1836E-04
17	3.4150E-06	3.1675E-06	2.9902E-06	2.9983E-06	3.1764E-06
18	1.7944E-08	1.9059E-08	1.6874E-08	3.1535E-08	3.3430E-08
19	2.3865E-11	4.6825E-11	4.9552E-11	3.9587E-11	6.5478E-11
20	4.5428E-15	5.4431E-15	4.3234E-15	6.2032E-15	6.1570E-15

Table C.68. Scattered Energy Flux Spectra, $I^S(b_1+b_2,E_i)/I^S(b_1+b_2)$, for 1MeV Photons in Slabs of Lead Followed by Iron.

LEAD-IRON, 1MEV, B1=1

GRP.	B2=1	B2=2	B2=3	B2=4	B2=5
1	1.8897E+00	1.7618E+00	1.6842E+00	1.6144E+00	1.5474E+00
2	1.7851E+00	1.6833E+00	1.6185E+00	1.5601E+00	1.5046E+00
3	1.5863E+00	1.5340E+00	1.4638E+00	1.4571E+00	1.4234E+00
4	1.4415E+00	1.4168E+00	1.3918E+00	1.3706E+00	1.3518E+00
5	1.3507E+00	1.3339E+00	1.3182E+00	1.3078E+00	1.3018E+00
6	1.2648E+00	1.2482E+00	1.2425E+00	1.2449E+00	1.2516E+00
7	1.0948E+00	1.0948E+00	1.1106E+00	1.1326E+00	1.1545E+00
8	7.6441E-01	8.2760E-01	8.8066E-01	9.2561E-01	9.6406E-01
9	4.3976E-01	5.4412E-01	6.0477E-01	6.4810E-01	6.8206E-01
10	3.4203E-01	4.0320E-01	4.4315E-01	4.6678E-01	4.8540E-01
11	1.6892E-01	1.9424E-01	2.0563E-01	2.1389E-01	2.2060E-01
12	4.1855E-02	4.8840E-02	5.2187E-02	5.4588E-02	5.6526E-02
13	1.7613E-02	2.0607E-02	2.2093E-02	2.3155E-02	2.4016E-02
14	5.3166E-03	6.2136E-03	6.6571E-03	6.9751E-03	7.2308E-03
15	1.0125E-03	1.1773E-03	1.2555E-03	1.3115E-03	1.3565E-03
16	1.2361E-04	1.1819E-04	1.1326E-04	1.1148E-04	1.1089E-04
17	2.1540E-06	2.4688E-06	2.6141E-06	2.7083E-06	2.7875E-06
18	1.1575E-08	1.3191E-08	1.4032E-08	1.4572E-08	2.1963E-08
19	9.6879E-12	1.1109E-11	2.3335E-11	4.1073E-11	4.7643E-11
20	9.1875E-16	2.7443E-15	3.5949E-15	4.3514E-15	5.0709E-15

LEAD-IRON, 1MEV, B1=2

GRP.	B2=1	B2=2	B2=3	B2=4	B2=5
1	2.0322E+00	1.8213E+00	1.7026E+00	1.6122E+00	1.5336E+00
2	1.9042E+00	1.7308E+00	1.6325E+00	1.5572E+00	1.4927E+00
3	1.6611E+00	1.5578E+00	1.4960E+00	1.4527E+00	1.4156E+00
4	1.4632E+00	1.4180E+00	1.3830E+00	1.3650E+00	1.3466E+00
5	1.3237E+00	1.3187E+00	1.3100E+00	1.3034E+00	1.2997E+00
6	1.2055E+00	1.2252E+00	1.2340E+00	1.2430E+00	1.2531E+00
7	1.0309E+00	1.0746E+00	1.1062E+00	1.1344E+00	1.1602E+00
8	7.2773E-01	8.2003E-01	8.8389E-01	9.3340E-01	9.7394E-01
9	4.2398E-01	5.4145E-01	6.0860E-01	6.5487E-01	6.9015E-01
10	3.2211E-01	4.0264E-01	4.4278E-01	4.6922E-01	4.8920E-01
11	1.5896E-01	1.9073E-01	2.0502E-01	2.1454E-01	2.2138E-01
12	3.9529E-02	4.8071E-02	5.2117E-02	5.4834E-02	5.6925E-02
13	1.6644E-02	2.0292E-02	2.2074E-02	2.3273E-02	2.4194E-02
14	5.0222E-03	6.1173E-03	6.6501E-03	7.0084E-03	7.2838E-03
15	9.5485E-04	1.1579E-03	1.2581E-03	1.3169E-03	1.3660E-03
16	1.0954E-04	1.1126E-04	1.0994E-04	1.0973E-04	1.1000E-04
17	2.0287E-06	2.4243E-06	2.5985E-06	2.7113E-06	2.8009E-06
18	1.0834E-08	1.2970E-08	1.3965E-08	1.4605E-08	2.2245E-08
19	9.0952E-12	1.6068E-11	3.2105E-11	4.1991E-11	4.8790E-11
20	1.3977E-15	2.9447E-15	3.9209E-15	3.7605E-15	4.9970E-15

Table C.68. Continued.

LEAD-IRON, 1MEV, B1=3

GRP.	B2=1	B2=2	B2=3	B2=4	B2=5
1	2.1547E+00	1.8786E+00	1.7243E+00	1.6152E+00	1.5254E+00
2	2.0005E+00	1.7741E+00	1.6479E+00	1.5585E+00	1.4855E+00
3	1.7076E+00	1.5756E+00	1.5028E+00	1.4509E+00	1.4098E+00
4	1.4670E+00	1.4165E+00	1.3850E+00	1.3615E+00	1.3432E+00
5	1.2987E+00	1.3060E+00	1.3035E+00	1.3002E+00	1.2984E+00
6	1.1663E+00	1.2082E+00	1.2272E+00	1.2411E+00	1.2540E+00
7	9.9131E-01	1.0594E+00	1.1016E+00	1.1350E+00	1.1637E+00
8	7.0408E-01	8.1257E-01	8.8407E-01	9.3750E-01	9.8019E-01
9	4.1209E-01	5.3728E-01	6.0935E-01	6.5834E-01	6.9514E-01
10	3.0935E-01	3.9700E-01	4.4139E-01	4.7012E-01	4.9140E-01
11	1.5265E-01	1.8787E-01	2.0412E-01	2.1467E-01	2.2251E-01
12	3.8032E-02	4.7416E-02	5.1946E-02	5.4620E-02	5.7157E-02
13	1.6018E-02	2.0021E-02	2.2007E-02	2.3316E-02	2.4299E-02
14	4.8321E-03	6.0346E-03	6.6292E-03	7.0207E-03	7.3149E-03
15	9.1795E-04	1.1414E-03	1.2485E-03	1.3186E-03	1.3712E-03
16	1.0163E-04	1.0647E-04	1.0766E-04	1.0846E-04	1.0934E-04
17	1.9471E-06	2.3878E-06	2.5828E-06	2.7107E-06	2.8082E-06
18	1.0383E-08	1.2799E-08	1.3883E-08	2.1103E-06	2.3034E-06
19	8.7240E-12	1.6564E-11	4.0422E-11	4.9056E-11	4.4696E-11
20	1.7998E-15	3.1938E-15	4.2885E-15	4.1274E-15	5.6227E-15

LEAD-IRON, 1MEV, B1=4

GRP.	B2=1	B2=2	B2=3	B2=4	B2=5
1	2.2539E+00	1.9274E+00	1.7449E+00	1.6204E+00	1.5210E+00
2	2.0761E+00	1.8106E+00	1.6628E+00	1.5617E+00	1.4814E+00
3	1.7382E+00	1.5887E+00	1.5069E+00	1.4501E+00	1.4061E+00
4	1.4654E+00	1.4141E+00	1.3824E+00	1.3590E+00	1.3406E+00
5	1.2790E+00	1.2959E+00	1.2935E+00	1.2977E+00	1.2974E+00
6	1.1385E+00	1.1953E+00	1.2216E+00	1.2394E+00	1.2545E+00
7	9.6405E-01	1.0477E+00	1.0976E+00	1.1343E+00	1.1660E+00
8	6.8754E-01	8.0622E-01	8.8335E-01	9.3933E-01	9.8453E-01
9	4.0322E-01	5.3339E-01	6.0913E-01	6.6033E-01	6.9851E-01
10	3.0043E-01	3.9247E-01	4.3990E-01	4.7041E-01	4.9281E-01
11	1.4827E-01	1.8552E-01	2.0326E-01	2.1460E-01	2.2304E-01
12	3.6985E-02	4.6892E-02	5.1768E-02	5.4642E-02	5.7304E-02
13	1.5578E-02	1.9802E-02	2.1945E-02	2.3320E-02	2.4345E-02
14	4.6986E-03	5.9582E-03	6.6072E-03	7.0243E-03	7.3345E-03
15	8.9221E-04	1.1284E-03	1.2439E-03	1.3188E-03	1.3745E-03
16	9.6818E-05	1.0360E-04	1.0539E-04	1.1301E-04	1.4522E-04
17	1.8841E-06	2.3547E-06	2.5683E-06	2.7051E-06	2.7602E-06
18	1.0050E-08	1.2634E-08	2.0231E-08	2.1000E-08	2.2879E-08
19	8.4537E-12	2.6565E-11	4.3958E-11	4.7654E-11	5.5559E-11
20	1.9059E-15	3.4384E-15	3.8777E-15	5.0762E-15	5.9306E-15

Table C.68. Continued.

LEAD-IRON, 1MEV, B1=5

GRP.	B2=1	B2=2	B2=3	B2=4	B2=5
1	2.3338E+00	1.9681E+00	1.7628E+00	1.6262E+00	1.5185E+00
2	2.1357E+00	1.8407E+00	1.6757E+00	1.5653E+00	1.4788E+00
3	1.7594E+00	1.5985E+00	1.5102E+00	1.4497E+00	1.4034E+00
4	1.4622E+00	1.4116E+00	1.3803E+00	1.3570E+00	1.3387E+00
5	1.2637E+00	1.2879E+00	1.2942E+00	1.2956E+00	1.2967E+00
6	1.1179E+00	1.1852E+00	1.2171E+00	1.2377E+00	1.2547E+00
7	9.4418E-01	1.0385E+00	1.0941E+00	1.1345E+00	1.1675E+00
8	6.7537E-01	8.0116E-01	8.8246E-01	9.4137E-01	9.8763E-01
9	3.9646E-01	5.3006E-01	6.0864E-01	6.6153E-01	7.0096E-01
10	2.9389E-01	3.8886E-01	4.3857E-01	4.7044E-01	4.9377E-01
11	1.4506E-01	1.8385E-01	2.0252E-01	2.1447E-01	2.2331E-01
12	3.6214E-02	4.6474E-02	5.1611E-02	5.4937E-02	5.7403E-02
13	1.5255E-02	1.9628E-02	2.1871E-02	2.3330E-02	2.4411E-02
14	4.6009E-03	5.9152E-03	6.5975E-03	7.0241E-03	7.3478E-03
15	8.7329E-04	1.1181E-03	1.2399E-03	1.3185E-03	1.3767E-03
16	9.3523E-05	1.0152E-04	1.0475E-04	1.1298E-04	1.1800E-04
17	1.8344E-06	2.3294E-06	2.5584E-06	2.7045E-06	2.8238E-06
18	9.7902E-09	1.2523E-08	2.1051E-08	2.2149E-08	3.3980E-08
19	8.2674E-12	3.5339E-11	3.9978E-11	5.0352E-11	5.8930E-11
20	2.0484E-15	3.7451E-15	4.3187E-15	5.3730E-15	6.2962E-15

Table C.69. Scattered Energy Flux Spectra, $I^S(b_1+b_2,E_i)/I^S(b_1+b_2)$, for 1MeV Photons in Slabs of Water Followed by Tin.

WATER-TIN, 1MEV, B1=2

GRP.	B2=1	B2=2	B2=3	B2=4	B2=5
1	2.0666E+00	2.1317E+00	2.1530E+00	2.1530E+00	2.1260E+00
2	1.9719E+00	2.0301E+00	2.0486E+00	2.0486E+00	2.0319E+00
3	1.7921E+00	1.8371E+00	1.8501E+00	1.8501E+00	1.8527E+00
4	1.6271E+00	1.6464E+00	1.6513E+00	1.6513E+00	1.6584E+00
5	1.4722E+00	1.4650E+00	1.4610E+00	1.4610E+00	1.4671E+00
6	1.2834E+00	1.2573E+00	1.2486E+00	1.2486E+00	1.2513E+00
7	9.9998E-01	9.6658E-01	9.5579E-01	9.5576E-01	9.6548E-01
8	6.0238E-01	5.6858E-01	5.5994E-01	5.5994E-01	5.5980E-01
9	2.1082E-01	1.9093E-01	1.8777E-01	1.8777E-01	1.8726E-01
10	5.4518E-02	4.9699E-02	4.8347E-02	4.8347E-02	4.7284E-02
11	6.6232E-03	6.1950E-03	6.0455E-03	6.0455E-03	5.9277E-03
12	3.0758E-04	2.8606E-04	2.7998E-04	2.7998E-04	2.7627E-04
13	8.2517E-05	7.6317E-05	7.4565E-05	7.4565E-05	7.3578E-05
14	1.2845E-05	1.2102E-05	1.1891E-05	1.1891E-05	1.1527E-05
15	6.3897E-07	8.6690E-07	5.8216E-07	5.8216E-07	8.7442E-07
16	3.0543E-08	3.6377E-08	3.0146E-08	3.0146E-08	6.3147E-08
17	1.8260E-10	4.1115E-10	3.5769E-10	3.5769E-10	3.7693E-10
18	3.5743E-13	3.3127E-13	3.9652E-13	3.9652E-13	4.0344E-13
19	3.1521E-16	5.3752E-16	4.6872E-16	4.6872E-16	5.4347E-16
20	5.5036E-20	5.7153E-20	5.0749E-20	5.0749E-20	6.3276E-20

WATER-TIN, 1MEV, B1=4

GRP.	B2=1	B2=2	B2=3	B2=4	B2=5
1	1.9638E+00	2.0374E+00	2.0592E+00	2.0592E+00	2.0361E+00
2	1.8895E+00	1.9576E+00	1.9776E+00	1.9776E+00	1.9669E+00
3	1.7485E+00	1.8059E+00	1.8244E+00	1.8244E+00	1.8354E+00
4	1.6078E+00	1.6424E+00	1.6539E+00	1.6539E+00	1.6699E+00
5	1.4698E+00	1.4776E+00	1.4791E+00	1.4791E+00	1.4830E+00
6	1.3014E+00	1.2825E+00	1.2742E+00	1.2742E+00	1.2739E+00
7	1.0456E+00	1.0062E+00	9.9229E-01	9.9209E-01	9.7331E-01
8	6.5288E-01	5.9840E-01	5.7963E-01	5.7963E-01	5.7086E-01
9	2.3566E-01	1.9950E-01	1.9303E-01	1.9303E-01	1.9062E-01
10	5.6069E-02	4.9473E-02	4.8137E-02	4.8137E-02	4.7152E-02
11	6.7014E-03	6.1667E-03	6.0283E-03	6.0283E-03	5.9207E-03
12	3.2094E-04	2.8948E-04	2.8223E-04	2.8223E-04	2.7755E-04
13	8.6801E-05	7.7533E-05	7.5229E-05	7.5229E-05	7.4736E-05
14	1.3579E-05	1.1837E-05	1.1709E-05	1.1709E-05	1.1195E-05
15	6.5711E-07	6.3478E-07	5.8696E-07	5.8696E-07	1.1515E-06
16	2.3792E-08	3.7778E-08	3.5115E-08	3.5115E-08	7.1347E-08
17	2.5301E-10	4.1538E-10	3.2294E-10	3.2294E-10	4.7524E-10
18	4.1187E-13	4.0934E-13	3.6491E-13	3.6491E-13	5.0516E-13
19	3.6505E-16	4.5313E-16	4.9432E-16	4.9432E-16	6.1617E-16
20	5.7220E-20	6.6891E-20	6.5144E-20	6.5144E-20	5.3634E-20

Table C.70. Scattered Energy Flux Spectra, $I^S(b_1+b_2,E_i)/I^S(b_1+b_2)$, for 1MeV Photons in Slabs of Water Followed by Lead.

WATER-LEAD, 1MEV, B1=1

GRP.	B2=1	B2=2	B2=3	B2=4	B2=5
1	2.7957E+00	3.1363E+00	3.3475E+00	3.4967E+00	3.6245E+00
2	2.5968E+00	2.8572E+00	3.0108E+00	3.1160E+00	3.2048E+00
3	2.2189E+00	2.3269E+00	2.3704E+00	2.3928E+00	2.4074E+00
4	1.8318E+00	1.7990E+00	1.7651E+00	1.7389E+00	1.7159E+00
5	1.4368E+00	1.3220E+00	1.2536E+00	1.2203E+00	1.1892E+00
6	1.0174E+00	8.9835E-01	8.4294E-01	8.0887E-01	7.8179E-01
7	5.9761E-01	5.2225E-01	4.8667E-01	4.6427E-01	4.4632E-01
8	2.3745E-01	2.0782E-01	1.9431E-01	1.8569E-01	1.7872E-01
9	4.0558E-02	3.6102E-02	3.4104E-02	3.2818E-02	3.1765E-02
10	5.3277E-03	4.6964E-03	4.3560E-03	4.1296E-03	3.9451E-03
11	3.9255E-04	3.5077E-04	3.2713E-04	3.1142E-04	2.9858E-04
12	4.3436E-06	3.8871E-06	3.5911E-06	3.7132E-06	3.9846E-06
13	2.4870E-06	2.2030E-06	2.0622E-06	1.9697E-06	1.8993E-06
14	4.1943E-07	3.7150E-07	3.4752E-07	3.3134E-07	3.1793E-07
15	3.5374E-08	3.1402E-08	2.9314E-08	2.7836E-08	3.7244E-08
16	7.3105E-10	6.3195E-10	8.7356E-10	1.1013E-09	1.1018E-09
17	4.4911E-12	4.6854E-12	5.9838E-12	7.7498E-12	1.0169E-11
18	3.7333E-15	3.7829E-15	4.0905E-15	4.3010E-15	4.8842E-15
19	7.0203E-20	8.4056E-20	8.7338E-20	9.2442E-20	8.8051E-20
20	8.0171E-26	1.0715E-25	1.1187E-25	1.0274E-25	1.2367E-25

WATER-LEAD, 1MEV, B1=2

GRP.	B2=1	B2=2	B2=3	B2=4	B2=5
1	2.8497E+00	3.2302E+00	3.4466E+00	3.5900E+00	3.6957E+00
2	2.6473E+00	2.9335E+00	3.0872E+00	3.1861E+00	3.2575E+00
3	2.2627E+00	2.3697E+00	2.4044E+00	2.4186E+00	2.4249E+00
4	1.8470E+00	1.8016E+00	1.7597E+00	1.7299E+00	1.7083E+00
5	1.4180E+00	1.2935E+00	1.2303E+00	1.1936E+00	1.1692E+00
6	9.7875E-01	8.5671E-01	8.0654E-01	7.7895E-01	7.6013E-01
7	5.6233E-01	4.8633E-01	4.5819E-01	4.4198E-01	4.3065E-01
8	2.2202E-01	1.9242E-01	1.8274E-01	1.7684E-01	1.7256E-01
9	3.9147E-02	3.4290E-02	3.2588E-02	3.1586E-02	3.0883E-02
10	4.6558E-03	4.2301E-03	4.0258E-03	3.8940E-03	3.7775E-03
11	3.4692E-04	3.1927E-04	3.0466E-04	2.9456E-04	2.8695E-04
12	4.2274E-06	3.5606E-06	3.5370E-06	3.3475E-06	3.2659E-06
13	2.2832E-06	2.0370E-06	1.9385E-06	1.8747E-06	1.8285E-06
14	3.8354E-07	3.4282E-07	3.2534E-07	3.1531E-07	3.0744E-07
15	3.1702E-08	2.8737E-08	2.7327E-08	2.6464E-08	3.5559E-08
16	8.8664E-10	8.4477E-10	8.4155E-10	8.2440E-10	8.8620E-10
17	4.6675E-12	5.4787E-12	7.1113E-12	9.3385E-12	9.6119E-12
18	4.1411E-15	4.1949E-15	4.4267E-15	4.6279E-15	4.6268E-15
19	6.8311E-20	8.3351E-20	8.7540E-20	8.1306E-20	7.6670E-20
20	1.0427E-25	1.0600E-25	1.1175E-25	1.1720E-25	1.1720E-25

Table C.70. Continued.

WATER-LEAD, 1MEV, B1=3

GRP.	B2=1	B2=2	B2=3	B2=4	B2=5
1	2.8333E+00	3.2398E+00	3.4693E+00	3.6196E+00	3.7246E+00
2	2.6372E+00	2.9454E+00	3.1087E+00	3.2116E+00	3.2820E+00
3	2.2646E+00	2.3860E+00	2.4235E+00	2.4366E+00	2.4410E+00
4	1.8523E+00	1.8112E+00	1.7658E+00	1.7322E+00	1.7085E+00
5	1.4221E+00	1.2913E+00	1.2223E+00	1.1829E+00	1.1583E+00
6	9.8083E-01	8.4449E-01	7.9055E-01	7.6279E-01	7.4585E-01
7	5.6148E-01	4.7137E-01	4.4203E-01	4.2877E-01	4.1972E-01
8	2.2033E-01	1.8526E-01	1.7636E-01	1.7153E-01	1.6822E-01
9	3.9097E-02	3.3472E-02	3.1762E-02	3.0846E-02	3.0245E-02
10	4.3716E-03	3.9826E-03	3.8312E-03	3.7293E-03	3.6521E-03
11	3.2820E-04	3.0292E-04	2.9149E-04	2.8382E-04	2.7900E-04
12	4.4923E-06	4.7931E-06	4.7456E-06	4.7416E-06	4.7455E-06
13	2.2187E-06	1.9552E-06	1.8674E-06	1.8175E-06	1.7729E-06
14	3.7230E-07	3.2835E-07	3.1406E-07	3.0514E-07	2.9858E-07
15	2.9172E-08	2.7205E-08	2.6356E-08	3.5171E-08	2.5232E-08
16	8.6321E-10	8.1305E-10	5.6618E-10	9.1928E-10	1.2073E-09
17	5.1794E-12	5.9646E-12	8.4220E-12	9.5119E-12	9.8532E-12
18	4.1052E-15	4.1129E-15	4.4538E-15	4.5468E-15	4.7467E-15
19	8.2162E-20	8.1474E-20	6.6621E-20	8.3621E-20	8.0622E-20
20	1.0362E-25	1.0392E-25	1.1037E-25	1.1975E-25	1.2042E-25

WATER-LEAD, 1MEV, B1=4

GRP.	B2=1	B2=2	B2=3	B2=4	B2=5
1	2.7846E+00	3.2099E+00	3.4557E+00	3.6160E+00	3.7310E+00
2	2.6021E+00	2.9284E+00	3.1044E+00	3.2144E+00	3.2909E+00
3	2.2554E+00	2.3935E+00	2.4370E+00	2.4514E+00	2.4548E+00
4	1.8579E+00	1.8244E+00	1.7772E+00	1.7403E+00	1.7130E+00
5	1.4356E+00	1.2999E+00	1.2237E+00	1.1801E+00	1.1528E+00
6	9.9580E-01	8.4411E-01	7.8316E-01	7.5341E-01	7.3600E-01
7	5.7065E-01	4.6501E-01	4.3381E-01	4.2001E-01	4.1173E-01
8	2.2261E-01	1.8155E-01	1.7237E-01	1.6795E-01	1.6503E-01
9	3.9406E-02	3.3052E-02	3.1237E-02	3.0338E-02	2.9775E-02
10	4.2226E-03	3.8266E-03	3.6973E-03	3.6172E-03	3.5579E-03
11	3.2405E-04	2.8932E-04	2.8032E-04	2.7922E-04	2.7350E-04
12	6.7049E-06	4.9332E-06	4.7952E-06	4.4320E-06	5.9154E-06
13	2.2627E-06	1.8572E-06	1.8247E-06	1.7609E-06	1.7263E-06
14	3.9193E-07	3.2707E-07	3.0636E-07	2.9640E-07	2.9129E-07
15	3.5670E-08	2.8300E-08	3.5203E-08	2.5466E-08	2.4989E-08
16	1.1926E-09	8.7732E-10	1.0171E-09	1.3585E-09	1.3583E-09
17	7.2080E-12	7.5344E-12	9.5464E-12	9.8202E-12	9.7724E-12
18	4.0535E-15	3.9065E-15	4.5831E-15	4.6886E-15	4.6749E-15
19	9.1363E-20	7.6282E-20	6.5034E-20	9.3383E-20	8.3410E-20
20	1.1651E-25	1.2177E-25	1.1560E-25	1.1927E-25	1.1898E-25

Table C.70. Continued.

WATER-LEAD, 1MEV, B1=5

GRP.	B2=1	B2=2	B2=3	B2=4	B2=5
1	2.7221E+00	3.1640E+00	3.4235E+00	3.5976E+00	3.7196E+00
2	2.5564E+00	2.8989E+00	3.0867E+00	3.2065E+00	3.2881E+00
3	2.2414E+00	2.3962E+00	2.4466E+00	2.4634E+00	2.4677E+00
4	1.8644E+00	1.8391E+00	1.7912E+00	1.7503E+00	1.7207E+00
5	1.4534E+00	1.3134E+00	1.2302E+00	1.1813E+00	1.1511E+00
6	1.0158E+00	8.4937E-01	7.3076E-01	7.4771E-01	7.2937E-01
7	5.8346E-01	4.6301E-01	4.2924E-01	4.1382E-01	4.0567E-01
8	2.2642E-01	1.7965E-01	1.6579E-01	1.6537E-01	1.6266E-01
9	3.9874E-02	3.2859E-02	3.0900E-02	2.9975E-02	2.9417E-02
10	4.1549E-03	3.7252E-03	3.6024E-03	3.5338E-03	3.4837E-03
11	2.9984E-04	2.8962E-04	2.8807E-04	2.7284E-04	2.7039E-04
12	6.4656E-06	6.1171E-06	6.0804E-06	4.5917E-06	6.3966E-06
13	2.9449E-06	2.5329E-06	1.7736E-06	2.4252E-06	2.4228E-06
14	4.7581E-07	3.2056E-07	2.9649E-07	2.8725E-07	3.9093E-07
15	3.7623E-08	3.5612E-08	2.6047E-08	3.4445E-08	2.5560E-08
16	1.4630E-09	7.5573E-10	1.4766E-09	1.4411E-09	1.6062E-09
17	1.0706E-11	9.6299E-12	9.8990E-12	7.0532E-12	8.7522E-12
18	4.8752E-15	4.6135E-15	4.4686E-15	4.5295E-15	4.3156E-15
19	9.8764E-20	7.0828E-20	9.5375E-20	7.8120E-20	9.3980E-20
20	1.2664E-25	1.2539E-25	1.1976E-25	1.0613E-25	1.0573E-25

Table C.71. Scattered Energy Flux Spectra, $I^S(b_1+b_2,E_i)/I^S(b_1+b_2)$, for 1MeV Photons in Slabs of Iron Followed by Lead.

IRON-LEAD, 1MEV, B1=1

GRP.	B2=1	B2=2	B2=3	B2=4	B2=5
1	2.8159E+00	3.1532E+00	3.3620E+00	3.5148E+00	3.6259E+00
2	2.6119E+00	2.8693E+00	3.0206E+00	3.1282E+00	3.2054E+00
3	2.2242E+00	2.3299E+00	2.3727E+00	2.3936E+00	2.4053E+00
4	1.8304E+00	1.7962E+00	1.7624E+00	1.7357E+00	1.7158E+00
5	1.4306E+00	1.3170E+00	1.2557E+00	1.2163E+00	1.1893E+00
6	1.0106E+00	8.9413E-01	8.3971E-01	8.0554E-01	7.8197E-01
7	5.9323E-01	5.1977E-01	4.8465E-01	4.6215E-01	4.4650E-01
8	2.3560E-01	2.0693E-01	1.9355E-01	1.8483E-01	1.7881E-01
9	4.0261E-02	3.5964E-02	3.3982E-02	3.2708E-02	3.1787E-02
10	5.3148E-03	4.6791E-03	4.3357E-03	4.1129E-03	3.9505E-03
11	3.9142E-04	3.4944E-04	3.2576E-04	3.1007E-04	2.9884E-04
12	4.3469E-06	3.8758E-06	3.7442E-06	3.5113E-06	3.6462E-06
13	2.4720E-06	2.1943E-06	2.0536E-06	1.9621E-06	1.8960E-06
14	4.1706E-07	3.7001E-07	3.4584E-07	3.3028E-07	3.1867E-07
15	3.5144E-08	3.1276E-08	2.9114E-08	2.7753E-08	2.6667E-08
16	7.1021E-10	6.3239E-10	8.8199E-10	8.4111E-10	1.0762E-09
17	3.5883E-12	4.8728E-12	7.8303E-12	7.4721E-12	9.3653E-12
18	1.8699E-15	4.0316E-15	4.8210E-15	4.3478E-15	4.6279E-15
19	6.2524E-20	7.9369E-20	9.3162E-20	8.5539E-20	9.4816E-20
20	8.2186E-26	1.0053E-25	9.4044E-26	9.9200E-26	1.0176E-25

IRON-LEAD, 1MEV, B1=2

GRP.	B2=1	B2=2	B2=3	B2=4	B2=5
1	2.8637E+00	3.2370E+00	3.4468E+00	3.5547E+00	3.6970E+00
2	2.6571E+00	2.9376E+00	3.0883E+00	3.1889E+00	3.2580E+00
3	2.2645E+00	2.3687E+00	2.4034E+00	2.4168E+00	2.4239E+00
4	1.8459E+00	1.8092E+00	1.7596E+00	1.7290E+00	1.7080E+00
5	1.4150E+00	1.2922E+00	1.2301E+00	1.1933E+00	1.1693E+00
6	9.7528E-01	8.9603E-01	8.0706E-01	7.7898E-01	7.6043E-01
7	5.5949E-01	4.8821E-01	4.5951E-01	4.4215E-01	4.3092E-01
8	2.2062E-01	1.9248E-01	1.8291E-01	1.7694E-01	1.7267E-01
9	3.8948E-02	3.4295E-02	3.2610E-02	3.1614E-02	3.0906E-02
10	4.6615E-03	4.2403E-03	4.0324E-03	3.8921E-03	3.7827E-03
11	3.4704E-04	3.1973E-04	3.0502E-04	2.9484E-04	2.8720E-04
12	4.0215E-06	3.6210E-06	3.5040E-06	3.3201E-06	4.7102E-06
13	2.2779E-06	2.0387E-06	1.9402E-06	1.8768E-06	1.8301E-06
14	3.8258E-07	3.4299E-07	3.2630E-07	3.1567E-07	3.0759E-07
15	3.1414E-08	2.8683E-08	2.7319E-08	2.6430E-08	2.5743E-08
16	6.3943E-10	5.8151E-10	9.6520E-10	8.0141E-10	1.0354E-09
17	3.2584E-12	4.5103E-12	7.4414E-12	5.6919E-12	9.0146E-12
18	1.6940E-15	3.7362E-15	4.3271E-15	3.6717E-15	4.6200E-15
19	5.7080E-20	6.7985E-20	8.5193E-20	8.1603E-20	7.5447E-20
20	7.2593E-26	8.3508E-26	1.0938E-25	9.4108E-26	1.1234E-25

Table C.71. Continued.

IRON-LEAD, 1MEV, B1=3

GRP.	B2=1	B2=2	B2=3	B2=4	B2=5
1	2.8527E+00	3.2466E+00	3.4783E+00	3.6246E+00	3.7280E+00
2	2.6515E+00	2.9501E+00	3.1140E+00	3.2143E+00	3.2837E+00
3	2.2692E+00	2.3868E+00	2.4218E+00	2.4347E+00	2.4395E+00
4	1.8516E+00	1.8095E+00	1.7639E+00	1.7311E+00	1.7077E+00
5	1.4179E+00	1.2893E+00	1.2209E+00	1.1824E+00	1.1581E+00
6	9.7505E-01	8.4307E-01	7.8991E-01	7.6287E-01	7.4604E-01
7	5.5604E-01	4.7078E-01	4.4290E-01	4.2903E-01	4.1999E-01
8	2.1757E-01	1.8519E-01	1.7641E-01	1.7166E-01	1.6833E-01
9	3.8714E-02	3.3438E-02	3.1775E-02	3.0874E-02	3.0269E-02
10	4.3634E-03	3.9869E-03	3.8400E-03	3.7373E-03	3.6579E-03
11	3.2770E-04	3.0335E-04	2.9193E-04	2.8432E-04	2.7875E-04
12	3.8993E-06	4.8963E-06	3.3202E-06	4.6023E-06	4.6855E-06
13	2.2073E-06	1.9477E-06	1.8693E-06	1.8185E-06	1.7788E-06
14	3.6967E-07	3.2866E-07	3.1415E-07	3.0550E-07	2.9990E-07
15	2.9843E-08	2.7201E-08	2.6190E-08	2.5513E-08	2.5464E-08
16	6.1244E-10	8.3819E-10	5.3255E-10	7.9348E-10	1.2572E-09
17	4.5108E-12	7.5149E-12	5.9854E-12	7.0529E-12	8.0589E-12
18	2.6420E-15	4.1751E-15	3.6174E-15	4.4198E-15	4.3501E-15
19	6.4954E-20	7.3402E-20	7.4905E-20	8.2942E-20	7.7369E-20
20	7.2811E-26	8.0017E-26	7.5710E-26	9.4980E-26	1.0619E-25

IRON-LEAD, 1MEV, B1=4

GRP.	B2=1	B2=2	B2=3	B2=4	B2=5
1	2.8125E+00	3.2257E+00	3.4699E+00	3.6256E+00	3.7351E+00
2	2.6226E+00	2.9390E+00	3.1130E+00	3.2200E+00	3.2932E+00
3	2.2618E+00	2.3941E+00	2.4350E+00	2.4492E+00	2.4535E+00
4	1.8571E+00	1.8215E+00	1.7742E+00	1.7391E+00	1.7119E+00
5	1.4238E+00	1.2960E+00	1.2212E+00	1.1787E+00	1.1524E+00
6	9.8750E-01	8.4105E-01	7.8131E-01	7.5296E-01	7.3614E-01
7	5.6257E-01	4.6347E-01	4.3397E-01	4.2006E-01	4.1200E-01
8	2.1858E-01	1.8121E-01	1.7233E-01	1.6800E-01	1.6515E-01
9	3.8892E-02	3.2909E-02	3.1239E-02	3.0355E-02	2.9793E-02
10	4.2088E-03	3.8315E-03	3.7060E-03	3.6247E-03	3.5623E-03
11	3.1805E-04	2.9330E-04	2.8306E-04	2.7697E-04	2.7276E-04
12	3.8627E-06	4.7837E-06	3.2107E-06	4.5798E-06	4.6270E-06
13	2.1834E-06	1.9275E-06	1.8229E-06	1.7764E-06	1.7453E-06
14	3.6402E-07	3.2029E-07	3.0613E-07	2.9682E-07	2.9306E-07
15	2.9097E-08	2.6347E-08	2.5435E-08	2.4955E-08	2.6430E-08
16	5.9562E-10	8.1375E-10	5.1546E-10	9.9116E-10	1.3590E-09
17	4.4421E-12	7.6709E-12	4.8550E-12	8.7057E-12	9.2712E-12
18	2.7236E-15	4.2422E-15	3.8508E-15	3.6224E-15	4.6617E-15
19	6.8164E-20	7.6022E-20	6.5464E-20	7.5259E-20	8.4612E-20
20	7.7710E-26	8.2134E-26	8.9923E-26	1.0397E-25	1.1610E-25

Table C.71. Continued.

IRON-LEAD, 1MEV, B1=5

GRP.	B2=1	B2=2	B2=3	B2=4	B2=5
1	2.7597E+00	3.1838E+00	3.4361E+00	3.6084E+00	3.7260E+00
2	2.5845E+00	2.9125E+00	3.0948E+00	3.2130E+00	3.2916E+00
3	2.2517E+00	2.3969E+00	2.4462E+00	2.4616E+00	2.4662E+00
4	1.8641E+00	1.8356E+00	1.7881E+00	1.7483E+00	1.7189E+00
5	1.4452E+00	1.3083E+00	1.2273E+00	1.1795E+00	1.1503E+00
6	1.0036E+00	8.4903E-01	7.7916E-01	7.4704E-01	7.2935E-01
7	5.7148E-01	4.6067E-01	4.2783E-01	4.1386E-01	4.0610E-01
8	2.2054E-01	1.7907E-01	1.6975E-01	1.6541E-01	1.6276E-01
9	3.9136E-02	3.2759E-02	3.0888E-02	2.9982E-02	2.9431E-02
10	4.1155E-03	3.7276E-03	3.6069E-03	3.5398E-03	3.4884E-03
11	3.1268E-04	2.8597E-04	2.7203E-04	2.7149E-04	2.7083E-04
12	3.8865E-06	4.1535E-06	4.9708E-06	4.5986E-06	5.8380E-06
13	2.1758E-06	1.9090E-06	1.9189E-06	1.7356E-06	2.4164E-06
14	3.6308E-07	3.1292E-07	2.9691E-07	2.9471E-07	3.9037E-07
15	2.8678E-08	2.5935E-08	3.5031E-08	2.4684E-08	3.1157E-08
16	5.9611E-10	6.6334E-10	1.3722E-09	1.0992E-09	1.5893E-09
17	3.4269E-12	6.7710E-12	9.7534E-12	7.8757E-12	8.0564E-12
18	3.2329E-15	4.3401E-15	4.2648E-15	4.4111E-15	4.7998E-15
19	7.0152E-20	8.5526E-20	8.9128E-20	8.2735E-20	8.3693E-20
20	8.3511E-26	1.0998E-25	1.1857E-25	1.1161E-25	1.2283E-25

Table C.72. Scattered Energy Flux Spectra, $I^S(b_1+b_2,E_i)/I^S(b_1+b_2)$, for 3MeV Photons in Slabs of Iron Followed by Water.

IRON-WATER, 3MEV, B1=1

GRP.	B2=1	B2=2	B2=3	B2=4	B2=5
1	5.1868E-01	5.1562E-01	5.1295E-01	5.0842E-01	5.0262E-01
2	5.0079E-01	4.9855E-01	4.9632E-01	4.9239E-01	4.8735E-01
3	4.6681E-01	4.6610E-01	4.6471E-01	4.6192E-01	4.5834E-01
4	4.3460E-01	4.3504E-01	4.3430E-01	4.3245E-01	4.3008E-01
5	4.0527E-01	4.0639E-01	4.0611E-01	4.0503E-01	4.0366E-01
6	3.7921E-01	3.8048E-01	3.8042E-01	3.7991E-01	3.7931E-01
7	3.5690E-01	3.5773E-01	3.5765E-01	3.5751E-01	3.5750E-01
8	3.3867E-01	3.3850E-01	3.3817E-01	3.3822E-01	3.3861E-01
9	3.2435E-01	3.2247E-01	3.2159E-01	3.2157E-01	3.2210E-01
10	3.1454E-01	3.1048E-01	3.0887E-01	3.0867E-01	3.0923E-01
11	3.0902E-01	3.0247E-01	3.0012E-01	2.9969E-01	3.0020E-01
12	3.0432E-01	2.9567E-01	2.9281E-01	2.9226E-01	2.9275E-01
13	2.9053E-01	2.8252E-01	2.8040E-01	2.8054E-01	2.8146E-01
14	2.4315E-01	2.4314E-01	2.4513E-01	2.4752E-01	2.4993E-01
15	1.7679E-01	1.8569E-01	1.9117E-01	1.9529E-01	1.9866E-01
16	1.9813E-01	2.1477E-01	2.2179E-01	2.2666E-01	2.3060E-01
17	2.1061E-01	2.3918E-01	2.4994E-01	2.5701E-01	2.6254E-01
18	1.9175E-01	2.3085E-01	2.4434E-01	2.5276E-01	2.5912E-01
19	1.3434E-01	1.7618E-01	1.8970E-01	1.9773E-01	2.0370E-01
20	1.4309E-02	1.8969E-02	2.0466E-02	2.1352E-02	2.2009E-02

IRON-WATER, 3MEV, B1=2

GRP.	B2=1	B2=2	B2=3	B2=4	B2=5
1	5.0823E-01	5.0944E-01	5.0516E-01	5.0029E-01	4.9440E-01
2	4.9244E-01	4.9355E-01	4.8974E-01	4.8549E-01	4.8038E-01
3	4.6244E-01	4.6336E-01	4.6044E-01	4.5737E-01	4.5375E-01
4	4.3323E-01	4.3410E-01	4.3176E-01	4.2968E-01	4.2727E-01
5	4.0586E-01	4.0681E-01	4.0489E-01	4.0351E-01	4.0223E-01
6	3.8072E-01	3.8187E-01	3.8006E-01	3.7944E-01	3.7888E-01
7	3.5839E-01	3.5938E-01	3.5791E-01	3.5777E-01	3.5783E-01
8	3.3921E-01	3.4139E-01	3.3876E-01	3.3895E-01	3.3944E-01
9	3.2274E-01	3.2567E-01	3.2216E-01	3.2247E-01	3.2318E-01
10	3.1000E-01	3.1359E-01	3.0926E-01	3.0959E-01	3.1041E-01
11	3.0119E-01	3.0541E-01	3.0025E-01	3.0059E-01	3.0130E-01
12	2.9385E-01	2.9838E-01	2.9283E-01	2.9312E-01	2.9397E-01
13	2.8148E-01	2.8488E-01	2.8111E-01	2.8182E-01	2.8297E-01
14	2.4595E-01	2.4481E-01	2.4801E-01	2.5029E-01	2.5247E-01
15	1.9154E-01	1.8515E-01	1.9564E-01	1.9891E-01	2.0172E-01
16	2.2108E-01	2.0462E-01	2.2692E-01	2.3079E-01	2.3415E-01
17	2.4843E-01	2.2001E-01	2.5723E-01	2.6284E-01	2.6730E-01
18	2.4165E-01	2.0182E-01	2.5284E-01	2.5946E-01	2.6466E-01
19	1.8612E-01	1.4246E-01	1.9761E-01	2.0390E-01	2.0870E-01
20	2.0066E-02	1.5196E-02	2.1337E-02	2.2029E-02	2.2556E-02

Table C.72. Continued.

IRON-WATER, 3MEV, B1=3

GRP.	B2=1	B2=2	B2=3	B2=4	B2=5
1	4.9954E-01	4.9841E-01	4.9542E-01	4.9079E-01	4.8529E-01
2	4.8539E-01	4.8418E-01	4.8151E-01	4.7747E-01	4.7270E-01
3	4.5852E-01	4.5716E-01	4.5508E-01	4.5214E-01	4.4879E-01
4	4.3180E-01	4.3021E-01	4.2861E-01	4.2656E-01	4.2432E-01
5	4.0628E-01	4.0447E-01	4.0330E-01	4.0206E-01	4.0091E-01
6	3.8244E-01	3.8043E-01	3.7962E-01	3.7903E-01	3.7855E-01
7	3.6121E-01	3.5890E-01	3.5831E-01	3.5820E-01	3.5832E-01
8	3.4282E-01	3.4017E-01	3.3972E-01	3.3995E-01	3.4048E-01
9	3.2671E-01	3.2374E-01	3.2333E-01	3.2374E-01	3.2450E-01
10	3.1381E-01	3.1079E-01	3.1045E-01	3.1097E-01	3.1185E-01
11	3.0477E-01	3.0171E-01	3.0138E-01	3.0195E-01	3.0288E-01
12	2.9716E-01	2.9424E-01	2.9396E-01	2.9454E-01	2.9549E-01
13	2.8439E-01	2.8247E-01	2.8267E-01	2.8356E-01	2.8473E-01
14	2.4819E-01	2.4927E-01	2.5108E-01	2.5305E-01	2.5497E-01
15	1.9111E-01	1.9635E-01	1.9958E-01	2.0222E-01	2.0452E-01
16	2.0955E-01	2.2633E-01	2.3147E-01	2.3472E-01	2.3744E-01
17	2.2667E-01	2.5577E-01	2.6346E-01	2.6804E-01	2.7178E-01
18	2.3870E-01	2.4997E-01	2.5994E-01	2.6533E-01	2.6957E-01
19	1.4786E-01	1.9360E-01	2.0409E-01	2.0923E-01	2.1312E-01
20	1.5784E-02	2.0887E-02	2.2048E-02	2.2614E-02	2.3040E-02

IRON-WATER, 3MEV, B1=4

GRP.	B2=1	B2=2	B2=3	B2=4	B2=5
1	4.8830E-01	4.8727E-01	4.8469E-01	4.8061E-01	4.7569E-01
2	4.7596E-01	4.7478E-01	4.7245E-01	4.6889E-01	4.6464E-01
3	4.5251E-01	4.5104E-01	4.4920E-01	4.4663E-01	4.4366E-01
4	4.2842E-01	4.2661E-01	4.2513E-01	4.2332E-01	4.2133E-01
5	4.0483E-01	4.0273E-01	4.0161E-01	4.0051E-01	3.9942E-01
6	3.8230E-01	3.8000E-01	3.7920E-01	3.7863E-01	3.7830E-01
7	3.6202E-01	3.5946E-01	3.5836E-01	3.5878E-01	3.5892E-01
8	3.4420E-01	3.4138E-01	3.4091E-01	3.4113E-01	3.4163E-01
9	3.2819E-01	3.2521E-01	3.2484E-01	3.2523E-01	3.2593E-01
10	3.1508E-01	3.1229E-01	3.1207E-01	3.1260E-01	3.1343E-01
11	3.0576E-01	3.0316E-01	3.0303E-01	3.0363E-01	3.0453E-01
12	2.9802E-01	2.9569E-01	2.9562E-01	2.9625E-01	2.9716E-01
13	2.8585E-01	2.8436E-01	2.8467E-01	2.8552E-01	2.8662E-01
14	2.5192E-01	2.5266E-01	2.5415E-01	2.5580E-01	2.5745E-01
15	1.9597E-01	2.0053E-01	2.0314E-01	2.0525E-01	2.0714E-01
16	2.1379E-01	2.3094E-01	2.3567E-01	2.3826E-01	2.4051E-01
17	2.3212E-01	2.6198E-01	2.6897E-01	2.7276E-01	2.7581E-01
18	2.1422E-01	2.5689E-01	2.6612E-01	2.7059E-01	2.7404E-01
19	1.5212E-01	1.9971E-01	2.0964E-01	2.1394E-01	2.1711E-01
20	1.6245E-02	2.1556E-02	2.2657E-02	2.3136E-02	2.3477E-02

Table C.72. Continued.

IRON-WATER, 3MEV, B1=5

GRP.	B2=1	B2=2	B2=3	B2=4	B2=5
1	4.7640E-01	4.7556E-01	4.7347E-01	4.6598E-01	4.6642E-01
2	4.6590E-01	4.6487E-01	4.6299E-01	4.5596E-01	4.5689E-01
3	4.4593E-01	4.4456E-01	4.4309E-01	4.4094E-01	4.3876E-01
4	4.2455E-01	4.2277E-01	4.2153E-01	4.2001E-01	4.1850E-01
5	4.0299E-01	4.0086E-01	3.9990E-01	3.9901E-01	3.9813E-01
6	3.8191E-01	3.7956E-01	3.7885E-01	3.7845E-01	3.7810E-01
7	3.6274E-01	3.6009E-01	3.5951E-01	3.5947E-01	3.5954E-01
8	3.4568E-01	3.4275E-01	3.4225E-01	3.4243E-01	3.4279E-01
9	3.2999E-01	3.2696E-01	3.2653E-01	3.2685E-01	3.2737E-01
10	3.1693E-01	3.1417E-01	3.1391E-01	3.1437E-01	3.1500E-01
11	3.0757E-01	3.0507E-01	3.0494E-01	3.0543E-01	3.0614E-01
12	2.9982E-01	2.9763E-01	2.9757E-01	2.9814E-01	2.9881E-01
13	2.8808E-01	2.8663E-01	2.8687E-01	2.8763E-01	2.8843E-01
14	2.5563E-01	2.5601E-01	2.5716E-01	2.5845E-01	2.5973E-01
15	2.0015E-01	2.0425E-01	2.0638E-01	2.0806E-01	2.0950E-01
16	2.1759E-01	2.3508E-01	2.3933E-01	2.4154E-01	2.4328E-01
17	2.3686E-01	2.6746E-01	2.7395E-01	2.7708E-01	2.7943E-01
18	2.1895E-01	2.6290E-01	2.7163E-01	2.7535E-01	2.7802E-01
19	1.5572E-01	2.0494E-01	2.1454E-01	2.1818E-01	2.2066E-01
20	1.6634E-02	2.2129E-02	2.3193E-02	2.3594E-02	2.3845E-02

Table C.73. Scattered Energy Flux Spectra, $I^S(b_1+b_2,E_i)/I^S(b_1+b_2)$, for 3MeV Photons in Slabs of Tin Followed by Water.

TIN-WATER, 3MEV, B1=2

GRP.	B2=1	B2=2	B2=3	B2=4	B2=5
1	5.0887E-01	5.0577E-01	5.0324E-01	5.0324E-01	4.9375E-01
2	4.9361E-01	4.9056E-01	4.8824E-01	4.8824E-01	4.7991E-01
3	4.6460E-01	4.6165E-01	4.5973E-01	4.5973E-01	4.5362E-01
4	4.3647E-01	4.3338E-01	4.3171E-01	4.3171E-01	4.2738E-01
5	4.1019E-01	4.0676E-01	4.0527E-01	4.0527E-01	4.0249E-01
6	3.8613E-01	3.8218E-01	3.8077E-01	3.8077E-01	3.7912E-01
7	3.6446E-01	3.6001E-01	3.5866E-01	3.5866E-01	3.5809E-01
8	3.4586E-01	3.4082E-01	3.3949E-01	3.3949E-01	3.3963E-01
9	3.3019E-01	3.2437E-01	3.2287E-01	3.2287E-01	3.2332E-01
10	3.1728E-01	3.1137E-01	3.0986E-01	3.0986E-01	3.1051E-01
11	3.0833E-01	3.0234E-01	3.0078E-01	3.0078E-01	3.0148E-01
12	3.0025E-01	2.9473E-01	2.9326E-01	2.9326E-01	2.9404E-01
13	2.8489E-01	2.8179E-01	2.8131E-01	2.8131E-01	2.8298E-01
14	2.4074E-01	2.4492E-01	2.4764E-01	2.4764E-01	2.5228E-01
15	1.7308E-01	1.8866E-01	1.9469E-01	1.9469E-01	2.0139E-01
16	1.8505E-01	2.1656E-01	2.2556E-01	2.2556E-01	2.3376E-01
17	1.9560E-01	2.4211E-01	2.5525E-01	2.5525E-01	2.6680E-01
18	1.7618E-01	2.3411E-01	2.5041E-01	2.5041E-01	2.6397E-01
19	1.2181E-01	1.7893E-01	1.9521E-01	1.9521E-01	2.0803E-01
20	1.2948E-02	1.9271E-02	2.1071E-02	2.1071E-02	2.2483E-02

TIN-WATER, 3MEV, B1=4

GRP.	B2=1	B2=2	B2=3	B2=4	B2=5
1	4.8128E-01	4.7915E-01	4.7805E-01	4.7805E-01	4.7205E-01
2	4.7099E-01	4.6832E-01	4.6709E-01	4.6709E-01	4.6175E-01
3	4.5145E-01	4.4773E-01	4.4627E-01	4.4627E-01	4.4217E-01
4	4.3091E-01	4.2603E-01	4.2421E-01	4.2421E-01	4.2091E-01
5	4.1033E-01	4.0432E-01	4.0220E-01	4.0220E-01	3.9970E-01
6	3.9020E-01	3.8320E-01	3.8083E-01	3.8083E-01	3.7899E-01
7	3.7065E-01	3.6313E-01	3.6076E-01	3.6076E-01	3.5965E-01
8	3.5283E-01	3.4507E-01	3.4261E-01	3.4261E-01	3.4232E-01
9	3.3671E-01	3.2887E-01	3.2671E-01	3.2671E-01	3.2658E-01
10	3.2164E-01	3.1519E-01	3.1361E-01	3.1361E-01	3.1399E-01
11	3.1039E-01	3.0539E-01	3.0431E-01	3.0431E-01	3.0504E-01
12	3.0038E-01	2.9720E-01	2.9664E-01	2.9664E-01	2.9763E-01
13	2.8467E-01	2.8474E-01	2.8525E-01	2.8525E-01	2.8699E-01
14	2.4451E-01	2.5102E-01	2.5393E-01	2.5393E-01	2.5758E-01
15	1.7837E-01	1.9627E-01	2.0206E-01	2.0206E-01	2.0706E-01
16	1.8730E-01	2.2425E-01	2.3387E-01	2.3387E-01	2.4039E-01
17	1.9943E-01	2.5275E-01	2.6647E-01	2.6647E-01	2.7555E-01
18	1.8028E-01	2.4600E-01	2.6299E-01	2.6299E-01	2.7366E-01
19	1.2507E-01	1.8937E-01	2.0649E-01	2.0649E-01	2.1663E-01
20	1.3304E-02	2.0416E-02	2.2309E-02	2.2309E-02	2.3429E-02

Table C.74. Scattered Energy Flux Spectra, $I^S(b_1+b_2,E_i)/I^S(b_1+b_2)$, for 3MeV Photons in Slabs of Lead Followed by Water.

LEAD-WATER, 3MEV, B1=1

GRP.	B2=1	B2=2	B2=3	B2=4	B2=5
1	5.2927E-01	5.1809E-01	5.1424E-01	5.0964E-01	5.0391E-01
2	5.1036E-01	5.0079E-01	4.9748E-01	4.9347E-01	4.8849E-01
3	4.7443E-01	4.6793E-01	4.6564E-01	4.6275E-01	4.5918E-01
4	4.4068E-01	4.3659E-01	4.3508E-01	4.3310E-01	4.3069E-01
5	4.1023E-01	4.0779E-01	4.0681E-01	4.0554E-01	4.0403E-01
6	3.8346E-01	3.8184E-01	3.8108E-01	3.8032E-01	3.7960E-01
7	3.6020E-01	3.5886E-01	3.5815E-01	3.5775E-01	3.5762E-01
8	3.4104E-01	3.3937E-01	3.3851E-01	3.3832E-01	3.3859E-01
9	3.2634E-01	3.2330E-01	3.2188E-01	3.2160E-01	3.2200E-01
10	3.1571E-01	3.1117E-01	3.0911E-01	3.0865E-01	3.0908E-01
11	3.0973E-01	3.0313E-01	3.0035E-01	2.9966E-01	3.0004E-01
12	3.0461E-01	2.9622E-01	2.9298E-01	2.9220E-01	2.9257E-01
13	2.8944E-01	2.8242E-01	2.8031E-01	2.8029E-01	2.8116E-01
14	2.3646E-01	2.4082E-01	2.4392E-01	2.4670E-01	2.4928E-01
15	1.6104E-01	1.8101E-01	1.8909E-01	1.9407E-01	1.9780E-01
16	1.7655E-01	2.0852E-01	2.1918E-01	2.2518E-01	2.2957E-01
17	1.8342E-01	2.2052E-01	2.4627E-01	2.5494E-01	2.6112E-01
18	1.6344E-01	2.2076E-01	2.3969E-01	2.5035E-01	2.5754E-01
19	1.1175E-01	1.6681E-01	1.8561E-01	1.9547E-01	2.0218E-01
20	1.1853E-02	1.7939E-02	2.0015E-02	2.1102E-02	2.1842E-02

LEAD-WATER, 3MEV, B1=2

GRP.	B2=1	B2=2	B2=3	B2=4	B2=5
1	5.2646E-01	5.1486E-01	5.0836E-01	5.0299E-01	4.9703E-01
2	5.0951E-01	4.9772E-01	4.9268E-01	4.8790E-01	4.8269E-01
3	4.7730E-01	4.6705E-01	4.6287E-01	4.5923E-01	4.5545E-01
4	4.4662E-01	4.3748E-01	4.3396E-01	4.3121E-01	4.2856E-01
5	4.1844E-01	4.0998E-01	4.0691E-01	4.0491E-01	4.0321E-01
6	3.9307E-01	3.8465E-01	3.8203E-01	3.8056E-01	3.7960E-01
7	3.6940E-01	3.6178E-01	3.5937E-01	3.5846E-01	3.5816E-01
8	3.4838E-01	3.4160E-01	3.3964E-01	3.3921E-01	3.3942E-01
9	3.3087E-01	3.2449E-01	3.2269E-01	3.2247E-01	3.2295E-01
10	3.1531E-01	3.1069E-01	3.0933E-01	3.0935E-01	3.1002E-01
11	3.0408E-01	3.0106E-01	3.0062E-01	3.0017E-01	3.0093E-01
12	2.9396E-01	2.9283E-01	2.9224E-01	2.9257E-01	2.9342E-01
13	2.7628E-01	2.7883E-01	2.7976E-01	2.8088E-01	2.8220E-01
14	2.2755E-01	2.3974E-01	2.4499E-01	2.4839E-01	2.5112E-01
15	1.5758E-01	1.8220E-01	1.9142E-01	1.9644E-01	2.0004E-01
16	1.7021E-01	2.0909E-01	2.2163E-01	2.2792E-01	2.3217E-01
17	1.7768E-01	2.3231E-01	2.5091E-01	2.5881E-01	2.6467E-01
18	1.5872E-01	2.2336E-01	2.4451E-01	2.5484E-01	2.6158E-01
19	1.0878E-01	1.6955E-01	1.8988E-01	1.9962E-01	2.0587E-01
20	1.1543E-02	1.8244E-02	2.0488E-02	2.1559E-02	2.2246E-02

Table C.74. Continued.

LEAD-WATER, 3MEV, B1=3

GRP.	B2=1	B2=2	B2=3	B2=4	B2=5
1	5.2127E-01	5.0675E-01	5.0029E-01	4.9474E-01	4.8892E-01
2	5.0615E-01	4.9211E-01	4.8602E-01	4.8101E-01	4.7595E-01
3	4.7744E-01	4.6428E-01	4.5890E-01	4.5492E-01	4.5119E-01
4	4.4964E-01	4.3704E-01	4.3214E-01	4.2893E-01	4.2621E-01
5	4.2365E-01	4.1132E-01	4.0675E-01	4.0419E-01	4.0232E-01
6	3.9974E-01	3.8743E-01	3.8305E-01	3.8097E-01	3.7976E-01
7	3.7588E-01	3.6460E-01	3.6087E-01	3.5844E-01	3.5893E-01
8	3.5352E-01	3.4402E-01	3.4119E-01	3.4043E-01	3.4051E-01
9	3.3417E-01	3.2624E-01	3.2406E-01	3.2374E-01	3.2417E-01
10	3.1531E-01	3.1119E-01	3.1024E-01	3.1048E-01	3.1123E-01
11	3.0093E-01	3.0041E-01	3.0049E-01	3.0114E-01	3.0210E-01
12	2.8807E-01	2.9125E-01	2.9237E-01	2.9340E-01	2.9454E-01
13	2.6897E-01	2.7701E-01	2.7996E-01	2.8185E-01	2.8346E-01
14	2.2252E-01	2.3946E-01	2.4629E-01	2.5019E-01	2.5298E-01
15	1.5530E-01	1.8319E-01	1.9347E-01	1.9873E-01	2.0218E-01
16	1.6632E-01	2.0967E-01	2.2382E-01	2.3047E-01	2.3464E-01
17	1.7410E-01	2.3371E-01	2.5321E-01	2.6233E-01	2.6794E-01
18	1.5572E-01	2.2530E-01	2.4826E-01	2.5883E-01	2.6530E-01
19	1.0685E-01	1.7150E-01	1.9236E-01	2.0327E-01	2.0923E-01
20	1.1342E-02	1.8461E-02	2.0870E-02	2.1959E-02	2.2614E-02

LEAD-WATER, 3MEV, B1=4

GRP.	B2=1	B2=2	B2=3	B2=4	B2=5
1	5.1323E-01	4.9756E-01	4.9074E-01	4.8538E-01	4.8006E-01
2	5.0008E-01	4.8465E-01	4.7810E-01	4.7320E-01	4.6849E-01
3	4.7509E-01	4.6011E-01	4.5407E-01	4.5005E-01	4.4651E-01
4	4.5042E-01	4.3560E-01	4.2982E-01	4.2638E-01	4.2367E-01
5	4.2687E-01	4.1200E-01	4.0638E-01	4.0341E-01	4.0143E-01
6	4.0475E-01	3.8962E-01	3.8410E-01	3.8149E-01	3.8004E-01
7	3.8109E-01	3.6734E-01	3.6254E-01	3.6062E-01	3.5986E-01
8	3.5793E-01	3.4661E-01	3.4301E-01	3.4190E-01	3.4176E-01
9	3.3740E-01	3.2941E-01	3.2581E-01	3.2520E-01	3.2550E-01
10	3.1610E-01	3.1239E-01	3.1161E-01	3.1191E-01	3.1263E-01
11	2.9969E-01	3.0073E-01	3.0150E-01	3.0243E-01	3.0347E-01
12	2.8494E-01	2.9083E-01	2.9306E-01	2.9456E-01	2.9585E-01
13	2.6482E-01	2.7634E-01	2.8065E-01	2.8310E-01	2.8490E-01
14	2.1974E-01	2.3978E-01	2.4779E-01	2.5206E-01	2.5491E-01
15	1.5402E-01	1.8424E-01	1.9541E-01	2.0086E-01	2.0424E-01
16	1.6402E-01	2.1047E-01	2.2593E-01	2.3291E-01	2.3703E-01
17	1.7200E-01	2.3516E-01	2.5617E-01	2.6561E-01	2.7116E-01
18	1.5398E-01	2.2710E-01	2.5164E-01	2.6252E-01	2.6882E-01
19	1.0574E-01	1.7322E-01	1.9644E-01	2.0659E-01	2.1238E-01
20	1.1225E-02	1.8652E-02	2.1208E-02	2.2322E-02	2.2957E-02

Table C.74. Continued.

LEAD-WATER, 3MEV, B1=5

GRP.	B2=1	B2=2	B2=3	B2=4	B2=5
1	5.0326E-01	4.8700E-01	4.8012E-01	4.7510E-01	4.7113E-01
2	4.9216E-01	4.7596E-01	4.6926E-01	4.6461E-01	4.6103E-01
3	4.7107E-01	4.5499E-01	4.4862E-01	4.4465E-01	4.4184E-01
4	4.4972E-01	4.3345E-01	4.2711E-01	4.2356E-01	4.2115E-01
5	4.2884E-01	4.1222E-01	4.0583E-01	4.0258E-01	4.0056E-01
6	4.0874E-01	3.9168E-01	3.8515E-01	3.8209E-01	3.8036E-01
7	3.8562E-01	3.7003E-01	3.6433E-01	3.6196E-01	3.6086E-01
8	3.6203E-01	3.4931E-01	3.4503E-01	3.4356E-01	3.4311E-01
9	3.4075E-01	3.3087E-01	3.2783E-01	3.2705E-01	3.2706E-01
10	3.1776E-01	3.1405E-01	3.1330E-01	3.1355E-01	3.1409E-01
11	2.9966E-01	3.0169E-01	3.0288E-01	3.0396E-01	3.0487E-01
12	2.8347E-01	2.9115E-01	2.9416E-01	2.9597E-01	2.9720E-01
13	2.6254E-01	2.7642E-01	2.8174E-01	2.8457E-01	2.8635E-01
14	2.1830E-01	2.4054E-01	2.4944E-01	2.5402E-01	2.5679E-01
15	1.5341E-01	1.8539E-01	1.9731E-01	2.0294E-01	2.0616E-01
16	1.6272E-01	2.1148E-01	2.2502E-01	2.3536E-01	2.3927E-01
17	1.7086E-01	2.3673E-01	2.5899E-01	2.6877E-01	2.7409E-01
18	1.5304E-01	2.2893E-01	2.5402E-01	2.6602E-01	2.7206E-01
19	1.0516E-01	1.7488E-01	1.9928E-01	2.0970E-01	2.1525E-01
20	1.1166E-02	1.8835E-02	2.1519E-02	2.2663E-02	2.3272E-02

Table C.75. Scattered Energy Flux Spectra, $I^S(b_1+b_2,E_i)/I^S(b_1+b_2)$, for 3MeV Photons in Slabs of Tin Followed by Aluminum.

TIN-ALUM., 3MEV, B1=2

GRP.	B2=1	B2=2	B2=3	B2=4	B2=5
1	5.0609E-01	5.0050E-01	4.9509E-01	4.9509E-01	4.8054E-01
2	4.9169E-01	4.8670E-01	4.8203E-01	4.8203E-01	4.6956E-01
3	4.6431E-01	4.6048E-01	4.5722E-01	4.5722E-01	4.4868E-01
4	4.3750E-01	4.3438E-01	4.3214E-01	4.3214E-01	4.2663E-01
5	4.1225E-01	4.0938E-01	4.0783E-01	4.0783E-01	4.0469E-01
6	3.8896E-01	3.8600E-01	3.8487E-01	3.8487E-01	3.8346E-01
7	3.6812E-01	3.6506E-01	3.6429E-01	3.6429E-01	3.6437E-01
8	3.5038E-01	3.4668E-01	3.4609E-01	3.4609E-01	3.4718E-01
9	3.3484E-01	3.3078E-01	3.3012E-01	3.3012E-01	3.3170E-01
10	3.2190E-01	3.1773E-01	3.1708E-01	3.1708E-01	3.1893E-01
11	3.1255E-01	3.0824E-01	3.0752E-01	3.0752E-01	3.0946E-01
12	3.0416E-01	3.0026E-01	2.9968E-01	2.9968E-01	3.0175E-01
13	2.8812E-01	2.8666E-01	2.8713E-01	2.8713E-01	2.9020E-01
14	2.4242E-01	2.4821E-01	2.5193E-01	2.5193E-01	2.5799E-01
15	1.7351E-01	1.9066E-01	1.9764E-01	1.9764E-01	2.0558E-01
16	1.7033E-01	1.9844E-01	2.0680E-01	2.0680E-01	2.1494E-01
17	1.3928E-01	1.6778E-01	1.7609E-01	1.7609E-01	1.8405E-01
18	8.2552E-02	1.0202E-01	1.0757E-01	1.0757E-01	1.1279E-01
19	1.5145E-02	1.8882E-02	1.9940E-02	1.9940E-02	2.0928E-02
20	1.2439E-04	1.5477E-04	1.6339E-04	1.6339E-04	1.7145E-04

TIN-ALUM., 3MEV, B1=4

GRP.	B2=1	B2=2	B2=3	B2=4	B2=5
1	4.7817E-01	4.7288E-01	4.6840E-01	4.6840E-01	4.5683E-01
2	4.6878E-01	4.6360E-01	4.5958E-01	4.5958E-01	4.4952E-01
3	4.5093E-01	4.4596E-01	4.4283E-01	4.4283E-01	4.3593E-01
4	4.3182E-01	4.2670E-01	4.2408E-01	4.2408E-01	4.1933E-01
5	4.1238E-01	4.0687E-01	4.0455E-01	4.0455E-01	4.0152E-01
6	3.9313E-01	3.8715E-01	3.8500E-01	3.8500E-01	3.8324E-01
7	3.7450E-01	3.6892E-01	3.6674E-01	3.6674E-01	3.6624E-01
8	3.5731E-01	3.5141E-01	3.4996E-01	3.4996E-01	3.5041E-01
9	3.4165E-01	3.3586E-01	3.3463E-01	3.3463E-01	3.3566E-01
10	3.2650E-01	3.2212E-01	3.2153E-01	3.2153E-01	3.2318E-01
11	3.1482E-01	3.1182E-01	3.1175E-01	3.1175E-01	3.1381E-01
12	3.0443E-01	3.0327E-01	3.0377E-01	3.0377E-01	3.0616E-01
13	2.8803E-01	2.9016E-01	2.9182E-01	2.9182E-01	2.9505E-01
14	2.4629E-01	2.5480E-01	2.5891E-01	2.5891E-01	2.6409E-01
15	1.7876E-01	1.9856E-01	2.0552E-01	2.0552E-01	2.1130E-01
16	1.7214E-01	2.0530E-01	2.1442E-01	2.1442E-01	2.2130E-01
17	1.4165E-01	1.7459E-01	1.8342E-01	1.8342E-01	1.9005E-01
18	8.4121E-02	1.0646E-01	1.1232E-01	1.1232E-01	1.1664E-01
19	1.5442E-02	1.9721E-02	2.0837E-02	2.0837E-02	2.1652E-02
20	1.2681E-04	1.6162E-04	1.7072E-04	1.7072E-04	1.7736E-04

Table C.76. Scattered Energy Flux Spectra, $I^S(b_1+b_2,E_i)/I^S(b_1+b_2)$, for 3MeV Photons in Slabs of Lead Followed by Aluminum.

LEAD-ALUM., 3MEV, B1=2

GRP.	B2=1	B2=2	B2=3	B2=4	B2=5
1	5.2387E-01	5.0895E-01	5.0068E-01	5.0068E-01	4.8434E-01
2	5.0777E-01	4.9418E-01	4.8658E-01	4.8658E-01	4.7278E-01
3	4.7719E-01	4.6611E-01	4.6066E-01	4.6066E-01	4.5082E-01
4	4.4781E-01	4.3964E-01	4.3457E-01	4.3457E-01	4.2709E-01
5	4.2062E-01	4.1270E-01	4.0958E-01	4.0958E-01	4.0552E-01
6	3.9600E-01	3.8871E-01	3.8618E-01	3.8618E-01	3.8392E-01
7	3.7308E-01	3.6680E-01	3.6498E-01	3.6498E-01	3.6442E-01
8	3.5252E-01	3.4734E-01	3.4615E-01	3.4615E-01	3.4588E-01
9	3.3533E-01	3.3071E-01	3.2978E-01	3.2978E-01	3.3119E-01
10	3.1958E-01	3.1676E-01	3.1634E-01	3.1634E-01	3.1828E-01
11	3.0782E-01	3.0660E-01	3.0651E-01	3.0651E-01	3.0872E-01
12	2.9721E-01	2.9793E-01	2.9835E-01	2.9835E-01	3.0093E-01
13	2.7874E-01	2.8320E-01	2.8522E-01	2.8522E-01	2.8918E-01
14	2.2845E-01	2.4247E-01	2.4887E-01	2.4887E-01	2.5658E-01
15	1.5734E-01	1.8367E-01	1.9398E-01	1.9398E-01	2.0402E-01
16	1.5643E-01	1.9143E-01	2.0304E-01	2.0306E-01	2.1336E-01
17	1.2664E-01	1.6114E-01	1.7252E-01	1.7252E-01	1.8255E-01
18	7.4707E-02	9.7758E-02	1.0527E-01	1.0527E-01	1.1182E-01
19	1.3681E-02	1.8078E-02	1.9506E-02	1.9506E-02	2.0745E-02
20	1.1241E-04	1.4821E-04	1.5994E-04	1.5994E-04	1.6996E-04

LEAD-ALUM., 3MEV, B1=4

GRP.	B2=1	B2=2	B2=3	B2=4	B2=5
1	5.1023E-01	4.9166E-01	4.9166E-01	4.8166E-01	4.6559E-01
2	4.9800E-01	4.8028E-01	4.7112E-01	4.7112E-01	4.5704E-01
3	4.7476E-01	4.5867E-01	4.5107E-01	4.5107E-01	4.4079E-01
4	4.5154E-01	4.3655E-01	4.3003E-01	4.3003E-01	4.2246E-01
5	4.2913E-01	4.1478E-01	4.0898E-01	4.0898E-01	4.0348E-01
6	4.0788E-01	3.9382E-01	3.8845E-01	3.8845E-01	3.8442E-01
7	3.8506E-01	3.7280E-01	3.6857E-01	3.6857E-01	3.6645E-01
8	3.6236E-01	3.5283E-01	3.5004E-01	3.5004E-01	3.4974E-01
9	3.4210E-01	3.3512E-01	3.3348E-01	3.3348E-01	3.3492E-01
10	3.2050E-01	3.1881E-01	3.1913E-01	3.1913E-01	3.2151E-01
11	3.0330E-01	3.0649E-01	3.0843E-01	3.0843E-01	3.1187E-01
12	2.8791E-01	2.9606E-01	2.9957E-01	2.9957E-01	3.0397E-01
13	2.6694E-01	2.8078E-01	2.8650E-01	2.8650E-01	2.9249E-01
14	2.2036E-01	2.4256E-01	2.5202E-01	2.5202E-01	2.6094E-01
15	1.5357E-01	1.8569E-01	1.9822E-01	1.9822E-01	2.0668E-01
16	1.5041E-01	1.9239E-01	2.0698E-01	2.0698E-01	2.1800E-01
17	1.2223E-01	1.6261E-01	1.7639E-01	1.7639E-01	1.8697E-01
18	7.2194E-02	9.8833E-02	1.0782E-01	1.0782E-01	1.1466E-01
19	1.3225E-02	1.8287E-02	1.9990E-02	1.9990E-02	2.1281E-02
20	1.0865E-04	1.4991E-04	1.6380E-04	1.6380E-04	1.7433E-04

Table C.77. Scattered Energy Flux Spectra, $I^S(b_1+b_2,E_i)/I^S(b_1+b_2)$, for 3MeV Photons in Slabs of Water Followed by Iron.

WATER-IRON, 3MEV, B1=1

GRP.	B2=1	B2=2	B2=3	B2=4	B2=5
1	5.1926E-01	3.1345E+00	4.9608E-01	4.8543E-01	4.7254E-01
2	5.0311E-01	2.1449E+00	4.8435E-01	4.7538E-01	4.6449E-01
3	4.7241E-01	2.6474E-01	4.6206E-01	4.5629E-01	4.4919E-01
4	4.4281E-01	2.6388E-01	4.3916E-01	4.3590E-01	4.3178E-01
5	4.1543E-01	2.4923E-01	4.1672E-01	4.1531E-01	4.1349E-01
6	3.9072E-01	2.3529E-01	3.9512E-01	3.9503E-01	3.9486E-01
7	3.6952E-01	2.2228E-01	3.7566E-01	3.7669E-01	3.7778E-01
8	3.5221E-01	2.1079E-01	3.5874E-01	3.6046E-01	3.6243E-01
9	3.3834E-01	2.0102E-01	3.4330E-01	3.4514E-01	3.4754E-01
10	3.2809E-01	1.9250E-01	3.2961E-01	3.3148E-01	3.3391E-01
11	3.2203E-01	1.8536E-01	3.2021E-01	3.2156E-01	3.2400E-01
12	3.1599E-01	1.8040E-01	3.1104E-01	3.1230E-01	3.1476E-01
13	2.9910E-01	1.7558E-01	2.9507E-01	2.9695E-01	2.9984E-01
14	2.4570E-01	1.6614E-01	2.5234E-01	2.5537E-01	2.6054E-01
15	1.6053E-01	1.3997E-01	1.7199E-01	1.7616E-01	1.7990E-01
16	8.4363E-02	1.8816E-01	8.5505E-02	8.6735E-02	8.8001E-02
17	9.4702E-03	2.3749E-01	9.6768E-03	9.8270E-03	9.9786E-03
18	9.4810E-04	5.3461E-03	9.6814E-04	9.8304E-04	9.9811E-04
19	1.5718E-05	5.3697E-04	1.6036E-05	1.6268E-05	1.6517E-05
20	1.6600E-08	8.8712E-06	4.5092E-08	3.4284E-08	5.6627E-08

WATER-IRON, 3MEV, B1=2

GRP.	B2=1	B2=2	B2=3	B2=4	B2=5
1	5.1677E-01	5.0216E-01	4.9035E-01	4.7624E-01	4.6244E-01
2	5.0154E-01	4.8941E-01	4.7943E-01	4.6752E-01	4.5583E-01
3	4.7262E-01	4.6518E-01	4.5870E-01	4.5094E-01	4.4327E-01
4	4.4441E-01	4.4076E-01	4.3706E-01	4.3253E-01	4.2809E-01
5	4.1795E-01	4.1720E-01	4.1558E-01	4.1363E-01	4.1160E-01
6	3.9353E-01	3.9465E-01	3.9473E-01	3.9460E-01	3.9436E-01
7	3.7227E-01	3.7485E-01	3.7605E-01	3.7730E-01	3.7846E-01
8	3.5418E-01	3.5754E-01	3.5962E-01	3.6183E-01	3.6398E-01
9	3.3864E-01	3.4192E-01	3.4425E-01	3.4690E-01	3.4955E-01
10	3.2606E-01	3.2946E-01	3.3056E-01	3.3326E-01	3.3606E-01
11	3.1733E-01	3.2087E-01	3.2059E-01	3.2330E-01	3.2624E-01
12	3.0902E-01	3.0976E-01	3.1134E-01	3.1407E-01	3.1705E-01
13	2.9270E-01	2.9388E-01	2.9602E-01	2.9916E-01	3.0245E-01
14	2.4702E-01	2.5138E-01	2.5557E-01	2.5996E-01	2.6402E-01
15	1.6772E-01	1.7157E-01	1.7565E-01	1.7952E-01	1.8296E-01
16	8.6160E-02	8.6317E-02	8.6487E-02	8.7811E-02	8.9062E-02
17	9.6768E-03	9.6538E-03	9.7987E-03	9.9570E-03	1.0105E-02
18	9.6848E-04	9.6593E-04	9.8020E-04	9.9594E-04	1.0107E-03
19	1.6055E-05	1.5864E-05	1.6221E-05	1.6486E-05	1.6737E-05
20	2.3248E-08	2.7954E-08	1.7779E-08	3.8502E-08	4.9444E-08

Table C.77 Continued.

WATER-IRON, 3MEV, B1=3

GRP.	B2=1	B2=2	B2=3	B2=4	B2=5
1	5.1399E-01	4.9624E-01	4.8270E-01	4.6749E-01	4.5315E-01
2	4.9930E-01	4.8436E-01	4.7286E-01	4.5998E-01	4.4785E-01
3	4.7139E-01	4.6178E-01	4.5416E-01	4.4572E-01	4.3777E-01
4	4.4399E-01	4.3871E-01	4.3421E-01	4.2929E-01	4.2463E-01
5	4.1811E-01	4.1623E-01	4.1409E-01	4.1190E-01	4.0981E-01
6	3.9411E-01	3.9468E-01	3.9431E-01	3.9411E-01	3.9390E-01
7	3.7287E-01	3.7529E-01	3.7651E-01	3.7786E-01	3.7911E-01
8	3.5464E-01	3.5835E-01	3.6071E-01	3.6315E-01	3.6543E-01
9	3.3858E-01	3.4275E-01	3.4565E-01	3.4864E-01	3.5142E-01
10	3.2521E-01	3.2910E-01	3.3200E-01	3.3517E-01	3.3822E-01
11	3.1570E-01	3.1929E-01	3.2201E-01	3.2527E-01	3.2845E-01
12	3.0690E-01	3.1010E-01	3.1278E-01	3.1607E-01	3.1932E-01
13	2.9147E-01	2.9485E-01	2.9789E-01	3.0148E-01	3.0494E-01
14	2.4969E-01	2.5453E-01	2.5879E-01	2.6317E-01	2.6717E-01
15	1.7245E-01	1.7516E-01	1.7872E-01	1.8232E-01	1.8553E-01
16	8.7549E-02	8.8310E-02	8.7450E-02	8.8770E-02	8.3993E-02
17	9.8378E-03	9.7760E-03	9.9153E-03	1.0072E-02	1.0216E-02
18	9.8444E-04	9.7792E-04	9.9178E-04	1.0073E-03	1.0217E-03
19	1.6315E-05	1.6876E-05	1.6410E-05	1.6666E-05	1.6844E-05
20	2.6441E-08	4.8092E-08	1.7769E-08	5.1736E-08	5.3137E-08

WATER-IRON, 3MEV, B1=4

GRP.	B2=1	B2=2	B2=3	B2=4	B2=5
1	5.0961E-01	4.9028E-01	4.7497E-01	4.5910E-01	4.4445E-01
2	4.9554E-01	4.7920E-01	4.6620E-01	4.5276E-01	4.4037E-01
3	4.6882E-01	4.5815E-01	4.4953E-01	4.4072E-01	4.3261E-01
4	4.4240E-01	4.3634E-01	4.3126E-01	4.2612E-01	4.2138E-01
5	4.1731E-01	4.1492E-01	4.1254E-01	4.1027E-01	4.0817E-01
6	3.9388E-01	3.9421E-01	3.9386E-01	3.9368E-01	3.9351E-01
7	3.7309E-01	3.7557E-01	3.7697E-01	3.7843E-01	3.7975E-01
8	3.5512E-01	3.5916E-01	3.6186E-01	3.6446E-01	3.6683E-01
9	3.3904E-01	3.4381E-01	3.4716E-01	3.5037E-01	3.5331E-01
10	3.2548E-01	3.3020E-01	3.3367E-01	3.3705E-01	3.4025E-01
11	3.1571E-01	3.2033E-01	3.2373E-01	3.2727E-01	3.3054E-01
12	3.0684E-01	3.1116E-01	3.1454E-01	3.1812E-01	3.2149E-01
13	2.9205E-01	2.9634E-01	2.9994E-01	3.0374E-01	3.0729E-01
14	2.5259E-01	2.5737E-01	2.6172E-01	2.6602E-01	2.6995E-01
15	1.7603E-01	1.7802E-01	1.8131E-01	1.8470E-01	1.8776E-01
16	8.8736E-02	8.7187E-02	8.8326E-02	8.9625E-02	9.0829E-02
17	9.9741E-03	9.8824E-03	1.0022E-02	1.0173E-02	1.0314E-02
18	9.9805E-04	9.8647E-04	1.0022E-03	1.0175E-03	1.0315E-03
19	1.6539E-05	1.7147E-05	1.6581E-05	1.6872E-05	1.7044E-05
20	2.4825E-08	4.7203E-08	2.7366E-08	4.8683E-08	5.6487E-08

Table C.77. Continued.

WATER-IRON, 3MEV, B1=5

GRP.	B2=1	B2=2	B2=3	B2=4	B2=5
1	5.0375E-01	4.8318E-01	4.6692E-01	4.5053E-01	4.3644E-01
2	4.9049E-01	4.7308E-01	4.5928E-01	4.4541E-01	4.3349E-01
3	4.6530E-01	4.5368E-01	4.4475E-01	4.3570E-01	4.2788E-01
4	4.4015E-01	4.3361E-01	4.2825E-01	4.2298E-01	4.1840E-01
5	4.1611E-01	4.1349E-01	4.1101E-01	4.0879E-01	4.0668E-01
6	3.9351E-01	3.9379E-01	3.9356E-01	3.9340E-01	3.9318E-01
7	3.7337E-01	3.7599E-01	3.7754E-01	3.7914E-01	3.8037E-01
8	3.5585E-01	3.6019E-01	3.6309E-01	3.6597E-01	3.6814E-01
9	3.3996E-01	3.4515E-01	3.4878E-01	3.5218E-01	3.5502E-01
10	3.2644E-01	3.3169E-01	3.3547E-01	3.3903E-01	3.4214E-01
11	3.1662E-01	3.2186E-01	3.2562E-01	3.2936E-01	3.3256E-01
12	3.0776E-01	3.1273E-01	3.1647E-01	3.1977E-01	3.2351E-01
13	2.9342E-01	2.9821E-01	3.0209E-01	3.0604E-01	3.0944E-01
14	2.5529E-01	2.6016E-01	2.6446E-01	2.6877E-01	2.7241E-01
15	1.7905E-01	1.8055E-01	1.8362E-01	1.8683E-01	1.8970E-01
16	8.9814E-02	8.8039E-02	8.9150E-02	9.0450E-02	9.1569E-02
17	1.0099E-02	9.9844E-03	1.0118E-02	1.0271E-02	1.0402E-02
18	1.0104E-03	9.9814E-04	1.0120E-03	1.0271E-03	1.0402E-03
19	1.6716E-05	1.8200E-05	1.6852E-05	1.7677E-05	2.3522E-05
20	2.6439E-08	4.9717E-08	4.6754E-08	5.4746E-08	5.9979E-08

Table C.78. Scattered Energy Flux Spectra, $I^S(b_1+b_2,E_i)/I^S(b_1+b_2)$, for 3MeV Photons in Slabs of Lead Followed by Iron.

LEAD-IRON, 3MEV, B1=1

GRP.	B2=1	B2=2	B2=3	B2=4	B2=5
1	5.2677E-01	5.1027E-01	4.9939E-01	4.8789E-01	4.7564E-01
2	5.0987E-01	4.9619E-01	4.8717E-01	4.7752E-01	4.6715E-01
3	4.7776E-01	4.6943E-01	4.6397E-01	4.5780E-01	4.5103E-01
4	4.4704E-01	4.4308E-01	4.4037E-01	4.3693E-01	4.3297E-01
5	4.1890E-01	4.1613E-01	4.1734E-01	4.1596E-01	4.1415E-01
6	3.9382E-01	3.9502E-01	3.9548E-01	3.9541E-01	3.9512E-01
7	3.7206E-01	3.7454E-01	3.7581E-01	3.7677E-01	3.7769E-01
8	3.5412E-01	3.5703E-01	3.5867E-01	3.6029E-01	3.6205E-01
9	3.4012E-01	3.4193E-01	3.4316E-01	3.4459E-01	3.4700E-01
10	3.2904E-01	3.2912E-01	3.2958E-01	3.3103E-01	3.3328E-01
11	3.2247E-01	3.2021E-01	3.1984E-01	3.2111E-01	3.2330E-01
12	3.1592E-01	3.1151E-01	3.1057E-01	3.1178E-01	3.1402E-01
13	2.9734E-01	2.9394E-01	2.9415E-01	2.9616E-01	2.9893E-01
14	2.3737E-01	2.4485E-01	2.5018E-01	2.5483E-01	2.5923E-01
15	1.4413E-01	1.6201E-01	1.6960E-01	1.7470E-01	1.7874E-01
16	7.6455E-02	8.2604E-02	8.4741E-02	8.6267E-02	8.7601E-02
17	8.6319E-03	9.3262E-03	9.5857E-03	9.7707E-03	9.9310E-03
18	8.6440E-04	9.3337E-04	9.5903E-04	9.7743E-04	9.9335E-04
19	1.4312E-05	1.5456E-05	1.5876E-05	1.6176E-05	1.6437E-05
20	1.5255E-08	1.6474E-08	1.6933E-08	1.7443E-08	3.4151E-08

LEAD-IRON, 3MEV, B1=2

GRP.	B2=1	B2=2	B2=3	B2=4	B2=5
1	5.2291E-01	5.0380E-01	4.9057E-01	4.7796E-01	4.6533E-01
2	5.0818E-01	4.9131E-01	4.7996E-01	4.6920E-01	4.5846E-01
3	4.8020E-01	4.6760E-01	4.5979E-01	4.5256E-01	4.4539E-01
4	4.5299E-01	4.4374E-01	4.3866E-01	4.3416E-01	4.2981E-01
5	4.2752E-01	4.2067E-01	4.1757E-01	4.1515E-01	4.1293E-01
6	4.0419E-01	3.9882E-01	3.9706E-01	3.9602E-01	3.9534E-01
7	3.8223E-01	3.7853E-01	3.7794E-01	3.7823E-01	3.7887E-01
8	3.6246E-01	3.6041E-01	3.6088E-01	3.6217E-01	3.6382E-01
9	3.4544E-01	3.4417E-01	3.4594E-01	3.4695E-01	3.4903E-01
10	3.2876E-01	3.2927E-01	3.3071E-01	3.3281E-01	3.3529E-01
11	3.1620E-01	3.1339E-01	3.2024E-01	3.2255E-01	3.2527E-01
12	3.0394E-01	3.0864E-01	3.1045E-01	3.1307E-01	3.1593E-01
13	2.9250E-01	2.9014E-01	2.9414E-01	2.9765E-01	3.0103E-01
14	2.2720E-01	2.4353E-01	2.5179E-01	2.5739E-01	2.6202E-01
15	1.4012E-01	1.6253E-01	1.7168E-01	1.7710E-01	1.8114E-01
16	7.2855E-02	8.2011E-02	8.5135E-02	8.6594E-02	8.7430E-02
17	8.2442E-03	9.2710E-03	9.6388E-03	9.8595E-03	1.0030E-02
18	8.2541E-04	9.2771E-04	9.6430E-04	9.8624E-04	1.0032E-03
19	1.3660E-05	1.5359E-05	1.5966E-05	1.6320E-05	1.6598E-05
20	1.4562E-08	1.6368E-08	1.6912E-08	3.4310E-08	5.6870E-08

Table C.78. Continued.

LEAD-IRON, 3MEV, B1=3

GRP.	B2=1	B2=2	B2=3	B2=4	B2=5
1	5.1701E-01	4.9512E-01	4.8035E-01	4.6719E-01	4.5457E-01
2	5.0425E-01	4.8442E-01	4.7149E-01	4.6019E-01	4.4936E-01
3	4.8000E-01	4.6408E-01	4.5464E-01	4.4679E-01	4.3948E-01
4	4.5593E-01	4.4305E-01	4.3629E-01	4.3112E-01	4.2651E-01
5	4.3290E-01	4.2218E-01	4.1739E-01	4.1424E-01	4.1170E-01
6	4.1126E-01	4.0153E-01	3.9844E-01	3.9670E-01	3.9556E-01
7	3.8921E-01	3.8209E-01	3.8016E-01	3.7980E-01	3.8019E-01
8	3.6808E-01	3.6365E-01	3.6332E-01	3.6427E-01	3.6574E-01
9	3.4910E-01	3.4669E-01	3.4738E-01	3.4910E-01	3.5123E-01
10	3.2873E-01	3.3026E-01	3.3240E-01	3.3480E-01	3.3749E-01
11	3.1268E-01	3.1800E-01	3.2138E-01	3.2443E-01	3.2741E-01
12	2.9738E-01	3.0654E-01	3.1114E-01	3.1474E-01	3.1800E-01
13	2.7441E-01	2.8829E-01	2.9482E-01	2.9939E-01	3.0321E-01
14	2.2157E-01	2.4326E-01	2.5342E-01	2.5982E-01	2.6468E-01
15	1.3759E-01	1.6317E-01	1.7345E-01	1.7929E-01	1.8334E-01
16	7.0748E-02	8.1700E-02	8.5563E-02	8.7701E-02	8.9226E-02
17	8.0166E-03	9.2438E-03	9.6934E-03	9.9447E-03	1.0125E-02
18	8.0255E-04	9.2491E-04	9.6971E-04	9.9470E-04	1.0126E-03
19	1.3278E-05	1.5310E-05	1.6047E-05	1.6459E-05	1.6749E-05
20	1.4155E-09	1.6302E-09	2.5565E-08	4.6441E-08	6.0588E-09

LEAD-IRON, 3MEV, B1=4

GRP.	B2=1	B2=2	B2=3	B2=4	B2=5
1	5.0833E-01	4.8478E-01	4.6920E-01	4.5592E-01	4.4355E-01
2	4.9768E-01	4.7538E-01	4.6218E-01	4.5066E-01	4.4005E-01
3	4.7733E-01	4.5927E-01	4.4884E-01	4.4067E-01	4.3341E-01
4	4.5658E-01	4.4133E-01	4.3346E-01	4.2703E-01	4.2311E-01
5	4.3620E-01	4.2294E-01	4.1693E-01	4.1322E-01	4.1046E-01
6	4.1651E-01	4.0455E-01	3.9979E-01	3.9741E-01	3.9606E-01
7	3.9477E-01	3.8543E-01	3.8242E-01	3.8157E-01	3.8161E-01
8	3.7283E-01	3.6689E-01	3.6539E-01	3.6650E-01	3.6776E-01
9	3.5260E-01	3.4751E-01	3.4975E-01	3.5152E-01	3.5354E-01
10	3.2965E-01	3.3191E-01	3.3447E-01	3.3717E-01	3.3979E-01
11	3.1128E-01	3.1861E-01	3.2299E-01	3.2650E-01	3.2966E-01
12	2.9393E-01	3.0627E-01	3.1236E-01	3.1663E-01	3.2017E-01
13	2.6987E-01	2.8756E-01	2.9596E-01	3.0131E-01	3.0544E-01
14	2.1847E-01	2.4356E-01	2.5521E-01	2.6223E-01	2.6725E-01
15	1.3614E-01	1.6388E-01	1.7511E-01	1.8126E-01	1.8540E-01
16	6.9500E-02	8.1626E-02	8.6044E-02	8.8402E-02	8.9994E-02
17	7.8827E-03	9.2414E-03	9.7527E-03	1.0027E-02	1.0216E-02
18	7.8909E-04	9.2462E-04	9.7558E-04	1.0030E-03	1.0217E-03
19	1.3053E-05	1.5303E-05	1.6143E-05	1.6597E-05	1.6927E-05
20	1.3917E-09	1.6380E-08	1.8048E-08	5.0218E-08	6.9690E-09

Table C.78. Continued.

LEAD-IRON, 3MEV, B1=5

GRP.	B2=1	B2=2	B2=3	B2=4	B2=5
1	4.9808E-01	4.7333E-01	4.5725E-01	4.4393E-01	4.3266E-01
2	4.8945E-01	4.6652E-01	4.5216E-01	4.4055E-01	4.3083E-01
3	4.7306E-01	4.5358E-01	4.4249E-01	4.3413E-01	4.2735E-01
4	4.5574E-01	4.3887E-01	4.3022E-01	4.2427E-01	4.1971E-01
5	4.3816E-01	4.2314E-01	4.1625E-01	4.1212E-01	4.0922E-01
6	4.2066E-01	4.0683E-01	4.0102E-01	3.9819E-01	3.9647E-01
7	3.9954E-01	3.8856E-01	3.8472E-01	3.8341E-01	3.8306E-01
8	3.7720E-01	3.7015E-01	3.6859E-01	3.6888E-01	3.6979E-01
9	3.5619E-01	3.5255E-01	3.5272E-01	3.5413E-01	3.5587E-01
10	3.3129E-01	3.3402E-01	3.3682E-01	3.3958E-01	3.4210E-01
11	3.1118E-01	3.1988E-01	3.2497E-01	3.2881E-01	3.3191E-01
12	2.9228E-01	3.0660E-01	3.1397E-01	3.1876E-01	3.2234E-01
13	2.6735E-01	2.8785E-01	2.9747E-01	3.0344E-01	3.0767E-01
14	2.1684E-01	2.4434E-01	2.5716E-01	2.6467E-01	2.6974E-01
15	1.3539E-01	1.6469E-01	1.7675E-01	1.8321E-01	1.8734E-01
16	6.8762E-02	8.1732E-02	8.6582E-02	8.9124E-02	9.0743E-02
17	7.8046E-03	9.2582E-03	9.8178E-03	1.0114E-02	1.0303E-02
18	7.8123E-04	9.2626E-04	9.8205E-04	1.0116E-03	1.0304E-03
19	1.2921E-05	1.5328E-05	1.6247E-05	1.6690E-05	1.6938E-05
20	1.3771E-08	2.3927E-08	5.2128E-08	6.3602E-08	5.8089E-09

Table C.79. Scattered Energy Flux Spectra, $I^S(b_1+b_2,E_i)/I^S(b_1+b_2)$, for 3MeV Photons in Slabs of Water Followed by Tin.

WATER-TIN, 3MEV, B1=2

GRP.	B2=1	B2=2	B2=3	B2=4	B2=5
1	5.3342E-01	5.1407E-01	4.9643E-01	4.9643E-01	4.5790E-01
2	5.1925E-01	5.0346E-01	4.8876E-01	4.8876E-01	4.5628E-01
3	4.9232E-01	4.8332E-01	4.7417E-01	4.7417E-01	4.5320E-01
4	4.6594E-01	4.6270E-01	4.5828E-01	4.5828E-01	4.4703E-01
5	4.4107E-01	4.4251E-01	4.4167E-01	4.4187E-01	4.3858E-01
6	4.1805E-01	4.2302E-01	4.2531E-01	4.2531E-01	4.2814E-01
7	3.9672E-01	4.0368E-01	4.0792E-01	4.0792E-01	4.1484E-01
8	3.7797E-01	3.8585E-01	3.9121E-01	3.9121E-01	4.0073E-01
9	3.6168E-01	3.6948E-01	3.7519E-01	3.7519E-01	3.8603E-01
10	3.4459E-01	3.4983E-01	3.5434E-01	3.5434E-01	3.6432E-01
11	3.2986E-01	3.3246E-01	3.3566E-01	3.3566E-01	3.4459E-01
12	3.1187E-01	3.1159E-01	3.1354E-01	3.1354E-01	3.2107E-01
13	2.7637E-01	2.7360E-01	2.7449E-01	2.7449E-01	2.8037E-01
14	1.9770E-01	1.9409E-01	1.9478E-01	1.9478E-01	1.9931E-01
15	6.3821E-02	6.1871E-02	6.2108E-02	6.2108E-02	6.3414E-02
16	4.1307E-03	3.9864E-03	3.9616E-03	3.9616E-03	3.9904E-03
17	1.1902E-04	1.1590E-04	1.1480E-04	1.1480E-04	1.1642E-04
18	5.4800E-06	5.1909E-06	5.3240E-06	5.3240E-06	1.0459E-05
19	2.3723E-08	2.2455E-08	2.8326E-08	2.8326E-08	6.0175E-08
20	4.1371E-11	5.1223E-11	4.0803E-11	4.0803E-11	5.5666E-11

WATER-TIN, 3MEV, B1=4

GRP.	B2=1	B2=2	B2=3	B2=4	B2=5
1	5.2731E-01	5.0133E-01	4.7900E-01	4.7900E-01	4.3599E-01
2	5.1433E-01	4.9272E-01	4.7389E-01	4.7389E-01	4.3745E-01
3	4.8967E-01	4.7635E-01	4.6418E-01	4.6418E-01	4.4022E-01
4	4.6513E-01	4.5890E-01	4.5246E-01	4.5246E-01	4.3917E-01
5	4.4167E-01	4.4135E-01	4.3953E-01	4.3953E-01	4.3520E-01
6	4.1959E-01	4.2391E-01	4.2590E-01	4.2590E-01	4.2847E-01
7	3.9877E-01	4.0611E-01	4.1073E-01	4.1073E-01	4.1810E-01
8	3.8005E-01	3.8927E-01	3.9558E-01	3.9558E-01	4.0609E-01
9	3.6309E-01	3.7320E-01	3.8042E-01	3.8042E-01	3.9260E-01
10	3.4482E-01	3.5305E-01	3.5933E-01	3.5933E-01	3.7101E-01
11	3.2888E-01	3.3501E-01	3.4022E-01	3.4022E-01	3.5093E-01
12	3.1017E-01	3.1347E-01	3.1739E-01	3.1739E-01	3.2666E-01
13	2.7564E-01	2.7523E-01	2.7758E-01	2.7758E-01	2.8491E-01
14	2.0057E-01	1.9691E-01	1.9757E-01	1.9757E-01	2.0280E-01
15	6.4932E-02	6.2495E-02	6.2846E-02	6.2846E-02	6.4363E-02
16	4.0672E-03	3.9498E-03	3.9554E-03	3.9554E-03	4.0194E-03
17	1.1804E-04	1.0937E-04	1.1504E-04	1.1504E-04	1.1417E-04
18	5.6850E-06	5.7069E-06	5.4372E-06	5.4372E-06	1.1437E-05
19	3.3625E-08	3.3610E-08	3.9666E-08	3.9666E-08	6.4651E-08
20	3.4813E-11	4.5570E-11	5.1365E-11	5.1365E-11	4.9767E-11

Table C.80. Scattered Energy Flux Spectra, $I^S(b_1+b_2,E_i)/I^S(b_1+b_2)$, for 3MeV Photons in Slabs of Aluminum Followed by Tin.

ALUM.-TIN, 3MEV, B1=2

GRP.	B2=1	B2=2	B2=3	B2=4	B2=5
1	5.2875E-01	5.1015E-01	4.9423E-01	4.9423E-01	4.5659E-01
2	5.1531E-01	5.0021E-01	4.8694E-01	4.8694E-01	4.5521E-01
3	4.8976E-01	4.8131E-01	4.7308E-01	4.7308E-01	4.5259E-01
4	4.6450E-01	4.6168E-01	4.5774E-01	4.5774E-01	4.4676E-01
5	4.4048E-01	4.4223E-01	4.4173E-01	4.4173E-01	4.3856E-01
6	4.1809E-01	4.2324E-01	4.2542E-01	4.2542E-01	4.2325E-01
7	3.9734E-01	4.0424E-01	4.0824E-01	4.0824E-01	4.1504E-01
8	3.7899E-01	3.8662E-01	3.9164E-01	3.9164E-01	4.0096E-01
9	3.6297E-01	3.7038E-01	3.7568E-01	3.7568E-01	3.8627E-01
10	3.4593E-01	3.5074E-01	3.5483E-01	3.5483E-01	3.6457E-01
11	3.3114E-01	3.3339E-01	3.3615E-01	3.3615E-01	3.4435E-01
12	3.1306E-01	3.1246E-01	3.1401E-01	3.1401E-01	3.2132E-01
13	2.7736E-01	2.7437E-01	2.7492E-01	2.7492E-01	2.8060E-01
14	1.9831E-01	1.9461E-01	1.9507E-01	1.9507E-01	1.9947E-01
15	6.4013E-02	6.2028E-02	6.2198E-02	6.2198E-02	6.3460E-02
16	4.1441E-03	3.9969E-03	3.9678E-03	3.9678E-03	3.9937E-03
17	1.1933E-04	1.1057E-04	1.1498E-04	1.1498E-04	1.1519E-04
18	5.2028E-06	9.6888E-06	5.2684E-06	5.2684E-06	1.2181E-05
19	2.7602E-08	3.0111E-08	3.6204E-08	3.6204E-08	2.9851E-08
20	4.5045E-11	4.4141E-11	4.1472E-11	4.1472E-11	4.7334E-11

ALUM.-TIN, 3MEV, B1=4

GRP.	B2=1	B2=2	B2=3	B2=4	B2=5
1	5.1794E-01	4.9514E-01	4.7181E-01	4.7181E-01	4.3293E-01
2	5.0652E-01	4.8758E-01	4.6795E-01	4.6795E-01	4.3494E-01
3	4.8482E-01	4.7324E-01	4.6062E-01	4.6062E-01	4.3875E-01
4	4.6257E-01	4.5732E-01	4.5070E-01	4.5070E-01	4.3348E-01
5	4.4073E-01	4.4078E-01	4.3918E-01	4.3918E-01	4.3201E-01
6	4.1979E-01	4.2405E-01	4.2636E-01	4.2636E-01	4.2861E-01
7	4.0008E-01	4.0697E-01	4.1180E-01	4.1180E-01	4.1852E-01
8	3.8205E-01	3.9056E-01	3.9698E-01	3.9698E-01	4.0667E-01
9	3.6552E-01	3.7475E-01	3.8198E-01	3.8198E-01	3.9337E-01
10	3.4725E-01	3.5459E-01	3.6094E-01	3.6094E-01	3.7169E-01
11	3.3110E-01	3.3641E-01	3.4182E-01	3.4182E-01	3.5159E-01
12	3.1223E-01	3.1480E-01	3.1891E-01	3.1891E-01	3.2730E-01
13	2.7746E-01	2.7642E-01	2.7892E-01	2.7892E-01	2.8547E-01
14	2.0190E-01	1.9738E-01	1.9852E-01	1.9852E-01	2.0310E-01
15	6.5373E-02	6.2773E-02	6.3124E-02	6.3124E-02	6.4484E-02
16	4.0909E-03	3.9650E-03	3.9715E-03	3.9715E-03	4.0253E-03
17	1.1886E-04	1.1466E-04	1.4592E-04	1.4592E-04	1.1287E-04
18	5.5506E-06	7.5371E-06	1.2457E-05	1.2457E-05	1.1372E-05
19	2.5924E-08	3.7494E-08	4.6347E-08	4.6347E-08	4.2441E-08
20	2.1360E-11	5.5122E-11	5.8765E-11	5.8765E-11	5.9729E-11

Table C.81. Scattered Energy Flux Spectra, $I^S(b_1+b_2,E_i)/I^S(b_1+b_2)$, for 3MeV Photons in Slabs of Water Followed by Lead.

WATER-LEAD, 3MEV, B1=1

GRP.	B2=1	B2=2	B2=3	B2=4	B2=5
1	5.8671E-01	5.8463E-01	5.7987E-01	5.6785E-01	5.5549E-01
2	5.6988E-01	5.7017E-01	5.6717E-01	5.5730E-01	5.4780E-01
3	5.3789E-01	5.4272E-01	5.4303E-01	5.3863E-01	5.3319E-01
4	5.0739E-01	5.1618E-01	5.1944E-01	5.1936E-01	5.1796E-01
5	4.7936E-01	4.9139E-01	4.9708E-01	5.0061E-01	5.0265E-01
6	4.5410E-01	4.6843E-01	4.7606E-01	4.8240E-01	4.8725E-01
7	4.2832E-01	4.4142E-01	4.4831E-01	4.5556E-01	4.6125E-01
8	4.0310E-01	4.1237E-01	4.1774E-01	4.2331E-01	4.2842E-01
9	3.8027E-01	3.8463E-01	3.8741E-01	3.9135E-01	3.9547E-01
10	3.4918E-01	3.4394E-01	3.4171E-01	3.4210E-01	3.4373E-01
11	3.1508E-01	3.0143E-01	2.9523E-01	2.9311E-01	2.9261E-01
12	2.6802E-01	2.4881E-01	2.4038E-01	2.3648E-01	2.3443E-01
13	1.9606E-01	1.7768E-01	1.6992E-01	1.6578E-01	1.6334E-01
14	9.5706E-02	8.6274E-02	8.2247E-02	8.0084E-02	7.8780E-02
15	1.4632E-02	1.3479E-02	1.2980E-02	1.2703E-02	1.2539E-02
16	3.3899E-04	3.0978E-04	2.8901E-04	2.7929E-04	2.7297E-04
17	3.5671E-06	4.3834E-06	3.0644E-06	4.0469E-06	3.4146E-06
18	6.9852E-07	6.6691E-07	6.0667E-07	5.9679E-07	5.7643E-07
19	2.4749E-09	2.4278E-09	2.9016E-09	2.3000E-09	2.9055E-09
20	1.9923E-12	2.7017E-12	2.2517E-12	2.3739E-12	2.3994E-12

WATER-LEAD, 3MEV, B1=2

GRP.	B2=1	B2=2	B2=3	B2=4	B2=5
1	5.8974E-01	5.8402E-01	5.7434E-01	5.5887E-01	5.4400E-01
2	5.7341E-01	5.7038E-01	5.6302E-01	5.5054E-01	5.3834E-01
3	5.4237E-01	5.4447E-01	5.4152E-01	5.3471E-01	5.2757E-01
4	5.1257E-01	5.1917E-01	5.2022E-01	5.1842E-01	5.1532E-01
5	4.8490E-01	4.9552E-01	4.9977E-01	5.0224E-01	5.0357E-01
6	4.5956E-01	4.7296E-01	4.8028E-01	4.8620E-01	4.9082E-01
7	4.3303E-01	4.4574E-01	4.5341E-01	4.6028E-01	4.6609E-01
8	4.0625E-01	4.1567E-01	4.2177E-01	4.2788E-01	4.3337E-01
9	3.8095E-01	3.8633E-01	3.9038E-01	3.9524E-01	3.9959E-01
10	3.4637E-01	3.4278E-01	3.4210E-01	3.4330E-01	3.4614E-01
11	3.0879E-01	2.9751E-01	2.9321E-01	2.9256E-01	2.9309E-01
12	2.5907E-01	2.4258E-01	2.3627E-01	2.3407E-01	2.3327E-01
13	1.8703E-01	1.7096E-01	1.6512E-01	1.6266E-01	1.6136E-01
14	9.0697E-02	8.2295E-02	7.9580E-02	7.8356E-02	7.7683E-02
15	1.4015E-02	1.2995E-02	1.2646E-02	1.2485E-02	1.2388E-02
16	3.0851E-04	2.8498E-04	2.7655E-04	2.7092E-04	2.6740E-04
17	3.4060E-06	3.4461E-06	2.9777E-06	3.0931E-06	3.9102E-06
18	6.6262E-07	5.9695E-07	5.8680E-07	5.7582E-07	5.6507E-07
19	2.4301E-09	3.6068E-09	2.7955E-09	2.6840E-09	2.8805E-09
20	1.7722E-12	2.9532E-12	2.2639E-12	2.4544E-12	1.9551E-12

Table C.81. Continued.

WATER-LEAD, 3MEV, B1=3

GRP.	B2=1	B2=2	B2=3	B2=4	B2=5
1	5.8997E-01	5.8061E-01	5.6747E-01	5.4988E-01	5.3329E-01
2	5.7396E-01	5.6778E-01	5.5744E-01	5.4309E-01	5.2932E-01
3	5.4353E-01	5.4341E-01	5.3838E-01	5.3020E-01	5.2197E-01
4	5.1419E-01	5.1943E-01	5.1523E-01	5.1053E-01	5.1325E-01
5	4.8680E-01	4.9567E-01	5.0063E-01	5.0268E-01	5.0371E-01
6	4.6156E-01	4.7518E-01	4.8270E-01	4.8869E-01	4.9334E-01
7	4.3484E-01	4.4838E-01	4.5668E-01	4.6389E-01	4.6937E-01
8	4.0755E-01	4.1821E-01	4.2519E-01	4.3180E-01	4.3758E-01
9	3.8138E-01	3.8839E-01	3.9353E-01	3.9902E-01	4.0423E-01
10	3.4556E-01	3.4352E-01	3.4382E-01	3.4611E-01	3.4894E-01
11	3.0679E-01	2.9680E-01	2.9335E-01	2.9329E-01	2.9429E-01
12	2.5625E-01	2.4038E-01	2.3486E-01	2.3330E-01	2.3305E-01
13	1.8408E-01	1.6789E-01	1.6285E-01	1.6112E-01	1.6043E-01
14	8.8814E-02	8.0403E-02	7.8243E-02	7.7467E-02	7.7109E-02
15	1.3756E-02	1.2759E-02	1.2477E-02	1.2370E-02	1.2324E-02
16	2.9476E-04	2.7491E-04	2.6976E-04	2.6824E-04	2.6400E-04
17	3.3163E-06	3.5185E-06	2.8140E-06	3.8545E-06	3.2704E-06
18	6.4680E-07	5.8096E-07	5.7809E-07	5.7420E-07	5.6441E-07
19	2.3855E-09	3.1837E-09	2.1231E-09	2.6359E-09	2.8556E-09
20	2.4529E-12	2.9784E-12	2.2104E-12	2.3511E-12	2.4167E-12

WATER-LEAD, 3MEV, B1=4

GRP.	B2=1	B2=2	B2=3	B2=4	B2=5
1	5.8675E-01	5.7490E-01	5.5935E-01	5.4027E-01	5.2274E-01
2	5.7134E-01	5.6307E-01	5.5068E-01	5.3505E-01	5.2056E-01
3	5.4208E-01	5.4060E-01	5.3422E-01	5.2515E-01	5.1634E-01
4	5.1369E-01	5.1824E-01	5.1732E-01	5.1410E-01	5.1046E-01
5	4.8708E-01	4.9689E-01	5.0072E-01	5.0261E-01	5.0351E-01
6	4.6242E-01	4.7656E-01	4.8446E-01	4.9061E-01	4.9539E-01
7	4.3608E-01	4.5054E-01	4.5949E-01	4.6709E-01	4.7338E-01
8	4.0833E-01	4.2073E-01	4.2846E-01	4.3552E-01	4.4165E-01
9	3.8263E-01	3.9091E-01	3.9685E-01	4.0281E-01	4.0825E-01
10	3.4633E-01	3.4531E-01	3.4617E-01	3.4878E-01	3.5179E-01
11	3.0714E-01	2.9764E-01	2.9453E-01	2.9470E-01	2.9536E-01
12	2.5608E-01	2.4004E-01	2.3471E-01	2.3341E-01	2.3339E-01
13	1.8340E-01	1.6660E-01	1.6182E-01	1.6044E-01	1.6026E-01
14	8.8175E-02	7.9484E-02	7.7576E-02	7.7019E-02	7.6934E-02
15	1.3655E-02	1.2643E-02	1.2391E-02	1.2311E-02	1.2296E-02
16	2.8776E-04	2.6753E-04	2.6573E-04	2.6218E-04	2.6116E-04
17	3.3491E-06	3.6756E-06	3.1294E-06	3.7859E-06	4.1372E-06
18	6.4193E-07	7.7988E-07	5.6844E-07	6.7151E-07	6.7263E-07
19	2.4110E-09	3.2409E-09	2.7846E-09	4.4690E-09	4.3446E-09
20	1.7665E-12	2.8914E-12	2.6761E-12	2.8938E-12	2.9166E-12

Table C.81. Continued.

WATER-LEAD, 3MEV, B1=5

GRP.	B2=1	B2=2	B2=3	B2=4	B2=5
1	5.8142E-01	5.6779E-01	5.5140E-01	5.3153E-01	5.1322E-01
2	5.6687E-01	5.5712E-01	5.4402E-01	5.2770E-01	5.1250E-01
3	5.3921E-01	5.3685E-01	5.2999E-01	5.2043E-01	5.1113E-01
4	5.1217E-01	5.1634E-01	5.1521E-01	5.1169E-01	5.0778E-01
5	4.8669E-01	4.9662E-01	5.0046E-01	5.0230E-01	5.0315E-01
6	4.6293E-01	4.7763E-01	4.8578E-01	4.9211E-01	4.9704E-01
7	4.3727E-01	4.5257E-01	4.6191E-01	4.6981E-01	4.7636E-01
8	4.1057E-01	4.2331E-01	4.3145E-01	4.3882E-01	4.4518E-01
9	3.8444E-01	3.9367E-01	4.0001E-01	4.0625E-01	4.1189E-01
10	3.4807E-01	3.4761E-01	3.4863E-01	3.5135E-01	3.5445E-01
11	3.0855E-01	2.9920E-01	2.9602E-01	2.9622E-01	2.9747E-01
12	2.5700E-01	2.4059E-01	2.3507E-01	2.3382E-01	2.3394E-01
13	1.8367E-01	1.6620E-01	1.6138E-01	1.6015E-01	1.5995E-01
14	8.8063E-02	7.9059E-02	7.7221E-02	7.6779E-02	7.6709E-02
15	1.3626E-02	1.2589E-02	1.2345E-02	1.2285E-02	1.2269E-02
16	2.8358E-04	2.5617E-04	2.6305E-04	2.5795E-04	2.6687E-04
17	3.5451E-06	3.9340E-06	3.3339E-06	4.3501E-06	3.1098E-06
18	6.1440E-07	8.1519E-07	5.6291E-07	7.5901E-07	5.8140E-07
19	2.4711E-09	3.5670E-09	1.9909E-09	4.6446E-09	3.1041E-09
20	2.0907E-12	3.1834E-12	2.3895E-12	2.9459E-12	2.2093E-12

Table C.82. Scattered Energy Flux Spectra, $I^S(b_1+b_2,E_i)/I^S(b_1+b_2)$, for 3MeV Photons in Slabs of Iron Followed by Lead.

IRON-LEAD, 3MEV, B1=1

GRP.	B2=1	B2=2	B2=3	B2=4	B2=5
1	5.8283E-01	5.8432E-01	5.7722E-01	5.6787E-01	5.5492E-01
2	5.6634E-01	5.6975E-01	5.6494E-01	5.5775E-01	5.4733E-01
3	5.3501E-01	5.4207E-01	5.4161E-01	5.3854E-01	5.3291E-01
4	5.0507E-01	5.1533E-01	5.1865E-01	5.1920E-01	5.1779E-01
5	4.7754E-01	4.9036E-01	4.9676E-01	5.0034E-01	5.0253E-01
6	4.5276E-01	4.6737E-01	4.7605E-01	4.8206E-01	4.8714E-01
7	4.2783E-01	4.4084E-01	4.4907E-01	4.5534E-01	4.6119E-01
8	4.0352E-01	4.1231E-01	4.1822E-01	4.2324E-01	4.2844E-01
9	3.8144E-01	3.8496E-01	3.8802E-01	3.9138E-01	3.9553E-01
10	3.5104E-01	3.4465E-01	3.4242E-01	3.4234E-01	3.4389E-01
11	3.1749E-01	3.0232E-01	2.9604E-01	2.9332E-01	2.9286E-01
12	2.7074E-01	2.4988E-01	2.4120E-01	2.3679E-01	2.3479E-01
13	1.9846E-01	1.7890E-01	1.7063E-01	1.6603E-01	1.6362E-01
14	9.6960E-02	8.6829E-02	8.2606E-02	8.0251E-02	7.8923E-02
15	1.4804E-02	1.3563E-02	1.3027E-02	1.2723E-02	1.2559E-02
16	3.4448E-04	3.0615E-04	2.9043E-04	2.8005E-04	2.7363E-04
17	3.5925E-06	3.2326E-06	3.1285E-06	2.9324E-06	3.9773E-06
18	7.1063E-07	6.4022E-07	6.1022E-07	5.9220E-07	5.8075E-07
19	2.3249E-09	2.0441E-09	2.9527E-09	2.1374E-09	2.0389E-09
20	2.0786E-12	2.5416E-12	2.7845E-12	2.3080E-12	2.1438E-12

IRON-LEAD, 3MEV, B1=2

GRP.	B2=1	B2=2	B2=3	B2=4	B2=5
1	5.7750E-01	5.7729E-01	5.6706E-01	5.5514E-01	5.4060E-01
2	5.6305E-01	5.6473E-01	5.5702E-01	5.4742E-01	5.3559E-01
3	5.3561E-01	5.4087E-01	5.3796E-01	5.3294E-01	5.2603E-01
4	5.0877E-01	5.1720E-01	5.1854E-01	5.1756E-01	5.1517E-01
5	4.8342E-01	4.9451E-01	4.9946E-01	5.0202E-01	5.0350E-01
6	4.5990E-01	4.7306E-01	4.8089E-01	4.8639E-01	4.9110E-01
7	4.3511E-01	4.4688E-01	4.5472E-01	4.6037E-01	4.6664E-01
8	4.0968E-01	4.1756E-01	4.2350E-01	4.2872E-01	4.3407E-01
9	3.8509E-01	3.8855E-01	3.9224E-01	3.9619E-01	4.0073E-01
10	3.6025E-01	3.4491E-01	3.4380E-01	3.4466E-01	3.4630E-01
11	3.1218E-01	2.9919E-01	2.9475E-01	2.9335E-01	2.9377E-01
12	2.6170E-01	2.4397E-01	2.3760E-01	2.3481E-01	2.3399E-01
13	1.8879E-01	1.7200E-01	1.6611E-01	1.6324E-01	1.6187E-01
14	9.1475E-02	8.2621E-02	8.0062E-02	7.8650E-02	7.7922E-02
15	1.4154E-02	1.3086E-02	1.2717E-02	1.2531E-02	1.2434E-02
16	3.1204E-04	2.8881E-04	2.7883E-04	2.7211E-04	2.6832E-04
17	3.3258E-06	3.0663E-06	3.0729E-06	2.8379E-06	3.9186E-06
18	6.6797E-07	6.1097E-07	5.9192E-07	5.8027E-07	5.7237E-07
19	2.1572E-09	2.7744E-09	2.8466E-09	2.1962E-09	2.5466E-09
20	1.9365E-12	2.4095E-12	2.6871E-12	2.3030E-12	2.3919E-12

Table C.82. Continued.

IRON-LEAD, 3MEV, B1=3

GRP.	B2=1	B2=2	B2=3	B2=4	B2=5
1	5.6921E-01	5.6634E-01	5.5392E-01	5.4108E-01	5.2571E-01
2	5.5662E-01	5.5597E-01	5.4633E-01	5.3591E-01	5.2323E-01
3	5.3270E-01	5.3628E-01	5.3191E-01	5.2609E-01	5.1850E-01
4	5.0859E-01	5.1597E-01	5.1632E-01	5.1475E-01	5.1180E-01
5	4.8519E-01	4.9587E-01	5.0036E-01	5.0252E-01	5.0368E-01
6	4.6288E-01	4.7629E-01	4.8419E-01	4.8959E-01	4.9422E-01
7	4.3868E-01	4.5114E-01	4.5938E-01	4.6562E-01	4.7147E-01
8	4.1321E-01	4.2204E-01	4.2854E-01	4.3396E-01	4.3947E-01
9	3.8783E-01	3.9259E-01	3.9702E-01	4.0128E-01	4.0604E-01
10	3.5141E-01	3.4719E-01	3.4685E-01	3.4805E-01	3.5051E-01
11	3.1178E-01	2.9982E-01	2.9596E-01	2.9491E-01	2.9565E-01
12	2.6006E-01	2.4272E-01	2.3691E-01	2.3460E-01	2.3414E-01
13	1.8648E-01	1.6946E-01	1.6425E-01	1.6202E-01	1.6119E-01
14	8.9843E-02	8.1124E-02	7.8894E-02	7.7886E-02	7.7464E-02
15	1.3938E-02	1.2882E-02	1.2574E-02	1.2437E-02	1.2377E-02
16	2.9844E-04	2.7930E-04	2.7121E-04	2.6766E-04	2.6554E-04
17	3.2250E-06	3.0786E-06	3.5005E-06	3.8618E-06	3.9500E-06
18	6.5368E-07	5.9914E-07	6.0044E-07	5.7270E-07	7.6597E-07
19	2.1028E-09	2.7825E-09	2.8363E-09	2.7300E-09	3.4508E-09
20	2.0120E-12	2.5285E-12	2.3235E-12	2.3601E-12	2.0159E-12

IRON-LEAD, 3MEV, B1=4

GRP.	B2=1	B2=2	B2=3	B2=4	B2=5
1	5.5822E-01	5.5340E-01	5.4210E-01	5.2693E-01	5.1127E-01
2	5.4764E-01	5.4534E-01	5.3655E-01	5.2420E-01	5.1118E-01
3	5.2752E-01	5.3004E-01	5.2600E-01	5.1891E-01	5.1101E-01
4	5.0640E-01	5.1328E-01	5.1367E-01	5.1142E-01	5.0821E-01
5	4.8524E-01	4.9598E-01	5.0031E-01	5.0240E-01	5.0348E-01
6	4.6449E-01	4.7851E-01	4.8627E-01	4.9208E-01	4.9677E-01
7	4.4137E-01	4.5477E-01	4.6299E-01	4.6981E-01	4.7579E-01
8	4.1648E-01	4.2638E-01	4.3290E-01	4.3890E-01	4.4491E-01
9	3.9111E-01	3.9702E-01	4.0152E-01	4.0632E-01	4.1117E-01
10	3.5407E-01	3.5066E-01	3.5019E-01	3.5177E-01	3.5426E-01
11	3.1375E-01	3.0207E-01	2.9782E-01	2.9712E-01	2.9790E-01
12	2.6119E-01	2.4342E-01	2.3719E-01	2.3523E-01	2.3493E-01
13	1.8665E-01	1.6875E-01	1.6341E-01	1.6162E-01	1.6106E-01
14	8.9532E-02	8.0431E-02	7.8288E-02	7.7553E-02	7.7293E-02
15	1.3886E-02	1.2801E-02	1.2506E-02	1.2398E-02	1.2357E-02
16	2.9193E-04	2.7348E-04	2.6804E-04	2.6490E-04	2.6307E-04
17	3.2101E-06	3.5070E-06	2.9688E-06	3.4470E-06	3.9459E-06
18	6.4970E-07	6.1284E-07	5.7771E-07	5.8130E-07	6.5819E-07
19	2.1458E-09	3.5169E-09	2.7371E-09	2.6000E-09	3.6707E-09
20	1.8755E-12	2.7251E-12	2.0916E-12	2.4597E-12	2.1623E-12

Table C.82. Continued.

IRON-LEAD, 3MEV, B1=5

GRP.	B2=1	B2=2	B2=3	B2=4	B2=5
1	5.4584E-01	5.4040E-01	5.2809E-01	5.1256E-01	4.9759E-01
2	5.3735E-01	5.3455E-01	5.2490E-01	5.1218E-01	4.9972E-01
3	5.2121E-01	5.2343E-01	5.1883E-01	5.1146E-01	5.0380E-01
4	5.0325E-01	5.1007E-01	5.1021E-01	5.0777E-01	5.0463E-01
5	4.8451E-01	4.9549E-01	4.9990E-01	5.0196E-01	5.0298E-01
6	4.6554E-01	4.8010E-01	4.8826E-01	4.9429E-01	4.9893E-01
7	4.4379E-01	4.5792E-01	4.6666E-01	4.7376E-01	4.7967E-01
8	4.1978E-01	4.3047E-01	4.3748E-01	4.4376E-01	4.4919E-01
9	3.9478E-01	4.0146E-01	4.0637E-01	4.1133E-01	4.1602E-01
10	3.5751E-01	3.5447E-01	3.5411E-01	3.5567E-01	3.5793E-01
11	3.1676E-01	3.0489E-01	3.0052E-01	2.9971E-01	3.0026E-01
12	2.6345E-01	2.4487E-01	2.3940E-01	2.3637E-01	2.3598E-01
13	1.8781E-01	1.6887E-01	1.6343E-01	1.6173E-01	1.6122E-01
14	8.9783E-02	8.0208E-02	7.8127E-02	7.7491E-02	7.7284E-02
15	1.3909E-02	1.2780E-02	1.2490E-02	1.2392E-02	1.2358E-02
16.	2.8875E-04	2.5964E-04	2.6559E-04	2.5742E-04	2.7219E-04
17	3.2362E-06	3.7123E-06	3.5217E-06	4.0455E-06	3.4036E-06
18	6.5036E-07	6.2447E-07	5.9174E-07	6.5441E-07	7.7866E-07
19	2.8079E-09	3.5248E-09	3.5066E-09	2.7984E-09	3.8825E-09
20	1.6742E-12	2.3329E-12	2.2560E-12	2.4391E-12	3.0278E-12

Table C.83. Scattered Energy Flux Spectra, $I^S(b_1+b_2,E_i)/I^S(b_1+b_2)$, for 6MeV Photons in Slabs of Iron Followed by Water.

IRON-WATER,6MEV,B1=1

GRP.	B2=1	B2=2	B2=3	B2=4	B2=5
1	2.6194E-01	2.6833E-01	2.7338E-01	2.7658E-01	2.7857E-01
2	2.5135E-01	2.5885E-01	2.6452E-01	2.6844E-01	2.7094E-01
3	2.3439E-01	2.4094E-01	2.4478E-01	2.4716E-01	2.4866E-01
4	2.1784E-01	2.2367E-01	2.2692E-01	2.2881E-01	2.2993E-01
5	2.0266E-01	2.0779E-01	2.1040E-01	2.1184E-01	2.1271E-01
6	1.8946E-01	1.9389E-01	1.9633E-01	1.9785E-01	1.9864E-01
7	1.7568E-01	1.7927E-01	1.8062E-01	1.8127E-01	1.8167E-01
8	1.6425E-01	1.6691E-01	1.6769E-01	1.6803E-01	1.6824E-01
9	1.5392E-01	1.5544E-01	1.5596E-01	1.5553E-01	1.5554E-01
10	1.4523E-01	1.4644E-01	1.4688E-01	1.4451E-01	1.4432E-01
11	1.3798E-01	1.3866E-01	1.3540E-01	1.3463E-01	1.3421E-01
12	1.3293E-01	1.2991E-01	1.2790E-01	1.2673E-01	1.2606E-01
13	1.3042E-01	1.2597E-01	1.2273E-01	1.2113E-01	1.2023E-01
14	1.2862E-01	1.2232E-01	1.1789E-01	1.1689E-01	1.1587E-01
15	1.2170E-01	1.1526E-01	1.1282E-01	1.1100E-01	1.0995E-01
16	1.5427E-01	1.3501E-01	1.2532E-01	1.2428E-01	1.2157E-01
17	1.0534E-01	2.4706E-02	3.1202E-02	8.9417E-02	8.8271E-02
18	1.1673E-01	1.0783E-01	1.0442E-01	1.0125E-01	9.9935E-02
19	1.2466E-01	1.1535E-01	1.1150E-01	1.0962E-01	1.0851E-01
20	2.5223E-02	2.3417E-02	2.2665E-02	2.2239E-02	2.2087E-02

IRON-WATER,6MEV,B1=2

GRP.	B2=1	B2=2	B2=3	B2=4	B2=5
1	2.5753E-01	2.6679E-01	2.7215E-01	2.7540E-01	2.7741E-01
2	2.4911E-01	2.5777E-01	2.6264E-01	2.6556E-01	2.6735E-01
3	2.3329E-01	2.4063E-01	2.4478E-01	2.4687E-01	2.4829E-01
4	2.1605E-01	2.2413E-01	2.2925E-01	2.2993E-01	2.3095E-01
5	2.0402E-01	2.0983E-01	2.1159E-01	2.1231E-01	2.1301E-01
6	1.9071E-01	1.9423E-01	1.9570E-01	1.9644E-01	1.9686E-01
7	1.7852E-01	1.8053E-01	1.8151E-01	1.8197E-01	1.8221E-01
8	1.6751E-01	1.6893E-01	1.6938E-01	1.6972E-01	1.6977E-01
9	1.5706E-01	1.5883E-01	1.5943E-01	1.5912E-01	1.5901E-01
10	1.4703E-01	1.4844E-01	1.4902E-01	1.4495E-01	1.4466E-01
11	1.3959E-01	1.3712E-01	1.3555E-01	1.3495E-01	1.3442E-01
12	1.3311E-01	1.2986E-01	1.2776E-01	1.2670E-01	1.2606E-01
13	1.2981E-01	1.2632E-01	1.2329E-01	1.2087E-01	1.2007E-01
14	1.2541E-01	1.1921E-01	1.1763E-01	1.1633E-01	1.1532E-01
15	1.1992E-01	1.1451E-01	1.1290E-01	1.1052E-01	1.0961E-01
16	1.4390E-01	1.3094E-01	1.2507E-01	1.2240E-01	1.2038E-01
17	1.0295E-01	2.3324E-02	3.0341E-02	8.8810E-02	8.7884E-02
18	1.1514E-01	1.0678E-01	1.0331E-01	1.0050E-01	9.9407E-02
19	1.2214E-01	1.1427E-01	1.1049E-01	1.0851E-01	1.0735E-01
20	2.4779E-02	2.3292E-02	2.2541E-02	2.2223E-02	2.2042E-02

Table C.83. Continued.

IRON-WATER, 6MEV, B1=3

GRP.	B2=1	B2=2	B2=3	B2=4	B2=5
1	2.5273E-01	2.6311E-01	2.6511E-01	2.7279E-01	2.7511E-01
2	2.4524E-01	2.5477E-01	2.5018E-01	2.6345E-01	2.6551E-01
3	2.3099E-01	2.3892E-01	2.4321E-01	2.4573E-01	2.4721E-01
4	2.1710E-01	2.2344E-01	2.2663E-01	2.2851E-01	2.2959E-01
5	2.0433E-01	2.0905E-01	2.1127E-01	2.1245E-01	2.1312E-01
6	1.9188E-01	1.9503E-01	1.9631E-01	1.9692E-01	1.9724E-01
7	1.8046E-01	1.8220E-01	1.8273E-01	1.8286E-01	1.8276E-01
8	1.6984E-01	1.7004E-01	1.6977E-01	1.6954E-01	1.6934E-01
9	1.5944E-01	1.5831E-01	1.5743E-01	1.5692E-01	1.5665E-01
10	1.5018E-01	1.4731E-01	1.4642E-01	1.4586E-01	1.4525E-01
11	1.4136E-01	1.3809E-01	1.3634E-01	1.3539E-01	1.3490E-01
12	1.3404E-01	1.3014E-01	1.2814E-01	1.2701E-01	1.2634E-01
13	1.2871E-01	1.2449E-01	1.2225E-01	1.2096E-01	1.2017E-01
14	1.2452E-01	1.2114E-01	1.1787E-01	1.1620E-01	1.1527E-01
15	1.1830E-01	1.1419E-01	1.1154E-01	1.1045E-01	1.0960E-01
16	1.3847E-01	1.2809E-01	1.2380E-01	1.2121E-01	1.1949E-01
17	1.0122E-01	9.2664E-02	8.9348E-02	8.3566E-02	8.7711E-02
18	1.1293E-01	1.0501E-01	1.0134E-01	1.0028E-01	9.9309E-02
19	1.2542E-01	1.1404E-01	1.1079E-01	1.0914E-01	1.0826E-01
20	2.4444E-02	2.3215E-02	2.2855E-02	2.2224E-02	2.2045E-02

IRON-WATER, 6MEV, B1=4

GRP.	B2=1	B2=2	B2=3	B2=4	B2=5
1	2.4691E-01	2.5824E-01	2.6063E-01	2.6733E-01	2.7214E-01
2	2.4032E-01	2.5069E-01	2.5570E-01	2.6052E-01	2.6306E-01
3	2.2777E-01	2.3635E-01	2.4117E-01	2.4402E-01	2.4591E-01
4	2.1535E-01	2.2216E-01	2.2568E-01	2.2776E-01	2.2902E-01
5	2.0392E-01	2.0977E-01	2.1115E-01	2.1242E-01	2.1314E-01
6	1.9243E-01	1.9551E-01	1.9676E-01	1.9733E-01	1.9765E-01
7	1.8181E-01	1.8314E-01	1.8341E-01	1.8342E-01	1.8337E-01
8	1.7173E-01	1.7147E-01	1.7090E-01	1.7047E-01	1.7019E-01
9	1.6154E-01	1.5954E-01	1.5861E-01	1.5794E-01	1.5739E-01
10	1.5231E-01	1.4933E-01	1.4796E-01	1.4652E-01	1.4578E-01
11	1.4318E-01	1.3937E-01	1.3762E-01	1.3610E-01	1.3544E-01
12	1.3583E-01	1.3110E-01	1.2903E-01	1.2794E-01	1.2678E-01
13	1.2945E-01	1.2503E-01	1.2296E-01	1.2122E-01	1.2043E-01
14	1.2477E-01	1.2023E-01	1.1783E-01	1.1633E-01	1.1543E-01
15	1.1967E-01	1.1446E-01	1.1206E-01	1.1054E-01	1.0977E-01
16	1.3563E-01	1.2653E-01	1.2279E-01	1.2048E-01	1.1994E-01
17	1.0054E-01	9.2574E-02	8.9348E-02	8.3546E-02	8.7707E-02
18	1.1134E-01	1.0477E-01	1.0161E-01	1.0023E-01	9.9301E-02
19	1.1774E-01	1.1435E-01	1.1097E-01	1.0935E-01	1.0842E-01
20	2.4321E-02	2.3215E-02	2.2602E-02	2.2275E-02	2.2088E-02

Table C.83. Continued.

IRON-WATER, 6MEV, B1=5

GRP.	B2=1	B2=2	B2=3	B2=4	B2=5
1	2.4063E-01	2.5258E-01	2.6018E-01	2.6507E-01	2.6883E-01
2	2.3495E-01	2.4539E-01	2.5274E-01	2.5709E-01	2.6040E-01
3	2.2416E-01	2.3327E-01	2.3961E-01	2.4193E-01	2.4437E-01
4	2.1319E-01	2.2035E-01	2.2432E-01	2.2668E-01	2.2833E-01
5	2.0311E-01	2.0821E-01	2.1079E-01	2.1219E-01	2.1309E-01
6	1.9261E-01	1.9576E-01	1.9762E-01	1.9766E-01	1.9795E-01
7	1.8284E-01	1.8497E-01	1.8625E-01	1.8716E-01	1.8392E-01
8	1.7343E-01	1.7267E-01	1.7204E-01	1.7148E-01	1.7095E-01
9	1.6347E-01	1.6141E-01	1.5993E-01	1.5891E-01	1.5817E-01
10	1.5438E-01	1.5034E-01	1.4803E-01	1.4756E-01	1.4668E-01
11	1.4506E-01	1.4082E-01	1.3841E-01	1.3701E-01	1.3607E-01
12	1.3697E-01	1.3230E-01	1.2975E-01	1.2827E-01	1.2727E-01
13	1.3062E-01	1.2592E-01	1.2334E-01	1.2183E-01	1.2079E-01
14	1.2553E-01	1.2093E-01	1.1840E-01	1.1673E-01	1.1562E-01
15	1.1953E-01	1.1514E-01	1.1253E-01	1.1107E-01	1.1002E-01
16	1.3421E-01	1.2578E-01	1.2225E-01	1.2012E-01	1.1859E-01
17	1.0050E-01	9.2831E-02	9.0123E-02	8.8721E-02	8.7781E-02
18	1.1179E-01	1.0517E-01	1.0203E-01	1.0046E-01	9.9389E-02
19	1.1956E-01	1.1503E-01	1.1152E-01	1.0978E-01	1.0867E-01
20	2.4356E-02	2.3446E-02	2.2724E-02	2.2369E-02	2.2143E-02

Table C.84. Scattered Energy Flux Spectra, $I^S(b_1+b_2,E_i)/I^S(b_1+b_2)$, for 6MeV Photons in Slabs of Tin Followed by Water.

TIN-WATER, 6MEV, B1=2

GRP.	B2=1	B2=2	B2=3	B2=4	B2=5
1	2.5135E-01	2.6274E-01	2.6348E-01	2.6549E-01	2.7615E-01
2	2.4334E-01	2.5409E-01	2.5924E-01	2.6026E-01	2.6725E-01
3	2.2841E-01	2.3766E-01	2.4272E-01	2.4272E-01	2.4743E-01
4	2.1404E-01	2.2165E-01	2.2556E-01	2.2558E-01	2.2340E-01
5	2.0198E-01	2.0722E-01	2.1025E-01	2.1025E-01	2.1271E-01
6	1.8836E-01	1.9341E-01	1.9552E-01	1.9932E-01	1.9676E-01
7	1.7767E-01	1.8061E-01	1.8152E-01	1.8159E-01	1.8221E-01
8	1.6754E-01	1.6820E-01	1.6853E-01	1.6933E-01	1.6850E-01
9	1.5795E-01	1.5752E-01	1.5744E-01	1.5894E-01	1.5820E-01
10	1.4957E-01	1.4747E-01	1.4603E-01	1.4603E-01	1.4491E-01
11	1.4201E-01	1.3837E-01	1.3637E-01	1.3637E-01	1.3479E-01
12	1.3594E-01	1.3103E-01	1.2855E-01	1.2856E-01	1.2640E-01
13	1.3179E-01	1.2681E-01	1.2311E-01	1.2311E-01	1.2044E-01
14	1.2827E-01	1.2229E-01	1.1893E-01	1.1893E-01	1.1575E-01
15	1.2126E-01	1.1605E-01	1.1294E-01	1.1294E-01	1.1001E-01
16	1.5157E-01	1.3391E-01	1.2723E-01	1.2723E-01	1.2104E-01
17	1.0605E-01	9.4931E-02	9.1231E-02	9.1231E-02	8.8236E-02
18	1.1559E-01	1.0754E-01	1.0233E-01	1.0233E-01	9.9508E-02
19	1.2328E-01	1.1599E-01	1.1179E-01	1.1179E-01	1.0864E-01
20	2.4716E-02	2.4541E-02	2.2758E-02	2.2758E-02	2.2118E-02

TIN-LATER, 6MEV, B1=4

GRP.	B2=1	B2=2	B2=3	B2=4	B2=5
1	2.3079E-01	2.4729E-01	2.5752E-01	2.5752E-01	2.6829E-01
2	2.2355E-01	2.4080E-01	2.5010E-01	2.5010E-01	2.5973E-01
3	2.1568E-01	2.2846E-01	2.3600E-01	2.3600E-01	2.4346E-01
4	2.0557E-01	2.1614E-01	2.2137E-01	2.2137E-01	2.2740E-01
5	1.9774E-01	2.0513E-01	2.0905E-01	2.0905E-01	2.1237E-01
6	1.8899E-01	1.9388E-01	1.9603E-01	1.9603E-01	1.9750E-01
7	1.8118E-01	1.8527E-01	1.8737E-01	1.8737E-01	1.8871E-01
8	1.7372E-01	1.7306E-01	1.7211E-01	1.7211E-01	1.7094E-01
9	1.6562E-01	1.6250E-01	1.6037E-01	1.6037E-01	1.5921E-01
10	1.5800E-01	1.5206E-01	1.4761E-01	1.4961E-01	1.4862E-01
11	1.5001E-01	1.4308E-01	1.3946E-01	1.3949E-01	1.3823E-01
12	1.4251E-01	1.3487E-01	1.3105E-01	1.3105E-01	1.2775E-01
13	1.3662E-01	1.2773E-01	1.2466E-01	1.2466E-01	1.2139E-01
14	1.3159E-01	1.2303E-01	1.2007E-01	1.2007E-01	1.1689E-01
15	1.2375E-01	1.1788E-01	1.1421E-01	1.1421E-01	1.1077E-01
16	1.4361E-01	1.3078E-01	1.2547E-01	1.2547E-01	1.2029E-01
17	1.0402E-01	9.5493E-02	9.1737E-02	9.1737E-02	8.8492E-02
18	1.1362E-01	1.0800E-01	1.0390E-01	1.0390E-01	1.0021E-01
19	1.1993E-01	1.1775E-01	1.1322E-01	1.1322E-01	1.0947E-01
20	2.4272E-02	2.3982E-02	2.3059E-02	2.3059E-02	2.2274E-02

Table C.85. Scattered Energy Flux Spectra, $I^S(b_1+b_2,E_i)/I^S(b_1+b_2)$, for 6MeV Photons in Slabs of Lead Followed by Water.

LEAD-WATER,6MEV,B1=1

GRP.	B2=1	B2=2	B2=3	B2=4	B2=5
1	2.6089E-01	2.6677E-01	2.7217E-01	2.7577E-01	2.7803E-01
2	2.5151E-01	2.5737E-01	2.6240E-01	2.6563E-01	2.6774E-01
3	2.3336E-01	2.3951E-01	2.4364E-01	2.4654E-01	2.4819E-01
4	2.1687E-01	2.2252E-01	2.2615E-01	2.2832E-01	2.2941E-01
5	2.0146E-01	2.0651E-01	2.0980E-01	2.1145E-01	2.1243E-01
6	1.8727E-01	1.9211E-01	1.9440E-01	1.9550E-01	1.9629E-01
7	1.7447E-01	1.7869E-01	1.8034E-01	1.8113E-01	1.8157E-01
8	1.6310E-01	1.6653E-01	1.6754E-01	1.6795E-01	1.6820E-01
9	1.5302E-01	1.5531E-01	1.5561E-01	1.5595E-01	1.5595E-01
10	1.4460E-01	1.4553E-01	1.4502E-01	1.4460E-01	1.4437E-01
11	1.3794E-01	1.3707E-01	1.3570E-01	1.3488E-01	1.3433E-01
12	1.3352E-01	1.3006E-01	1.2837E-01	1.2702E-01	1.2624E-01
13	1.3194E-01	1.2566E-01	1.2344E-01	1.2195E-01	1.2049E-01
14	1.3080E-01	1.2369E-01	1.1970E-01	1.1748E-01	1.1600E-01
15	1.2333E-01	1.1715E-01	1.1355E-01	1.1144E-01	1.1013E-01
16	1.6225E-01	1.3916E-01	1.3023E-01	1.2537E-01	1.2230E-01
17	1.0596E-01	9.6022E-02	9.2038E-02	8.9884E-02	8.8574E-02
18	1.1697E-01	1.0875E-01	1.0426E-01	1.0177E-01	1.0029E-01
19	1.2007E-01	1.1504E-01	1.1217E-01	1.1060E-01	1.0881E-01
20	2.4156E-02	2.3536E-02	2.2763E-02	2.2368E-02	2.2142E-02

LEAD-WATER,6MEV,B1=2

GRP.	B2=1	B2=2	B2=3	B2=4	B2=5
1	2.5445E-01	2.6135E-01	2.6593E-01	2.7389E-01	2.7639E-01
2	2.4622E-01	2.5472E-01	2.6051E-01	2.6415E-01	2.6640E-01
3	2.3055E-01	2.3803E-01	2.4261E-01	2.4571E-01	2.4747E-01
4	2.1567E-01	2.2232E-01	2.2582E-01	2.2804E-01	2.2935E-01
5	2.0213E-01	2.0725E-01	2.1069E-01	2.1156E-01	2.1270E-01
6	1.8945E-01	1.9323E-01	1.9510E-01	1.9601E-01	1.9663E-01
7	1.7729E-01	1.8030E-01	1.8151E-01	1.8179E-01	1.8207E-01
8	1.6742E-01	1.6842E-01	1.6864E-01	1.6870E-01	1.6876E-01
9	1.5772E-01	1.5713E-01	1.5660E-01	1.5621E-01	1.5601E-01
10	1.4907E-01	1.4713E-01	1.4589E-01	1.4514E-01	1.4481E-01
11	1.4165E-01	1.3818E-01	1.3627E-01	1.3522E-01	1.3465E-01
12	1.3569E-01	1.3105E-01	1.2858E-01	1.2720E-01	1.2641E-01
13	1.3152E-01	1.2623E-01	1.2322E-01	1.2159E-01	1.2052E-01
14	1.2777E-01	1.2254E-01	1.1912E-01	1.1716E-01	1.1597E-01
15	1.2063E-01	1.1612E-01	1.1313E-01	1.1129E-01	1.1013E-01
16	1.5023E-01	1.3447E-01	1.2815E-01	1.2412E-01	1.2151E-01
17	1.0025E-01	9.4755E-02	9.1429E-02	8.9557E-02	8.8384E-02
18	1.1023E-01	1.0713E-01	1.0355E-01	1.0142E-01	1.0004E-01
19	1.1428E-01	1.1091E-01	1.1180E-01	1.0973E-01	1.0875E-01
20	2.3614E-02	2.3322E-02	2.2731E-02	2.2362E-02	2.2137E-02

Table C.85. Continued.

LEAD-WATER, 6MEV, B1=3

GRP.	B2=1	B2=2	B2=3	B2=4	B2=5
1	2.4573E-01	2.5752E-01	2.6534E-01	2.7C3CE-01	2.7344E-01
2	2.3873E-01	2.4964E-01	2.5675E-01	2.6119E-01	2.6399E-01
3	2.2556E-01	2.3469E-01	2.4042E-01	2.4330E-01	2.4604E-01
4	2.1286E-01	2.2019E-01	2.2457E-01	2.2715E-01	2.2869E-01
5	2.0148E-01	2.0668E-01	2.0987E-01	2.1197E-01	2.1255E-01
6	1.9063E-01	1.9399E-01	1.9752E-01	1.9951E-01	1.9999E-01
7	1.8053E-01	1.8312E-01	1.8537E-01	1.8753E-01	1.8826E-01
8	1.7121E-01	1.7353E-01	1.7534E-01	1.7671E-01	1.7752E-01
9	1.6212E-01	1.6451E-01	1.6608E-01	1.6726E-01	1.6786E-01
10	1.5348E-01	1.4935E-01	1.4725E-01	1.4613E-01	1.4552E-01
11	1.4561E-01	1.4060E-01	1.3741E-01	1.3560E-01	1.3523E-01
12	1.3844E-01	1.3234E-01	1.2838E-01	1.2577E-01	1.2695E-01
13	1.3244E-01	1.2670E-01	1.2286E-01	1.2165E-01	1.2091E-01
14	1.2584E-01	1.2247E-01	1.1930E-01	1.1736E-01	1.1604E-01
15	1.1983E-01	1.1610E-01	1.1280E-01	1.1145E-01	1.1036E-01
16	1.4235E-01	1.3232E-01	1.2694E-01	1.2433E-01	1.2102E-01
17	9.7753E-02	9.4103E-02	9.1305E-02	8.9534E-02	8.8398E-02
18	1.0716E-01	1.0644E-01	1.0334E-01	1.0139E-01	1.0010E-01
19	1.1074E-01	1.1467E-01	1.1193E-01	1.1012E-01	1.0834E-01
20	2.2315E-02	2.3507E-02	2.2763E-02	2.2414E-02	2.2181E-02

LEAD-WATER, 6MEV, B1=4

GRP.	B2=1	B2=2	B2=3	B2=4	B2=5
1	2.3544E-01	2.4967E-01	2.5924E-01	2.6542E-01	2.6945E-01
2	2.2983E-01	2.4289E-01	2.5155E-01	2.5775E-01	2.6066E-01
3	2.1917E-01	2.2993E-01	2.3693E-01	2.4125E-01	2.4397E-01
4	2.0881E-01	2.1723E-01	2.2254E-01	2.2570E-01	2.2763E-01
5	1.9980E-01	2.0560E-01	2.0918E-01	2.1117E-01	2.1232E-01
6	1.9093E-01	1.9416E-01	1.9556E-01	1.9684E-01	1.9731E-01
7	1.8255E-01	1.8522E-01	1.8747E-01	1.8934E-01	1.8942E-01
8	1.7461E-01	1.7275E-01	1.7106E-01	1.7063E-01	1.7048E-01
9	1.6633E-01	1.6219E-01	1.5931E-01	1.5862E-01	1.5787E-01
10	1.5797E-01	1.5295E-01	1.5000E-01	1.4741E-01	1.4642E-01
11	1.4990E-01	1.4284E-01	1.3811E-01	1.3713E-01	1.3607E-01
12	1.4183E-01	1.3431E-01	1.3047E-01	1.2868E-01	1.2753E-01
13	1.3446E-01	1.2712E-01	1.2463E-01	1.2259E-01	1.2133E-01
14	1.2740E-01	1.2322E-01	1.1902E-01	1.1779E-01	1.1643E-01
15	1.1993E-01	1.1674E-01	1.1286E-01	1.1133E-01	1.1070E-01
16	1.3865E-01	1.3022E-01	1.2516E-01	1.2259E-01	1.2075E-01
17	9.5162E-02	9.1207E-02	8.8172E-02	8.6774E-02	8.5885E-02
18	1.0514E-01	1.0451E-01	1.0176E-01	1.0016E-01	1.0031E-01
19	1.0943E-01	1.1317E-01	1.1065E-01	1.0885E-01	1.0734E-01
20	2.1961E-02	2.3424E-02	2.2730E-02	2.2529E-02	2.2208E-02

Table C.85. Continued.

LEAD-WATER, 6MEV, B1=5

GRP.	B2=1	B2=2	B2=3	B2=4	B2=5
1	2.2426E-01	2.4057E-01	2.5186E-01	2.5936E-01	2.6480E-01
2	2.2001E-01	2.3449E-01	2.4520E-01	2.5193E-01	2.5677E-01
3	2.1191E-01	2.2427E-01	2.3253E-01	2.3782E-01	2.4150E-01
4	2.0393E-01	2.1359E-01	2.1994E-01	2.2371E-01	2.2630E-01
5	1.9733E-01	2.0336E-01	2.0804E-01	2.1044E-01	2.1195E-01
6	1.9055E-01	1.9405E-01	1.9607E-01	1.9710E-01	1.9763E-01
7	1.8408E-01	1.8445E-01	1.8456E-01	1.8444E-01	1.8420E-01
8	1.7771E-01	1.7562E-01	1.7343E-01	1.7236E-01	1.7155E-01
9	1.7052E-01	1.6504E-01	1.6204E-01	1.6024E-01	1.5903E-01
10	1.6254E-01	1.5510E-01	1.5122E-01	1.4901E-01	1.4761E-01
11	1.5446E-01	1.4548E-01	1.4104E-01	1.3860E-01	1.3708E-01
12	1.4573E-01	1.3642E-01	1.3233E-01	1.2993E-01	1.2837E-01
13	1.3711E-01	1.3004E-01	1.2601E-01	1.2361E-01	1.2201E-01
14	1.2886E-01	1.2440E-01	1.2038E-01	1.1861E-01	1.1696E-01
15	1.2015E-01	1.1613E-01	1.1504E-01	1.1231E-01	1.1124E-01
16	1.3627E-01	1.3062E-01	1.2608E-01	1.2299E-01	1.2073E-01
17	9.5624E-02	9.4810E-02	9.2196E-02	9.0255E-02	8.8892E-02
18	1.0435E-01	1.0715E-01	1.0490E-01	1.0222E-01	1.0067E-01
19	1.0429E-01	1.1625E-01	1.1372E-01	1.1143E-01	1.0995E-01
20	2.1883E-02	2.3657E-02	2.3159E-02	2.2707E-02	2.2395E-02

Table C.86. Scattered Energy Flux Spectra, $I^S(b_1+b_2,E_i)/I^S(b_1+b_2)$, for 6MeV Photons in Slabs of Tin Followed by Aluminum.

TIN-ALUM.,6MEV,B1=2

GRP.	B2=1	B2=2	B2=3	B2=4	B2=5
1	2.3[illegible]E-01	2.4575E-01	2.4877E-01	2.4877E-01	2.4917E-01
2	2.3201E-01	2.3865E-01	2.4160E-01	2.4160E-01	2.4226E-01
3	2.1890E-01	2.2515E-01	2.2798E-01	2.2798E-01	2.2911E-01
4	2.0634E-01	2.1208E-01	2.1470E-01	2.1470E-01	2.1614E-01
5	1.9524E-01	2.0037E-01	2.0276E-01	2.0276E-01	2.0446E-01
6	1.8456E-01	1.8939E-01	1.9099E-01	1.9099E-01	1.9267E-01
7	1.7513E-01	1.7954E-01	1.8014E-01	1.8014E-01	1.8174E-01
8	1.6651E-01	1.6885E-01	1.6997E-01	1.6997E-01	1.7143E-01
9	1.5924E-01	1.5929E-01	1.6080E-01	1.6080E-01	1.6087E-01
10	1.5111E-01	1.5088E-01	1.5080E-01	1.5080E-01	1.5148E-01
11	1.4462E-01	1.4224E-01	1.4210E-01	1.4210E-01	1.4224E-01
12	1.3920E-01	1.3609E-01	1.3476E-01	1.3476E-01	1.3432E-01
13	1.3512E-01	1.3105E-01	1.2918E-01	1.2918E-01	1.2814E-01
14	1.3104E-01	1.2669E-01	1.2444E-01	1.2444E-01	1.2283E-01
15	1.2385E-01	1.2043E-01	1.1845E-01	1.1848E-01	1.1714E-01
16	1.9298E-01	1.6962E-01	1.6014E-01	1.6014E-01	1.5097E-01
17	1.2482E-01	1.1339E-01	1.0866E-01	1.0866E-01	1.0479E-01
18	1.2031E-01	1.1937E-01	1.1446E-01	1.1446E-01	1.1032E-01
19	8.9080E-02	8.5365E-02	8.2025E-02	8.2025E-02	7.9315E-02
20	1.7825E-03	1.7028E-03	1.6356E-03	1.6356E-03	1.5808E-03

TIN-ALUM.,6MEV,B1=4

GRP.	B2=1	B2=2	B2=3	B2=4	B2=5
1	2.1061E-01	2.2874E-01	2.3433E-01	2.3439E-01	2.3836E-01
2	2.1432E-01	2.2395E-01	2.2917E-01	2.2917E-01	2.3303E-01
3	2.0717E-01	2.1463E-01	2.1923E-01	2.1929E-01	2.2289E-01
4	1.9813E-01	2.0532E-01	2.0932E-01	2.0925E-01	2.1243E-01
5	1.9172E-01	1.9743E-01	2.0050E-01	2.0050E-01	2.0304E-01
6	1.8502E-01	1.9007E-01	1.9110E-01	1.9110E-01	1.9297E-01
7	1.7901E-01	1.8129E-01	1.8239E-01	1.8239E-01	1.8342E-01
8	1.7330E-01	1.7367E-01	1.7375E-01	1.7375E-01	1.7402E-01
9	1.6674E-01	1.6521E-01	1.6434E-01	1.6434E-01	1.6388E-01
10	1.6070E-01	1.5732E-01	1.5566E-01	1.5566E-01	1.5465E-01
11	1.5385E-01	1.4904E-01	1.4673E-01	1.4673E-01	1.4523E-01
12	1.4700E-01	1.4140E-01	1.3874E-01	1.3874E-01	1.3664E-01
13	1.4066E-01	1.3513E-01	1.3242E-01	1.3242E-01	1.3035E-01
14	1.3446E-01	1.2866E-01	1.2605E-01	1.2605E-01	1.2465E-01
15	1.2736E-01	1.2288E-01	1.2113E-01	1.2113E-01	1.1964E-01
16	1.7404E-01	1.6112E-01	1.5553E-01	1.5553E-01	1.4913E-01
17	1.1831E-01	1.1127E-01	1.0833E-01	1.0833E-01	1.0499E-01
18	1.1947E-01	1.1769E-01	1.1405E-01	1.1405E-01	1.1052E-01
19	8.4243E-02	8.0422E-02	7.7855E-02	7.7855E-02	7.5944E-02
20	1.6554E-03	1.5471E-03	1.4958E-03	1.4958E-03	1.4568E-03

Table C.87. Scattered Energy Flux Spectra, $I^S(b_1+b_2,E_i)/I^S(b_1+b_2)$, for 6MeV Photons in Slabs of Lead Followed by Aluminum.

LEAD-ALUM.,6MEV,B1=2

GRP.	B2=1	B2=2	B2=3	B2=4	B2=5
1	2.4217E-01	2.4695E-01	2.4995E-01	2.4996E-01	2.4996E-01
2	2.3494E-01	2.3967E-01	2.4234E-01	2.4234E-01	2.4291E-01
3	2.2121E-01	2.2583E-01	2.2843E-01	2.2843E-01	2.2952E-01
4	2.0210E-01	2.0642E-01	2.0882E-01	2.0882E-01	2.0985E-01
5	1.9639E-01	2.0045E-01	2.0273E-01	2.0273E-01	2.0447E-01
6	1.8536E-01	1.8905E-01	1.9096E-01	1.9096E-01	1.9255E-01
7	1.7537E-01	1.7879E-01	1.7966E-01	1.7980E-01	1.8154E-01
8	1.6633E-01	1.6935E-01	1.6954E-01	1.6954E-01	1.7115E-01
9	1.5791E-01	1.5977E-01	1.5934E-01	1.5936E-01	1.6057E-01
10	1.5051E-01	1.5029E-01	1.5034E-01	1.5034E-01	1.5116E-01
11	1.4406E-01	1.4238E-01	1.4174E-01	1.4174E-01	1.4197E-01
12	1.3866E-01	1.3577E-01	1.3451E-01	1.3451E-01	1.3412E-01
13	1.3445E-01	1.3088E-01	1.2907E-01	1.2907E-01	1.2902E-01
14	1.2995E-01	1.2659E-01	1.2443E-01	1.2443E-01	1.2278E-01
15	1.2184E-01	1.2006E-01	1.1837E-01	1.1837E-01	1.1706E-01
16	1.1396E-01	1.1230E-01	1.1193E-01	1.1193E-01	1.1518E-01
17	1.1934E-01	1.1333E-01	1.0903E-01	1.0905E-01	1.0503E-01
18	1.2147E-01	1.1924E-01	1.1491E-01	1.1491E-01	1.1054E-01
19	8.4200E-02	8.4979E-02	8.2241E-02	8.2241E-02	7.9466E-02
20	1.6715E-03	1.6980E-03	1.6563E-03	1.6563E-03	1.5863E-03

LEAD-ALUM.,6MEV,B1=4

GRP.	B2=1	B2=2	B2=3	B2=4	B2=5
1	2.2335E-01	2.3161E-01	2.3663E-01	2.3680E-01	2.4044E-01
2	2.1972E-01	2.2642E-01	2.3127E-01	2.3127E-01	2.3491E-01
3	2.0391E-01	2.1055E-01	2.2076E-01	2.2076E-01	2.2407E-01
4	2.0134E-01	2.0677E-01	2.1022E-01	2.1025E-01	2.1314E-01
5	1.9423E-01	1.9827E-01	2.0092E-01	2.0092E-01	2.0325E-01
6	1.8714E-01	1.9059E-01	1.9312E-01	1.9312E-01	1.9290E-01
7	1.8059E-01	1.8361E-01	1.8212E-01	1.8212E-01	1.8307E-01
8	1.7437E-01	1.7733E-01	1.7720E-01	1.7720E-01	1.7349E-01
9	1.6765E-01	1.6943E-01	1.6870E-01	1.6870E-01	1.6824E-01
10	1.6072E-01	1.6059E-01	1.6083E-01	1.6083E-01	1.6096E-01
11	1.5373E-01	1.5225E-01	1.5162E-01	1.5162E-01	1.5165E-01
12	1.4715E-01	1.4604E-01	1.4469E-01	1.4469E-01	1.4464E-01
13	1.4034E-01	1.3901E-01	1.3769E-01	1.3769E-01	1.3665E-01
14	1.3018E-01	1.2879E-01	1.2629E-01	1.2629E-01	1.2436E-01
15	1.2127E-01	1.2178E-01	1.2034E-01	1.2034E-01	1.1854E-01
16	1.7112E-01	1.6277E-01	1.5703E-01	1.5703E-01	1.5007E-01
17	1.0903E-01	1.0951E-01	1.0827E-01	1.0827E-01	1.0512E-01
18	1.1124E-01	1.1619E-01	1.1300E-01	1.1300E-01	1.1067E-01
19	7.7465E-02	8.3163E-02	8.1870E-02	8.1870E-02	7.9689E-02
20	1.5522E-03	1.6063E-03	1.6322E-03	1.6322E-03	1.5874E-03

Table C.88. Scattered Energy Flux Spectra, $I^S(b_1+b_2,E_i)/I^S(b_1+b_2)$, for 6MeV Photons in Slabs of Water Followed by Iron.

WATER-IRON,6MEV,B1=1

GRP.	B2=1	B2=2	B2=3	B2=4	B2=5
1	2.3764E-01	2.3138E-01	2.2500E-01	2.1901E-01	2.1221E-01
2	2.3059E-01	2.2538E-01	2.2002E-01	2.1436E-01	2.0902E-01
3	2.1719E-01	2.1328E-01	2.1050E-01	2.0708E-01	2.0296E-01
4	2.0436E-01	2.0292E-01	2.0113E-01	1.9951E-01	1.9659E-01
5	1.9271E-01	1.9305E-01	1.9284E-01	1.9232E-01	1.9122E-01
6	1.8171E-01	1.8345E-01	1.8454E-01	1.8506E-01	1.8512E-01
7	1.7190E-01	1.7406E-01	1.7713E-01	1.7869E-01	1.7981E-01
8	1.6317E-01	1.6731E-01	1.7045E-01	1.7272E-01	1.7470E-01
9	1.5511E-01	1.5972E-01	1.6326E-01	1.6594E-01	1.6836E-01
10	1.4836E-01	1.5344E-01	1.5717E-01	1.6012E-01	1.6290E-01
11	1.4295E-01	1.4719E-01	1.5055E-01	1.5332E-01	1.5606E-01
12	1.3898E-01	1.4196E-01	1.4459E-01	1.4688E-01	1.4945E-01
13	1.3664E-01	1.3771E-01	1.3940E-01	1.4119E-01	1.4332E-01
14	1.3357E-01	1.3284E-01	1.3276E-01	1.3503E-01	1.3696E-01
15	1.2477E-01	1.2446E-01	1.2570E-01	1.2722E-01	1.2910E-01
16	2.7299E-01	2.4576E-01	2.2909E-01	2.1692E-01	2.0993E-01
17	1.3464E-01	1.3099E-01	1.2586E-01	1.2232E-01	1.2029E-01
18	5.8074E-02	5.9811E-02	5.7050E-02	5.5222E-02	5.4153E-02
19	3.9226E-03	3.7246E-03	3.5527E-03	3.4376E-03	3.3723E-03
20	9.5866E-06	9.0944E-06	8.5670E-06	8.4082E-06	8.3459E-06

WATER-IRON,6MEV,B1=2

GRP.	B2=1	B2=2	B2=3	B2=4	B2=5
1	2.4431E-01	2.3272E-01	2.2487E-01	2.1641E-01	2.0850E-01
2	2.3661E-01	2.2690E-01	2.2010E-01	2.1273E-01	2.0593E-01
3	2.2293E-01	2.1564E-01	2.1103E-01	2.0579E-01	2.0077E-01
4	2.0977E-01	2.0505E-01	2.0197E-01	1.9854E-01	1.9524E-01
5	1.9762E-01	1.9545E-01	1.9405E-01	1.9240E-01	1.9074E-01
6	1.8669E-01	1.8590E-01	1.8588E-01	1.8564E-01	1.8529E-01
7	1.7514E-01	1.7745E-01	1.7866E-01	1.7974E-01	1.8059E-01
8	1.6683E-01	1.6976E-01	1.7201E-01	1.7416E-01	1.7598E-01
9	1.5797E-01	1.6181E-01	1.6473E-01	1.6751E-01	1.6964E-01
10	1.5044E-01	1.5506E-01	1.5853E-01	1.6117E-01	1.6407E-01
11	1.4341E-01	1.4809E-01	1.5154E-01	1.5493E-01	1.5779E-01
12	1.3775E-01	1.4196E-01	1.4511E-01	1.4813E-01	1.5101E-01
13	1.3350E-01	1.3652E-01	1.3933E-01	1.4204E-01	1.4459E-01
14	1.2895E-01	1.3126E-01	1.3324E-01	1.3594E-01	1.3774E-01
15	1.2095E-01	1.2327E-01	1.2543E-01	1.2744E-01	1.3017E-01
16	2.3244E-01	2.2301E-01	2.1376E-01	2.0772E-01	2.0369E-01
17	1.2043E-01	1.2229E-01	1.2036E-01	1.1902E-01	1.1923E-01
18	5.5974E-02	5.5574E-02	5.4273E-02	5.3592E-02	5.3113E-02
19	3.4799E-03	3.4605E-03	3.3859E-03	3.3374E-03	3.3076E-03
20	8.4366E-06	1.1104E-05	8.2691E-06	8.1132E-06	7.6650E-06

Table C.88. Continued.

WATER-IRON, 6MEV, B1=3

GRP.	B2=1	B2=2	B2=3	B2=4	B2=5
1	2.4884E-01	2.3439E-01	2.2429E-01	2.1452E-01	2.0577E-01
2	2.4094E-01	2.2556E-01	2.1970E-01	2.1114E-01	2.0349E-01
3	2.2676E-01	2.1747E-01	2.1099E-01	2.0473E-01	1.9912E-01
4	2.1311E-01	2.0560E-01	2.0221E-01	1.9801E-01	1.9423E-01
5	2.0073E-01	1.9634E-01	1.9496E-01	1.9234E-01	1.9036E-01
6	1.8931E-01	1.8727E-01	1.8695E-01	1.8594E-01	1.8532E-01
7	1.7810E-01	1.7872E-01	1.7952E-01	1.8038E-01	1.8110E-01
8	1.6839E-01	1.7033E-01	1.7302E-01	1.7507E-01	1.7695E-01
9	1.5691E-01	1.6270E-01	1.6572E-01	1.6954E-01	1.7104E-01
10	1.5081E-01	1.5570E-01	1.5947E-01	1.6294E-01	1.6596E-01
11	1.4305E-01	1.4834E-01	1.5221E-01	1.5591E-01	1.5907E-01
12	1.3661E-01	1.4179E-01	1.4563E-01	1.4911E-01	1.5219E-01
13	1.3156E-01	1.3616E-01	1.3952E-01	1.4271E-01	1.4559E-01
14	1.2543E-01	1.3022E-01	1.3315E-01	1.3602E-01	1.3861E-01
15	1.1870E-01	1.2247E-01	1.2543E-01	1.2840E-01	1.3100E-01
16	2.1246E-01	2.1006E-01	2.0517E-01	2.0123E-01	1.9952E-01
17	1.1320E-01	1.1774E-01	1.1714E-01	1.1694E-01	1.1798E-01
18	5.2353E-02	5.3127E-02	5.2801E-02	5.2559E-02	5.2429E-02
19	3.2529E-03	3.3089E-03	3.2979E-03	3.2730E-03	3.2643E-03
20	7.2827E-06	1.0619E-05	8.0375E-06	8.1255E-06	9.1741E-06

WATER-IRON, 6MEV, B1=4

GRP.	B2=1	B2=2	B2=3	B2=4	B2=5
1	2.5129E-01	2.3539E-01	2.2362E-01	2.1295E-01	2.0347E-01
2	2.4353E-01	2.2954E-01	2.1912E-01	2.0974E-01	2.0147E-01
3	2.2709E-01	2.1843E-01	2.1075E-01	2.0378E-01	1.9767E-01
4	2.1509E-01	2.0751E-01	2.0221E-01	1.9740E-01	1.9330E-01
5	2.0242E-01	1.9782E-01	1.9462E-01	1.9217E-01	1.8995E-01
6	1.9019E-01	1.8837E-01	1.8799E-01	1.8607E-01	1.8529E-01
7	1.7913E-01	1.7947E-01	1.8012E-01	1.8081E-01	1.8142E-01
8	1.6929E-01	1.7197E-01	1.7472E-01	1.7674E-01	1.7854E-01
9	1.5938E-01	1.6329E-01	1.6748E-01	1.6939E-01	1.7193E-01
10	1.5077E-01	1.5614E-01	1.6022E-01	1.6384E-01	1.6700E-01
11	1.4251E-01	1.4856E-01	1.5295E-01	1.5621E-01	1.6013E-01
12	1.3596E-01	1.4177E-01	1.4611E-01	1.4990E-01	1.5319E-01
13	1.3046E-01	1.3583E-01	1.3972E-01	1.4232E-01	1.4639E-01
14	1.2480E-01	1.2967E-01	1.3321E-01	1.3644E-01	1.3963E-01
15	1.1749E-01	1.2205E-01	1.2564E-01	1.2890E-01	1.3174E-01
16	2.0375E-01	2.0119E-01	1.9594E-01	1.9178E-01	1.9061E-01
17	1.0971E-01	1.1407E-01	1.1347E-01	1.1554E-01	1.1907E-01
18	5.0226E-02	5.1208E-02	5.1777E-02	5.1866E-02	5.1987E-02
19	3.1201E-03	3.2120E-03	3.2044E-03	3.2298E-03	3.2360E-03
20	7.5576E-06	1.0314E-05	7.8122E-06	1.0488E-05	9.0744E-06

Table C.88. Continued.

WATER-IRON, 6MEV, B1=5

GRP.	B2=1	B2=2	B2=3	B2=4	B2=5
1	2.5303E-01	2.3591E-01	2.2297E-01	2.1137E-01	2.0179E-01
2	2.4526E-01	2.2935E-01	2.1856E-01	2.0843E-01	2.0000E-01
3	2.3649E-01	2.1834E-01	2.1027E-01	2.0285E-01	1.9661E-01
4	2.1628E-01	2.0779E-01	2.0206E-01	1.9689E-01	1.9261E-01
5	2.0344E-01	1.9822E-01	1.9418E-01	1.9152E-01	1.8951E-01
6	1.9099E-01	1.8856E-01	1.8719E-01	1.8610E-01	1.8523E-01
7	1.7985E-01	1.7997E-01	1.8031E-01	1.8112E-01	1.8167E-01
8	1.6973E-01	1.7208E-01	1.7426E-01	1.7631E-01	1.7804E-01
9	1.5973E-01	1.6372E-01	1.6705E-01	1.7007E-01	1.7258E-01
10	1.5113E-01	1.5654E-01	1.6025E-01	1.6464E-01	1.6780E-01
11	1.4274E-01	1.4853E-01	1.5312E-01	1.5759E-01	1.6094E-01
12	1.3563E-01	1.4137E-01	1.4656E-01	1.5059E-01	1.5393E-01
13	1.2924E-01	1.3572E-01	1.4062E-01	1.4388E-01	1.4704E-01
14	1.2415E-01	1.2937E-01	1.3337E-01	1.3690E-01	1.3982E-01
15	1.1672E-01	1.2186E-01	1.2586E-01	1.2938E-01	1.3229E-01
16	1.0315E-01	1.0634E-01	1.0960E-01	1.1299E-01	1.1637E-01
17	1.0615E-01	1.1195E-01	1.1760E-01	1.1496E-01	1.1527E-01
18	4.8854E-02	5.0556E-02	5.1671E-02	5.1365E-02	5.1606E-02
19	3.0345E-03	3.1477E-03	3.1801E-03	3.1933E-03	3.2136E-03
20	1.2325E-05	1.0229E-05	1.0160E-05	1.0054E-05	1.0075E-05

Table C.89. Scattered Energy Flux Spectra, $I^S(b_1+b_2,E_i)/I^S(b_1+b_2)$, for 6MeV Photons in Slabs of Lead Followed by Iron.

LEAD-IRON, 6MEV, B1=1

GRP.	B2=1	B2=2	B2=3	B2=4	B2=5
1	2.3935E-01	2.2783E-01	2.2445E-01	2.1953E-01	2.1387E-01
2	2.2348E-01	2.2192E-01	2.1933E-01	2.1525E-01	2.1040E-01
3	2.1041E-01	2.0876E-01	2.0561E-01	2.0713E-01	2.0392E-01
4	1.9794E-01	1.9655E-01	2.0006E-01	1.9893E-01	1.9701E-01
5	1.8672E-01	1.8511E-01	1.8157E-01	1.8183E-01	1.8124E-01
6	1.7623E-01	1.7492E-01	1.7230E-01	1.7442E-01	1.7485E-01
7	1.6596E-01	1.6727E-01	1.6591E-01	1.6776E-01	1.6929E-01
8	1.5630E-01	1.5542E-01	1.5619E-01	1.6183E-01	1.6391E-01
9	1.5171E-01	1.5035E-01	1.5220E-01	1.5507E-01	1.5751E-01
10	1.4619E-01	1.4960E-01	1.5033E-01	1.5326E-01	1.5619E-01
11	1.4191E-01	1.4703E-01	1.4908E-01	1.5267E-01	1.5518E-01
12	1.3954E-01	1.4261E-01	1.4452E-01	1.4654E-01	1.4871E-01
13	1.3883E-01	1.3911E-01	1.3972E-01	1.4103E-01	1.4277E-01
14	1.3678E-01	1.3471E-01	1.3437E-01	1.3514E-01	1.3646E-01
15	1.2695E-01	1.2582E-01	1.2607E-01	1.2714E-01	1.2865E-01
16	3.2929E-01	2.6233E-01	2.4005E-01	2.2435E-01	2.1477E-01
17	1.5534E-01	1.4034E-01	1.3062E-01	1.2515E-01	1.2201E-01
18	7.2117E-02	6.4203E-02	5.9326E-02	5.6536E-02	5.5001E-02
19	4.5055E-03	3.9701E-03	3.6948E-03	3.5245E-03	3.4252E-03
20	1.0998E-05	9.7685E-06	9.0250E-06	8.6093E-06	8.3740E-06

LEAD-IRON, 6MEV, B1=2

GRP.	B2=1	B2=2	B2=3	B2=4	B2=5
1	2.2432E-01	2.2192E-01	2.1842E-01	2.1356E-01	2.0917E-01
2	2.1565E-01	2.1655E-01	2.1416E-01	2.1015E-01	2.0543E-01
3	2.0797E-01	2.0791E-01	2.0605E-01	2.0347E-01	2.0023E-01
4	1.9753E-01	1.9529E-01	1.9736E-01	1.9662E-01	1.9444E-01
5	1.8953E-01	1.9029E-01	1.9102E-01	1.9034E-01	1.8911E-01
6	1.7992E-01	1.8238E-01	1.8364E-01	1.8452E-01	1.8472E-01
7	1.7235E-01	1.7598E-01	1.7750E-01	1.7856E-01	1.8001E-01
8	1.6567E-01	1.6903E-01	1.7161E-01	1.7366E-01	1.7540E-01
9	1.5934E-01	1.6274E-01	1.6508E-01	1.6735E-01	1.6945E-01
10	1.5567E-01	1.5864E-01	1.5940E-01	1.6192E-01	1.6414E-01
11	1.4914E-01	1.5079E-01	1.5297E-01	1.5514E-01	1.5740E-01
12	1.4482E-01	1.4553E-01	1.4693E-01	1.4873E-01	1.5077E-01
13	1.4066E-01	1.4062E-01	1.4143E-01	1.4284E-01	1.4457E-01
14	1.3452E-01	1.3496E-01	1.3591E-01	1.3655E-01	1.3803E-01
15	1.2383E-01	1.2613E-01	1.2731E-01	1.2866E-01	1.3023E-01
16	2.8059E-01	2.4759E-01	2.2926E-01	2.1803E-01	2.1096E-01
17	1.3714E-01	1.3275E-01	1.2693E-01	1.2323E-01	1.2099E-01
18	6.3704E-02	5.8658E-02	5.5481E-02	5.3602E-02	5.4459E-02
19	3.9533E-03	3.7033E-03	3.5796E-03	3.4027E-03	3.3911E-03
20	9.6529E-06	9.1977E-06	8.7435E-06	8.4537E-06	8.2243E-06

Table C.89. Continued.

LEAD-IRON, 6MEV, B1=3

GRP.	B2=1	B2=2	B2=3	B2=4	B2=5
1	2.15994E-01	2.13854E-01	2.10756E-01	2.07428E-01	2.04150E-01
2	2.11538E-01	2.09377E-01	2.06245E-01	2.02965E-01	1.99761E-01
3	2.03148E-01	2.02970E-01	2.01188E-01	1.98844E-01	1.95687E-01
4	1.95036E-01	1.93241E-01	1.90477E-01	1.87521E-01	1.84717E-01
5	1.89311E-01	1.87517E-01	1.84756E-01	1.81928E-01	1.79155E-01
6	1.81751E-01	1.80202E-01	1.77838E-01	1.75426E-01	1.73434E-01
7	1.76001E-01	1.74405E-01	1.72079E-01	1.69589E-01	1.67069E-01
8	1.70065E-01	1.68228E-01	1.65337E-01	1.62552E-01	1.59954E-01
9	1.65493E-01	1.63649E-01	1.60811E-01	1.57984E-01	1.55157E-01
10	1.60441E-01	1.58118E-01	1.55270E-01	1.52467E-01	1.49665E-01
11	1.55533E-01	1.53518E-01	1.50438E-01	1.47603E-01	1.44907E-01
12	1.49625E-01	1.47031E-01	1.43976E-01	1.41405E-01	1.38821E-01
13	1.42934E-01	1.41362E-01	1.38322E-01	1.35914E-01	1.33475E-01
14	1.34351E-01	1.32634E-01	1.29737E-01	1.26956E-01	1.24399E-01
15	1.23011E-01	1.21744E-01	1.19191E-01	1.16654E-01	1.14217E-01
16	2.51206E-01	2.33445E-01	2.21446E-01	2.13411E-01	2.07301E-01
17	1.25107E-01	1.23767E-01	1.21454E-01	1.19207E-01	1.17047E-01
18	5.80211E-02	5.73971E-02	5.62956E-02	5.52369E-02	5.41285E-02
19	3.62231E-03	3.61201E-03	3.58331E-03	3.54232E-03	3.37056E-03
20	3.89441E-06	3.82321E-06	3.55569E-06	3.33359E-06	7.99463E-06

LEAD-IRON, 6MEV, B1=4

GRP.	B2=1	B2=2	B2=3	B2=4	B2=5
1	2.03665E-01	2.02450E-01	2.02055E-01	1.98451E-01	1.94178E-01
2	2.02309E-01	2.01731E-01	1.99778E-01	1.96776E-01	1.93044E-01
3	1.96911E-01	1.96478E-01	1.95982E-01	1.93491E-01	1.90595E-01
4	1.91095E-01	1.91159E-01	1.90034E-01	1.89981E-01	1.89029E-01
5	1.86579E-01	1.87115E-01	1.87469E-01	1.87231E-01	1.86618E-01
6	1.82311E-01	1.82744E-01	1.83361E-01	1.83267E-01	1.83729E-01
7	1.79511E-01	1.78905E-01	1.79794E-01	1.80601E-01	1.81278E-01
8	1.76978E-01	1.76921E-01	1.76228E-01	1.77332E-01	1.78555E-01
9	1.75868E-01	1.75041E-01	1.74124E-01	1.72440E-01	1.73941E-01
10	1.66356E-01	1.66426E-01	1.66412E-01	1.66777E-01	1.66339E-01
11	1.61236E-01	1.59765E-01	1.60344E-01	1.61125E-01	1.62725E-01
12	1.54956E-01	1.54802E-01	1.53355E-01	1.54406E-01	1.55559E-01
13	1.48115E-01	1.48001E-01	1.46741E-01	1.47885E-01	1.48324E-01
14	1.39556E-01	1.40951E-01	1.39771E-01	1.40692E-01	1.42117E-01
15	1.28659E-01	1.29471E-01	1.31584E-01	1.33001E-01	1.34356E-01
16	2.32489E-01	2.23701E-01	2.15911E-01	2.10021E-01	2.05283E-01
17	1.19211E-01	1.24491E-01	1.23121E-01	1.21497E-01	1.20133E-01
18	5.47231E-02	5.44021E-02	5.54231E-02	5.46061E-02	5.30245E-02
19	3.41621E-03	3.51271E-03	3.45221E-03	3.40071E-03	3.36201E-03
20	5.34021E-06	6.53085E-06	6.44361E-06	6.42821E-06	5.21595E-06

Table C.89. Continued.

LEAD-IRON, 6MEV, B1=5

GRP.	B2=1	B2=2	B2=3	B2=4	B2=5
1	1.9554E-01	1.9443E-01	1.9266E-01	1.8979E-01	1.8647E-01
2	1.9343E-01	1.9277E-01	1.9133E-01	1.8950E-01	1.8619E-01
3	1.8[illegible]E-01	1.8960E-01	1.8[illegible]E-01	1.8751E-01	1.8565E-01
4	1.8[illegible]E-01	1.8[illegible]E-01	1.8[illegible]E-01	1.8[illegible]E-01	1.8449E-01
5	1.8[illegible]E-01	1.8[illegible]E-01	1.8[illegible]E-01	1.8[illegible]E-01	1.8438E-01
6	1.8[illegible]E-01	1.8[illegible]E-01	1.8[illegible]E-01	1.8270E-01	1.8289E-01
7	1.8[illegible]E-01	1.8[illegible]E-01	1.8[illegible]E-01	1.8114E-01	1.8171E-01
8	1.7866E-01	1.7797E-01	1.7846E-01	1.7924E-01	1.8011E-01
9	1.7577E-01	1.7624E-01	1.7443E-01	1.7522E-01	1.7618E-01
10	1.7196E-01	1.7012E-01	1.7[illegible]E-01	1.7111E-01	1.7225E-01
11	1.6702E-01	1.6439E-01	1.6413E-01	1.6480E-01	1.6589E-01
12	1.5972E-01	1.5733E-01	1.5717E-01	1.5787E-01	1.5893E-01
13	1.4[illegible]E-01	1.4967E-01	1.5[illegible]E-01	1.5095E-01	1.5197E-01
14	1.3766E-01	1.4126E-01	1.4262E-01	1.4356E-01	1.4469E-01
15	1.2510E-01	1.3202E-01	1.3433E-01	1.3570E-01	1.3683E-01
16	2.1987E-01	2.1693E-01	2.1296E-01	2.0793E-01	2.0447E-01
17	1.1481E-01	1.2256E-01	1.2743E-01	1.2141E-01	1.2049E-01
18	5.2606E-02	5.3416E-02	5.3670E-02	5.4479E-02	5.3380E-02
19	3.2832E-03	3.4508E-03	3.4735E-03	3.3529E-03	3.3618E-03
20	8.0157E-06	8.4295E-06	9.2738E-06	1.1344E-05	1.1468E-05

Table C.90. Scattered Energy Flux Spectra, $I^S(b_1+b_2,E_i)/I^S(b_1+b_2)$, for 6MeV Photons in Slabs of Water Followed by Tin.

WATER-TIN, 6MEV, B1=2

GRP.	B2=1	B2=2	B2=3	B2=4	B2=5
1	2.3316E-01	2.1369E-01	1.9832E-01	1.9832E-01	1.6961E-01
2	2.2705E-01	2.0769E-01	1.9589E-01	1.9589E-01	1.6993E-01
3	2.1553E-01	2.0294E-01	1.9128E-01	1.9128E-01	1.7056E-01
4	2.0450E-01	1.9470E-01	1.8679E-01	1.8679E-01	1.7117E-01
5	1.9500E-01	1.8918E-01	1.8439E-01	1.8439E-01	1.7434E-01
6	1.8591E-01	1.8360E-01	1.8164E-01	1.8164E-01	1.7679E-01
7	1.7780E-01	1.7932E-01	1.7983E-01	1.7983E-01	1.8019E-01
8	1.7075E-01	1.7510E-01	1.7849E-01	1.7845E-01	1.8381E-01
9	1.6373E-01	1.7054E-01	1.7601E-01	1.7601E-01	1.8528E-01
10	1.5720E-01	1.6573E-01	1.7399E-01	1.7399E-01	1.8665E-01
11	1.5218E-01	1.6233E-01	1.7055E-01	1.7055E-01	1.8516E-01
12	1.4703E-01	1.5717E-01	1.6541E-01	1.6541E-01	1.8040E-01
13	1.4171E-01	1.5033E-01	1.5762E-01	1.5762E-01	1.7156E-01
14	1.3198E-01	1.3782E-01	1.4345E-01	1.4345E-01	1.5525E-01
15	1.1403E-01	1.1900E-01	1.2262E-01	1.2262E-01	1.3262E-01
16	2.8134E-01	2.6476E-01	2.4832E-01	2.4832E-01	2.2924E-01
17	5.9464E-02	5.7331E-02	5.5787E-02	5.5787E-02	5.3651E-02
18	5.4473E-03	5.1829E-03	4.9493E-03	4.9493E-03	4.7093E-03
19	3.0208E-05	2.7146E-05	2.7630E-05	2.7630E-05	2.5829E-05
20	1.6621E-05	3.3389E-05	2.7135E-05	2.6135E-05	3.5329E-05

WATER-TIN, 6MEV, B1=4

GRP.	B2=1	B2=2	B2=3	B2=4	B2=5
1	2.4123E-01	2.1578E-01	1.9552E-01	1.9552E-01	1.6191E-01
2	2.3468E-01	2.1140E-01	1.9357E-01	1.9357E-01	1.6301E-01
3	2.2240E-01	2.0436E-01	1.8985E-01	1.8985E-01	1.6511E-01
4	2.1053E-01	1.9709E-01	1.8619E-01	1.8619E-01	1.6715E-01
5	2.0031E-01	1.9177E-01	1.8471E-01	1.8471E-01	1.7188E-01
6	1.9037E-01	1.8617E-01	1.8267E-01	1.8267E-01	1.7576E-01
7	1.8159E-01	1.8160E-01	1.8157E-01	1.8157E-01	1.8063E-01
8	1.7386E-01	1.7762E-01	1.8004E-01	1.8004E-01	1.8571E-01
9	1.6666E-01	1.7276E-01	1.7864E-01	1.7864E-01	1.8285E-01
10	1.6056E-01	1.6900E-01	1.7632E-01	1.7632E-01	1.8069E-01
11	1.5477E-01	1.6553E-01	1.7324E-01	1.7324E-01	1.8972E-01
12	1.4927E-01	1.5758E-01	1.6770E-01	1.6770E-01	1.8504E-01
13	1.3884E-01	1.4791E-01	1.5922E-01	1.5922E-01	1.7561E-01
14	1.2804E-01	1.3705E-01	1.4439E-01	1.4439E-01	1.5865E-01
15	1.1041E-01	1.1797E-01	1.2341E-01	1.2341E-01	1.3549E-01
16	2.3192E-01	2.2967E-01	2.2258E-01	2.2258E-01	2.1591E-01
17	5.1171E-02	5.1283E-02	5.1681E-02	5.1681E-02	5.1647E-02
18	4.6299E-03	4.6107E-03	4.5954E-03	4.5954E-03	4.5110E-03
19	2.9343E-05	3.2760E-05	2.8330E-05	2.8330E-05	3.3756E-05
20	2.0576E-05	3.7503E-05	3.4610E-05	3.6010E-05	4.2019E-05

Table C.91. Scattered Energy Flux Spectra, $I^S(b_1+b_2,E_i)/I^S(b_1+b_2)$, for 6MeV Photons in Slabs of Aluminum Followed by Tin.

ALUM.-TIN,6MEV,B1=2

GRP.	B2=1	B2=2	B2=3	B2=4	B2=5
1	2.2657E-01	2.0937E-01	1.9521E-01	1.9521E-01	1.8812E-01
2	2.2109E-01	2.0575E-01	1.9306E-01	1.9306E-01	1.8657E-01
3	2.1067E-01	1.9896E-01	1.8899E-01	1.8899E-01	1.8342E-01
4	2.0069E-01	1.9222E-01	1.8501E-01	1.8501E-01	1.7927E-01
5	1.9230E-01	1.8745E-01	1.8316E-01	1.8316E-01	1.7870E-01
6	1.8421E-01	1.8295E-01	1.8091E-01	1.8091E-01	1.7839E-01
7	1.7715E-01	1.7963E-01	1.7955E-01	1.7955E-01	1.8004E-01
8	1.7091E-01	1.7531E-01	1.7869E-01	1.7869E-01	1.8391E-01
9	1.6466E-01	1.7122E-01	1.7657E-01	1.7657E-01	1.8556E-01
10	1.5950E-01	1.6796E-01	1.7490E-01	1.7490E-01	1.8709E-01
11	1.5444E-01	1.6391E-01	1.7159E-01	1.7159E-01	1.8571E-01
12	1.4963E-01	1.5983E-01	1.6665E-01	1.6665E-01	1.8099E-01
13	1.4438E-01	1.5218E-01	1.5890E-01	1.5890E-01	1.7219E-01
14	1.3443E-01	1.3949E-01	1.4467E-01	1.4467E-01	1.5586E-01
15	1.1616E-01	1.1945E-01	1.2367E-01	1.2367E-01	1.3315E-01
16	2.0097E-01	2.0976E-01	2.0169E-01	2.0169E-01	2.3109E-01
17	6.1647E-02	5.8904E-02	5.6479E-02	5.6479E-02	5.4020E-02
18	5.6212E-03	5.2715E-03	5.0095E-03	5.0095E-03	4.7417E-03
19	3.1203E-05	2.7531E-05	2.7951E-05	2.7951E-05	3.5054E-05
20	2.6881E-08	2.5915E-08	4.0995E-08	4.0995E-08	4.3203E-08

ALUM.-TIN,6MEV,B1=4

GRP.	B2=1	B2=2	B2=3	B2=4	B2=5
1	2.2642E-01	2.0822E-01	1.8832E-01	1.8832E-01	1.8776E-01
2	2.2329E-01	2.0329E-01	1.8710E-01	1.8710E-01	1.8524E-01
3	2.1355E-01	1.9773E-01	1.8479E-01	1.8479E-01	1.8204E-01
4	2.0407E-01	1.9224E-01	1.8242E-01	1.8242E-01	1.8047E-01
5	1.9623E-01	1.8870E-01	1.8223E-01	1.8223E-01	1.8027E-01
6	1.8844E-01	1.8470E-01	1.8146E-01	1.8146E-01	1.8027E-01
7	1.8154E-01	1.8159E-01	1.8149E-01	1.8149E-01	1.8046E-01
8	1.7524E-01	1.7937E-01	1.8176E-01	1.8176E-01	1.8617E-01
9	1.6945E-01	1.7463E-01	1.8034E-01	1.8034E-01	1.8624E-01
10	1.6262E-01	1.7166E-01	1.7921E-01	1.7921E-01	1.8721E-01
11	1.5637E-01	1.6710E-01	1.7603E-01	1.7603E-01	1.8514E-01
12	1.5011E-01	1.6132E-01	1.7064E-01	1.7064E-01	1.8064E-01
13	1.4329E-01	1.5365E-01	1.6211E-01	1.6211E-01	1.7178E-01
14	1.3232E-01	1.3708E-01	1.4703E-01	1.4703E-01	1.5603E-01
15	1.1974E-01	1.1993E-01	1.2569E-01	1.2569E-01	1.3099E-01
16	2.3840E-01	2.4323E-01	2.2613E-01	2.2613E-01	2.1743E-01
17	5.3943E-02	5.2539E-02	5.2362E-02	5.2362E-02	5.2073E-02
18	4.7644E-03	4.6269E-03	4.4116E-03	4.4116E-03	4.2465E-03
19	2.6423E-05	2.4322E-05	2.5630E-05	2.5630E-05	3.3215E-05
20	1.6052E-08	1.5235E-08	4.0617E-08	4.0617E-08	3.6038E-08

Table C.92. Scattered Energy Flux Spectra, $I^S(b_1+b_2,E_i)/I^S(b_1+b_2)$, for 6MeV Photons in Slabs of Water Followed by Lead.

Water-Lead, 6MeV, B1=1

Grp.	B2=1	B2=2	B2-3	B2-4	B2=5
1	2.3637E-01	2.2435E-01	2.1064E-01	1.9796E-01	1.8471E-01
2	2.3039E-01	2.2002E-01	2.0797E-01	1.9667E-01	1.8474E-01
3	2.1903E-01	2.1180E-01	2.0289E-01	1.9423E-01	1.8481E-01
4	2.0828E-01	2.0403E-01	1.9814E-01	1.9205E-01	1.8514E-01
5	1.9898E-01	1.9791E-01	1.9525E-01	1.9194E-01	1.8780E-01
6	1.9027E-01	1.9216E-01	1.9244E-01	1.9178E-01	1.9032E-01
7	1.8255E-01	1.8721E-01	1.9027E-01	1.9216E-01	1.9336E-01
8	1.7580E-01	1.8296E-01	1.8857E-01	1.9283E-01	1.9657E-01
9	1.6959E-01	1.7865E-01	1.8617E-01	1.9237E-01	1.9821E-01
10	1.6377E-01	1.7368E-01	1.8215E-01	1.8946E-01	1.9656E-01
11	1.5907E-01	1.6929E-01	1.7816E-01	1.8604E-01	1.9393E-01
12	1.5343E-01	1.6157E-01	1.6901E-01	1.7594E-01	1.8316E-01
13	1.4328E-01	1.4614E-01	1.5018E-01	1.5456E-01	1.5968E-01
14	1.1787E-01	1.1404E-01	1.1426E-01	1.1572E-01	1.1815E-01
15	7.9206E-02	7.4324E-02	7.3496E-02	7.3781E-02	7.4818E-02
16	2.7706E-01	2.3018E-01	2.0065E-01	1.8091E-01	1.6724E-01
17	1.8669E-02	1.6130E-02	1.4575E-02	1.3567E-02	1.2903E-02
18	5.1451E-04	4.3325E-04	3.8450E-04	3.5310E-04	3.3171E-04
19	4.3659E-06	3.6781E-06	3.4807E-06	2.9714E-06	3.7705E-06
20	2.4594E-09	3.5263E-09	6.1487E-09	5.3448E-09	5.5571E-09

Water-Lead, 6MeV, B1=2

Grp.	B2=1	B2=2	B2=3	B2=4	B2=5
1	2.4463E-01	2.2590E-01	2.0922E-01	1.9254E-01	1.7768E-01
2	2.3839E-01	2.2185E-01	2.0692E-01	1.9199E-01	1.7849E-01
3	2.2654E-01	2.1416E-01	2.0254E-01	1.9092E-01	1.8004E-01
4	2.1526E-01	2.0684E-01	1.9845E-01	1.9006E-01	1.8182E-01
5	2.0544E-01	2.0121E-01	1.9629E-01	1.9136E-01	1.8606E-01
6	1.9616E-01	1.9572E-01	1.9410E-01	1.9246E-01	1.9008E-01
7	1.8779E-01	1.9098E-01	1.9247E-01	1.9402E-01	1.9457E-01
8	1.8027E-01	1.8668E-01	1.9121E-01	1.9573E-01	1.9914E-01
9	1.7293E-01	1.8194E-01	1.8895E-01	1.9596E-01	2.0185E-01
10	1.6568E-01	1.7619E-01	1.8475E-01	1.9330E-01	2.0086E-01
11	1.5913E-01	1.7068E-01	1.8027E-01	1.8986E-01	1.9858E-01
12	1.5117E-01	1.6143E-01	1.7026E-01	1.7908E-01	1.8738E-01
13	1.3858E-01	1.4430E-01	1.5032E-01	1.5633E-01	1.6253E-01
14	1.1205E-01	1.1098E-01	1.1336E-01	1.1573E-01	1.1905E-01
15	7.4802E-02	7.1525E-02	7.2371E-02	7.3216E-02	7.4917E-02
16	2.1092E-01	1.8843E-01	1.7449E-01	1.6054E-01	1.5194E-01
17	1.4991E-02	1.3795E-02	1.3129E-02	1.2463E-02	1.2097E-02
18	4.0154E-04	3.6590E-04	3.4280E-04	3.1960E-04	3.0685E-04
19	3.4201E-06	4.1073E-06	3.8560E-06	3.6047E-06	2.7190E-06
20	2.3195E-09	5.7806E-09	4.9270E-09	4.0733E-09	4.1648E-09

Table C.92. Continued.

WATER-LEAD,6MEV,B1=3

GRP.	B2=1	B2=2	B2=3	B2=4	B2=5
1	2.5011E-01	2.2762E-01	2.0902E-01	1.9943E-01	1.7307E-01
2	2.4355E-01	2.2360E-01	2.0605E-01	1.9527E-01	1.7438E-01
3	2.3110E-01	2.1597E-01	2.0231E-01	1.8997E-01	1.7685E-01
4	2.1420E-01	2.0076E-01	1.9074E-01	1.8283E-01	1.7955E-01
5	2.0984E-01	2.0336E-01	1.9711E-01	1.9091E-01	1.8477E-01
6	1.9895E-01	1.9720E-01	1.9537E-01	1.9270E-01	1.8973E-01
7	1.8093E-01	1.8262E-01	1.8410E-01	1.8434E-01	1.8517E-01
8	1.8185E-01	1.8323E-01	1.8307E-01	1.8272E-01	2.0065E-01
9	1.7375E-01	1.7331E-01	1.7269E-01	1.7192E-01	2.0405E-01
10	1.6571E-01	1.7701E-01	1.8655E-01	1.9550E-01	2.0360E-01
11	1.5923E-01	1.7166E-01	1.8115E-01	1.9213E-01	2.0163E-01
12	1.4933E-01	1.6156E-01	1.7127E-01	1.8107E-01	1.9025E-01
13	1.3593E-01	1.4325E-01	1.5072E-01	1.5754E-01	1.6455E-01
14	1.0924E-01	1.0940E-01	1.1210E-01	1.1584E-01	1.1980E-01
15	7.2734E-02	7.0107E-02	7.1045E-02	7.2981E-02	7.5115E-02
16	1.8205E-01	1.6793E-01	1.5724E-01	1.4918E-01	1.4313E-01
17	1.3366E-02	1.2641E-02	1.2153E-02	1.1847E-02	1.1635E-02
18	3.5206E-04	3.3140E-04	3.1284E-04	3.0070E-04	2.9240E-04
19	3.0009E-06	3.7161E-06	2.6412E-06	2.8284E-06	2.9922E-06
20	2.0873E-09	5.2350E-09	4.5732E-09	4.4208E-09	4.8772E-09

WATER-LEAD,6MEV,B1=4

GRP.	B2=1	B2=2	B2=3	B2=4	B2=5
1	2.5336E-01	2.2957E-01	2.0899E-01	1.9714E-01	1.8991E-01
2	2.4661E-01	2.2456E-01	2.0952E-01	1.8725E-01	1.7145E-01
3	2.3374E-01	2.1695E-01	2.0116E-01	1.8747E-01	1.7455E-01
4	2.2144E-01	2.0992E-01	1.9557E-01	1.8783E-01	1.7727E-01
5	2.1073E-01	2.0405E-01	1.9733E-01	1.9045E-01	1.8377E-01
6	2.0044E-01	1.9846E-01	1.9538E-01	1.9272E-01	1.8937E-01
7	1.9113E-01	1.9355E-01	1.9404E-01	1.9146E-01	1.9554E-01
8	1.8254E-01	1.8991E-01	1.9405E-01	1.9529E-01	2.0164E-01
9	1.7411E-01	1.8361E-01	1.9136E-01	1.9525E-01	2.0562E-01
10	1.6554E-01	1.7754E-01	1.8769E-01	1.9704E-01	2.0554E-01
11	1.5709E-01	1.7121E-01	1.8240E-01	1.9338E-01	2.0394E-01
12	1.4832E-01	1.6039E-01	1.7209E-01	1.8259E-01	1.9236E-01
13	1.3452E-01	1.4277E-01	1.5295E-01	1.6354E-01	1.6607E-01
14	1.0774E-01	1.0957E-01	1.1197E-01	1.1600E-01	1.2041E-01
15	7.1614E-02	6.9329E-02	7.0662E-02	7.2914E-02	7.5317E-02
16	1.6595E-01	1.5593E-01	1.4744E-01	1.4196E-01	1.3734E-01
17	1.2459E-02	1.1960E-02	1.1665E-02	1.1458E-02	1.1336E-02
18	3.2443E-04	3.1107E-04	2.9832E-04	2.8596E-04	2.8521E-04
19	2.7642E-06	3.4284E-06	2.4513E-06	3.2163E-06	3.2976E-06
20	1.9311E-09	4.9061E-09	4.2094E-09	4.2403E-09	2.2155E-09

Table C.92. Continued.

WATER-LEAD,.6MEV,B1=5

GRP.	B2=1	B2=2	B2=3	B2=4	B2=5
1	2.5473E-01	2.2902E-01	2.0603E-01	1.8528E-01	1.6733E-01
2	2.4789E-01	2.2502E-01	2.0439E-01	1.8560E-01	1.6925E-01
3	2.3491E-01	2.1744E-01	2.0127E-01	1.8621E-01	1.7280E-01
4	2.2250E-01	2.1014E-01	1.9829E-01	1.8696E-01	1.7657E-01
5	2.1170E-01	2.0461E-01	1.9732E-01	1.8959E-01	1.8296E-01
6	2.0126E-01	1.9902E-01	1.9660E-01	1.9324E-01	1.9050E-01
7	1.9186E-01	1.9412E-01	1.9531E-01	1.9573E-01	1.9568E-01
8	1.8327E-01	1.8958E-01	1.9474E-01	1.9837E-01	2.0234E-01
9	1.7454E-01	1.8442E-01	1.9279E-01	2.0027E-01	2.0675E-01
10	1.6584E-01	1.7737E-01	1.8857E-01	1.9827E-01	2.0693E-01
11	1.5762E-01	1.7150E-01	1.8379E-01	1.9513E-01	2.0592E-01
12	1.4795E-01	1.6107E-01	1.7291E-01	1.8381E-01	1.9342E-01
13	1.3394E-01	1.4259E-01	1.5309E-01	1.6293E-01	1.6725E-01
14	1.0701E-01	1.0911E-01	1.1161E-01	1.1434E-01	1.2091E-01
15	7.1033E-02	6.8869E-02	7.0464E-02	7.2929E-02	7.5500E-02
16	1.5597E-01	1.4786E-01	1.4163E-01	1.3696E-01	1.3329E-01
17	1.1990E-02	1.1513E-02	1.1304E-02	1.1192E-02	1.1127E-02
18	2.8669E-04	2.9772E-04	2.9473E-04	2.8554E-04	2.7013E-04
19	3.5994E-06	3.3330E-06	3.2247E-06	2.6549E-06	3.2606E-06
20	2.5205E-09	4.9553E-09	3.0677E-09	3.4874E-09	4.1365E-09

Table C.93. Scattered Energy Flux Spectra, $I^S(b_1+b_2,E_i)/I^S(b_1+b_2)$, for 6MeV Photons in Slabs of Iron Followed by Lead.

IRON-LEAD,6MEV,B1=1

GRP.	B2=1	B2=2	B2=3	B2=4	B2=5
1	2.2853E-01	2.1989E-01	2.0965E-01	1.9715E-01	1.8506E-01
2	2.2306E-01	2.1548E-01	2.0666E-01	1.9596E-01	1.8499E-01
3	2.1268E-01	2.0816E-01	2.0113E-01	1.9343E-01	1.8487E-01
4	2.0227E-01	2.0072E-01	1.9653E-01	1.9124E-01	1.8504E-01
5	1.9449E-01	1.9533E-01	1.9279E-01	1.9112E-01	1.8751E-01
6	1.8676E-01	1.9012E-01	1.9118E-01	1.9100E-01	1.8985E-01
7	1.8005E-01	1.8576E-01	1.9027E-01	1.9140E-01	1.9284E-01
8	1.7434E-01	1.8215E-01	1.8976E-01	1.9225E-01	1.9559E-01
9	1.6921E-01	1.7859E-01	1.8956E-01	1.9397E-01	1.9744E-01
10	1.6466E-01	1.7632E-01	1.8933E-01	1.9534E-01	1.9611E-01
11	1.6120E-01	1.7072E-01	1.8978E-01	1.9618E-01	1.9359E-01
12	1.5573E-01	1.6369E-01	1.8006E-01	1.7634E-01	1.8300E-01
13	1.4750E-01	1.4866E-01	1.5150E-01	1.5521E-01	1.5977E-01
14	1.2190E-01	1.1642E-01	1.1562E-01	1.1652E-01	1.1810E-01
15	8.1738E-02	7.6058E-02	7.4535E-02	7.4424E-02	7.5149E-02
16	3.0615E-01	2.4511E-01	2.1006E-01	1.8747E-01	1.7200E-01
17	2.0395E-02	1.7008E-02	1.5126E-02	1.3946E-02	1.3172E-02
18	5.6141E-04	4.5369E-04	4.0003E-04	3.6422E-04	3.3904E-04
19	4.7832E-06	3.7029E-06	3.2183E-06	3.0179E-06	2.8316E-06
20	2.6125E-09	3.3454E-09	5.7034E-09	4.4447E-09	4.5668E-09

IRON-LEAD,6MEV,B1=2

GRP.	B2=1	B2=2	B2=3	B2=4	B2=5
1	2.2683E-01	2.1418E-01	2.0017E-01	1.8709E-01	1.7395E-01
2	2.2221E-01	2.1113E-01	1.9872E-01	1.8699E-01	1.7505E-01
3	2.1344E-01	2.0547E-01	1.9596E-01	1.8606E-01	1.7706E-01
4	2.0506E-01	2.0003E-01	1.9341E-01	1.8663E-01	1.7938E-01
5	1.9816E-01	1.9621E-01	1.9282E-01	1.8673E-01	1.8411E-01
6	1.9159E-01	1.9265E-01	1.9210E-01	1.9079E-01	1.8874E-01
7	1.8594E-01	1.8973E-01	1.9133E-01	1.9224E-01	1.9359E-01
8	1.8106E-01	1.8732E-01	1.9217E-01	1.9395E-01	1.9923E-01
9	1.7613E-01	1.8430E-01	1.9121E-01	1.9711E-01	2.0262E-01
10	1.7134E-01	1.8027E-01	1.9022E-01	1.9534E-01	2.0230E-01
11	1.6654E-01	1.7533E-01	1.8458E-01	1.9253E-01	2.0044E-01
12	1.5983E-01	1.6736E-01	1.7450E-01	1.8200E-01	1.8943E-01
13	1.4702E-01	1.4938E-01	1.5422E-01	1.6004E-01	1.6447E-01
14	1.1656E-01	1.1524E-01	1.1593E-01	1.1788E-01	1.2062E-01
15	7.9015E-02	7.4280E-02	7.2803E-02	7.4613E-02	7.5944E-02
16	2.2332E-01	1.9341E-01	1.7011E-01	1.6044E-01	1.5665E-01
17	1.6276E-02	1.4552E-02	1.3523E-02	1.2851E-02	1.2337E-02
18	4.3236E-04	3.8274E-04	3.5163E-04	3.2013E-04	3.1512E-04
19	3.6736E-06	3.2541E-06	3.1143E-06	2.7650E-06	2.6345E-06
20	2.5139E-09	2.8271E-09	4.7783E-09	4.0352E-09	4.3144E-09

Table C.93. Continued.

IRON-LEAF, GMIV, B1=3

GRP.	B2=1	B2=2	B2=3	B2=4	B2=5
1	2.2275E-01	2.0770E-01	1.9213E-01	1.7912E-01	1.6443E-01
2	2.1495E-01	2.0544E-01	1.9168E-01	1.7954E-01	1.6647E-01
3	2.1174E-01	2.0171E-01	1.8975E-01	1.8051E-01	1.7023E-01
4	2.0472E-01	1.9789E-01	1.8994E-01	1.8221E-01	1.7426E-01
5	1.9921E-01	1.9534E-01	1.9119E-01	1.8628E-01	1.8034E-01
6	1.9366E-01	1.9356E-01	1.9006E-01	1.8599E-01	1.8139E-01
7	1.8699E-01	1.9139E-01	1.9351E-01	1.8942E-01	1.8445E-01
8	1.8484E-01	1.9362E-01	1.9111E-01	1.8958E-01	2.0159E-01
9	1.8014E-01	1.8823E-01	1.9515E-01	2.0102E-01	2.0651E-01
10	1.7538E-01	1.8452E-01	1.9226E-01	2.0020E-01	2.0735E-01
11	1.6995E-01	1.8002E-01	1.8931E-01	1.9783E-01	2.0623E-01
12	1.6202E-01	1.7066E-01	1.7905E-01	1.8701E-01	1.9504E-01
13	1.4739E-01	1.5194E-01	1.5774E-01	1.6222E-01	1.6880E-01
14	1.1638E-01	1.1501E-01	1.1717E-01	1.1966E-01	1.2284E-01
15	7.8579E-02	7.4050E-02	7.4136E-02	7.5286E-02	7.6953E-02
16	1.9507E-01	1.7569E-01	1.6314E-01	1.5225E-01	1.4690E-01
17	1.4409E-02	1.3264E-02	1.2637E-02	1.2219E-02	1.1932E-02
18	3.7474E-04	3.4370E-04	3.2473E-04	3.1013E-04	3.0042E-04
19	3.1991E-06	2.9361E-06	3.6643E-06	2.6001E-06	3.4419E-06
20	2.0556E-09	2.7223E-09	4.2885E-09	4.0471E-09	4.3676E-09

IRON-LEAC, GMLV, B1=4

GRP.	B2=1	B2=2	B2=3	B2=4	B2=5
1	2.1722E-01	2.0371E-01	1.9519E-01	1.7017E-01	1.5623E-01
2	2.1427E-01	1.9954E-01	1.9581E-01	1.7182E-01	1.5907E-01
3	2.0986E-01	1.9732E-01	1.9017E-01	1.7430E-01	1.6425E-01
4	2.0307E-01	1.9507E-01	1.9021E-01	1.7912E-01	1.6973E-01
5	1.9897E-01	1.9461E-01	1.9044E-01	1.8277E-01	1.7728E-01
6	1.9453E-01	1.9366E-01	1.9165E-01	1.8830E-01	1.8505E-01
7	1.9066E-01	1.9352E-01	1.9441E-01	1.9479E-01	1.9464E-01
8	1.8754E-01	1.9314E-01	1.9721E-01	2.0001E-01	2.0340E-01
9	1.8322E-01	1.9146E-01	1.9913E-01	2.0420E-01	2.0977E-01
10	1.7855E-01	1.8821E-01	1.9634E-01	2.0429E-01	2.1155E-01
11	1.7294E-01	1.8376E-01	1.9224E-01	2.0245E-01	2.1120E-01
12	1.6445E-01	1.7402E-01	1.8172E-01	1.9191E-01	1.9956E-01
13	1.4052E-01	1.5451E-01	1.6014E-01	1.6639E-01	1.7265E-01
14	1.1938E-01	1.1711E-01	1.1847E-01	1.2149E-01	1.2452E-01
15	7.9021E-02	7.4471E-02	7.4434E-02	7.5167E-02	7.7583E-02
16	1.7538E-01	1.6139E-01	1.5219E-01	1.4294E-01	1.4027E-01
17	1.3372E-02	1.2521E-02	1.2078E-02	1.1823E-02	1.1627E-02
18	3.4224E-04	3.1944E-04	3.0355E-04	2.9457E-04	2.8466E-04
19	2.9234E-06	2.7349E-06	3.3511E-06	2.5795E-06	2.8220E-06
20	2.3457E-09	2.6441E-09	3.4778E-09	4.1922E-09	4.2078E-09

Table C.93. Continued.

IRON-LEAD,SALV,B1=5

GRP.	B2=1	B2=2	B2=3	B2=4	B2=5
1	2.1109E-01	1.9335E-01	1.7793E-01	1.6269E-01	1.4907E-01
2	2.0599E-01	1.8861E-01	1.7904E-01	1.6505E-01	1.5245E-01
3	2.0436E-01	1.9293E-01	1.8114E-01	1.6654E-01	1.5488E-01
4	2.0078E-01	1.8212E-01	1.8316E-01	1.7415E-01	1.6599E-01
5	1.9606E-01	1.8310E-01	1.8734E-01	1.8127E-01	1.7521E-01
6	1.9477E-01	1.8360E-01	1.9033E-01	1.8794E-01	1.8453E-01
7	1.9215E-01	1.9027E-01	1.9520E-01	1.9516E-01	1.9446E-01
8	1.8963E-01	1.9514E-01	1.9938E-01	2.0231E-01	2.0487E-01
9	1.8596E-01	1.9418E-01	2.0093E-01	2.0702E-01	2.1237E-01
10	1.8156E-01	1.9148E-01	2.0001E-01	2.0800E-01	2.1532E-01
11	1.7589E-01	1.8720E-01	1.9719E-01	2.0471E-01	2.1562E-01
12	1.6706E-01	1.7727E-01	1.8841E-01	1.9572E-01	2.0440E-01
13	1.5163E-01	1.5714E-01	1.6721E-01	1.7379E-01	1.7624E-01
14	1.2071E-01	1.1952E-01	1.2027E-01	1.2334E-01	1.2691E-01
15	7.0834E-02	7.5132E-02	7.9414E-02	7.7037E-02	7.9001E-02
16	1.6297E-01	1.5175E-01	1.4474E-01	1.2959E-01	1.3550E-01
17	1.2736E-02	1.2043E-02	1.1721E-02	1.1538E-02	1.1420E-02
18	3.2155E-04	3.0734E-04	2.9472E-04	2.8438E-04	2.7594E-04
19	2.7336E-06	3.4360E-06	2.5735E-06	2.8260E-06	3.2978E-06
20	2.5112E-07	4.0502E-09	2.8640E-08	4.2244E-08	4.4794E-08

APPENDIX D

D.1. Graphical Display of Results

The figures in this appendix are arranged as follows:

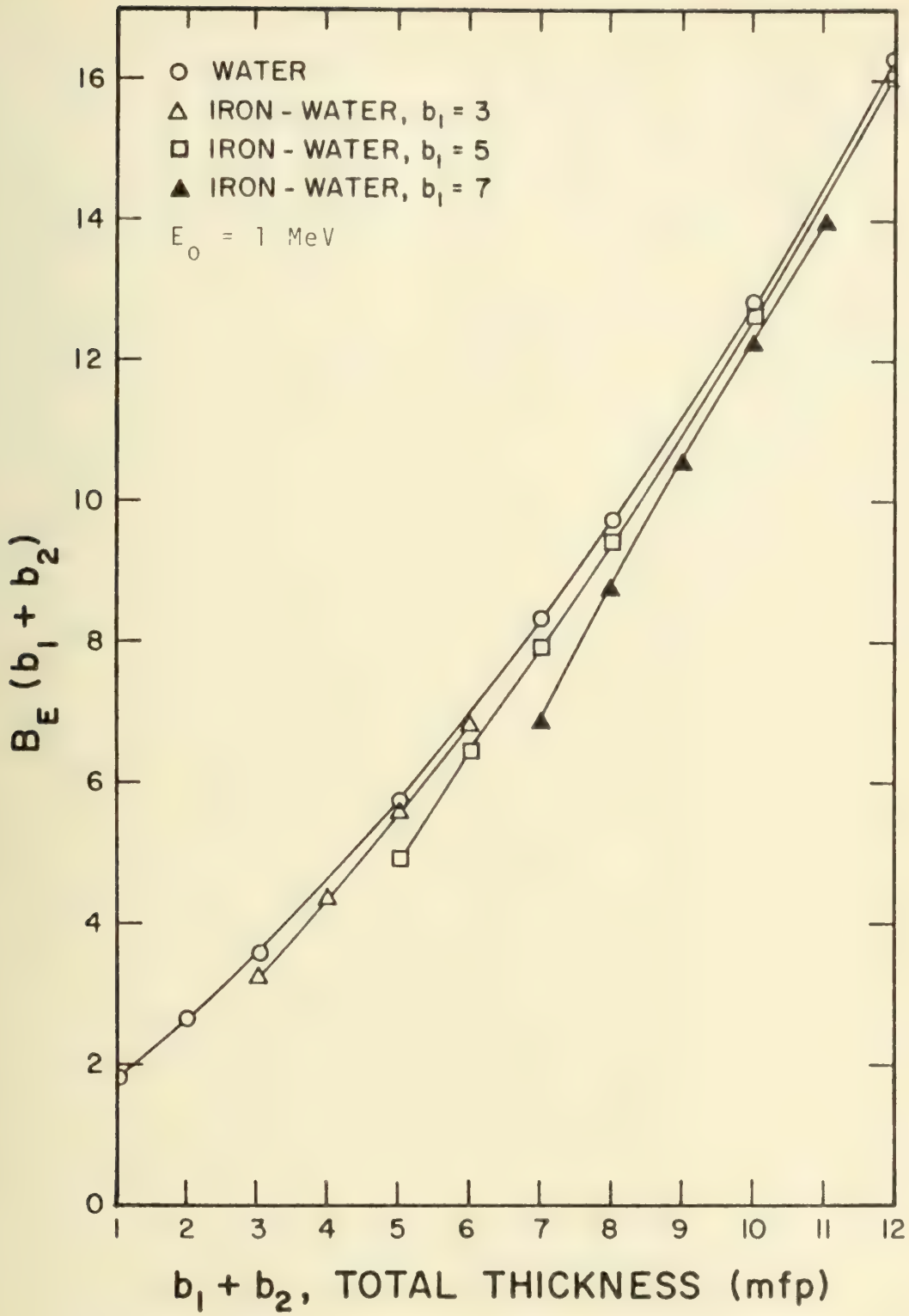

Figure D.1. The Energy Buildup Factor, $B_E(b_1+b_2)$ vs. b_1 and b_2 for 1MeV Photons in Slabs of Iron Followed by Water.

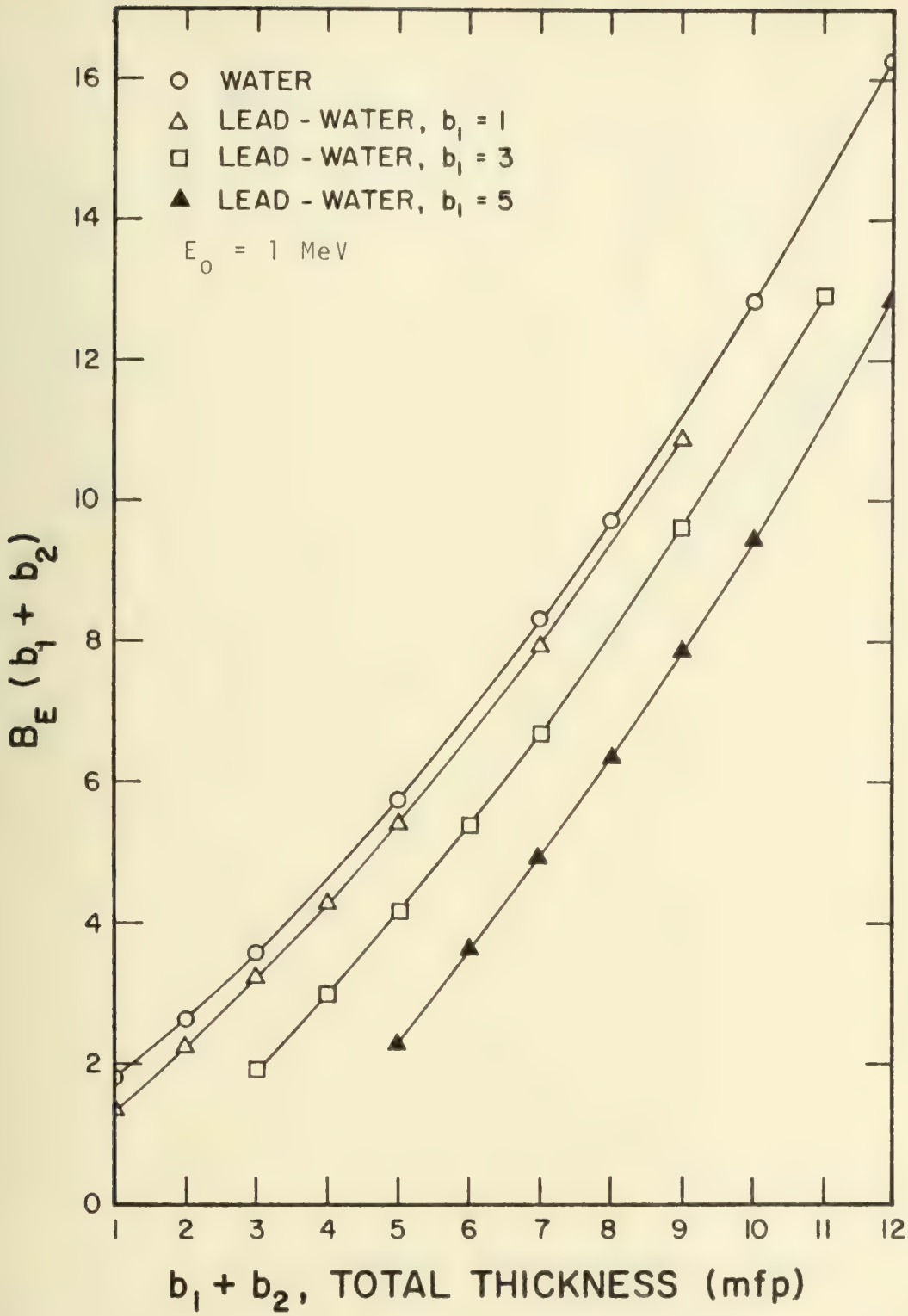

Figure D.2. The Energy Buildup Factor, $B_E(b_1+b_2)$ vs. b_1 and b_2 for 1MeV Photons in Slabs of Lead Followed by Water.

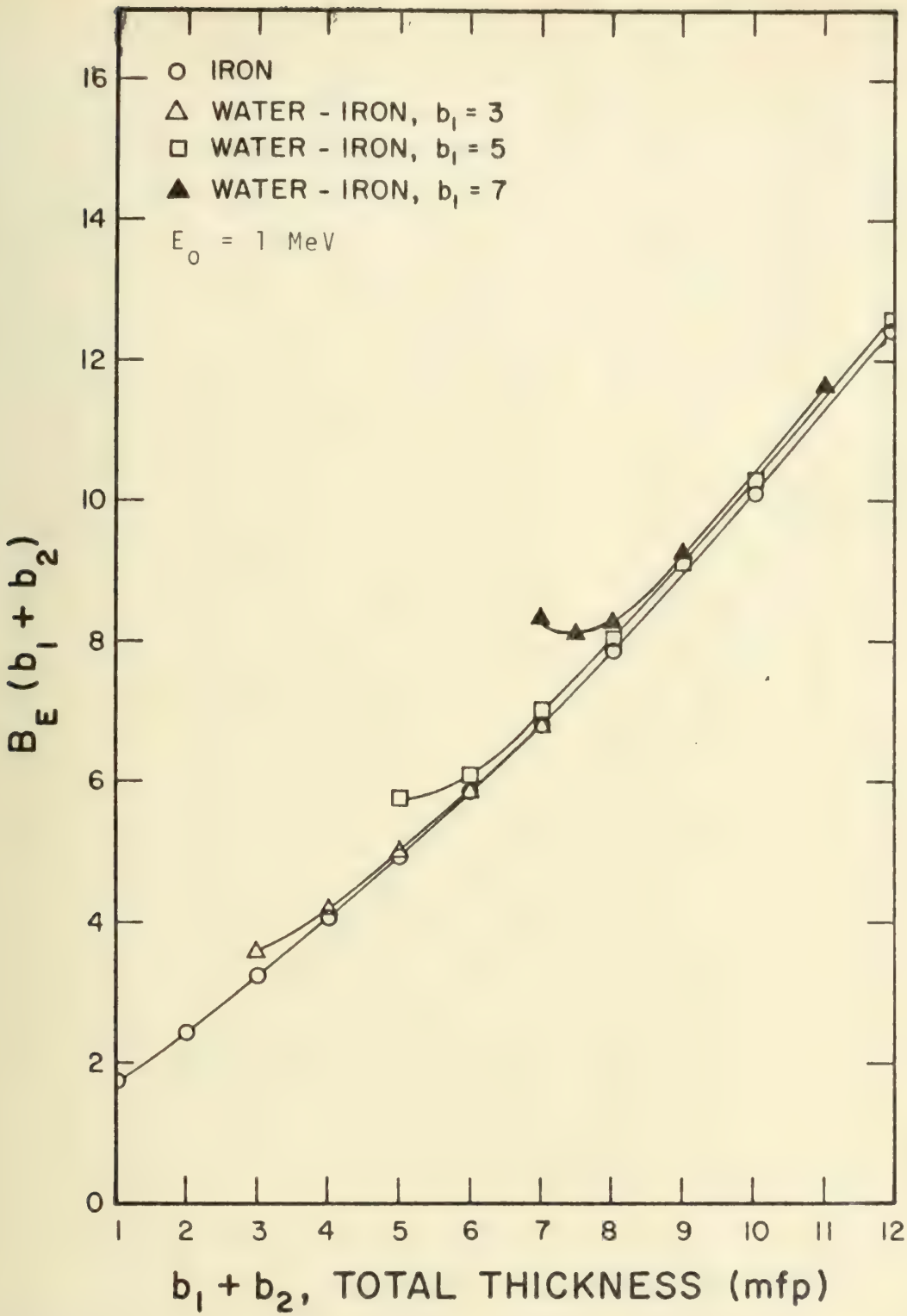

Figure D.3. The Energy Buildup Factor, $B_E(b_1+b_2)$ vs. b_1 and b_2 for 1MeV Photons in Slabs of Water Followed by Iron.

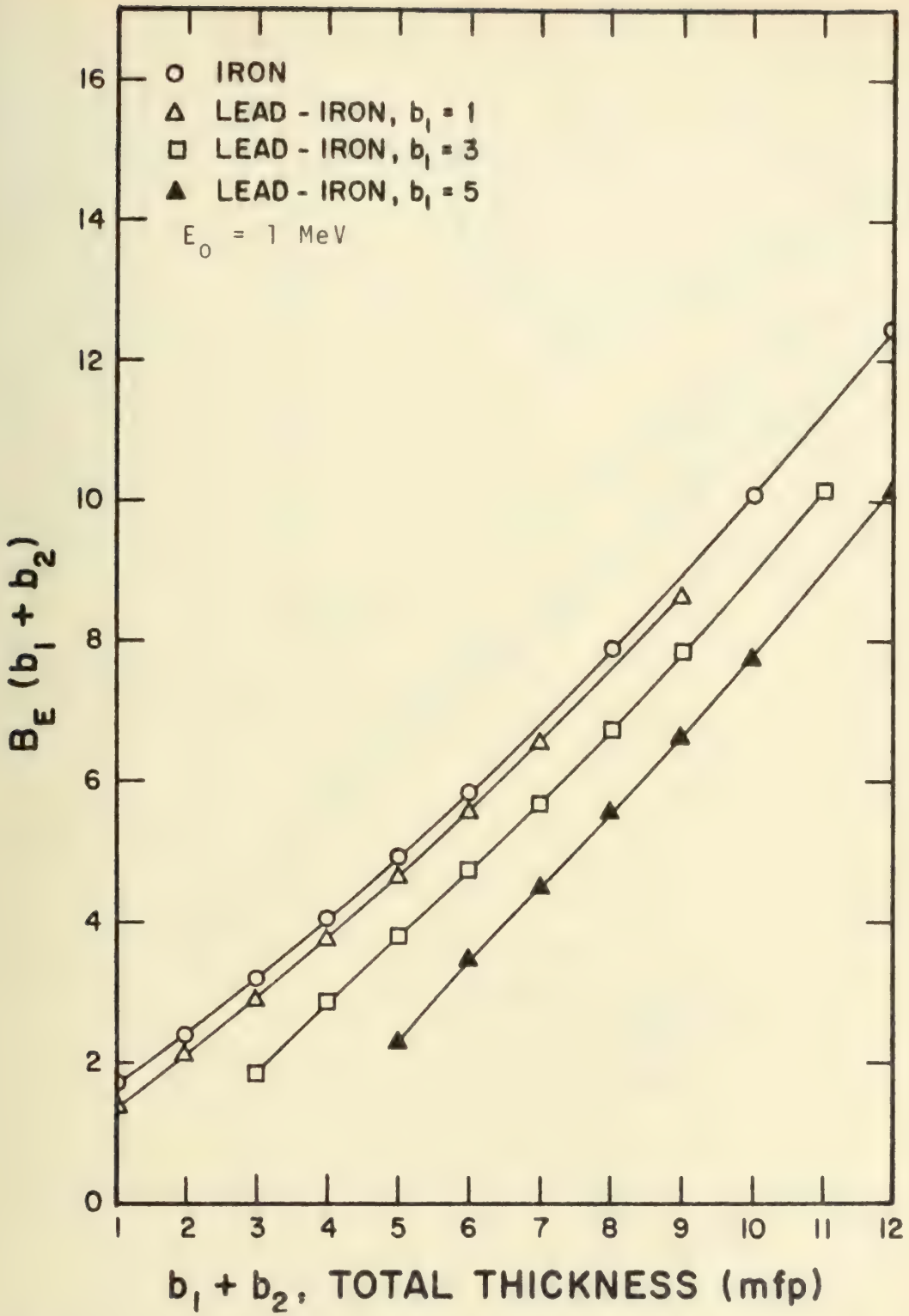

Figure D.4. The Energy Buildup Factor, $B_E(b_1+b_2)$ vs. b_1 and b_2 for 1MeV Photons in Slabs of Lead Followed by Iron.

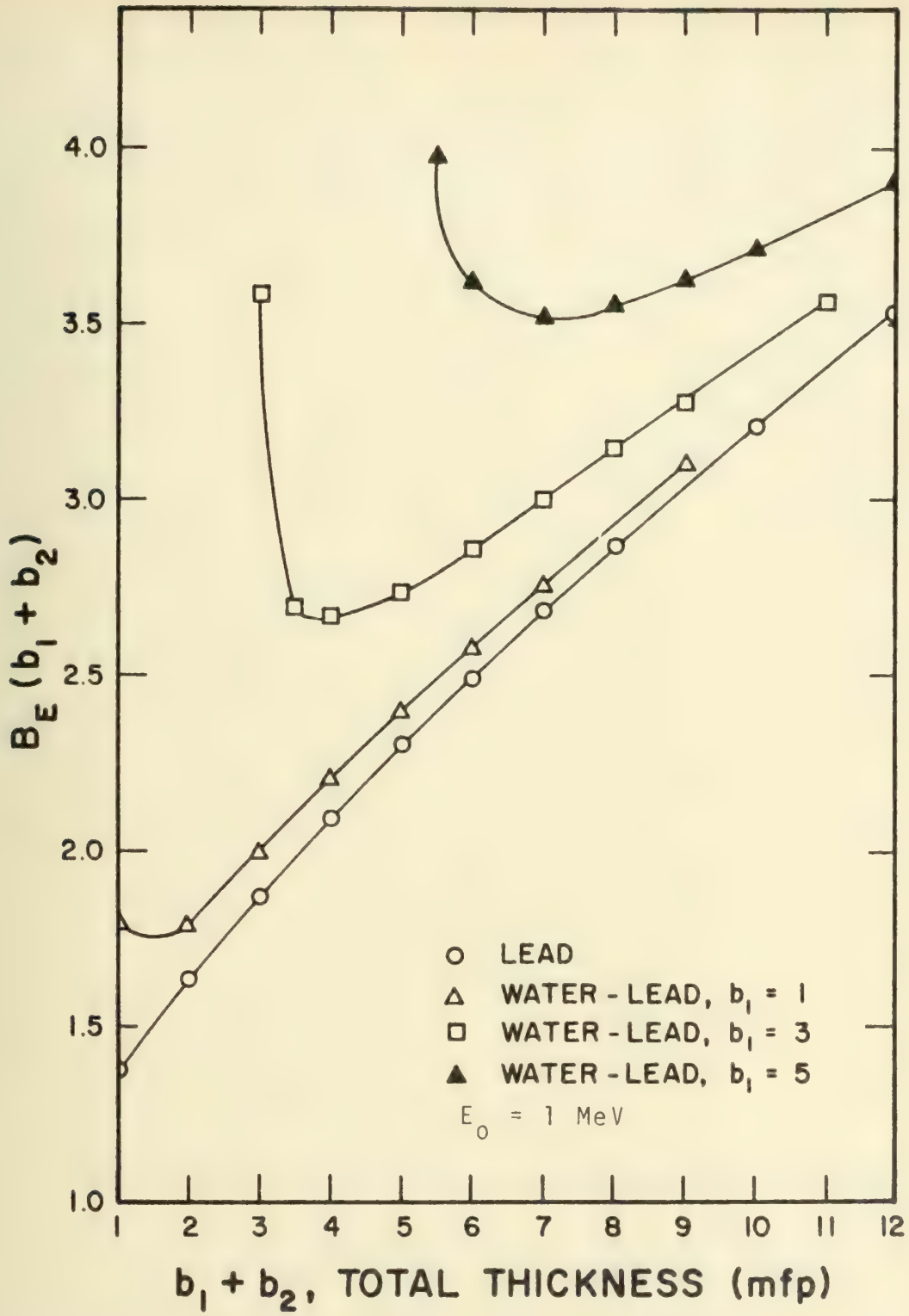

Figure D.5. The Energy Buildup Factor, $B_E(b_1+b_2)$ vs. b_1 and b_2 for 1MeV Photons in Slabs of Water Followed by Lead.

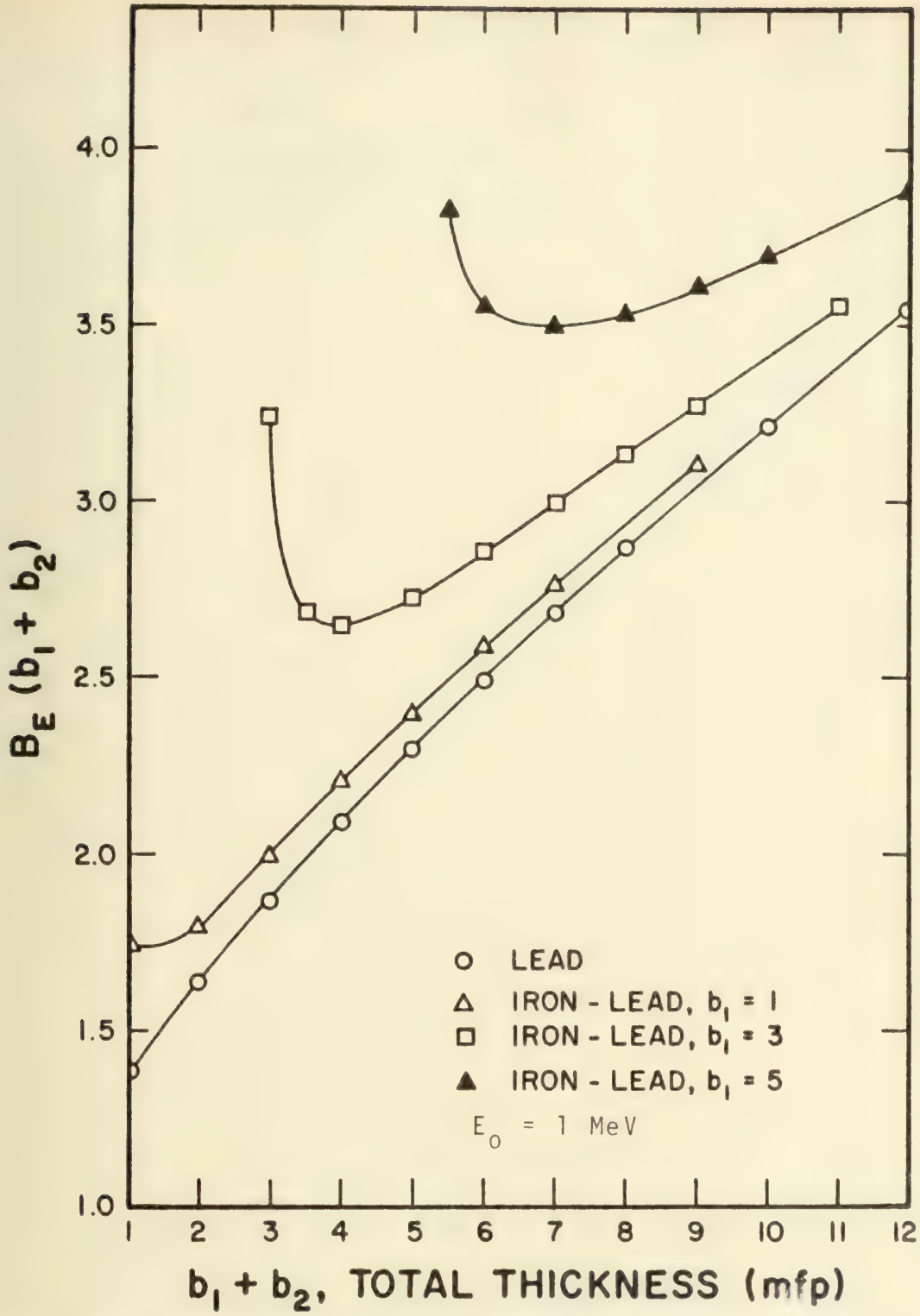

Figure D.6. The Energy Buildup Factor, $B_E(b_1+b_2)$ vs. b_1 and b_2 for 1MeV Photons in Slabs of Iron Followed by Lead.

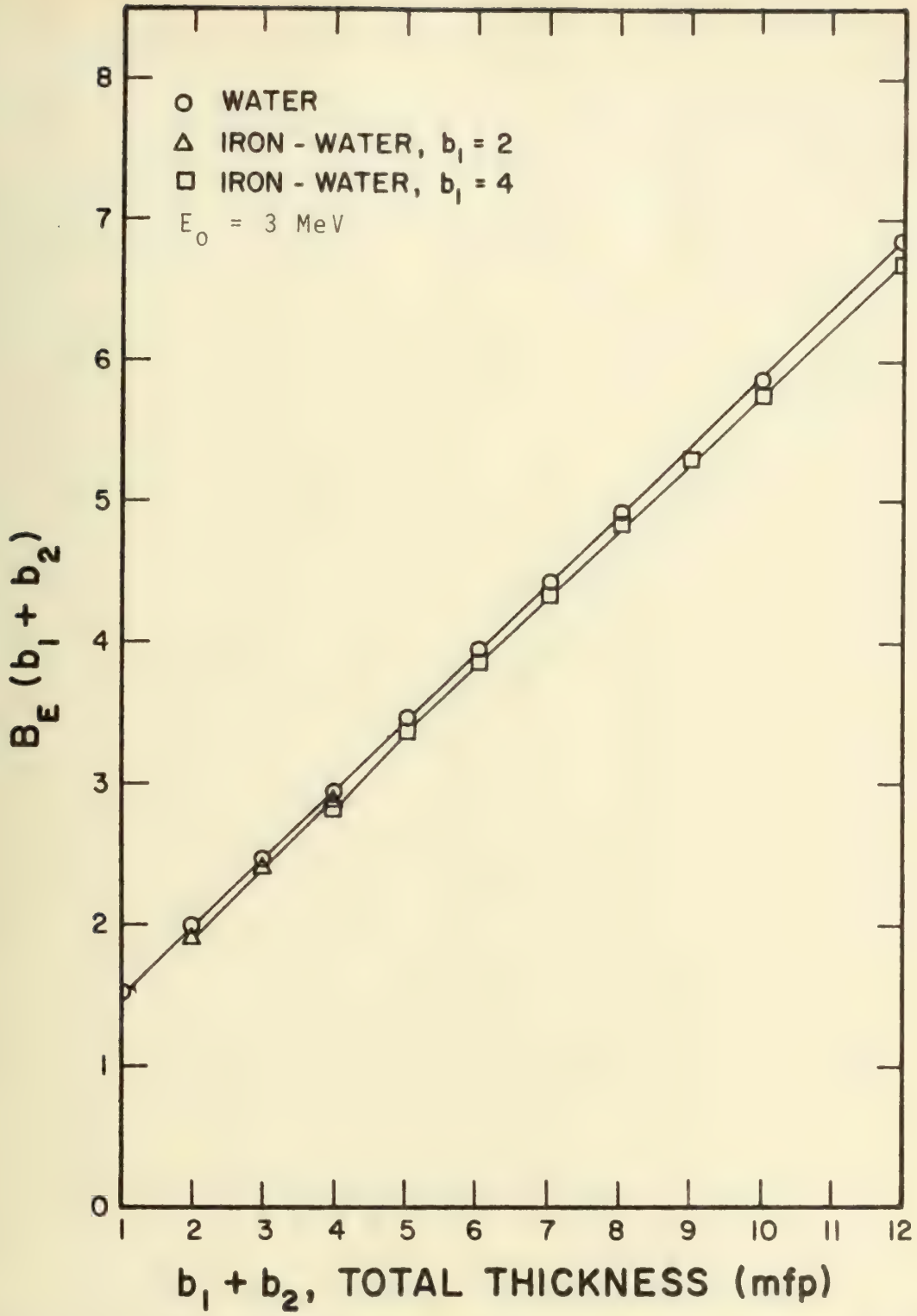

Figure D.7. The Energy Buildup Factor, $B_E(b_1+b_2)$ vs. b_1 and b_2 for 3MeV Photons in Slabs of Iron Followed by Water.

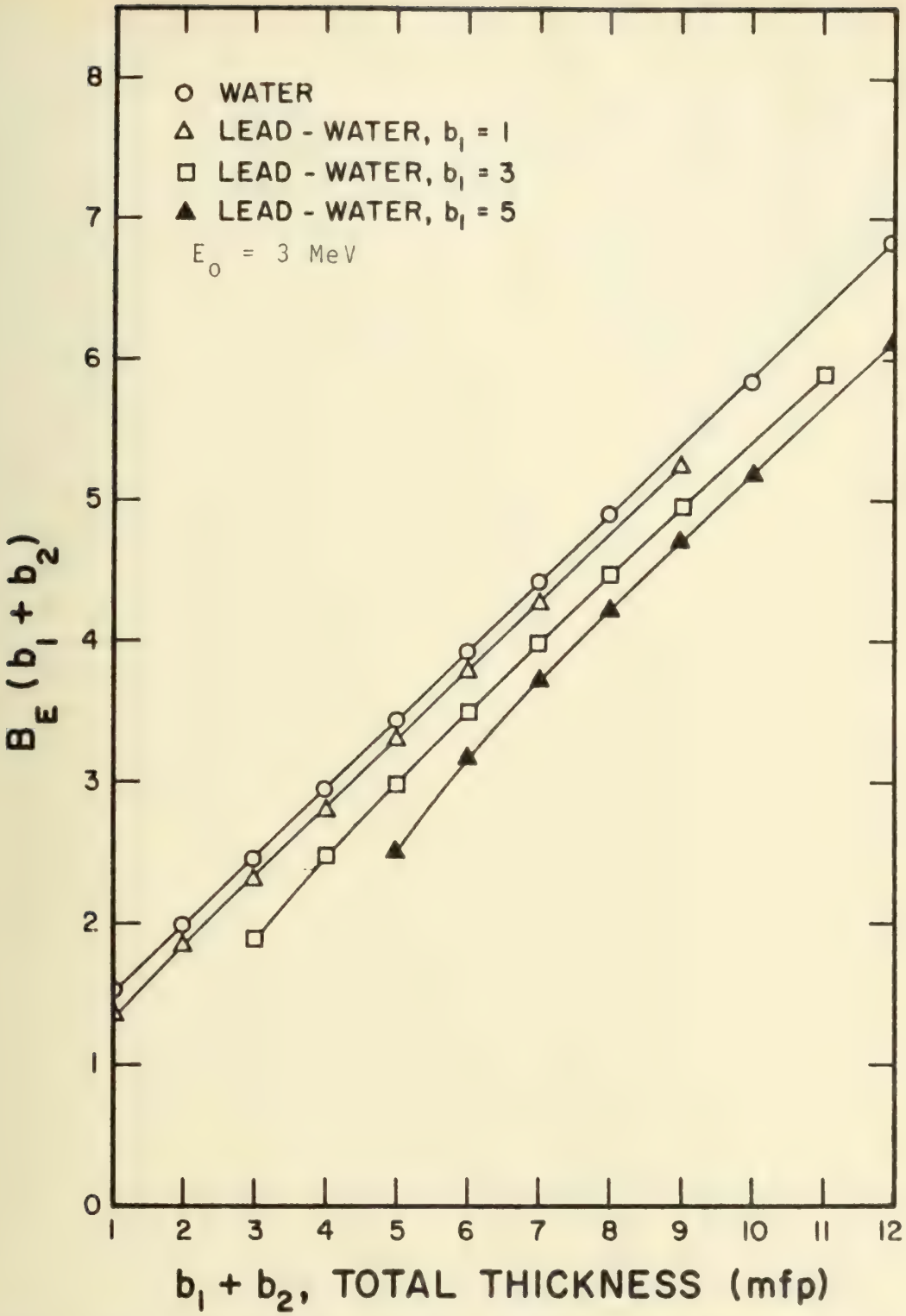

Figure D.8. The Energy Buildup Factor, $B_E(b_1+b_2)$ vs. b_1 and b_2 for 3MeV Photons in Slabs of Lead Followed by Water.

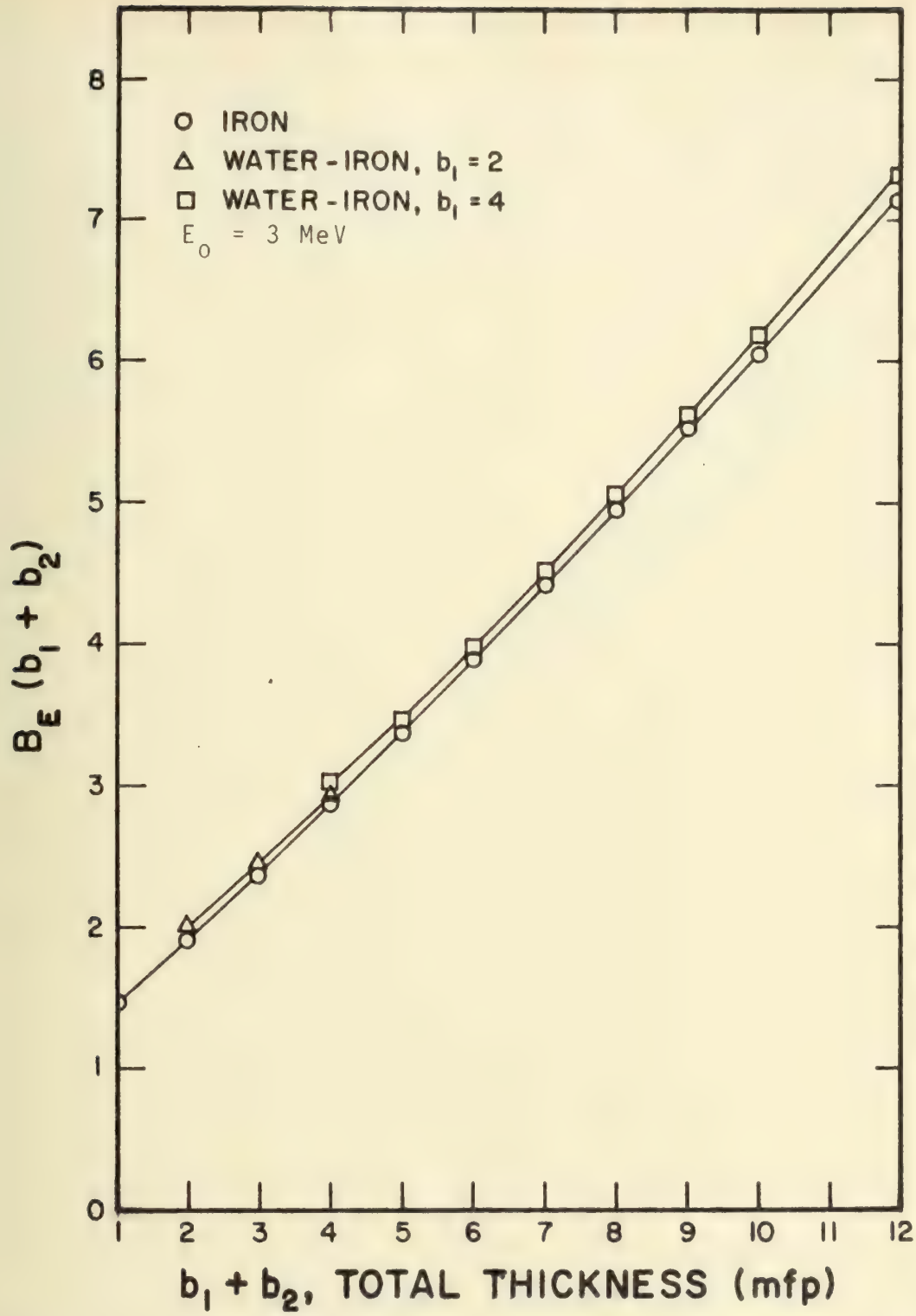

Figure D.9. The Energy Buildup Factor, $B_E(b_1+b_2)$ vs. b_1 and b_2 for 3MeV Photons in Slabs of Water Followed by Iron.

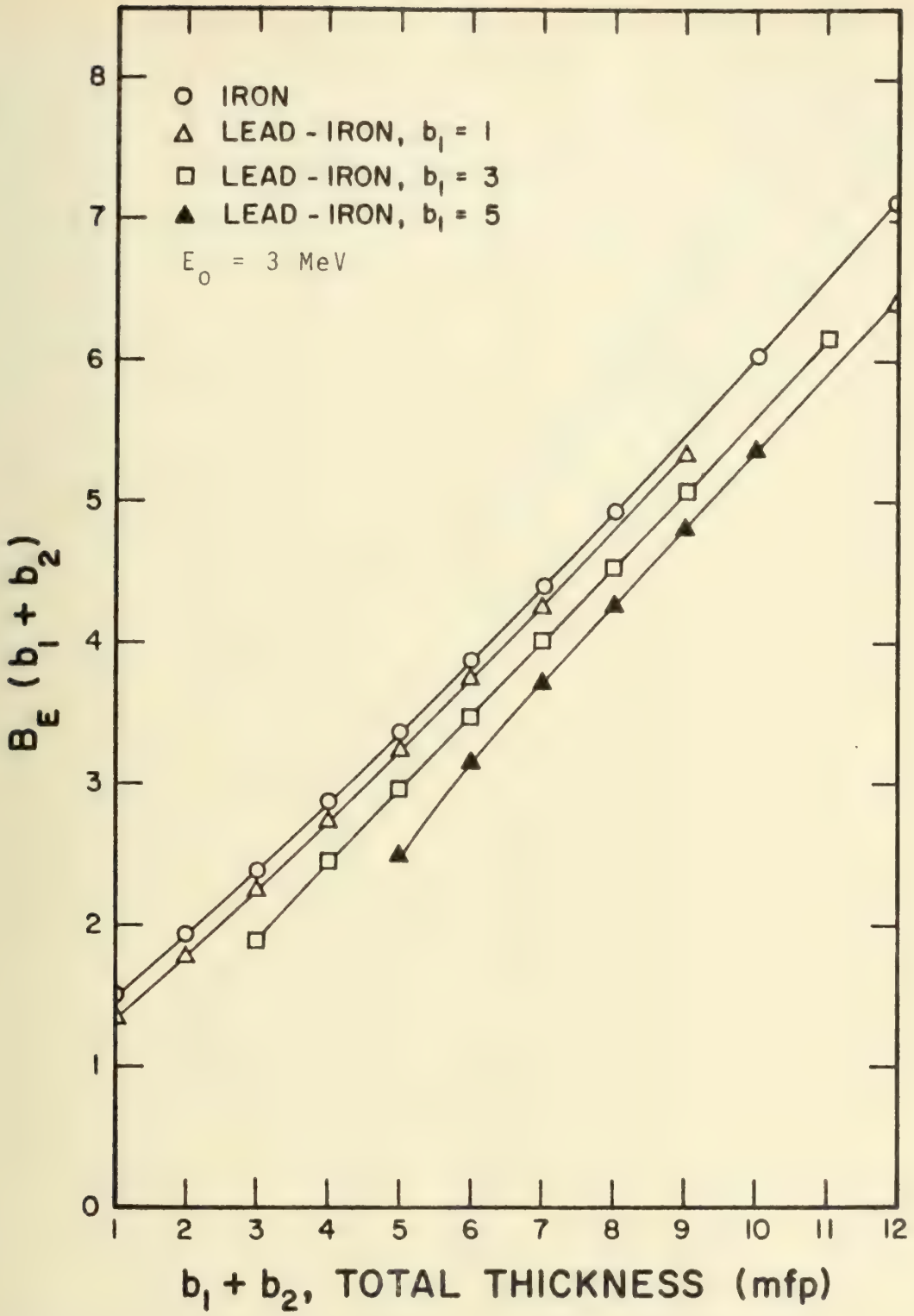

Figure D.10. The Energy Buildup Factor, $B_E(b_1+b_2)$ vs. b_1 and b_2 for 3MeV Photons in Slabs of Lead Followed by Iron.

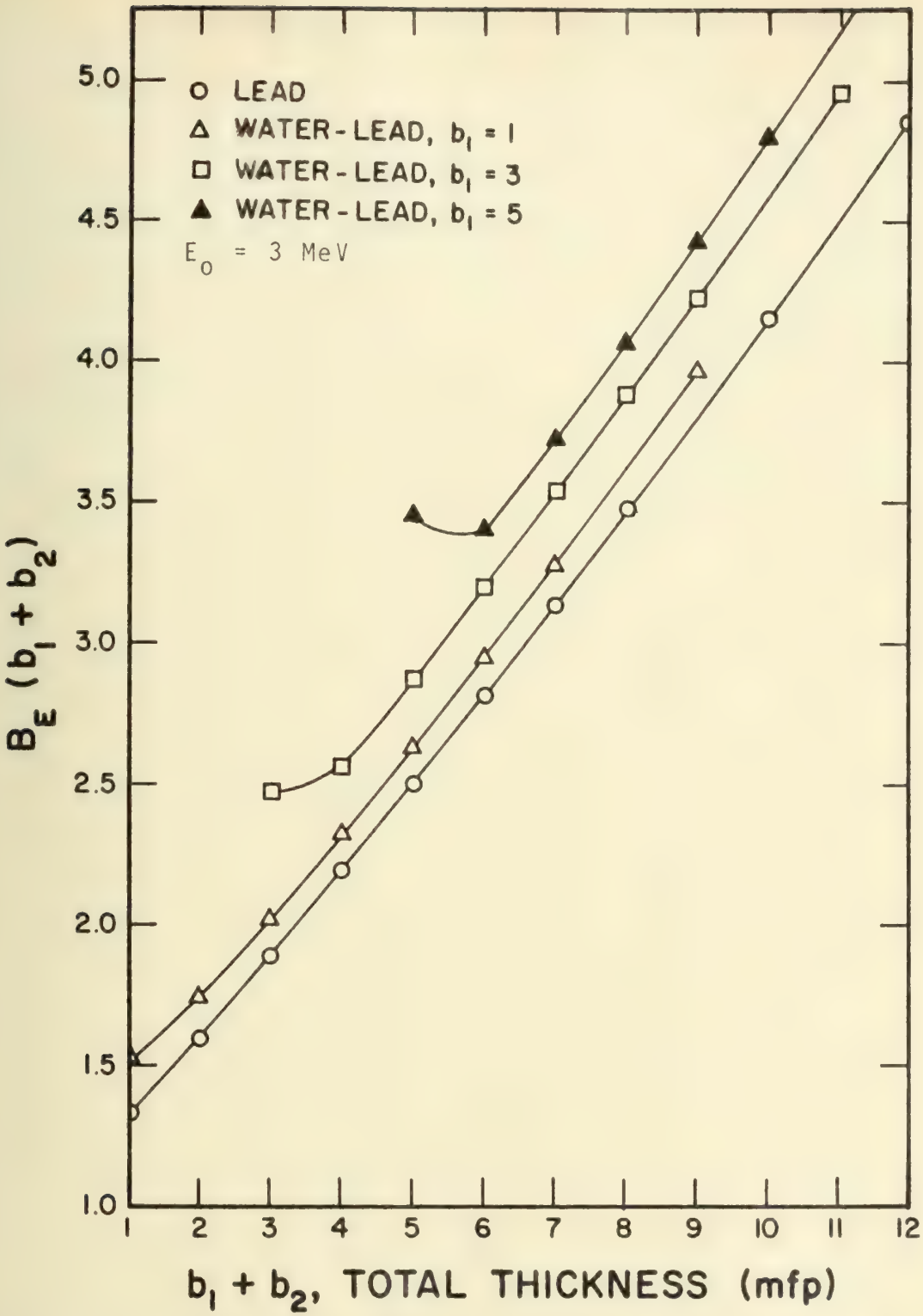

Figure D.11. The Energy Buildup Factor, $B_E(b_1+b_2)$ vs. b_1 and b_2 for 3MeV Photons in Slabs of Water Followed by Lead.

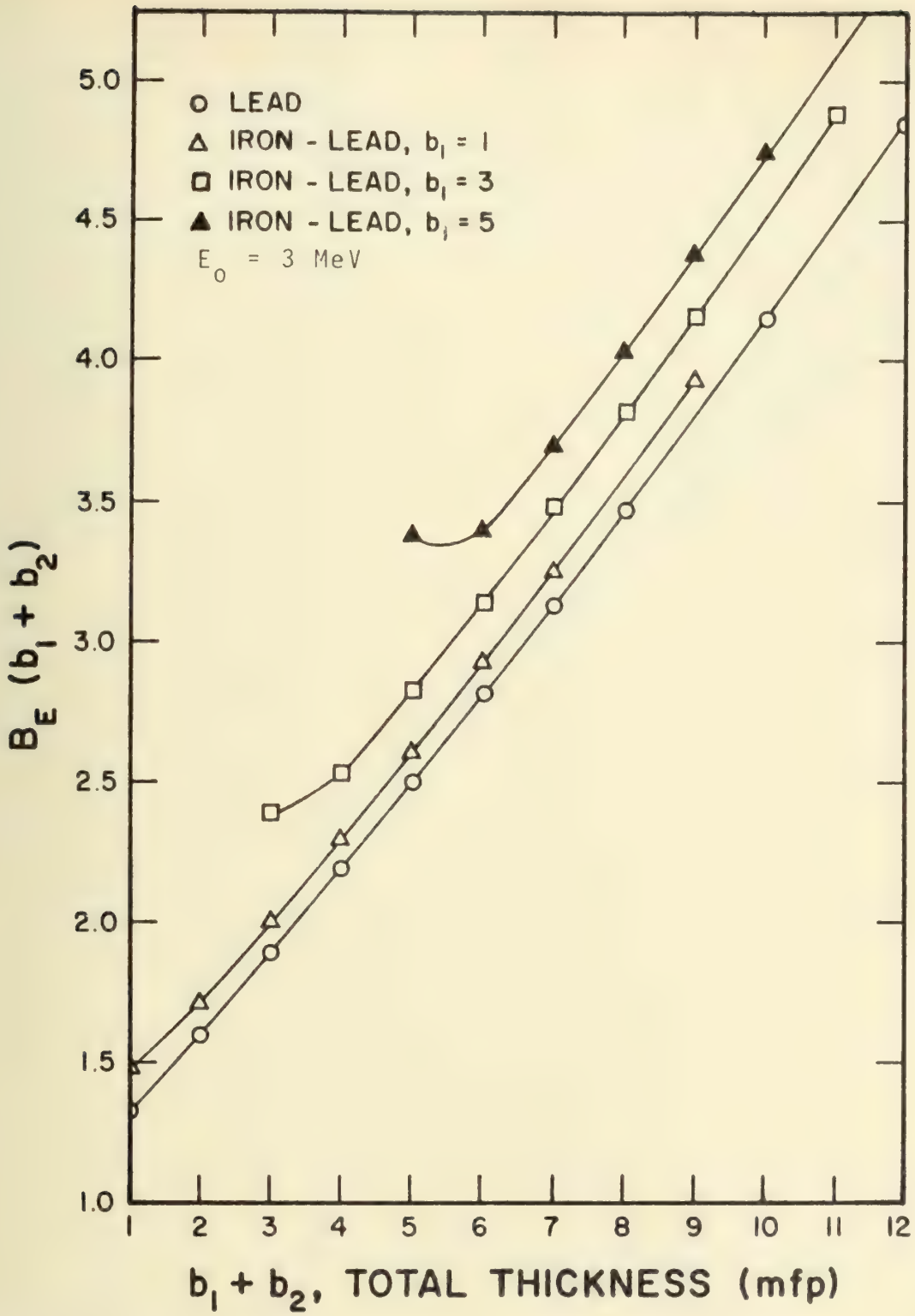

Figure D.12. The Energy Buildup Factor, $B_E(b_1+b_2)$ vs. b_1 and b_2 for 3MeV Photons in Slabs of Iron Followed by Lead.

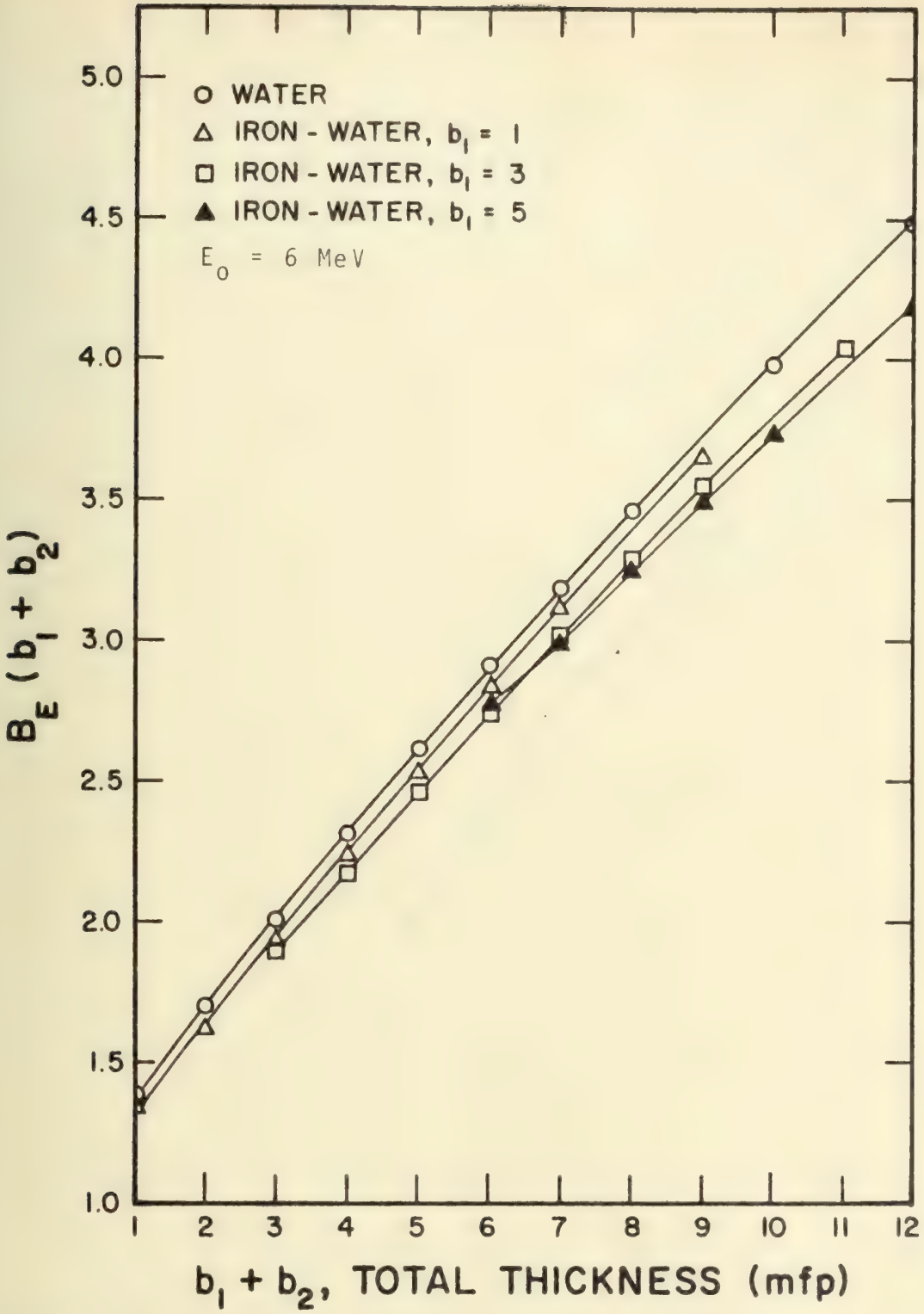

Figure D.13. The Energy Buildup Factor, $B_E(b_1+b_2)$ vs. b_1 and b_2 for 6MeV Photons in Slabs of Iron Followed by Water.

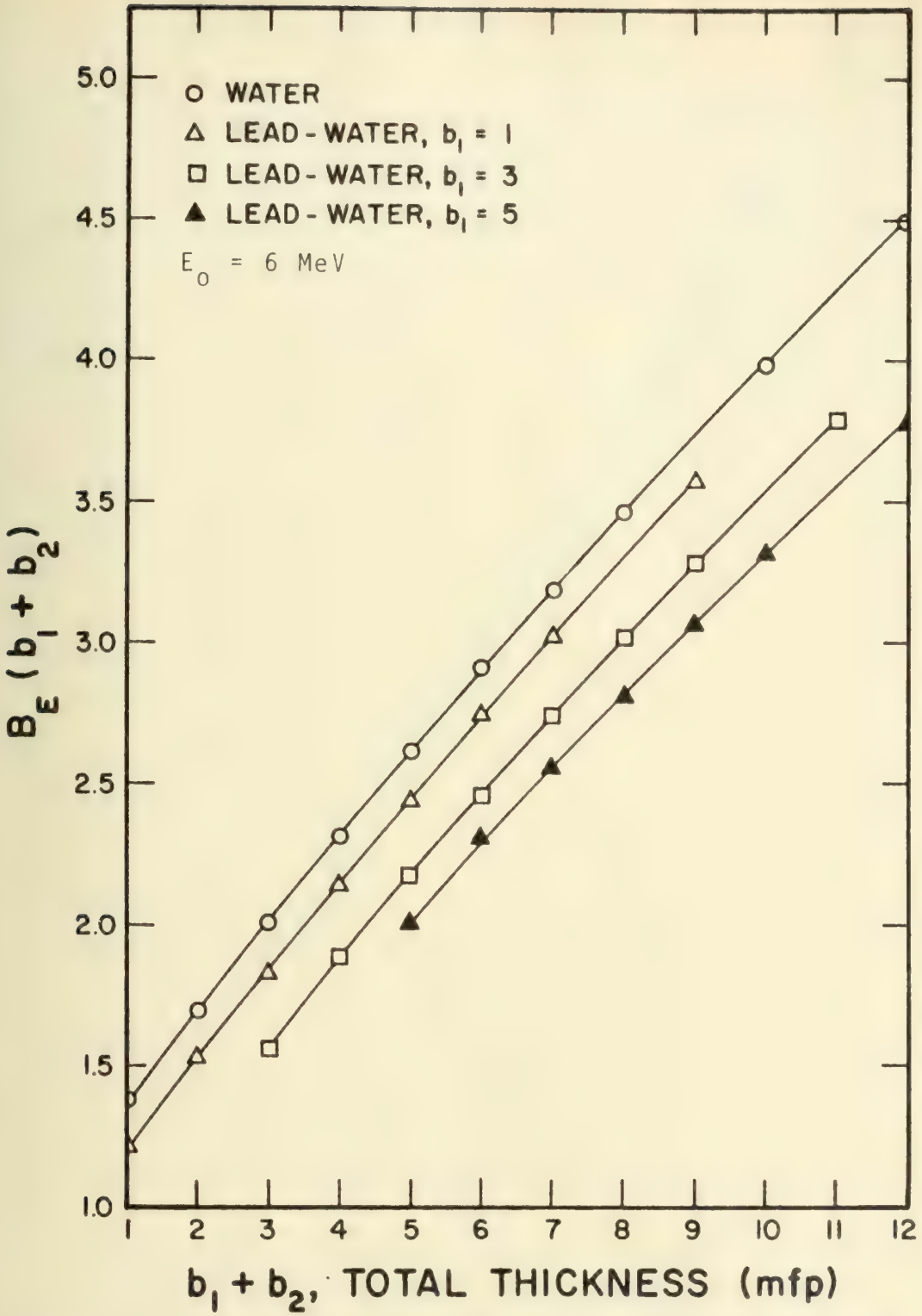

Figure D.14. The Energy Buildup Factor, $B_E(b_1+b_2)$ vs. b_1 and b_2 for 6MeV Photons in Slabs of Lead Followed by Water.

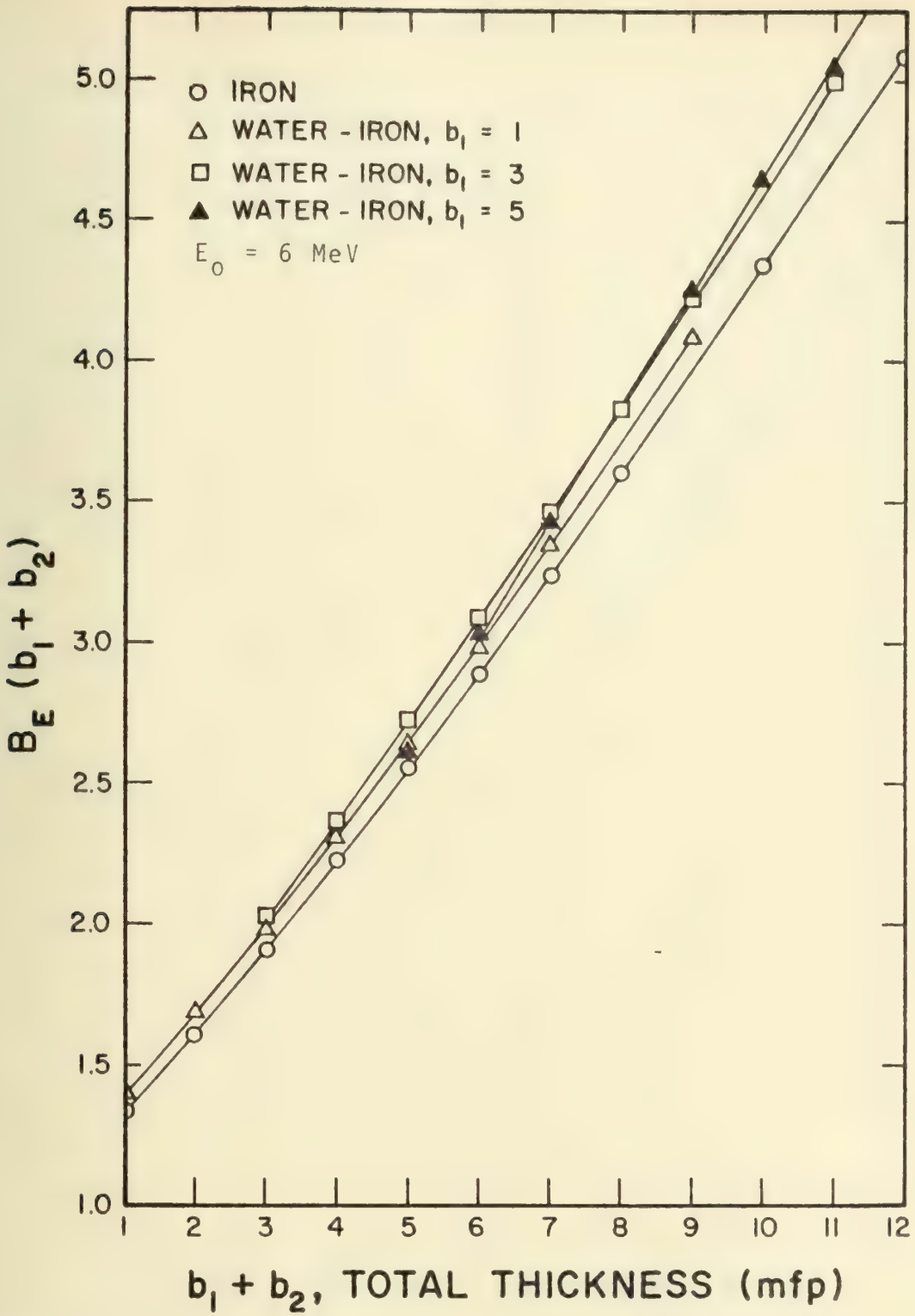

Figure D.15. The Energy Buildup Factor, $B_E(b_1+b_2)$ vs. b_1 and b_2 for 6MeV Photons in Slabs of Water Followed by Iron.

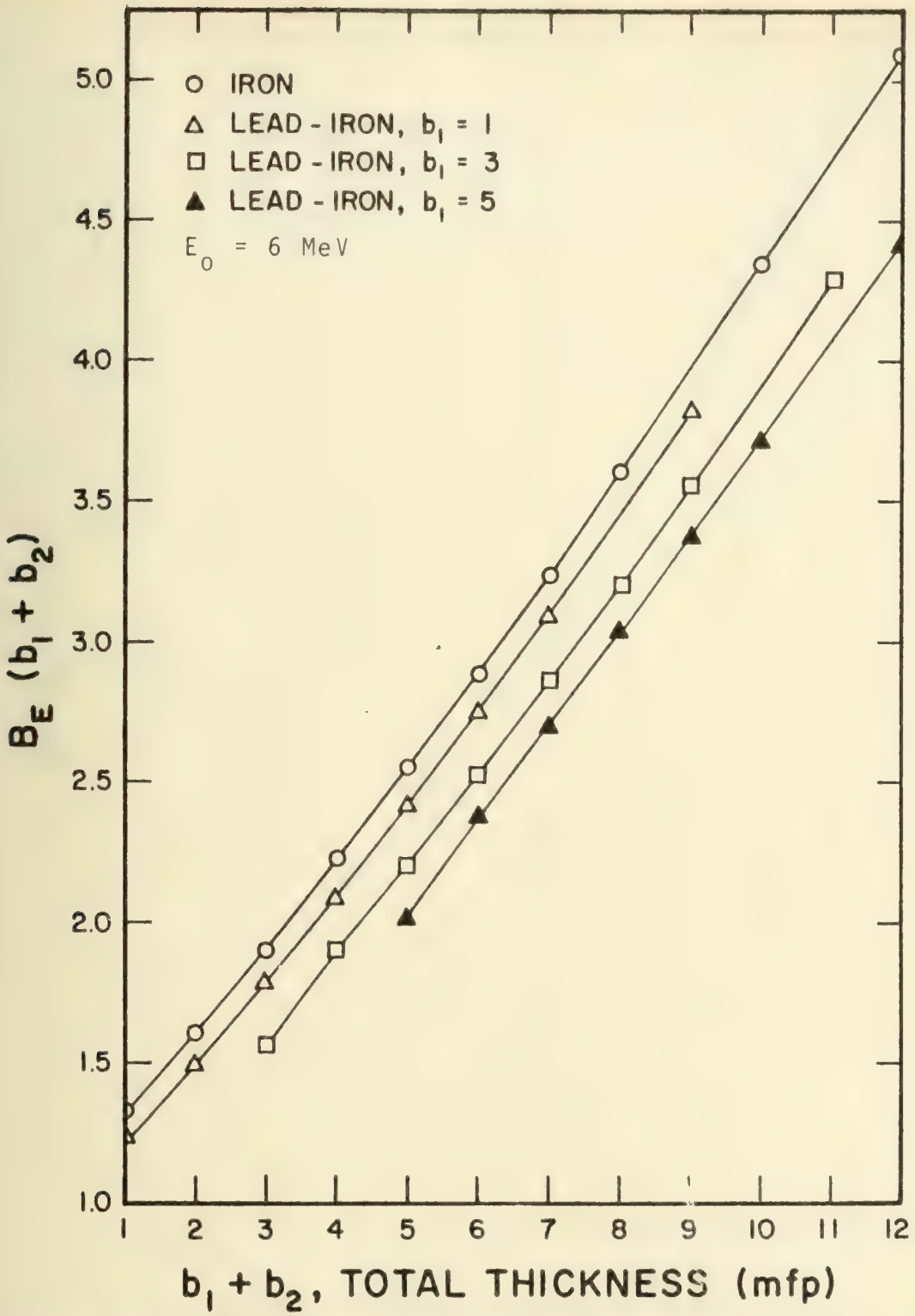

Figure D.16. The Energy Buildup Factor, $B_E(b_1+b_2)$ vs. b_1 and b_2 for 6MeV Photons in Slabs of Lead Followed by Iron.

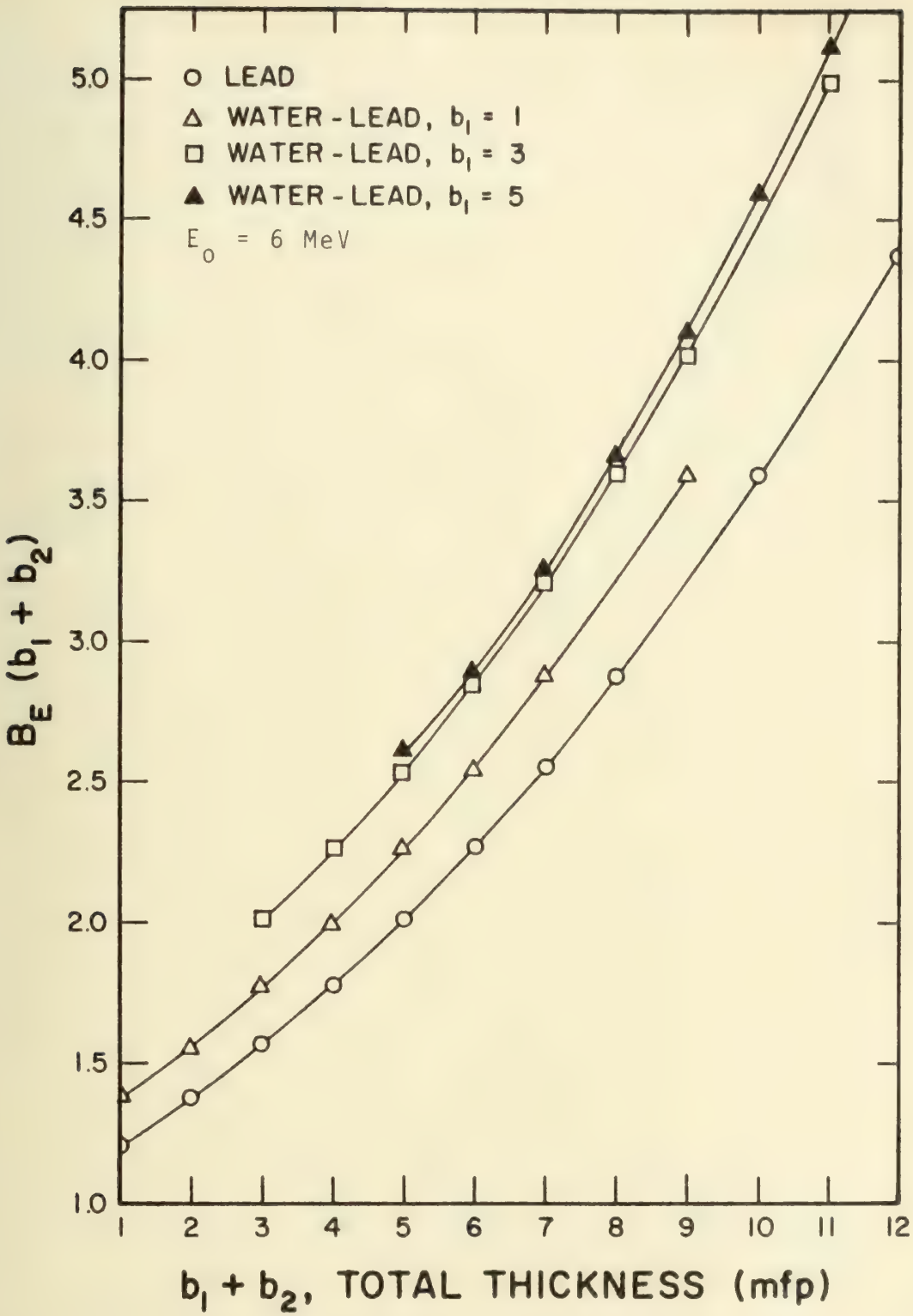

Figure D.17. The Energy Buildup Factor, $B_E(b_1+b_2)$ vs. b_1 and b_2 for 6MeV Photons in Slabs of Water Followed by Lead.

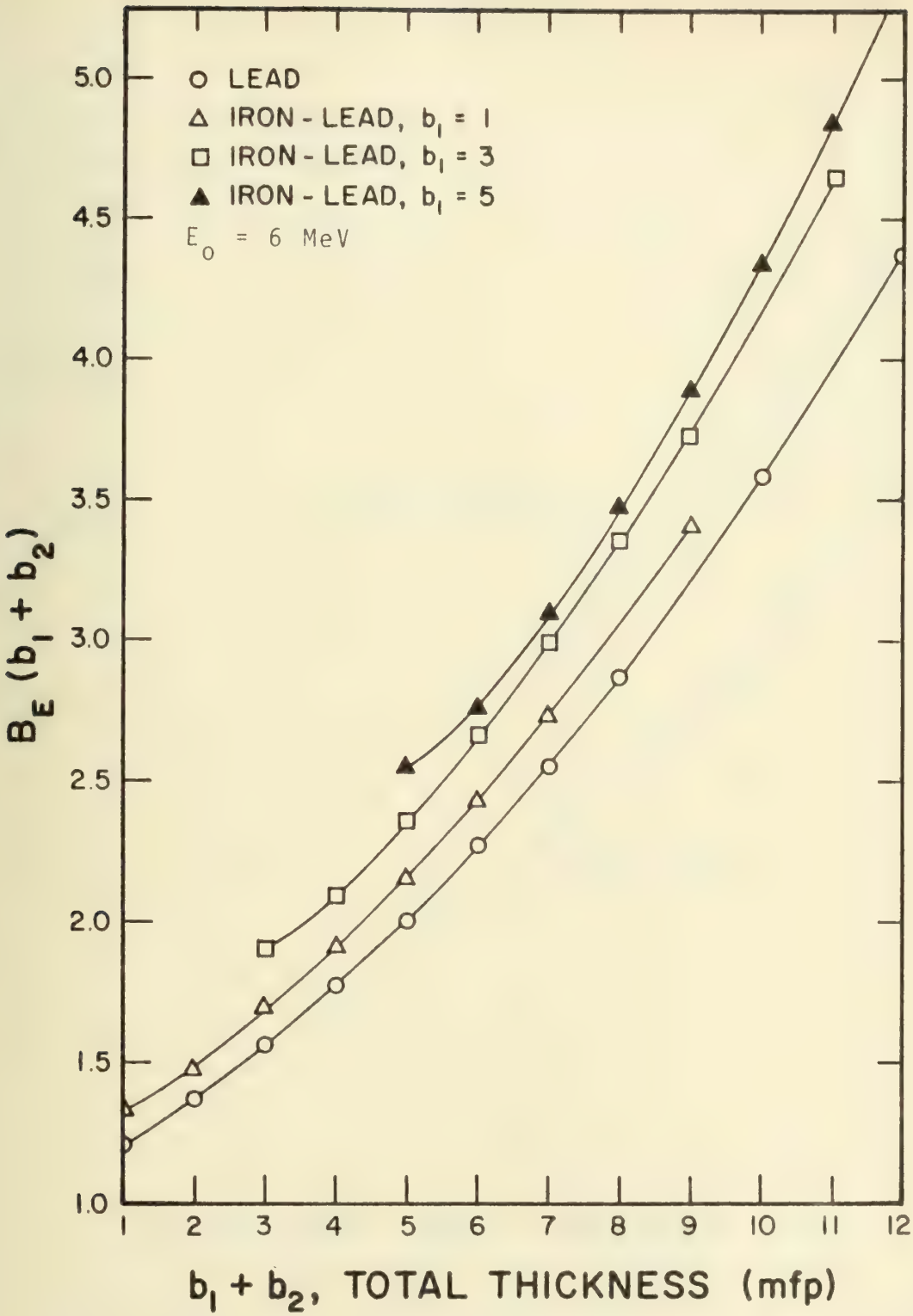

Figure D.18. The Energy Buildup Factor, $B_E(b_1+b_2)$ vs. b_1 and b_2 for 6MeV Photons in Slabs of Iron Followed by Lead.

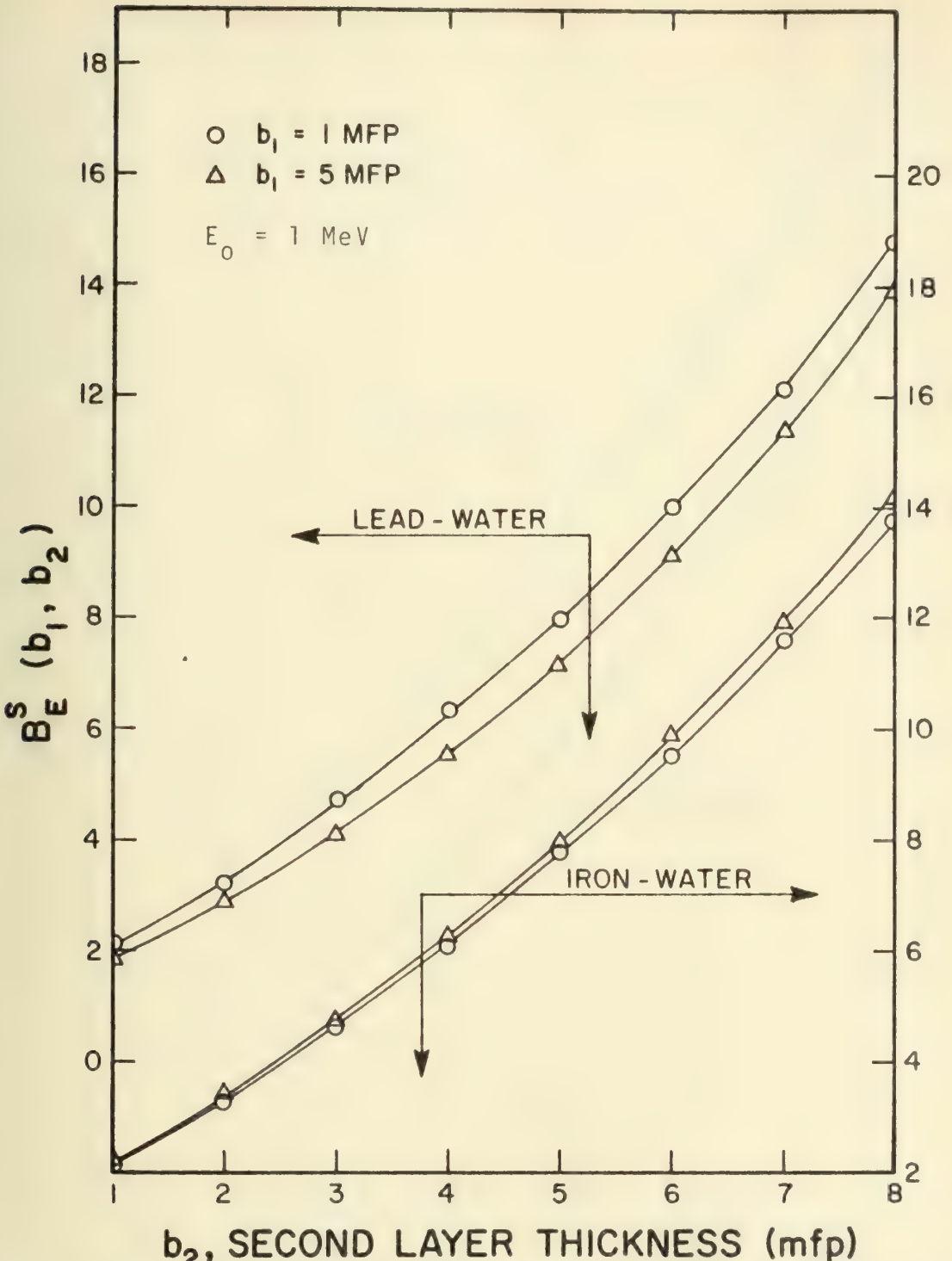

Figure D.19. The Scattered Energy Buildup Factor, $B^S_E(b_1,b_2)$ vs. b_1 and b_2 for 1MeV Photons in Two-Layered Slabs of Iron-Water and Lead-Water.

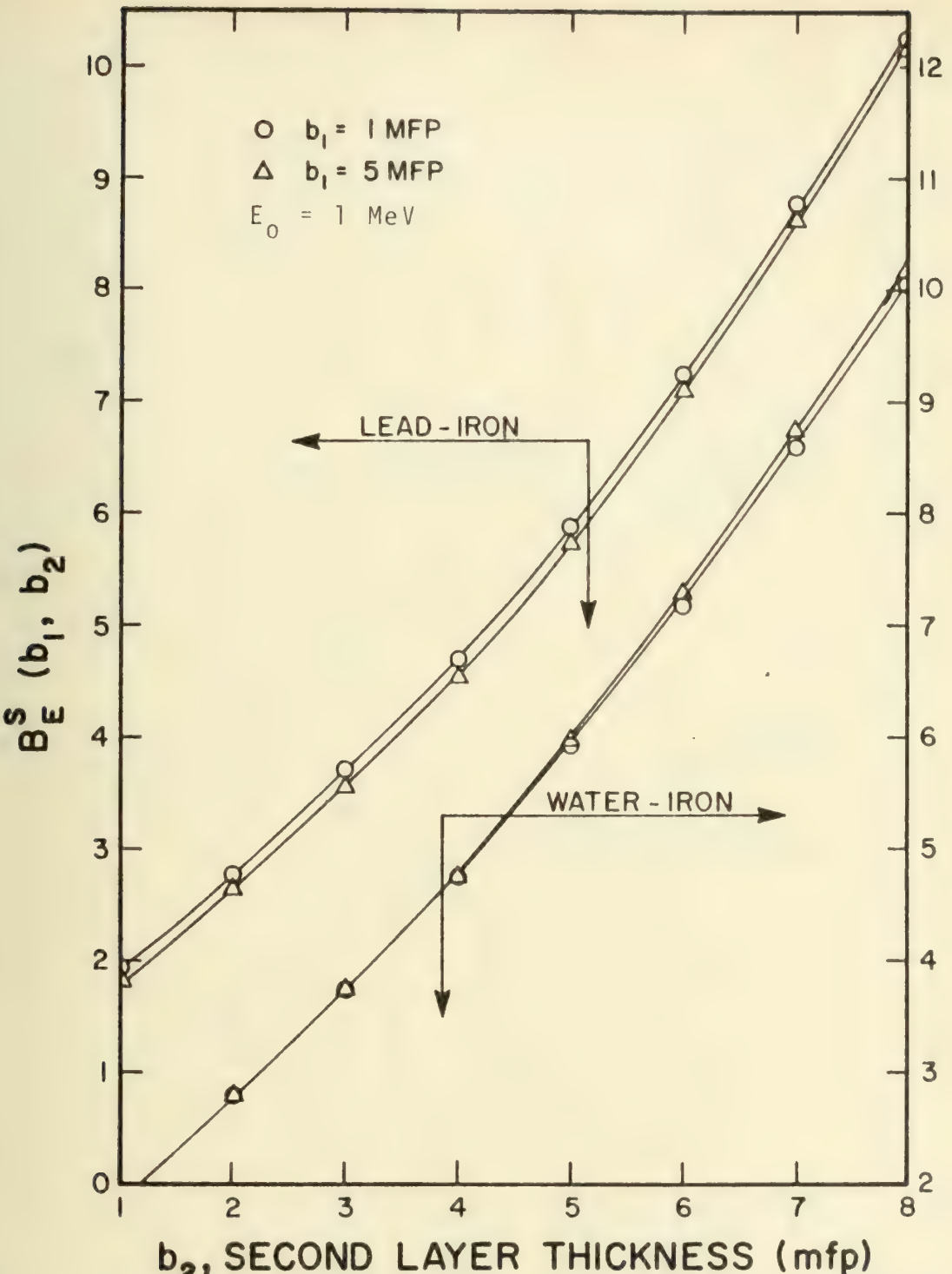

Figure D.20. The Scattered Energy Buildup Factor, $B_E^S(b_1, b_2)$ vs. b_1 and b_2 for 1MeV Photons in Two-Layered Slabs of Water-Iron and Lead-Iron.

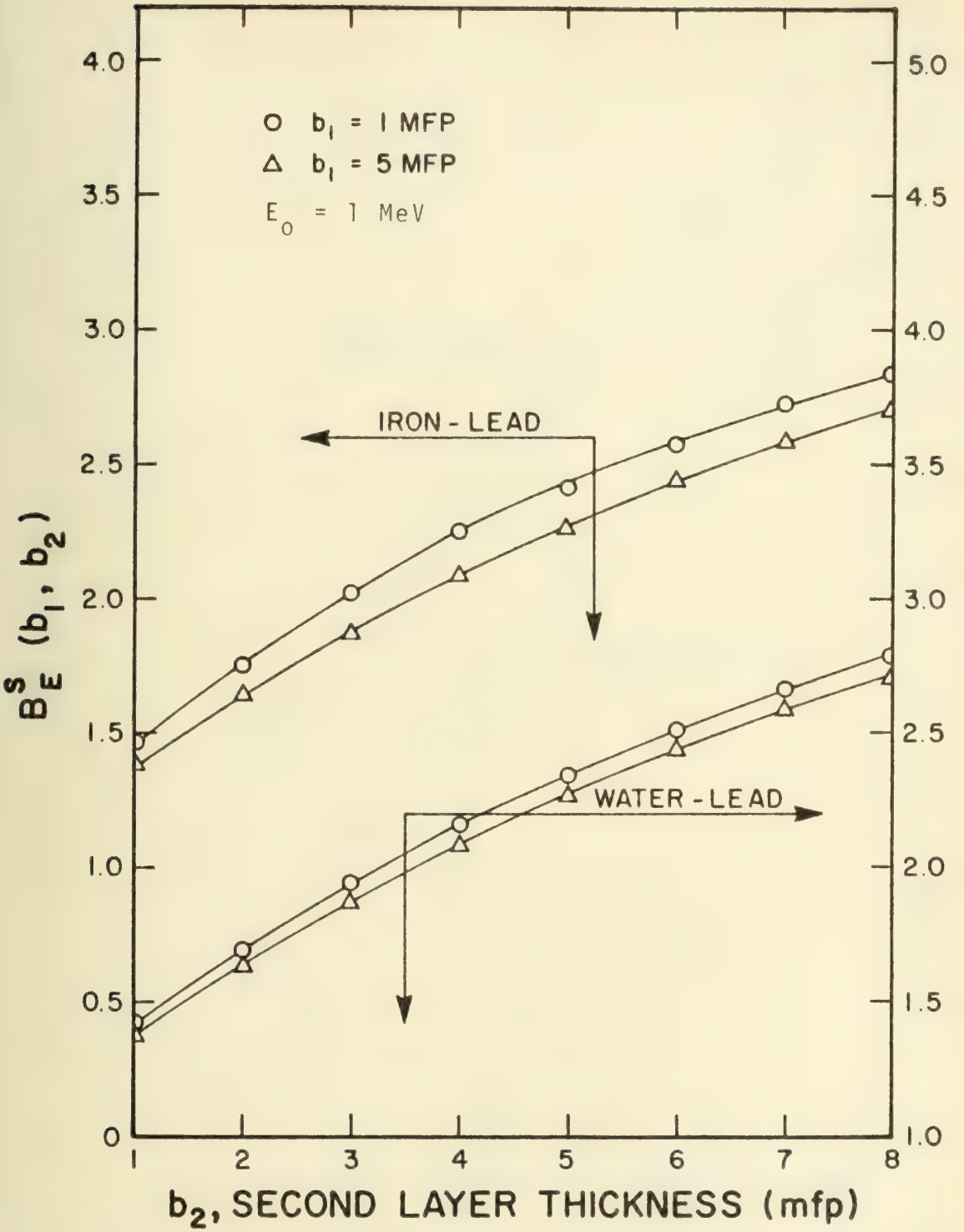

Figure D.21. The Scattered Energy Buildup Factor, $B^S_E(b_1,b_2)$ vs. b_1 and b_2 for 1MeV Photons in Two-Layered Slabs of Water-Lead and Iron-Lead.

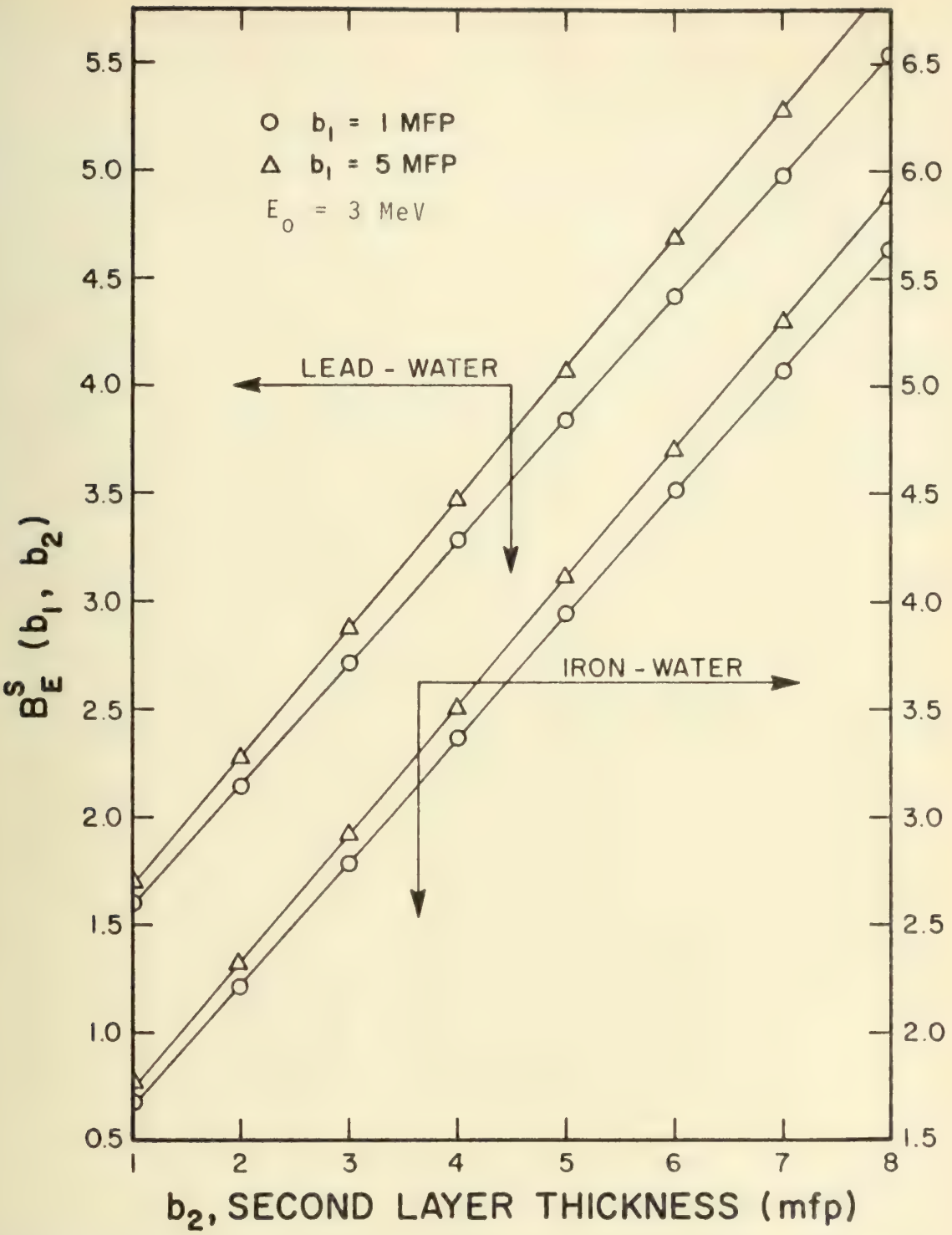

Figure D.22. The Scattered Energy Buildup Factor, $B_E^S(b_1,b_2)$ vs. b_1 and b_2 for 3MeV Photons in Two-Layered Slabs of Iron-Water and Lead-Water.

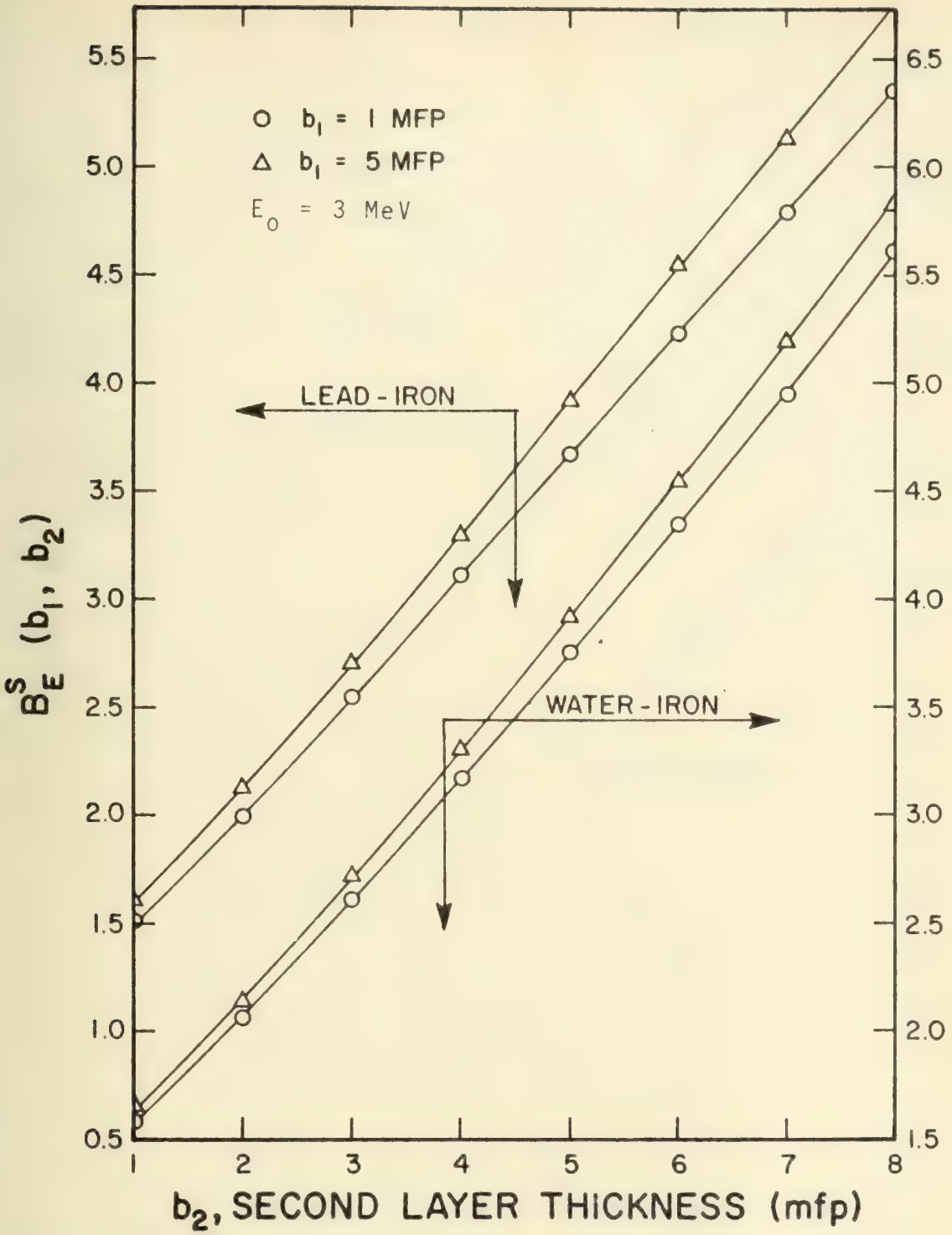

Figure D.23. The Scattered Energy Buildup Factor, $B_E^S(b_1,b_2)$ vs. b_1 and b_2 for 3MeV Photons in Two-Layered Slabs of Water-Iron and Lead-Iron.

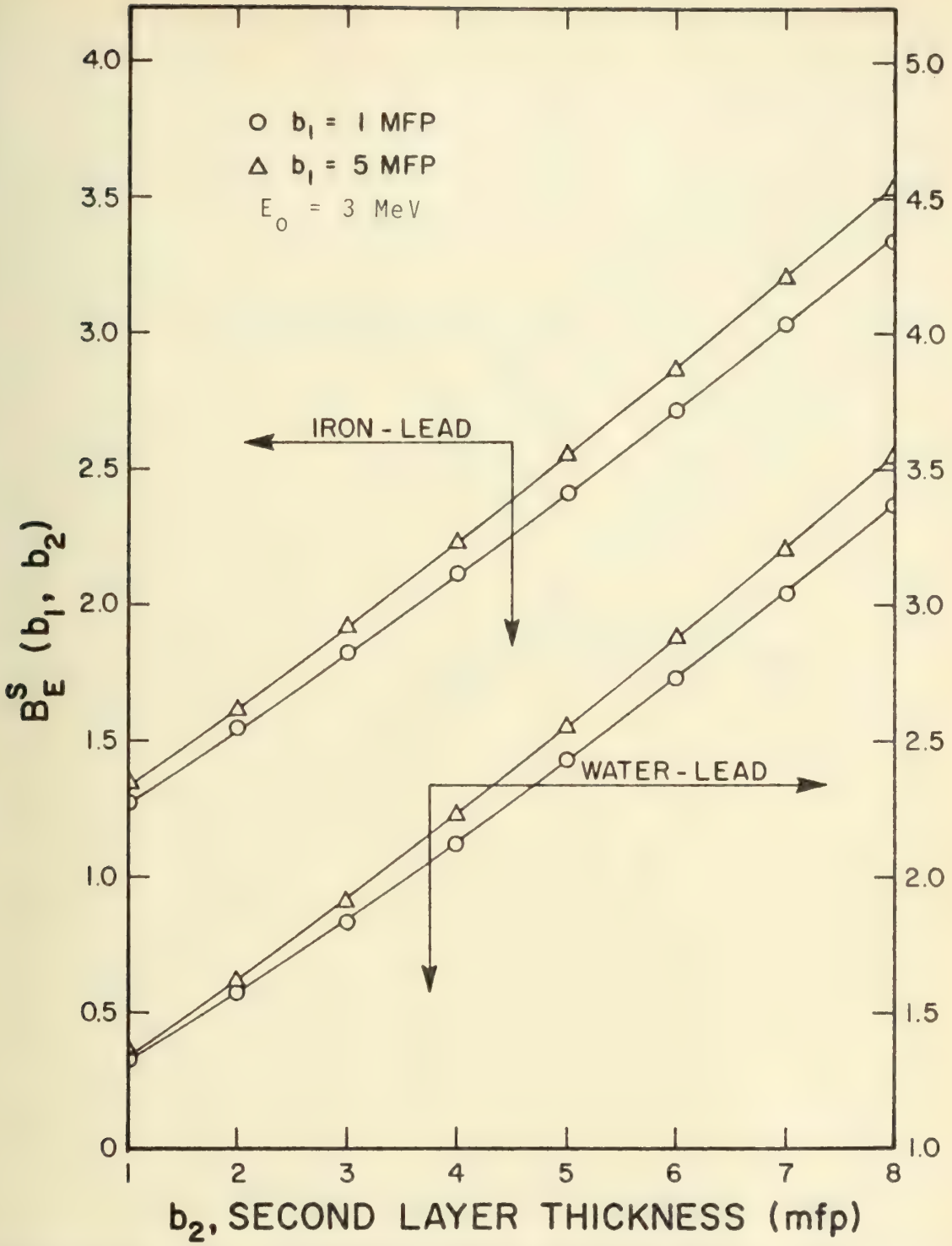

Figure D.24. The Scattered Energy Buildup Factor, $B_E^S(b_1,b_2)$ vs. b_1 and b_2 for 3MeV Photons in Two-Layered Slabs of Water-Lead and Iron-Lead.

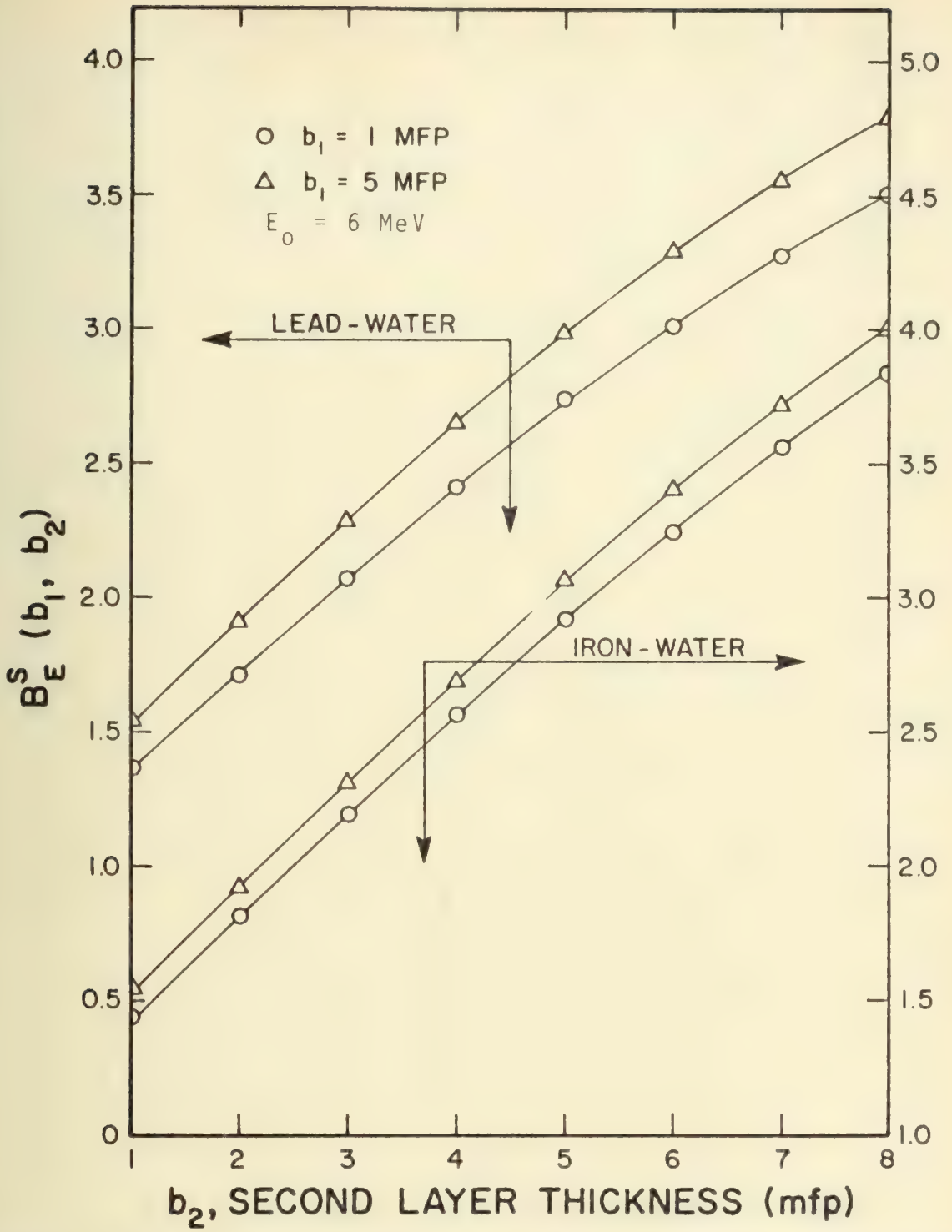

Figure D.25. The Scattered Energy Buildup Factor, $B_E^S(b_1,b_2)$ vs. b_1 and b_2 for 6MeV Photons in Two-Layered Slabs of Iron-Water and Lead-Water.

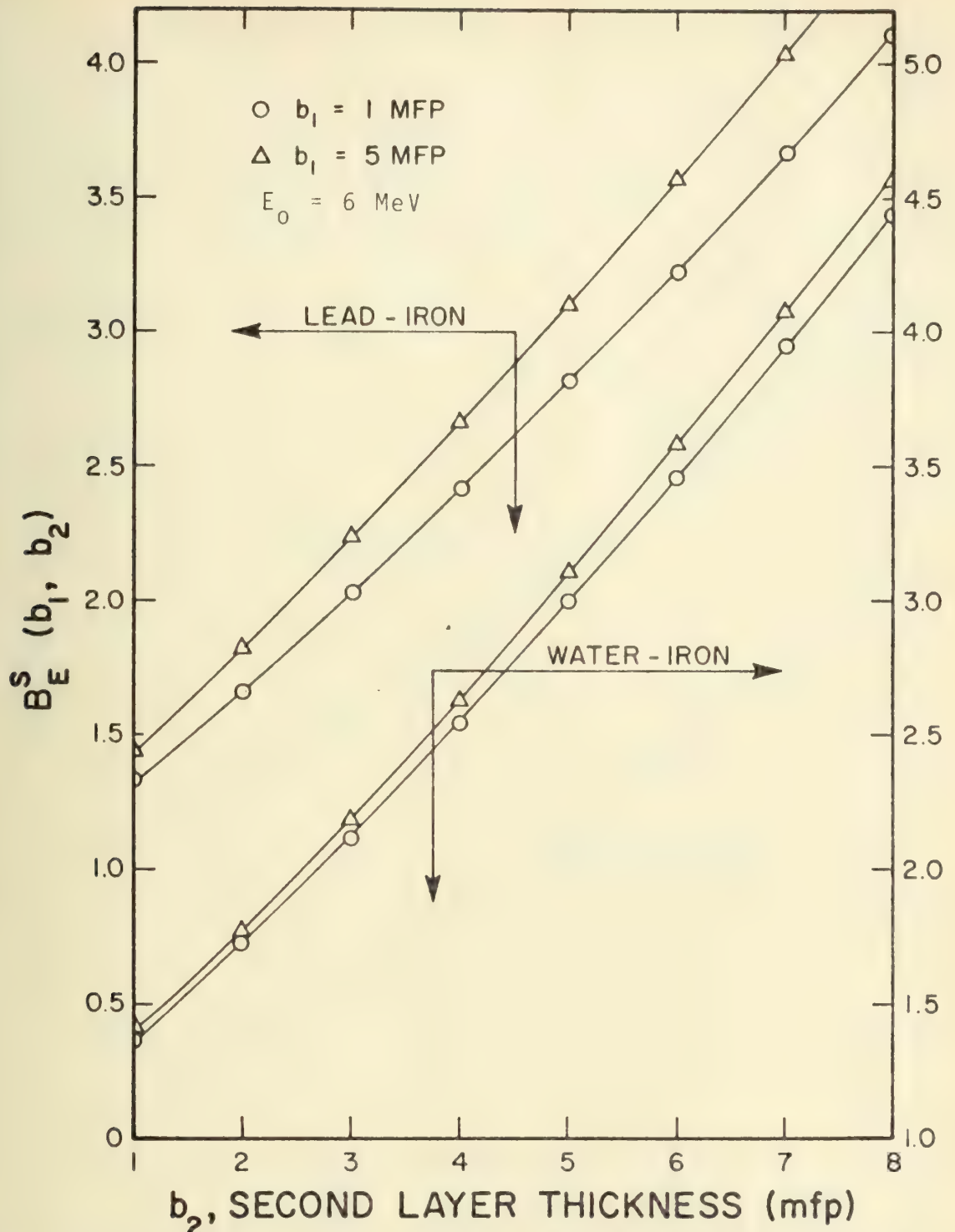

Figure D.26. The Scattered Energy Buildup Factor, $B^S_E(b_1,b_2)$ vs. b_1 and b_2 for 6MeV Photon in Two-Layered Slabs of Water-Iron and Lead-Iron.

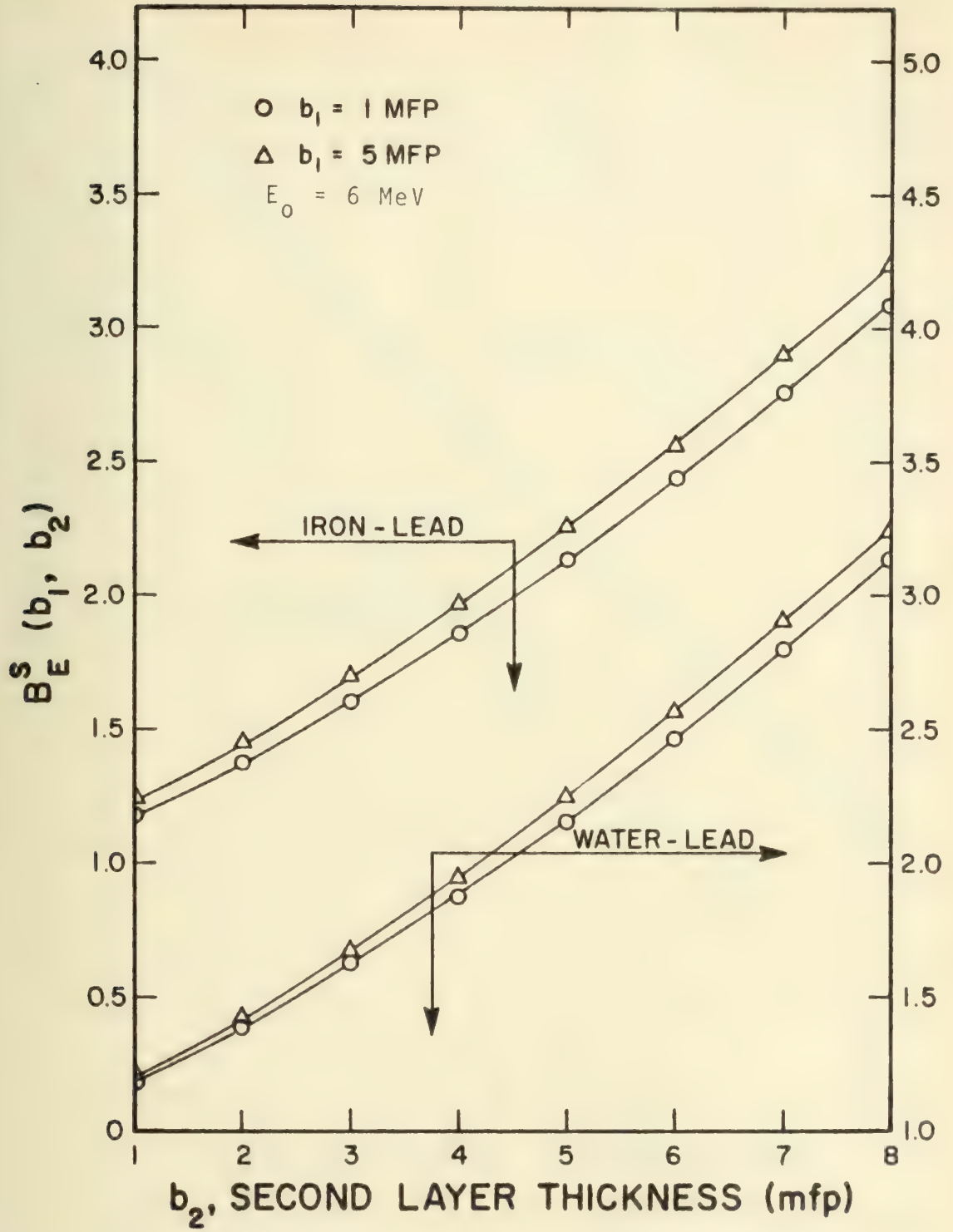

Figure D.27. The Scattered Energy Buildup Factor, $B_E^S(b_1,b_2)$ vs. b_1 and b_2 for 6MeV Photons in Two-Layered Slabs of Water-Lead and Iron-Lead.

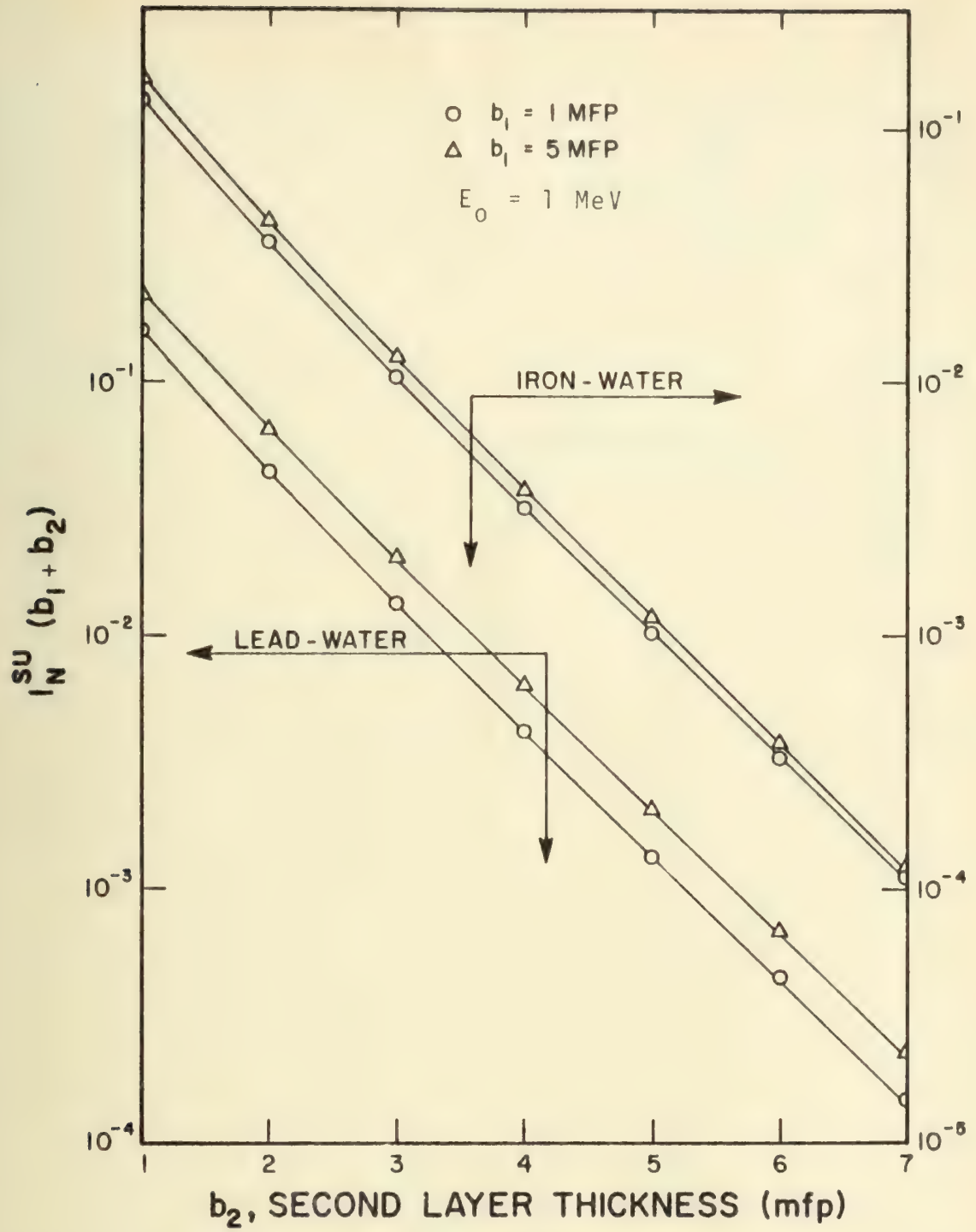

Figure D.28. The Energy Flux, $I_n^{su}(b_1+b_2)$ vs. b_1 and b_2 for 1MeV Photons in Two-Layered Slabs of Iron-Water and Lead-Water.

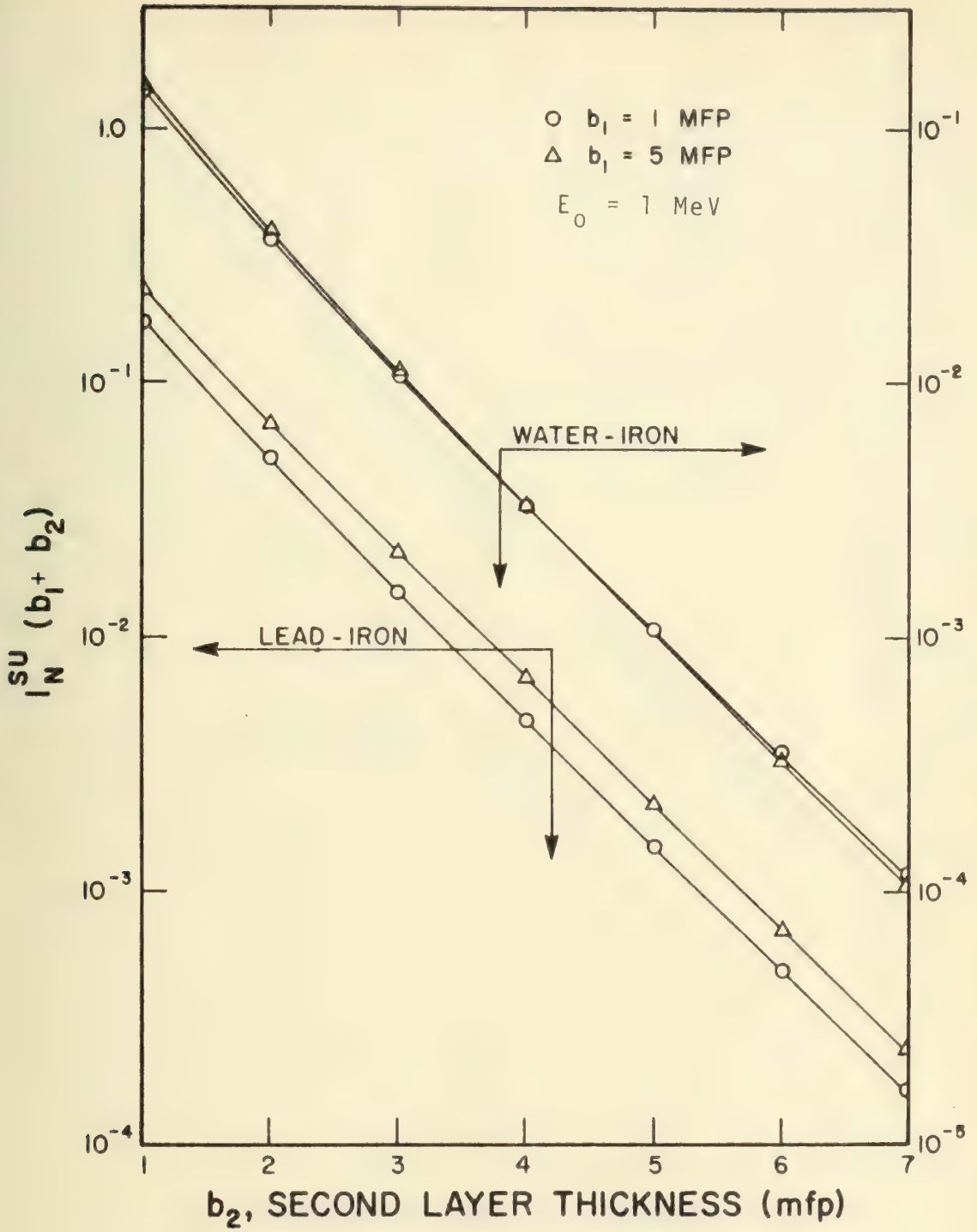

Figure D.29. The Energy Flux, $I_n^{su}(b_1+b_2)$ vs. b_1 and b_2 for 1MeV Photons in Two-Layered Slabs of Water-Iron and Lead-Iron.

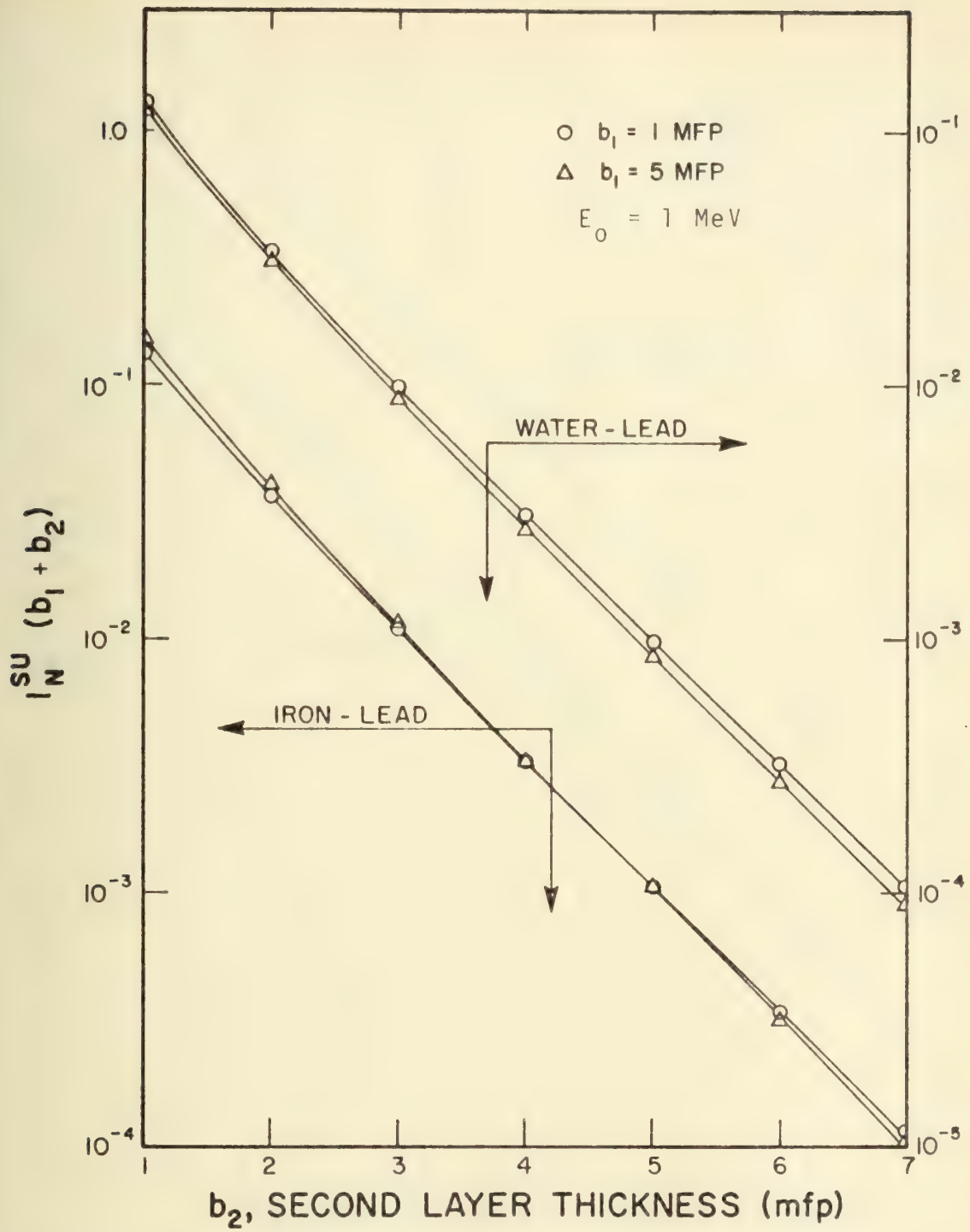

Figure D.30. The Energy Flux, $I_n^{su}(b_1+b_2)$ vs. b_1 and b_2 for 1MeV Photons in Two-Layered Slabs of Water-Lead and Iron-Lead.

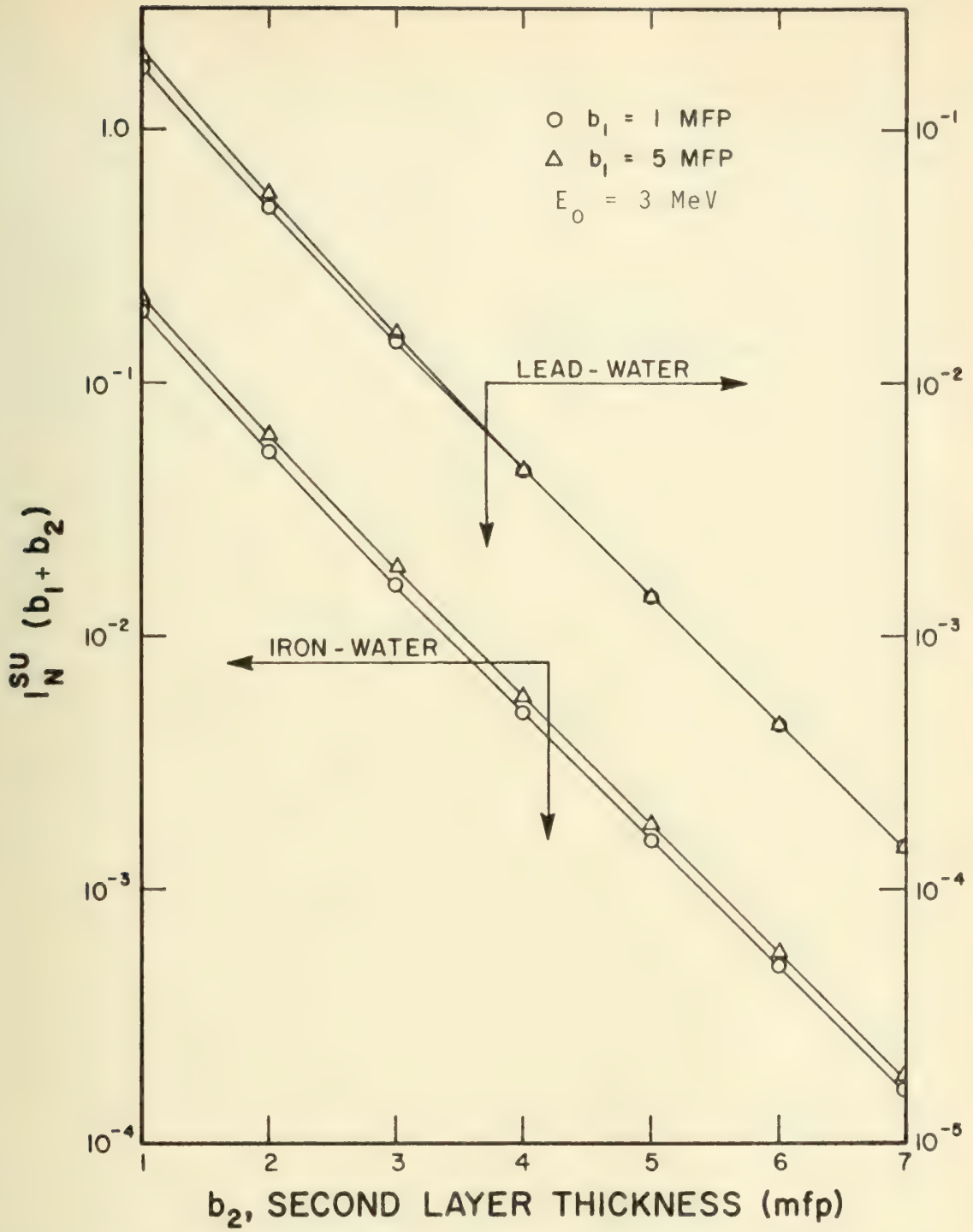

Figure D.31. The Energy Flux, $I_n^{su}(b_1+b_2)$ vs b_1 and b_2 for 3MeV Photons in Two-Layered Slabs of Iron-water and Lead-Water.

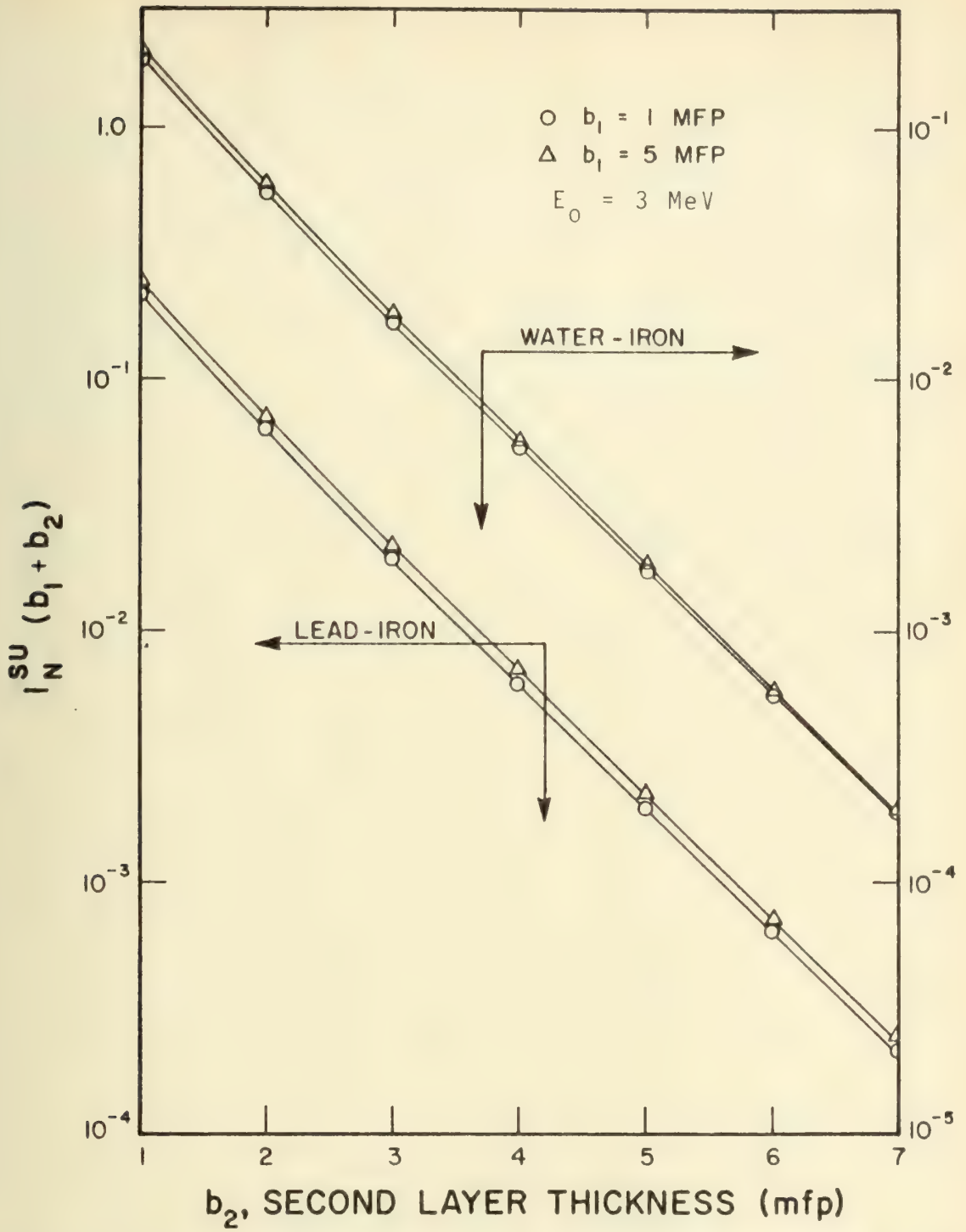

Figure D.32. The Energy Flux, $I_n^{su}(b_1+b_2)$ vs. b_1 and b_2 for 3MeV Photons in Two-Layered Slabs of Water-Iron and Lead-Iron.

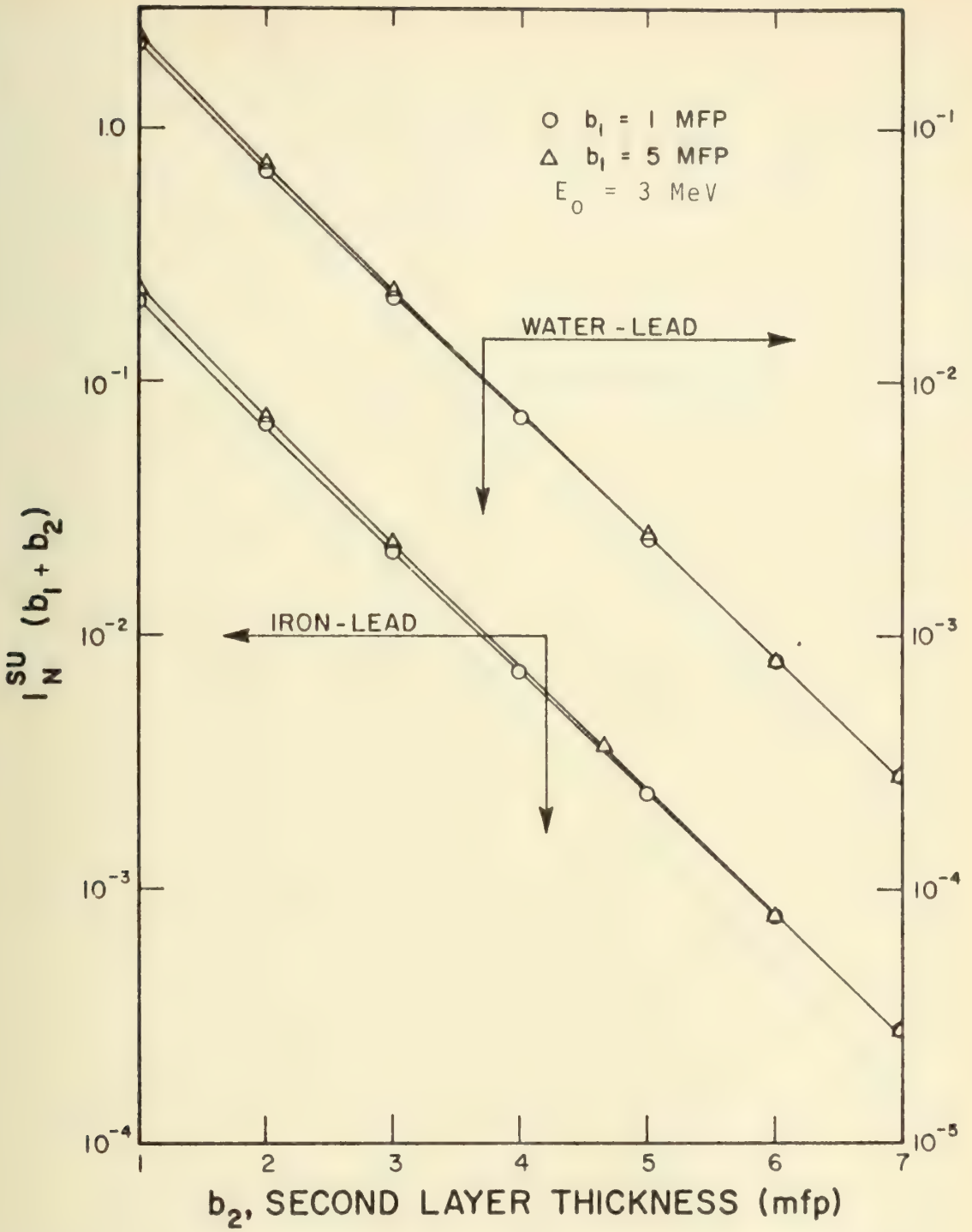

Figure D.33. The Energy Flux, $I_n^{su}(b_1+b_2)$ vs. b_1 and b_2 for 3MeV Photons in Two-Layered Slabs of Water-Lead and Iron-Lead.

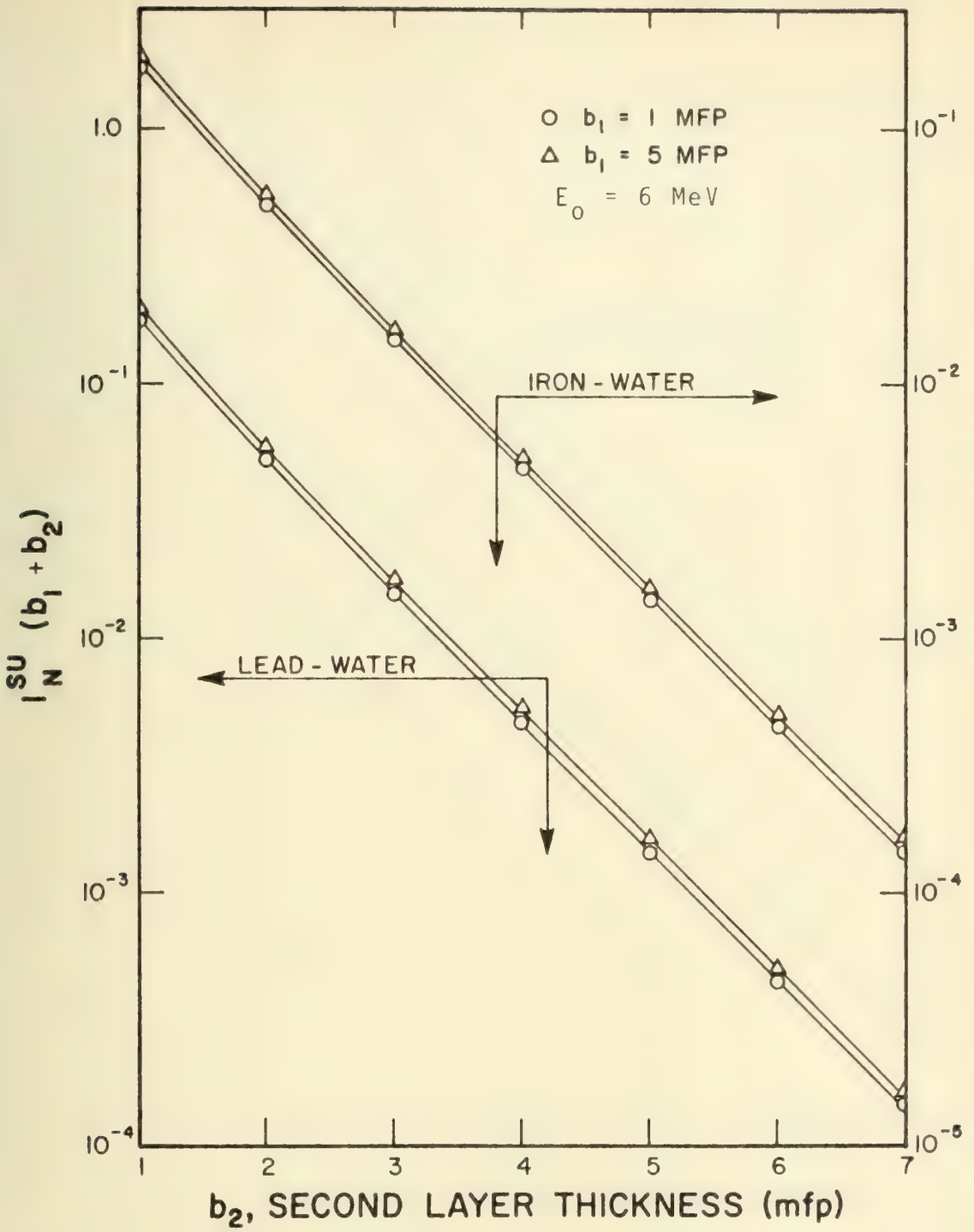

Figure D.34. The Energy Flux, $I_n^{su}(b_1+b_2)$ vs. b_1 and b_2 for 6MeV Photon in Two-Layered Slabs of Iron-Water and Lead-Water.

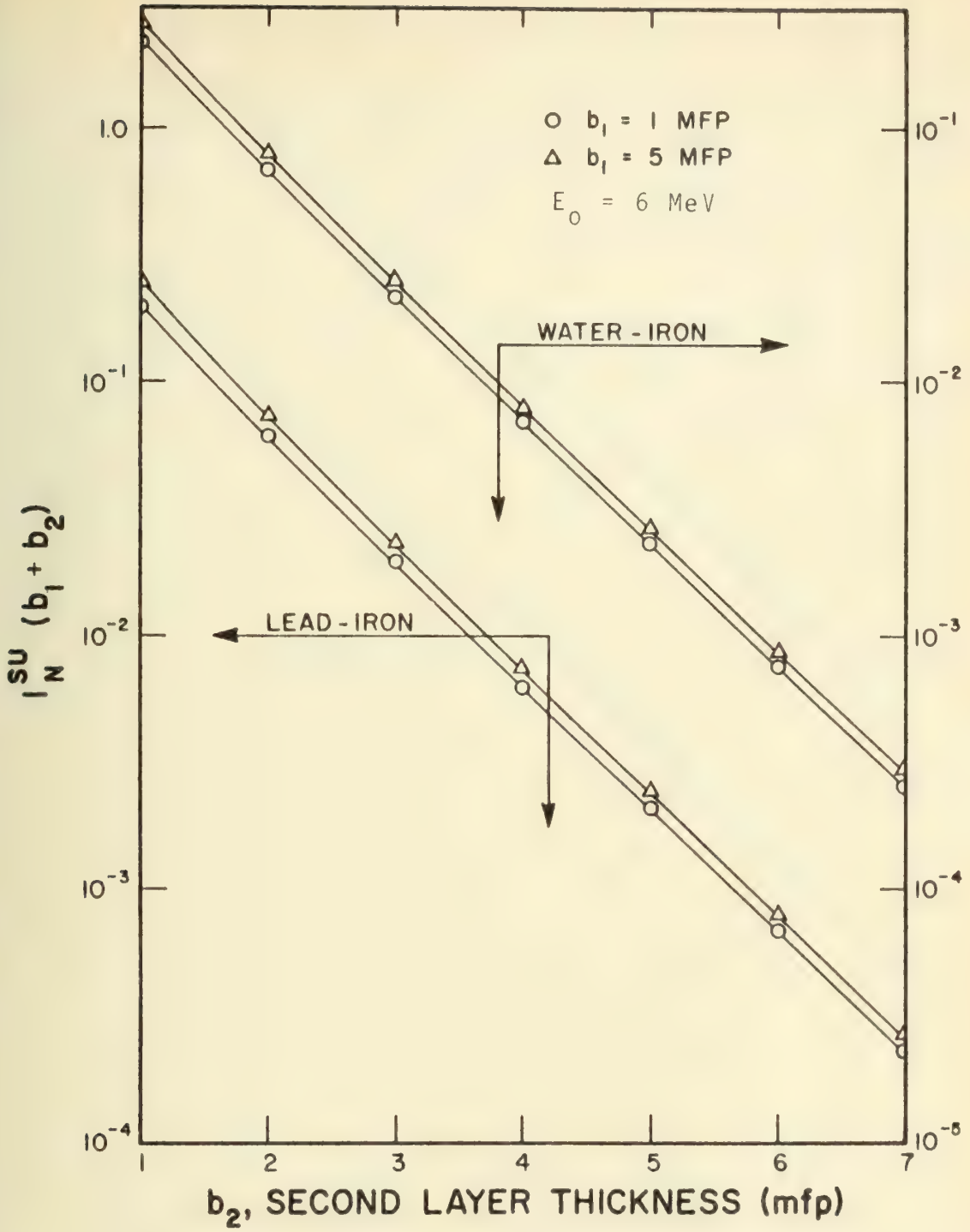

Figure D.35. The Energy Flux, $I_n^{su}(b_1+b_2)$ vs. b_1 and b_2 for 6MeV Photons in Two-Layered Slabs of Water-Iron and Lead-Iron.

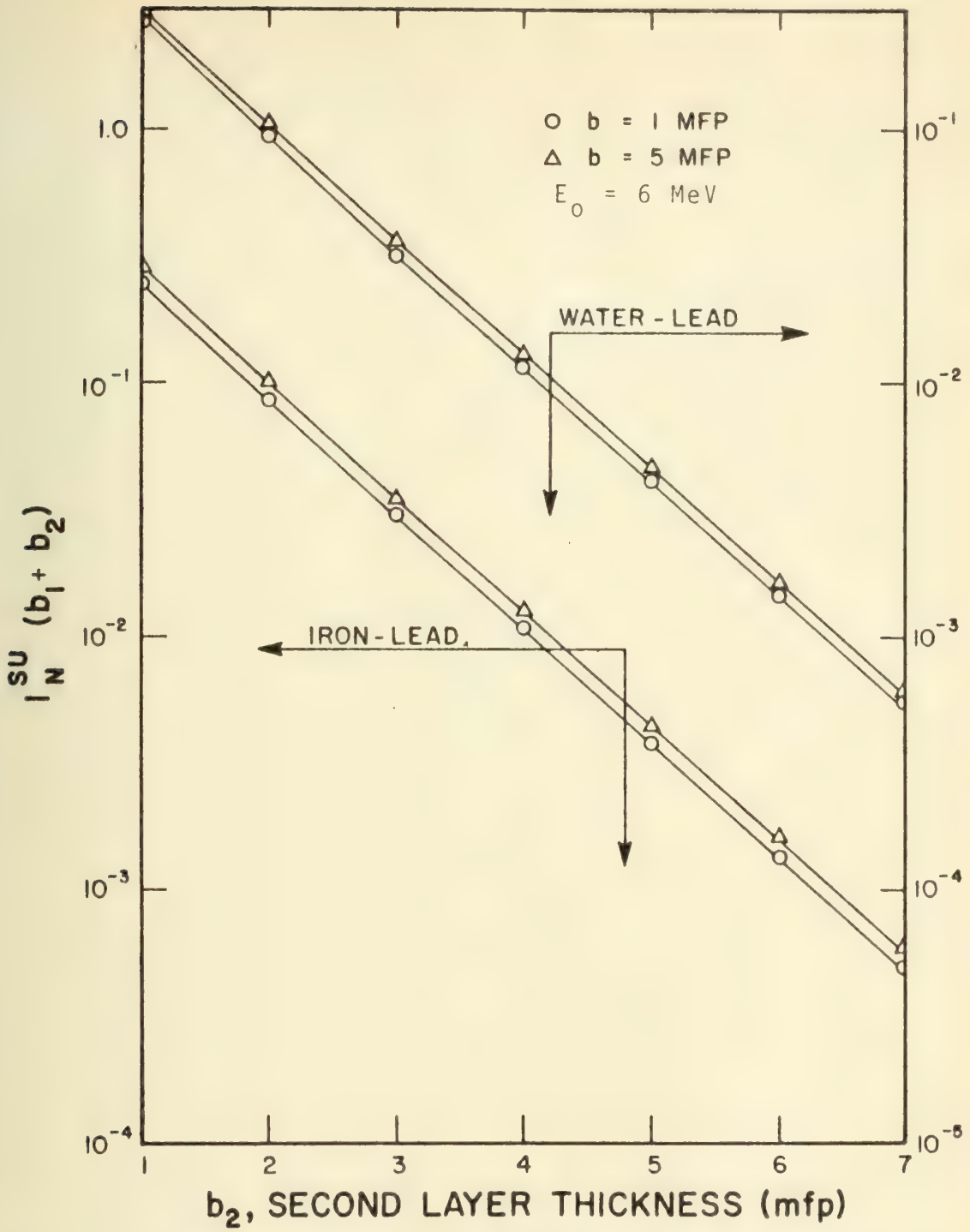

Figure D.36. The Energy Flux, $I_n^{su}(b_1+b_2)$ vs. b_1 and b_2 for 6MeV Photons in Two-Layered Slabs of Water-Lead and Iron-Lead.

VITA

VITA

James Andrew Maniscalco was born in Lawrence, Massachusetts on August 8, 1942. He attended Tenney High School in Methuen, Massachusetts; and joined the U.S. Navy in December of his Senior year. After two years of enlisted service he was selected to attend the Naval Academy Preparatory School in Bainbridge, Maryland. As a result of his work there, he was given a Secretary of the Navy Appointment to the U.S. Naval Academy, Annapolis, Maryland. In June, 1966 Mr. Maniscalco was graduated with distinction and was a recipient of both Fulbright and Burke program scholarships. On the Fulbright he spent a year studying at the University of Turin, Italy and teaching English in the Italian Public High School system.

From 1967 to 1969, Mr. Maniscalco attended Submarine School in New London, Connecticut and subsequently served aboard the submarine USS Cobbler. His duties included that of Electronics and Weapon Officer.

In September 1969, now a Lieutenant in the Navy, Mr. Maniscalco began his graduate work in nuclear engineering at Purdue University under the Junior Line Officer Advanced Scientific Educational (Burke) Program. He received his

Master of Science Degree in Nuclear Engineering in June of 1971. Upon completion of his doctorate, Mr. Maniscalco hopes to put his energy and education to work in the U.S. Navy.

142175
Thesis
M2797 Maniscalco
An analytical treatment of photon transport in two-layered media.